Molecular and circuit analysis of stable contrast processing in the visual system

Dissertation for the award of the degree

Doctor rerum naturalium (Dr.rer.nat.)

of the Georg-August-Universität Göttingen

within the doctoral program Neurosciences of the Georg-August University School of Science (GAUSS)

submitted by

Burak Gür

from Istanbul, Turkey

Göttingen - Mainz 2022

Thesis Committee

Prof. Dr. Marion Silies Neural Circuits Lab, Institute of Developmental Biology and Neurobiology (iDN), Johannes Gutenberg University of Mainz

Prof. Dr. Silvio Rizzoli Dept. of Neuro- and Sensory Physiology, University Medical Center Göttingen

Dr. Jan Clemens Neural Computation and Behavior group, European Neuroscience Institute Göttingen

Members of the examination board

First referee: Prof. Dr. Marion Silies Neural Circuits Lab, Institute of Developmental Biology and Neurobiology (iDN), Johannes Gutenberg University of Mainz

Second referee: Prof. Dr. Silvio Rizzoli Dept. of Neuro- and Sensory Physiology, University Medical Center Göttingen

Further members of the examination board

Dr. Jan Clemens Neural Computation and Behavior group, European Neuroscience Institute Göttingen

Prof. Dr. Jochen Staiger Center for Anatomy, Dept. of Neuroanatomy, University Medical Center Göttingen

Prof. Dr. Tobias Moser Institute for Auditory Neuroscience, University Medical Center Göttingen

Dr. Alexander Ecker Neural Data Science Group, Department of Computer Science, Georg August University Göttingen

Date of oral examination 14.07.2022

Contents

1 | Thesis Abstract

Visual perception gives us a reliable estimate of the world throughout the day, thanks to the computations implemented in visual circuits. In a given space or time, the relative change in luminance, contrast, forms the basis for many downstream computations like the detection of edges, shape, orientation and motion. Stable contrast estimation is challenged by the immensely changing lightning conditions that can slowly change throughout the day or much more rapidly when viewing natural scenes. To ensure reliable behavioral responses to the same (contrast) stimulus, visual systems face the monumental task of keeping contrast representations stable.

Gain mechanisms operate across the nervous system to match neural responses to relevant stimulus distribution. In visual systems, photoreceptors have numerous mechanisms that implement sensory gain to keep contrast representations stable across the slow changes of luminance occurring throughout the day. However, major changes in luminance also occur at fast timescales due to the luminance distributions within natural scenes which we view or through which we navigate. The extend of photoreceptor gain is often insufficient in these conditions but vision can still operate luminance-invariantly as shown in human perception, neurons in the vertebrate cortex, lateral geniculate nucleus and the retina. This highlights the necessity of post-receptor luminance gain mechanisms and evidence from a few studies suggests that this happens in the retina. However, a detailed understanding of the underlying circuitry, including the contribution of different cell types, their specialization and the molecular mechanisms underlying the post-receptor gain, is not understood in any visual system.

A recent study from *Drosophila melanogaster* showed that fly behavior to stimuli containing contrast decrements (OFF stimuli) is also luminance-invariant in rapidly changing conditions (Ketkar et al. 2020). Two second order neurons located in the lamina and post-synaptic to photoreceptors, L2 and L3, contribute to the OFF behavior by encoding contrast and luminance respectively. L3 neurons underlie the luminance-invariant behavior by providing a rapid luminance gain to the OFF pathway (Ketkar et al. 2020). This opened up the possibility of investigating post-receptor gain using the advanced fly genetic arsenal. **In the first part** of this thesis, we asked if the ON pathway also utilizes a post-receptor gain and which second-order neurons support this. The fly ON pathway was thought to receive major inputs only from a single second-order neuron type, L1 neurons, instead of the contrast and luminance sensitive parallel pathways formed by L2 and L3 within the OFF pathway. Using calcium imaging and behavioral paradigms, we revealed that all lamina neurons encode distinct features of the visual scenery and distribute these to both ON and OFF pathways showing that ON and OFF pathways only arise downstream of the lamina neurons. ON behavior also requires a luminance gain and this is provided by both L1 as well as L3 inputs. For the rapid luminance gain, L1 and L3 provide distinct contributions since their luminance encoding differ. Thus, a combination of temporal filtering leading to distinct contrast-luminance specializations in the second-order visual neurons is vital for downstream stable contrast processing. The bipolar cells, the second-order vi-

sual neurons of the vertebrate retina, also form parallel temporal channels suggesting that these specializations can serve distinct behavioral roles like in the fly visual system.

In the second study, I investigated the molecular factors shaping the distinct feature encoding properties of the lamina cell-types. Biophysical properties of neurons that are largely shaped by ion channel expression underlie a significant fraction of their signal processing properties. Using RNA-seq data and endogenous protein tagging, I have identified a specific subtype of voltage gated potassium channels, the K_a channels Shaker and Shal, as being highly expressed in the contrast sensitive L2 neurons. Using pharmacological manipulations, I have revealed the circuit wide role of K_a channels in enhancing L2 contrast responses. Additionally using cell-type specific RNAi, I have shown that K_a channels are involved in sharpening the L2 contrast responses. Similarities in the other fly species suggest the conserved role of K_a channels in shaping distinct cell-types and conferring their computational role within visual circuits for contrast processing.

In the third study I investigated visual circuits of the OFF pathway that implement the rapid luminance gain. I characterized the contrast encoding properties of all major cell-types in the OFF circuitry and identified the dendrites of two distinct third-order medulla neurons as the location where the rapid luminance gain arises. Using the specific features provided by the lamina neurons, the medulla neurons Tm1 and Tm9 implement a rapid luminance gain which scale their representations of contrast in distinct ways. Whereas Tm1 neurons reach luminance-invariant estimations of contrast, Tm9 neurons boost contrast signals in low luminances. Spatial pooling underlies the luminance gain in both neurons and both neurons receive wide glutamatergic signals yet use distinct molecular mechanisms to the implement luminance gain. Genetic analysis shows that Tm9 relies on inhibition mediated by GluClα channels whereas the molecular basis for luminance-invariance in Tm1 remains yet to be identified. This study reveals the details of how visual systems implement a gain mechanisms vital for stable vision in natural scenes. A post-receptor gain acting specifically in dim light in vertebrates is also implemented in the third-order neurons suggesting the presence of convergent strategies for stable vision. Testing if distinct luminance gain channels exist in vertebrates and whether similar spatial and molecular properties underlie the luminance gain can reveal if convergent strategies are implemented for natural scene processing across species.

My initial studies added to the numerous examples of convergent and divergent processing happening within neural circuits. One outcome of such complex wiring of neural circuits is that specific synaptic connections made between distinct synaptic partners, can contribute to information processing differently. To get a detailed causal understanding of specific cell-type to cell-type connections, manipulations restricted to specific synapses are necessary. However current manipulations maximally achieve specificity that affects all presynapses of one cell-type and thus limit the level of detail at which can understand neural circuit function. **In my final study**, we are developing a genetic tool, Synapse Targeted Activity Block (STAB), to manipulate synaptic connections between distinct partners. STAB is based on two components each expressed in one of the partners and only activates when these components coincide, which happens in the synaptic connections. One component is a viral protease (TEV protease - TEVp) which cleaves a conditionally integrated cleavage site (TEV cleavage site - TEVcs) in an endogenous synaptic protein which constitutes the second component. We generated TEVp fusion proteins that localize to synaptic regions and function extracellularly both *in vitro* and *in vivo*. Concentrating on the transsynaptic cleavage of postsynaptic receptors that are known to be essential for visual circuit function, *in vitro* experiments suggested that TEVp cleavage leads to degradation of post-synaptic receptor GluClα containing a TEVcs but the levels of degradation was not enough to recapitulate LOF phenotypes *in vivo*. We generated an optimized TEVp

version which showed higher levels of GluClα degradation. STAB with the enhanced TEVp needs to be validated *in vivo* before applying it for investigating specific synaptic connections. STAB is the first example of synapse specific manipulations that opens up a door of highly specific investigations of neural circuits and get detailed causal insights on neural circuits, computations and behavior.

Overall, my work thus combined the molecular and circuit analysis of stable contrast computation in dynamically changing environments. The development of the genetic STAB tool will allow circuit analysis at higher resolution than possible to date, and can be applied to studying visual computations, as well as any other type of circuit level analysis.

2 | General introduction

Throughout the history of humanity, theories to understand the mind emerged as humans tried to make sense of their existence. Aristotle, the great thinker, scientist, and the inventor of formal logic who lived around ~350 BC thought that the heart is the organ that senses and enables human intelligence. The great philosopher and mathematician of the 17th century, René Descartes, came closer. He described the pineal gland as the "Seat of the Soul" assigning it the tasks of sensation, memory, and motor control (Hall 1972). Today it is considered "common sense" that our rich daily experiences arise from the brain and the rest of the nervous system, composed of neurons organized into neural circuits connecting through synapses. How did we get from mere speculations of the origins of behavior to a structured, detailed and causal understanding of the processes driving it?

2.1 Our understanding of the brain advances parallel to the development of methods

"The history of neuroscience is the history of its methods." (Yuste 2015). Our current understanding of the brain emerged from a massive boom of development of methods over the last century. In the late 19th century, Santiago Ramón y Cajal formulated the neuron doctrine, placing individual neurons as the functional units of the nervous system (Ramón y Cajal 1888). His achievement was possible thanks to the Golgi staining method (Golgi 1873) which enabled him to visualize neurons in a sparse and random fashion. The proposal of single neurons as the building blocks of the nervous system caused a conceptual quantum leap in neurosciences and focused on single neuron techniques. In 1957, the development of tungsten micro-electrode (Hubel 1957) enabled the landmark discoveries of Hubel and Wiesel in the cat visual cortex. Their discoveries opened a door to understanding how neurons are organized to generate perception by showing the topographical tiling of receptive fields in cortical columns (Hubel et al. 1959; Hubel et al. 1962). Recording neural population activities using EEG (Berger 1929) lead to the discovery of spontaneous activity throughout the brain that is now associated with a plethora of important roles, from sleep to attention to decision making and consciousness (Fries et al. 1997; Llinás et al. 1993; Llinás 2002; Gray et al. 1989; Crick et al. 1990). More recent advances on recording neuronal activity such as tetrodes (McNaughton et al. 1983), multi-electrode arrays (Meister et al. 1994) and neuropixel silicon probes (Jun et al. 2017) along with the computational methods of neural network modeling, originating from the work of McCulloch and Pitts (McCulloch et al. 1943) gave a platform to capture and analyze the emergent computations arising from the interactions of many individual neurons. Today, thanks to the data acquired and analyses done through the collection of the last-century neuroscientific methods, we reached a level of knowledge of our mental faculties that astronomically exceeds the knowledge gained throughout human history before these methods. Unsurprisingly, further progress will only be achieved with an ever-developing toolbox of methods to investigate the brain.

2.1.1 Individual cell-types define key aspects of neural computation

Today, one major goal of neuroscience is to understand how neural circuits guide behavior. To reach such understanding, it is critical to know what kind of computations are implemented, how they are implemented, and why they are implemented (Marr 1982). Computations in neural circuits are implemented on different scales, from molecular to cellular to interactions between large neural assemblies. Individual cell types, which make up neural circuits, are key players on which all these levels depend. Cell types are defined by several parameters, including gene expression, developmental path, connections, morphology, physiology, and function (Zeng et al. 2017). Even though a unanimous description of a cell type does not exist, it serves as an instrumental concept to systematically analyze and reproducibly investigate information processing within the brain.

Players at the molecular scale shape distinct physiology of cell types, and together with their wiring, a diversity of computations emerges within and between neural circuits. Thus, understanding how neural representations arise in cell types and how they contribute to the workings of the neural circuit function to drive behavior is now central in systems neuroscience. An immense wealth of knowledge has been acquired about cell-types and their contributions to neural computations in the brain again thanks to neuroscientific methods. A major part of these methods rely on genetic tools or are used in conjunction with genetic tools.

In this thesis, I use genetic methods in the *Drosophila melanogaster* visual system to provide insights into the circuitry involved in contrast processing. First, I give insights into feature-encoding properties of different cell-types and causally link them to animal behavior; second, I reveal how distinct cell-type physiologies are shaped to facilitate distinct feature extractions; and third, I reveal the neural and molecular implementation of a vital peripheral visual computation that enables stable contrast processing. Last but not least, I develop genetic methods to achieve neural manipulations at higher resolutions than so far achieved. Thus, in the following sections, I will start by covering genetic tools for investigating neural circuits, and how causal links between different scales can be established. Afterwards, I will highlight the importance of specific synaptic connections between cell-types and thus the need for methods to address this scale. Later, I will introduce *Drosophila melanogaster* as an optimal platform for using and developing genetic tools. In the second section, I will delve deeper into a specific visual computation that facilitates stable contrast processing. First, I will shortly emphasize why contrast is a fundamental feature in visual scenes and how it is extracted. Then I will cover the challenges encountered by the visual system in computing contrast throughout the day and known solutions to these challenges in peripheral circuits. Throughout these sections, I will mainly focus on the fly visual system and complement this with knowledge gathered in other animals. In the last section, I will define the aims of my thesis.

2.1.2 Genetic tools to investigate neural circuits at the level of individual cell-types

Genetic tools provide numerous ways of visualizing neurons, measuring their activity, and manipulating their function. Combination of different methods further broadens their usage. A crucial advantage of genetic methods is that they give reliable and reproducible access to defined cell types. Thus the role of cell types can be investigated with different experimental paradigms, data can be integrated between studies and laboratories, and comparisons can be made between species.

Achieving genetic access to cell types

The description and categorization of cell-types relies mainly on parameters such as gene expression, morphology and physiology. Usually these different definitions overlap since they depend on each other. Recent studies using single-cell RNA-seq approaches show a major correspondence between gene expression, morphology, physiology and function (Li et al. 2017; Shekhar et al. 2016; Tasic et al. 2016). Accordingly, the most common way of accessing cell-types is to mimic or capture the endogenous gene expression.

Endogenous gene expression patterns are mostly mimicked by using or capturing the regulatory elements of genes, enhancers and promoters. Today, the most common strategy to access cell-types is the use of binary expression systems. Binary systems are composed of two main elements: a driver gene that encodes for a driver protein, and a "responder" gene that encodes for a protein of interest (e.g. effector or reporter proteins) that is used for visualizing, measuring or manipulating cells. The driver gene captures a specific expression pattern by utilizing nearby (or provided) regulatory elements (enhancers and promoters) and thus the driver protein can be expressed in distinct cell types. The driver protein is commonly a transcription factor that binds to its target sequence upstream of the responder gene. The big advantage of these binary systems is their modularity: one can combine driver and responder lines to in principle achieve expression of any protein of interest in any cell-type.

A great example of a binary expression system is the Gal4-UAS system (Brand et al. 1993). The yeast transcriptional activator Gal4 binds to the Upstream Activator Sequence (UAS) to drive a protein of interest. This system is particularly popular in *Drosophila melanogaster* where vast libraries of Gal4 lines are available (Jenett et al. 2012; Gohl et al. 2011) and also used in zebrafish (Scott et al. 2007; Davison et al. 2007) and mice (Rowitch et al. 1999). Additionally, several other binary systems are available which enables simultaneous expression of different proteins in different cell types (Potter et al. 2010; Lai et al. 2006). Some binary systems depend on recombinases like the Cre-loxP system that is widely used in mice (Nagy 2000; García-Otín et al. 2006). Binary expression systems allow reliable genetic access to thousands of different expression patterns that include specific cell-types.

Cell-type specificity combined with other methods (e.g. microscopy, electrophysiolgy, behavioral paradigms) provided immense insights into workings of neural circuits. In the last decades, generation of such genetic elements sped-up thanks to the usage of techniques such as CRISPR-Cas9 which also opens up a promising avenue to implement these methods in non model organisms and model organisms where genetic tools are not extensive, such as non-human primates.

Using the cell-type specific access provided by the driver genes, one can drive effector proteins that allow characterizing the anatomy, connectivity, molecular composition, physiology and function of cell-types. In the following paragraphs I will mention common ways to characterize the molecular composition, physiology and function of cell-types which form the main focus of this thesis.

Measuring the protein composition of cell-types using genetic methods

The molecular composition of cell-types is crucial to investigate since development, connectivity and physiology of neurons are shaped by protein expression. Information about protein localization in the nervous system is essential for determining the molecular composition of cell-types. One simple strategy to figure out if a neuron expresses a certain protein is to utilize the specific antibodies against proteins while labeling the neuron with

the previously mentioned genetic approaches. However, especially in invertebrate systems, specific antibodies of proteins are not always available, only 3% of the proteins encoded by the fly genome have antibodies against them (St. Pierre et al. 2014). Genetic approaches again circumvent this problem in several ways. A powerful recent way to capture endogenous protein expression patterns is achieved by inserting an exon with a protein tag to the endogenous gene locus (Nagarkar-Jaiswal et al. 2015). A conditional approach where one can restrict the tag integration to defined cell-types provides a more specific way of visualizing protein expression (Fendl et al. 2020). Another method to check the molecular composition of a cell is to use a driver line that is driven by the regulatory elements of proteins-of-interest. For example, a driver line using the regulatory elements of the gene encoding the $GABA_A$ receptors will give access only to the cells that are GABAergic. Intersecting these with the known drivers of cell-types will show if a defined cell-type expresses a certain set of neurotransmitters or receptors. Combining genetic tools to mark cell-types using reporter proteins (such as GFP) and isolating them for RNA-seq analysis is a powerful way to access the expression profile of distinct cell-types (Henry et al. 2012; Mo et al. 2015). Recent studies for example provided the molecular composition of distinct cell-types in the olfactory system (Crocker et al. 2016) and the visual system (Tan et al. 2015; Pankova et al. 2016; Konstantinides et al. 2018; Davis et al. 2018) which provides a basis for specific and testable hypotheses in terms of mechanisms leading to connectivity and physiology of neurons (Molina-Obando et al. 2019).

Characterizing the physiology of cell-types using genetic methods

The physiology of cell-types are crucial for encoding of distinct features within neural circuits. In the last decade, our knowledge on neural physiology and how it relates to information processing greatly expanded thanks to genetic methods. Electrophysiological recordings of same cell-types require reliably localizing the cell-type based on their morphology before targeting the electrode. Expressing fluorescent reports facilitate this process immensely. The most common genetic method to characterize the physiology of cell-types are the genetically encoded indicators of neural activity that infer voltage or calcium levels, synaptic vesicle fusion and neurotransmitter release (Lin et al. 2016b). Combined with two-photon imaging, Genetically Encoded Calcium Indicators (GECIs), especially the GFP based sensor GCaMP6 (Chen et al. 2013) provided physiological descriptions of neural circuits in diverse organisms (Ahrens et al. 2013; Peron et al. 2015). Additionally, using different types of indicators one can also get insights into the signal transformations happening within a neuron, such as voltage to calcium transformations happening in the axon terminals (Yang et al. 2016). Furthermore, using the indicators for detecting specific neurotransmitters, one can characterize the input properties of a neuron and how these inputs are transformed to get the calcium signal at the axon terminals. Combined, genetically encoded activity indicators provide a diverse set of effector proteins to characterize cell-type physiology ranging from input dynamics to dendrite to axon transformations to release dynamics.

A causal understanding of cell-types requires manipulation methods

Observing neurons and measuring their activity through genetic methods is instrumental to understand neural circuit function. They provide invaluable information to form hypotheses on how neural circuits function and contribute to behavior. However, to test these hypotheses and to establish causal links between different scales of neural computation and behavior one needs methods to manipulate activity.

The manipulation methods can be broadly classified into two: loss of function techniques (LOF) where entities are removed or inactivated and gain of function techniques (GOF)

where entities are activated outside of their natural context. Origins of LOF studies extending from human brain lesion studies along with experiments done with surgically induced lesions provided initial insights on a causal relationship between neural circuits and behavior (Izquierdo et al. 1998) and are still important for assessing theories in cognitive and behavioral neuroscience (Vaidya et al. 2019). However, they do not provide cell-type specificity and also lead to post-lesion plasticity that hinder conclusions (Otchy et al. 2015). Similarly, pharmacological LOF or GOF studies provided the basis for understanding how neurotransmitters and receptors contribute to information processing in neural circuits and drive behavior. As a major GOF technique microstimulations have also provided important insights (Cohen et al. 2004) but similar to other techniques, they lack specificity. The extensive genetic tools now provide numerous methods to manipulate neural activity down to cell-type level and enable testing detailed hypotheses about brain function.

Chemogenetic approaches are widely used in larger brains where small molecule ligands bind to engineered receptors that activate downstream pathways which manipulate activity (Sternson et al. 2014). Here the receptors can be expressed in distinct cell-types, restricting the manipulations to neurons of interest. Chemogenetic methods are suitable for long-term manipulation of activity in larger brains since they can be delivered systematically however thus limited in temporal resolution and hard to conduct investigations on temporally defined periods of neural circuit activity. Furthermore the unspecific effects of the applied small molecules throughout the brain is another major concern in these approaches (Gomez et al. 2017).

Optogenetics, on the other hand, give an excellent millisecond temporal resolution to neural manipulations (Fenno et al. 2011). Optogenetics rely on activation of native or modified microbial opsin proteins with light to either induce neuronal depolarization (in case of most Channelrhodopsins - ChRs) or hyperpolarization (Halorhodopsins). For depolarization, different excitatory ChRs provide experimenters a set of different manipulation options with different absorption spectra, activation strengths, kinetics and temporal properties (Berndt et al. 2009; Gunaydin et al. 2010; Lin et al. 2013; Klapoetke et al. 2014). For hyperpolarization, halorhodopsins (Zhang et al. 2007) and Cl- conducting ChRs (Wietek et al. 2014) are used. With its excellent temporal resolution and ease of application optogenetics lead to major discoveries on how the neural circuits work (Deisseroth 2015).

When it comes to tissue-wide manipulation of neurons, a variety of cell-type specific silencing or activation methods are used. In *Drosophila melanogaster*, where genetic methods to achieve cell-type specificity are advanced, a common neural silencing method is the temperature dependent inactivation of synaptic transmission using a dominant-negative dynamin allele, Shibire^{ts} (Kitamoto 2001). What makes Shibire^{ts} manipulations so attractive is that they are easily achievable and temporally controllable by elevating temperature for desired durations. After the animals return to normal temperatures, the Shibire^{ts} manipulations are reversed so that the experimenter can still continue with paradigms that were designed to last after the manipulations, for example learning and memory assays. Another temperature dependent method is the expression of temperature-sensitive transient receptor potential (TRP) channels. The TRP channel family have different members that offer temporally defined activation of cell-types by either heating (Hamada et al. 2008; Krashes et al. 2009) or cooling down (McKemy et al. 2002; Peabody et al. 2009) the ambient temperature. Temperature dependent methods thus give a good temporal resolution and act over the whole nervous tissue. However shifting temperature for very long durations is not desirable. For chronic manipulations of neurons, one can inactivate neural activity using expression of neurotoxins for example tetanus light chain (Yamamoto et al. 2003). In addition to neurotoxins, one can express constantly active hyperpolariz-

ing ion channels, such as the potassium channels (Hodge 2009). A widely used example of this is the expression of the inward rectifying potassium channel $K_{ir}2.1$ (Baines et al. 2001).

The development of tools to achieve cell-type specific manipulations gave us causal insights into how neural computations are implemented in different scales and drive behavior. A big arsenal of tools that have different spatial and temporal properties provide experimenters a long list of options to choose from depending on their question. Now these methods are routinely applied to crack neural circuits in almost all animal models.

2.1.3 Moving beyond cell-type specificity: the need for methods targeting specific synaptic connections

A plethora of genetic approaches combined with other methods provide the rich experimental possibilities offered for understanding neural circuits down to the single cell-type level. Consequently cell-types can be considered as the fundamental units of neural computation. However, neural circuits are organized into a finer level of detail, the synaptic connections. Recent advances in high-throughput electron microscopy (EM) allowed the reconstructions of large neural tissue leading to very precise connectomes of neural circuits. Detailed wiring diagrams of *C. elegans* (Chen et al. 2006), fly (Takemura et al. 2013; Schlegel et al. 2017; Takemura et al. 2017; Horne et al. 2018; Shinomiya et al. 2019a; Scheffer et al. 2020) and mammalian (Briggman et al. 2011; Lee et al. 2016) neural circuits are readily available (Figure 2.1A, B). These reconstructions reveal that neuronal connectivity is very intricate.

Each neuron contributes to different neural pathways by sending outputs to multiple neurons and gets information from multiple pathways by receiving input from multiple cell-types. Many studies have shown that the boundaries between processing of different types of information are not clear-cut but such divergence and convergence happens at many stages within neural processing streams (Cohen et al. 1990; Jeanne et al. 2015; Takagi et al. 2017; Luo 2021). These architectures have many implications from noise reduction (Faisal et al. 2008) and gain increase (Cohen et al. 1990) to improving sensory decoding accuracy (Jeanne et al. 2015). An important property of these architectures is that a diverging cell can affect its post-synaptic partners differentially (e.g. depending on the connection strength, or the neurotransmitter profile) and thus contribute to neural processing in a complex way. Furthermore, through learning, specific synapses between partners participating in the learning process are modified and other synapses could stay unaffected. This synaptic heterogeneity within a cell-type enables its synapses to act as unique computational units. Thus, an ultimate understanding of neural circuits requires an understanding of the roles of synaptic connections.

A well-studied example of synaptic heterogeneity include wide-field amacrine cells in the vertebrate retina (Masland 2012). The A17 amacrine cells with their electronically isolated varicosities operates up to more than 100 independent microcircuits (Grimes et al. 2010). A counterpart of this neuron is available in the *Drosophila* visual system suggesting evolutionary convergent computational strategies depending on specific synapses in a single neuron (Meier et al. 2019). Similarly, starburst amacrine cells in vertebrates compute direction selectivity locally in dendritic regions and thus also act as independent computational units (Euler et al. 2002). Another example comes from the olfactory system, where specific olfactory projection neurons project to two distinct regions with very different functions, the mushroom body and the lateral horn (Masse et al. 2009; Bates et al. 2020). Thus, synaptic connections from one cell type contributes to two different neural computation streams, even using different molecular pathways supporting the idea that specific

synaptic connections are elementary units of information processing.

To obtain a causal understanding of how specific synaptic connections contribute to neural processing one require manipulations (Figure 2.1). However, so far no suitable manipulation method exists to either do LOF or GOF experiments in specific synaptic connections. What is an optimal platform to develop new genetic methods?

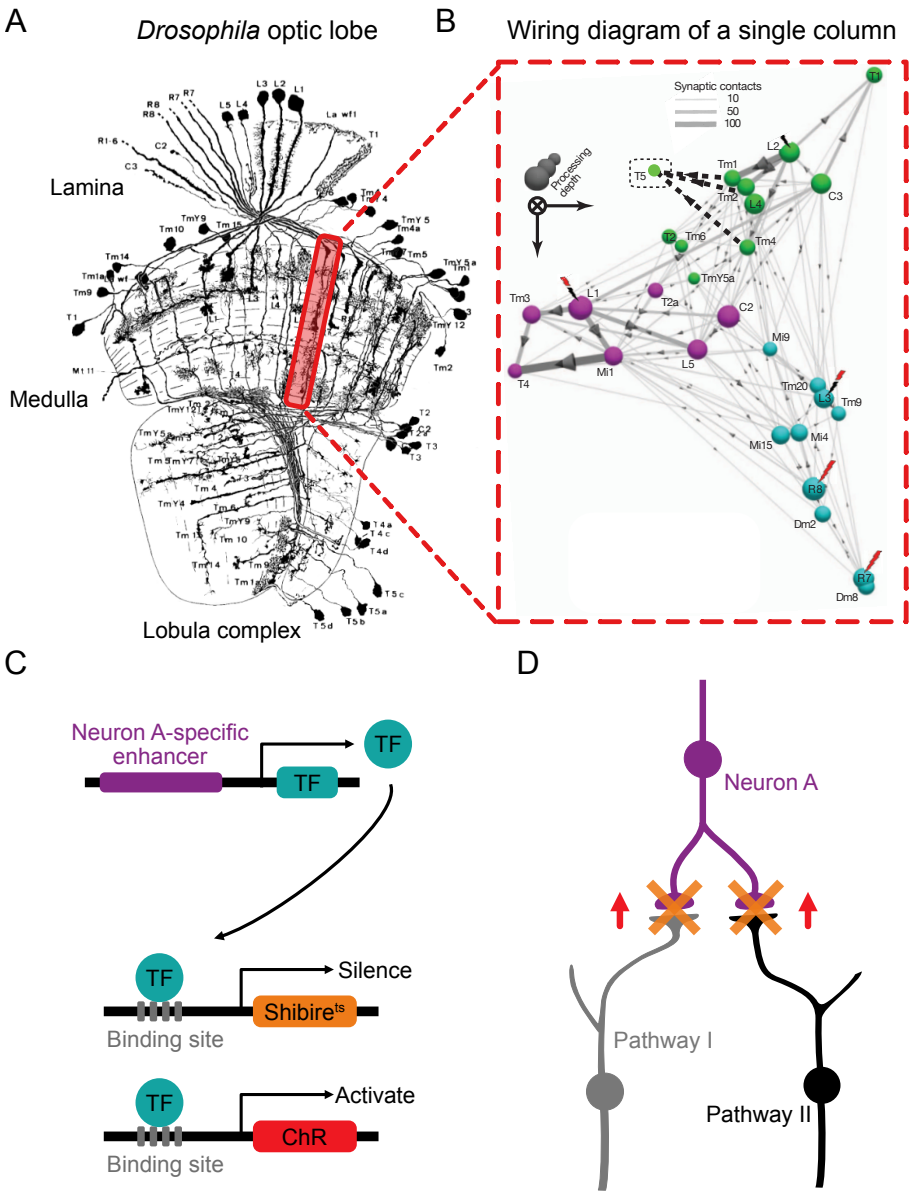

Figure 2.1: Neural circuits have intricate wiring but current manipulations go down to cell-type resolution. (A) The *Drosophila* optic lobe contains > 60 neural cell-types (adapted from Fischbach et al. 1989). **(B)** Circuit diagram of a single visual processing column in the medulla reveals complex connectivity where cell-types take input from and project to multiple other cell-types (adapted from Takemura et al. 2013). Cell-types are depicted as colored balls. **(C)** Binary expression systems give access to defined cell-types enabling manipulations down to cell-type level. **(D)** Cell-type specific manipulations simultaneously affect distinct synaptic connections, potentially different roles in information processing, thus obstructing a detailed causal understanding of neural computations.

2.1.4 *Drosophila melanogaster* as the model organism for both developing and using genetic tools to study cell-types and neural circuits

Drosophila melanogaster contains the most advanced arsenal of genetic tools available of all higher eukaryotes. This genetic arsenal enables both gene-centric (identifying the genetic basis of nervous system function) and neuron-centric (the neural basis of nervous system function) research to be done in the fly (Venken et al. 2011a). The nervous system of *Drosophila melanogaster* provides a good compromise between complexity and accessibility. Almost all of the neuron-types of the fly brain are accessible through binary expression systems (Gohl et al. 2011; Jenett et al. 2012). Plus, connectomes of different neural circuits are known to their finest detail (Takemura et al. 2013; Schlegel et al. 2017; Takemura et al. 2017; Horne et al. 2018; Shinomiya et al. 2019a; Scheffer et al. 2020). Compared to the vertebrate models, it has fewer neurons but many more than the worm, giving it a complexity level appropriate for studying the neural underpinnings of behavior. Arising from this complexity, it exhibits a rich set of quantifiable behaviors such as feeding, courtship, learning, sleep, aggression and motivation, making it optimal for cracking neural circuits underlying behavior (Olsen et al. 2008a; Owald et al. 2015). From development to synaptic function to neural circuits to behavior, *Drosophila* research has provided fundamental insights into our understanding of the brain (Collins et al. 2007; Bellen et al. 2010; Sanes et al. 2020) including the origins of neurological disorders (Lessing et al. 2009; O'Kane 2011).

The current genetic arsenal of the fruit fly offers a versatile platform for developing genetic tools. The presence of multiple binary expression systems such as Gal4/UAS, LexA/lexAop, QF/QUAS enables expression of multiple genetic constructs in different cell-types. One can easily convert binary expression systems to each other (Gohl et al. 2011; Lin et al. 2016a) to repurpose well-established expression patterns or use intersectional approaches to refine expression patterns (Luan et al. 2006). Several of newly developed fly genetic tools depend on multiple binary expression systems. Especially for the trans-synaptic tools where the focus is labeling synaptic partners, multiple binary expression systems are utilized (Talay et al. 2017; Huang et al. 2017; Cachero et al. 2020). Thus, any trans-synaptic manipulation approach would also benefit from multiple binary expression systems.

For manipulation of synapses, one requires targeting of engineered proteins to synaptic regions. Current genetic tools in *Drosophila* already utilize such protein fusions and achieve localization in synaptic regions. For example the *Drosophila* Synaptobrevin is suitable for targeting proteins to pre-synapses as demonstrated in trans-synaptic labeling approaches (Huang et al. 2017; Macpherson et al. 2015). For post-synaptic targeting, Neuroligin and the ICAM proteins localize to post-synapses and can be used in fusion proteins to target other proteins to the post-synapse (Huang et al. 2017; Nicolaï et al. 2010).

A manipulation method targeted to specific synapses requires manipulation of the activity of endogenous synaptic proteins, conditionally in specific synapses. Thus, methods to engineer endogenous proteins are useful. Engineering of endogenous proteins is possible using recombinase-mediated cassette exchange (RMCE). The base of this approach depends on MiMIC insertions which are available throughout the fly genome including developmentally important genes, neurotransmitter encoding genes, receptors, and ion channel genes (Venken et al. 2011b). FlpStop, a recent genetic approach, used RMCE to generate a strategy to conditionally knock-out specific genes (Fisher et al. 2017). Another application of RMCE provided endogenous tagging of proteins in the visual system (Nagarkar-Jaiswal et al. 2015), even conditionally to specific cell-types (Fendl et al. 2020). RMCE was also used to generate driver lines by integrating a Gal4 construct into endogenous genes (Lee et al. 2018). In addition to RMCE, the recent advances in CRISPR/Cas9-based genome

engineering and their diverse application methods in the fly offers yet another avenue for very specific genome editing (Marr et al. 2021).

One important part of genetic tool development is the time and cost of transgenic animal generation since tool development procedures may require iterations of transgenic animal creation during optimization processes. The fly provides a very time and cost efficient platform for transgenesis (Venken et al. 2005). Furthermore, transgenes can be inserted using optimized vectors into well characterized genomic sites leading to suitable expression levels for *in vivo* studies (Pfeiffer et al. 2010; Pfeiffer et al. 2012). The ease of fly husbandry and short generation time is also vital for tool development procedures. Combined, these factors make the *Drosophila* system optimal for genetic tool development.

2.2 Neural circuits ensuring stable visual contrast processing

Sighted animals depend heavily on their visual system for survival. Neural circuits in the visual system implement a diverse set of parallel and serial computations that enable the extraction of features such as shape, size, color, texture and motion. All of these features are built on the fundamental signal that informs about the luminance levels reflected by different objects. Objects are visible because of the difference of luminance levels they reflect compared to their background or compared to other objects. For example, a snake on a grass field reflects lower amounts of light than the grass behind it enabling our brains to detect and avoid it. This difference in luminance levels between objects or, objects and their background is called luminance contrast (I will simply refer to it as contrast). A majority of extraordinary feats of our visual systems depend on the processing of this fundamental visual feature, contrast.

The eye receives photons from defined locations in the visual field. The optics of the eye guide the incoming photons to the retina where light is transduced into electrical signals. From these absolute number of photons, the visual system first has to extract the photon differences, contrast. Extraction of contrast is already achieved in the initial stages of retinal circuits. Starting from the light capturing cells, the photoreceptors, one can observe contrast signals. Along the circuitry in the retina, these contrast signals are transformed and refined by spatial and temporal processing. A plethora of mechanisms ranging from molecular to circuit aid these processes. Almost all of the output cells of the mammalian retina, RGCs, are activated by contrast and act as parallel streams that represent features of the visual scenery such as orientation and motion (Demb et al. 2015). Similar to the mammalian retina, the output cells of the fly retina are activated by contrast and encode different features (Clark et al. 2016).

A common challenge for all visual animals is to deal with the wide intensity in the range of visual inputs encountered throughout the day. The most extensive changes occur from day to night. Visual systems have to function reliably in light intensities varying over 10 orders of magnitude (Rieke et al. 2009). Even in given a natural scene, visual systems are faced with light intensity differences up to 3-4 orders of magnitude (Hateren 1997; Hateren et al. 1998; Mante et al. 2005; Frazor et al. 2006). Natural signals highly exceed the dynamic range of photoreceptor signalling which can go up to only 1-2 orders of magnitude (Normann et al. 1979; Schnapf et al. 1990; Choi et al. 2005). Adaptation mechanisms that change the gain of neural responses must be implemented in the visual system to compensate for the changing statistics of the visual inputs and achieve a stable estimation of contrast. Without such mechanisms, the fidelity of all downstream computations are compromised.

2.2.1 An overview of the vertebrate and invertebrate eyes

The eye of different animals can differ significantly according to the environmental niche and evolutionary distance, but they also exhibit many analogous developmental, structural and functional features (Sanes et al. 2010; Wernet et al. 2014; Clark et al. 2016). For example, both invertebrate and vertebrate eyes use lenses to focus light onto the photoreceptors. Photoreceptors express different types of opsin molecules that undergo a conformational change upon isomerization of their retinal molecules upon light activation. Adjacent neurons throughout the retina receive information from adjacent points in space which forms a retionotopic topographical representation of the visual space. Retinotopy is preserved throughout many of the downstream processing stages forming a columnar structure of visual processing. Within these columns, specific cell-types exhibit stereotypical connectivity by extending their dendritic processes and axon terminals to distinct areas forming horizontal layered structure within the visual system. In both taxa, inter-columnar neurons further support signal processing (Sanes et al. 2010).

Two eye patterns emerged through evolution: the lens eye common in vertebrates and the compound eye typical for arthropods (Figure 2.2A, B, C). In vertebrates, vision begins with the light entering the eye through its outermost lens, the cornea. The focused light enters through the pupil and further adjusted with the lens before hitting the retina where it is transduced into electrical signals by two distinct types of photoreceptors, rods and cones (Figure 2.2B, D). Upon the capture of light, photoreceptors hyperpolarize and reduce the release of glutamate in their synaptic terminals (Arshavsky et al. 2002). These signals are picked up in the outer plexiform layer (OPL) by the bipolar cells (BPCs) (Figure 2.2D). There are typically more than ten types of BPCs which transform photoreceptor signals in numerous ways with respect to polarity and signal dynamics (Euler et al. 2014). In the OPL, horizontal cells provide inter-columnar input and also feedback to the photoreceptors (Thoreson et al. 2012). Retinal processing then continues with the numerous types of retinal ganglion cells (RGCs) that act as parallel feature detectors sending the highly preprocessed visual information to higher brain areas (Baden et al. 2016) (Figure 2.2D).

The compound eye consists of repeating hexagonally arranged lens-capped optical units, called ommatidia, which harbor the eight photoreceptor cells (retinula - R - cells) of the *Drosophila* retina (Katz et al. 2009) (Figure 2.2C). Unlike vertebrate photoreceptors, *Drosophila* photoreceptors depolarize upon light capture. R1-R6 are the major class that are involved in achromatic processing of the image such as orientation and motion (Heisenberg et al. 1977; Ramos-Traslosheros et al. 2018). Here, transduction of light is mediated by the Rh1 opsin which ensures a broad sensitivity to light. *Drosophila* R7-R8 cells express different opsins and are involved in color vision and the detection of polarized light (Wernet et al. 2006). R1-R6 project to the second optic neuropile, the lamina, where lamina monopolar cells (LMCs) reside (Figure 2.2E). LMCs send their signals to the medulla neurons where approximately 60 types of columnar and non-columnar cells provide further spatiotemporal transformation of signals (Fischbach et al. 1989; Yang et al. 2018). Medulla neurons project to the neurons in the lobula complex which encode distinct features such as local motion and orientation (Maisak et al. 2013; Yang et al. 2018) (Figure 2.2E).

2.2.2 Extracting contrast signals in the visual system

Vertebrate rods are extremely sensitive to light and thus cover the scotopic ranges of vision (Baylor et al. 1974) and saturate at photopic conditions which characterize most of the day (Green 1971). In contrast to rods, cones are not extremely sensitive to light and thus do not work in the scotopic ranges but have optimal mechanisms to adjust their sensitivity

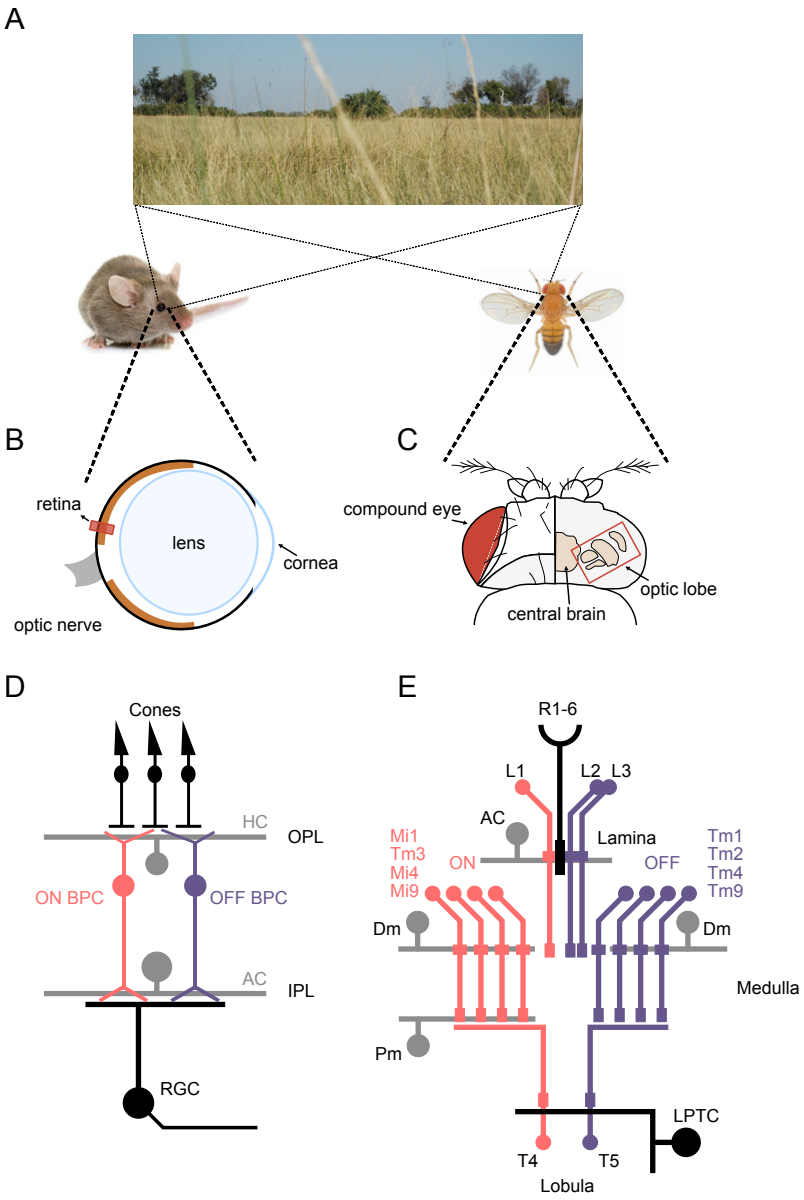

Figure 2.2: Overview of vertebrate and invertebrate peripheral vision. (A) Vertebrates (e.g., mouse) and invertebrates (e.g., fly) are exposed to similar natural scenes and thus their visual systems are subjected to similar challenges (e.g., the wide variance of luminance). (image from Tkačik et al. 2011) **(B)** Light enters the lens eyes through the cornea where it is focused and further adjusted by the lens before hitting the retina where photoreceptors and peripheral visual neurons reside. After pre-processing of visual information in the retina, information is sent to the higher brain areas through the optic nerve. **(C)** Compound eyes consist of lens-capped optical units (ommatidia) where photoreceptors reside. The signals are pre-processed in the optic lobe before going to the central brain. (adapted from Shinomiya et al. 2019b) **(D)** Circuit diagram of the vertebrate retina starting from cone photoreceptors (rods work in dim light and thus omitted) that connect to bipolar cells (BPC) in the outer plexiform layer (OPL). Horizontal processing is mediated by the horizontal cells (HC) in the OPL. Contrast increments (ON) and decrements (OFF) are processed in different BPCs (ON and OFF BPCs). BPCs connect with the downstream retinal ganglion cells (RGCs) in the inner plexiform layer (IPL) where amacrine cells support horizontal processing. RGCs are sensitive to a plethora of visual features such as motion. **(E)** Circuit diagram of the fly peripheral visual system starting from photoreceptors R1-6 that connect to lamina monopolar cells (LMCs) located in the lamina. L1 gives major inputs to ON and L2-L3 gives major inputs to the OFF pathway. Horizontal processing is mediated by the amacrine cells in the lamina. LMCs project to medulla where ON and OFF selective medulla neurons reside. At the medulla horizontal distal medulla (Dm) and proximal medulla (Pm) neurons reside. Medulla neurons converge onto the dendrites of the first-direction selective neurons T4 and T5 located in the lobula. T4 and T5 signals are pooled in wide-field lobula plate tangential cells (LPTCs) (adapted from Clark et al. 2016).

to cover the whole photopic range (Boynton et al. 1970). Cones also underlie the basis of color vision. Even though insects just have a single photoreceptor type that covers all light ranges, many different adaptation mechanisms exist to enable vision in dark ranging enabling insects to have robust vision throughout the day with a single opsin (Laughlin 1989; Honkanen et al. 2017).

Rapid adaptation mechanisms ensure photoreceptors to encode both contrast amplitudes in their transient responses and luminance in their sustained responses simultaneously (Laughlin et al. 1978; Normann et al. 1974; Normann et al. 1979; Laughlin 1989). Fly photoreceptors use a plethora of molecular mechanisms to extract and enhance contrast signals. Voltage-gated conductances mediated via potassium (K_v) and sodium channels (Na_v) form an important fraction of this (Weckström et al. 1995; Frolov et al. 2016). For example fast-flying fly species use a delayed K_v current in the photoreceptors that promotes the rapid repolarization of the membrane and prevents the sustained level to be saturated. In slower flies, a less energy demanding type of K_v conductance serves this purpose (Weckström et al. 1991; Weckström et al. 1995). Na_v conductances mainly facilitate the amplification of the contrast response (Weckström et al. 1995). The Arrestin molecule is essential for the inactivation of metarhodopsin, leading to the rapid termination of the response (Dolph et al. 1993; Katz et al. 2009).The inhibitory feedback provided by the calcium ions entering after the transduction cascade also contributes to the rapid loss of depolarization. Phospolipase C mediated pathways are also involved in the response termination of the photoreceptors (Katz et al. 2009). Accordingly, PLC mutants have slower response dynamics (Cook et al. 2000).

Circuit mechanisms add to the diverse molecular mechanisms of contrast encoding in photoreceptors. For example *Drosophila* amacrine-like cells take input from photoreceptors and form feedback synapses back onto them (Meinertzhagen et al. 2001; Rivera-Alba et al. 2011, Figure 2.2E)). These feedback synapses mediate a negative feedback loop controlling the speed and amplitude of the photoreceptor contrast response (Zheng et al. 2006).

Similar to the fly photoreceptors, vertebrate photoreceptors use a plethora of molecular mechanisms to extract and enhance contrast signals. The transduction cascade allows amplification of signals and similar rapid adaptation mechanisms use members of the transduction cascade, Ca^{2+} dependent mechanisms and the arrestin molecule (Pugh et al. 1999; Burns et al. 2001). Circuit mechanisms are also involved, including horizontal cell feedback that provides a fast mechanism to shape contrast sensitive transient responses (Demb et al. 2015). One major mechanism underlying this feedback is GABAergic inhibition from horizontal cells to cones (Wu 1992).

The photoreceptor signals undergo numerous spatiotemporal transformations in the second- and third-order visual neurons leading to differential luminance and contrast sensitivities in both vertebrates and invertebrates. Fly photoreceptors feed into three major LMC types, L1, L2 and L3, in the first neuropile of the visual system (Figure 2.2E). Photoreceptors use histamine as their neurotransmitter (Hardie 1989) which binds to the histamine-gated chloride channels and leads to the hyperpolarization of LMCs (Gengs et al. 2002). Thus, all of the second-order visual neurons of the fly respond in an inverted fashion than the upstream photoreceptors. Signal amplification occurs in the array of 1200 high-gain chemical synapses (Laughlin 1989), which then leads to around 6.5 times signal amplification (Laughlin et al. 1987). Furthermore, in some LMCs, the luminance components are altered or removed, for example in the L1 and L2-type LMCs (Laughlin et al. 1987). These LMCs are characterized by their transient responses and their biphasic filters which also represent their signal transformation (Reiff et al. 2010; Clark et al. 2011; Fisher et al.

2015. Lateral-inhibition, possibly mediated by the horizontally projecting amacrine cells, provides a basis for this removal (Laughlin et al. 1989; Freifeld et al. 2013; Wu et al. 2021). Another distinct LMC type, the L3 neuron, exhibits sustained responses and a monophasic linear filter (Silies et al. 2013; Silies et al. 2013). However, the biophysical properties shaping the responses distinct type of LMCs are widely unexplored.

LMCs project to distinct layers of the medulla and make contacts with the columnar medulla neurons that further transform LMC signals in spatial and temporal domains (Figure 2.2E). Medulla neurons exhibit distinct spatiotemporal properties and the medulla is the first processing layer where contrast polarity selectivity (ON and OFF pathways) is established (Strother et al. 2014; Ammer et al. 2015; Fisher et al. 2015; Serbe et al. 2016). Medulla contains different types of distal medulla (Dm) neurons that span horizontally and possibly further refine contrast signals (Nern et al. 2015). One of the main outputs of the medulla neurons are the first direction-selective cells T4 and T5 neurons which mediate the motion behavior of the fly (Maisak et al. 2013). Different populations of T4 and T5 cells encode optic flow patterns (Henning et al. 2022) and give inputs to optic flow sensitive wide-field lobula plate tangential cells (LPTC) which send their signals to the central brain of the fly (Krapp et al. 1998; Krapp et al. 1996) (Figure 2.2E).

Vertebrate first-order visual neurons, the BPCs, also exhibit diverse spatial and temporal properties (Euler et al. 2014) (Figure 2.2D). This diversity also leads to differential encoding of contrast and luminance signals. Several mechanisms in the photoreceptor-BPC synapse contribute to their temporal specializations such as expression of different glutamate receptors like AMPA or kainate (DeVries 2000), vesicle depletion and calcium channel inactivation (Jarsky et al. 2011; Oesch et al. 2011). Furthermore differential expression of calcium and sodium channels shape BPC membrane properties (Hu et al. 2009; Cui et al. 2008) adding to the plethora of mechanisms shaping temporal filtering of contrast and luminance signals. In contrast to the fly, contrast polarity specific processing is already achieved in the first-order neurons of the vertebrates (Figure 2.2D). The outputs of the BPCs are integrated in a weighted fashion in the RGC dendrites before reaching the brain (Figure 2.2D). The mouse retina has more than 40 types of RGCs which encode distinct features of the visual field, from simple contrast signals to orientation and motion (Baden et al. 2016; Bae et al. 2018; Tran et al. 2019). Molecular mechanisms mediated by AMPA and NMDA receptors play roles in shaping the temporal properties of RGCs (Crook et al. 2014).

Horizontal processing is also important for shaping BPC-RGC transmission (Figure 2.2D). Narrow-field glycinergic amacrine cells fine tune local glutamatergic inputs and GABAergic wide-field amacrine cells contribute to the surround generation (Zhang et al. 2012). A specific type of amacrine cell, the starburst amacrine cell, is direction selective and also forms the basis of direction selectivity in the RGCs (Vaney et al. 2012; Vlasits et al. 2014).

2.2.3 Stable contrast estimation: a challenge that spans different temporal and spatial scales

Visual systems face two major challenges arising from the width in the range of visual inputs. The first major problem arises because the neurons have limited dynamic range for encoding inputs. Natural signals highly exceed the dynamic range of light sensitive neurons which can go up to only 1-2 orders of magnitude (Normann et al. 1979; Schnapf et al. 1990; Choi et al. 2005). Thus, encoding the natural signals requires adaptation mechanisms that shift neural operating ranges. These shifts in operating ranges should preserve the representations of contrast. The representations of contrast will be highly variable if the neurons were sensitive to absolute differences in reflected luminance levels. This

is because the difference of luminance levels between a given object and a background depends on mean luminance levels. In brighter contexts this absolute difference will be much higher than in darker contexts. Thus, to achieve a stable representation, visual systems require computations of contrast relative to luminance levels.

Both invertebrate and vertebrate photoreceptors can estimate contrast relative to the luminance changes occurring throughout the day (Figure 2.3). The operating ranges of photoreceptors shift according to the mean background luminance, leading to a contrast representation following Weber's law (Normann et al. 1974; Laughlin et al. 1978; Burkhardt 1994). The shifts in the operating ranges represent luminance-dependent gain changes in the photoreceptors. This luminance gain reduces when the luminance levels increase (Shapley et al. 1984) (Figure 2.3).

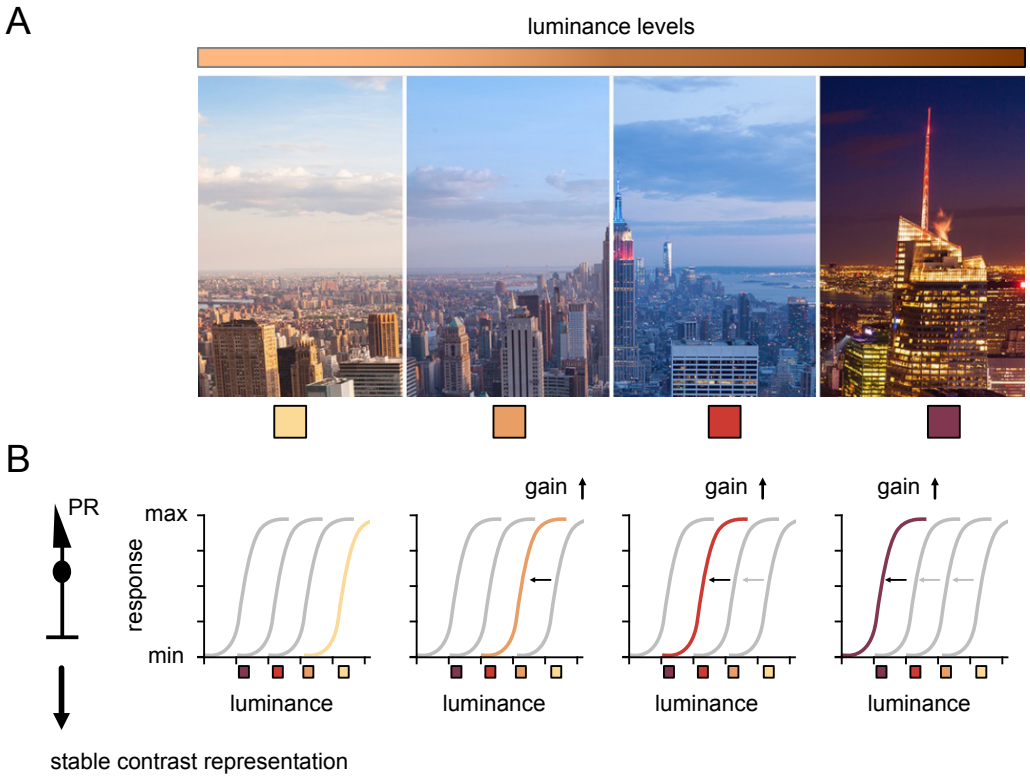

Figure 2.3: Photoreceptor adaptation provides stable vision throughout the day. **(A)** Natural scene luminance levels change up to 10 orders of magnitude throughout the day. (image from Kroll 2014) **(B)** Photoreceptor adaptation leads to changes of gain in the photoreceptor response and adjusts the PR operating curves accordingly to ensure stable contrast representations throughout the day (adapted from Carandini et al. 2011).

The luminance gain in photoreceptors originate from a plethora of mechanisms that have multiple timescales (Pugh et al. 1999; Burns et al. 2001; Fain et al. 2001; Katz et al. 2009). Molecular adaptation mechanisms decrease the gain of photoreceptors through the reduction of the amplification in the transduction cascade. In fly photoreceptors, for example, this leads to a decrease in the number of channels activated by a single rhodopsin isomerization (Laughlin 1989). A key player in both vertebrate and invertebrates are the calcium-dependent mechanisms (Fain et al. 2001; Katz et al. 2009). These lead to the inhibition of TRP channels in invertebrates, regulation of second messenger pathways, and inactivation of metarhodopsin (Gu et al. 2005; Liu et al. 2008). Another important mechanism is the relocation of TRP-like channels to the cell body upon calcium entry (Katz et al. 2009). This process works at two temporal scales, a fast one is completed within around 5 minutes and the slower one lasts over 6 hours (Cronin et al. 2006). Arrestin

protein inactivates opsins in bright daylight, both in vertebrates and invertebrates (Katz et al. 2009; Burns et al. 2001). Additionally, other voltage-dependent conductances such as K_v based conductances also shape insect photoreceptor adaptation during the day via changing membrane properties (Weckström et al. 1991; Cuttle et al. 1995; Weckström et al. 1995; Juusola et al. 2001; Frolov et al. 2016). The combination of these mechanisms with multiple timescales make photoreceptors sensitive to a considerable history of visual inputs that can range from milliseconds to hours. Even though these adaptations enable vision throughout the slow and astronomical changes in the luminance levels, they are not sufficient for precise correction of rapid changes occurring within the natural scenes.

Many mammals perform rapid eye movements, saccades, leading to substantial changes in local luminance and contrast statistics at around 200-300ms (Binda et al. 2018; Frazor et al. 2006, Figure 2.4A). Similarly, many fly species perform sharp turns (body saccades) to explore their environment or during a prey-predator chase (Wehrhahn et al. 1982; Tammero et al. 2002; Geurten et al. 2014). Accordingly, different types of experiments showed that visual systems are able to handle these changes and achieve a stable representations of contrast. Humans can perceive the amplitudes of contrasts in changing luminances correctly (Burkhardt et al. 1984) and accurate contrast perception can be achieved rapidly, around 300 ms, matching the speed of eye saccades (Kilpeläinen et al. 2011). Stable contrast representations are also achieved rapidly in the cat brain, where neurons in the visual cortex (MacEvoy et al. 2001), the LGN (Mante et al. 2005) and also the cat Y RGCs respond in a luminance invariant manner (Shapley et al. 1984). This suggests a post-receptor luminance gain that is implemented in the visual system, post-synaptic to photoreceptors (Figure 2.4C).

Post-receptor gain mechanisms were already described in the retina acting in dim light conditions. In this range, even though photoreceptor sensitivities were unaltered, RGCs changed their contrast representations (Green et al. 1975; Green et al. 1982). A similar dim light dependent post-receptor mechanism is also found in the primate retina which occurred in signal transfer from cone BPCs to RGCs (Dunn et al. 2007). However these adaptation mechanisms also acted on a longer time course which makes it unlikely to explain the stable contrast representations achieved in rapid luminance changes (Green et al. 1975; Green et al. 1982). Thus, the rapid luminance gain mechanism that ensures vision within natural scenes is unknown.

In Ketkar*, Sporar*, **Gür** et al 2020 (not included in this thesis), we showed that fly OFF behavior is luminance invariant in rapidly changing conditions, similar to human behavior (Burkhardt et al. 1984; Ketkar et al. 2020). Fly behavioral responses to OFF contrast stimuli depend on the interactions of LMCs in the lamina. A specific type of LMCs, L3 neurons, encode luminance and are the source of a rapid luminance gain that enables fly behavior to be luminance-invariant. This reveals a crucial role for retaining luminance signals past photoreceptors. However where this luminance gain is implemented in the neuronal level and how L3 neuron luminance information leads to luminance gain in the visual circuitry is unknown.

For a rapid luminance gain mechanism to work, local luminance levels have to be accurately and rapidly estimated. However rapid estimations can be sensitive to noise levels since time-averaging will be minimal. Thus spatial pooling at a post-receptor site could be used as a noise reduction mechanism in implementing gain (Dunn et al. 2007). However, luminance correlations in natural scenes fall rapidly with the distance indicating a problem of estimating luminances over large spatial extends (Frazor et al. 2006). The optimal spatial extent of luminance that can provide both reliable (rapid but noise free) and accurate (representative for the relevant contrast computations) is also not known.

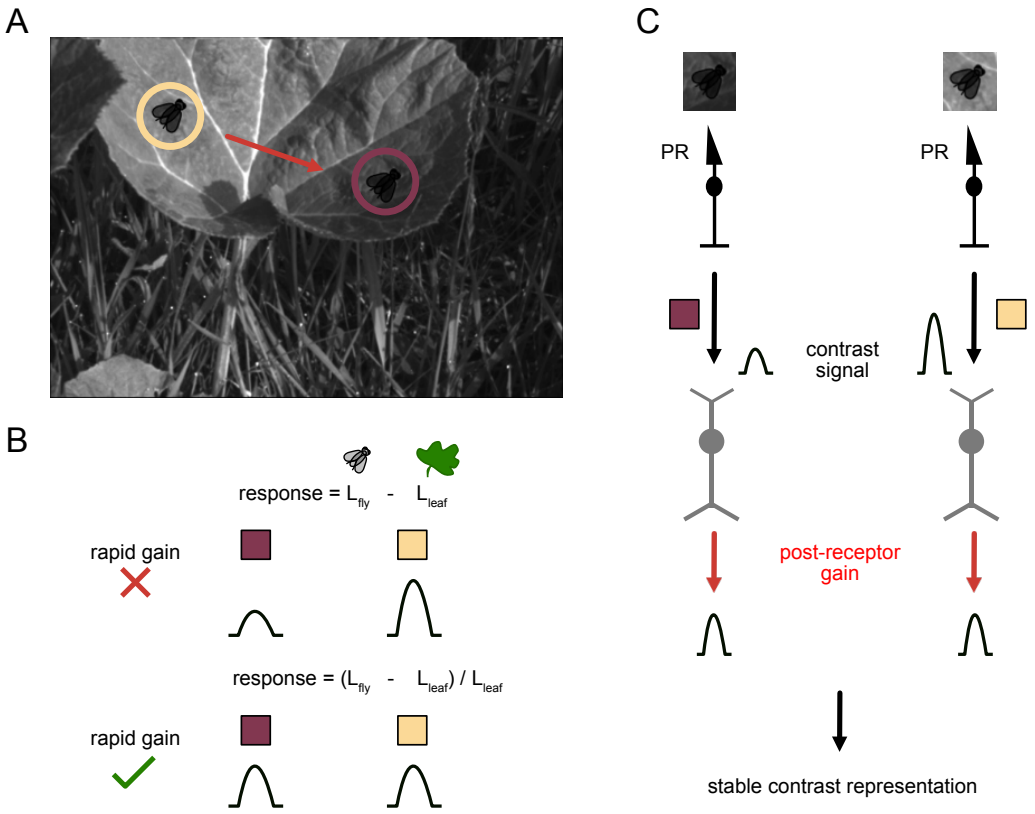

Figure 2.4: Rapid post-receptor gain mechanisms are required for stable visual processing. **(A)** Luminance levels can change up to three orders of magnitude within natural scenes upon eye (vertebrates) or body (invertebrates) saccades. In the example, the RF of a photoreceptor switches its location from a high luminance (bright circle) to a low luminance (dark circle) (natural image from Hateren 1997) **(B)** Within this switch not accounting for the novel background luminance leads to a luminance dependent contrast signal that in turn leads to different representations of the same object on the same background (fly on a leaf). Keeping contrast representations stable can be achieved by a rapid luminance gain mechanism that account for the local luminance changes. **(C)** Incomplete photoreceptor adaptation leads to unstable contrast estimations in rapidly changing luminances. A post-receptor gain mechanism can correct the contrast representations coming from the photoreceptors.

2.2.4 Polarity of contrast signals: ON and OFF pathways in visual circuits

One hallmark of visual systems is the parallel processing of contrast polarity (Figure 2.2D, E). Pathway splitting improves the efficiency of the neural code by reducing metabolic costs, preserving sensitivity to both contrast polarities and for rapid information processing (Schiller et al. 1986; Gjorgjieva et al. 2014). In vertebrates, processing of contrast decrements (OFF) and contrast increments (ON) are split one synapse downstream of the photoreceptors in distinct BPC types (Euler et al. 2014). ON BPCs utilize the metabotropic glutamate receptors to invert the OFF photoreceptor inputs and OFF BPCs preserve the photoreceptor sign using ionotropic glutamate receptors (Demb et al. 2015). In the fly, this split is thought to happen at the LMC level based on behavioral experiments (Joesch et al. 2010) but only at the third-order medulla neurons ON and OFF neurons exist in parallel (Yang et al. 2018). The LMC OFF signals are inverted by a glutamate-gated chloride channel as well as GABAergic mechanisms in the ON pathway medulla neurons (Molina-Obando et al. 2019). In both taxa, the same visual features are processed in ON and OFF parallel channels (Maisak et al. 2013; Baden et al. 2016). This highlights the importance of stable contrast processing and thus the rapid luminance gain for both channels. Accordingly, at the level of human perception, both ON and OFF contrasts are represented stably in rapidly changing conditions (Burkhardt et al. 1984). In flies, the neural signa-

tures of OFF luminance-invariance has been revealed but ON luminance-invariance is still unexplored.

In the fly visual system, L1 neurons are thought to be the sole inputs to the ON pathway whereas OFF pathway receive inputs from L2 and L3 neurons (Joesch et al. 2010; Clark et al. 2011; Shinomiya et al. 2019a). The OFF luminance-invariant behavior depends on the luminance sensitive L3 neurons (Ketkar et al. 2020) but the counterpart of a luminance sensitive neuron is not known for the ON pathway since L1 neurons are reported to have identical characteristics as L2 neurons (Clark et al. 2011).

Natural scenes contain ON and OFF asymmetries in image structure (Ruderman et al. 1994). ON and OFF pathways are not simple flipped versions of each other but implement some computations asymmetrically, for example in motion processing (Leonhardt et al. 2016; Ravi et al. 2018). Thus, luminance gain mechanisms can also differ between ON and OFF pathways especially considering the differences in ON and OFF contrast distributions (Ruderman et al. 1994).

2.2.5 Aims and structure of this thesis

Contrast processing depends on distinct feature-selective cell types that can filter visual information to aid achieving stable contrast representations. A rapid luminance gain, implemented post photoreceptors is required for stable contrast representations in fast luminance changes like the ones happen in natural scene viewing. In the first three studies of this thesis, I investigate the cell types involved in stable contrast processing. Using the *Drosophila* genetic tools, I aimed to identify the cell types, characterise their contrast-encoding properties, and causally link their feature selectivity to molecular mechanisms. In the last study, I aimed to develop a genetic tool that enables manipulations down to specific synapses between defined partners.

Fly OFF behavior is luminance-invariant in rapidly changing conditions (Ketkar et al. 2020). Interactions between LMCs having distinct feature encoding is required for this behavior, showing a necessity of a post-receptor gain mechanism. In the first study of this thesis, me and my colleagues investigated how stable contrast processing in both ON and OFF pathways benefits from the distinct feature encoding of LMCs. Using genetically encoded calcium indicators and two-photon imaging we described the feature encoding properties of L1, L2 and L3 LMCs and revealed that they segregate distinct contrast and luminance information to both ON and OFF pathways. Using genetic silencing experiments, we showed that L1 and L3 LMCs ensure the post-receptor gain for both ON and OFF pathways, causally linking cell-type function to behavior. Furthermore, our findings corrected the view that LMCs provide inputs to only either to ON or OFF pathway by showing that the genetic silencing of LMCs affect behavior for both ON and OFF contrasts.

In the second study I asked how diversity in feature selectivity in LMCs arise. Since biophysical properties are crucial for neural signal processing, based on RNA-seq data I identified molecular candidates that shape L2 contrast encoding. I then localised these candidates using endogenous protein tagging approaches and found potassium channels that are distinctly expressed by L2 neurons. I targeted these channels using pharmacology and cell-type specific manipulations to reveal cell-type specific and circuit wide requirements of potassium channels in shaping L2 contrast selectivity.

In my third study, I dissected the circuits that implement the rapid luminance gain in the OFF pathway. First I showed that none of the LMCs have stable contrast representations in rapidly changing luminances. In contrast to LMCs, the direction sensitive cells in the OFF pathway had luminance-invariant motion responses in rapidly changing luminances,

highlighting a post-LMC luminance gain implemented before the emergence of direction selectivity. I then characterised the contrast-encoding properties of medulla OFF neurons and revealed that the rapid luminance gain first arises in two specific types of medulla neurons, Tm1 and Tm9. This luminance gain also generalises to different contrasts. I also showed that Tm1 and Tm9 neurons have distinct luminance gain properties forming two parallel channels that aid downstream contrast processing. Spatial pooling mediated via the circuitry is required for the luminance gain in both Tm1 and Tm9 neurons. Both neurons receive wide-field glutamatergic signals along with their main inputs which are cholinergic. Tm9 neurons use the glutamate gated chloride channel GluClα to achieve their luminance gain properties but Tm1 does not indicating distinct mechanisms underlying these parallel channels. Interestingly, two of the other major OFF pathway Tm neurons, Tm2 and Tm4, display luminance-dependent contrast representations highlighting the importance of parallel pathways for optimal contrast processing.

Besides showing the computational principles underlying contrast processing, our studies added to the numerous evidence that neural circuits are inter-woven, where cell-types diverge into distinct processing streams. For example, all LMCs give input to both distinct ON and OFF pathways or luminance and contrast information coming from distinct cell-types is integrated on the medulla neuron dendrites. Achieving the detailed causal underpinnings of such circuit motifs is instrumental for our understanding of neural circuit function. The current resolution of genetic manipulations which can go down to the specific cell-type level is not sufficient because specific connections between defined cell-types can contribute differentially to downstream information processing. In the fourth study I developed a novel genetic tool, called Synapse Targeted Activity Block (STAB), that aims to manipulate neural activity at synaptic resolution. This approach is based on protease-mediated cleavage of important synaptic proteins to achieve silencing of specific synapses. We characterised and optimised the tool components *in vitro* and *in vivo* and validated them. Fly genetic toolbox provided us with the necessary basis to develop our genetic tool. In its current status, STAB achieves cleavage of important synaptic proteins but requires further validations to be used in manipulating synaptic partners and revealing their functional role for information processing.

3 | Manuscript 1: First-order visual interneurons distribute distinct contrast and luminance information across ON and OFF pathways to achieve stable behavior

This manuscript is published as a research article in *eLife* and is available under DOI: https://doi.org/10.7554/eLife.74937

Authors and affiliations

Madhura D Ketkar[1,2,*], **Burak Gür**[1,2,*], Sebastian Molina Obando[1,2,*] , Maria Ioannidou[1], Carlotta Martelli[1], Marion Silies[1,X]

1 - Institute of Developmental Biology and Neurobiology, Johannes-Gutenberg University Mainz, Mainz, Germany

2 - Göttingen Graduate School for Neurosciences, Biophysics, and Molecular Biosciences (GGNB) and International Max Planck Research School (IMPRS) for Neurosciences at the University of Göttingen, Göttingen, Germany

* - These authors contributed equally.

X - For correspondence: msilies@uni-mainz.de

Contribution statement

Marion Silies, Madhura D Ketkar, Sebastian Molina-Obando and I designed and planned the study. I performed the imaging experiments and analyzed the imaging data. Madhura D Ketkar performed and analyzed most of the behavioral experiments with help from Sebastian Molina-Obando and Maria Ioannidou. The original draft was mainly written by Marion Silies, Sebastian Molina-Obando and Madhura D Ketkar. I reviewed and edited the manuscript together with Marion Silies, Sebastian Molina-Obando and Madhura D Ketkar.

RESEARCH ARTICLE

First-order visual interneurons distribute distinct contrast and luminance information across ON and OFF pathways to achieve stable behavior

Madhura D Ketkar[1,2†], Burak Gür[1,2†], Sebastian Molina-Obando[1,2†], Maria Ioannidou[1], Carlotta Martelli[1], Marion Silies[1]*

[1]Institute of Developmental Biology and Neurobiology, Johannes-Gutenberg University Mainz, Mainz, Germany; [2]Göttingen Graduate School for Neurosciences, Biophysics, and Molecular Biosciences (GGNB) and International Max Planck Research School (IMPRS) for Neurosciences at the University of Göttingen, Göttingen, Germany

Abstract The accurate processing of contrast is the basis for all visually guided behaviors. Visual scenes with rapidly changing illumination challenge contrast computation because photoreceptor adaptation is not fast enough to compensate for such changes. Yet, human perception of contrast is stable even when the visual environment is quickly changing, suggesting rapid post receptor luminance gain control. Similarly, in the fruit fly *Drosophila*, such gain control leads to luminance invariant behavior for moving OFF stimuli. Here, we show that behavioral responses to moving ON stimuli also utilize a luminance gain, and that ON-motion guided behavior depends on inputs from three first-order interneurons L1, L2, and L3. Each of these neurons encodes contrast and luminance differently and distributes information asymmetrically across both ON and OFF contrast-selective pathways. Behavioral responses to both ON and OFF stimuli rely on a luminance-based correction provided by L1 and L3, wherein L1 supports contrast computation linearly, and L3 non-linearly amplifies dim stimuli. Therefore, L1, L2, and L3 are not specific inputs to ON and OFF pathways but the lamina serves as a separate processing layer that distributes distinct luminance and contrast information across ON and OFF pathways to support behavior in varying conditions.

Editor's evaluation

This paper combines silencing and rescue experiments with measurements of cellular responses and behavior to investigate how three early visual neurons in the fly eye encode both scene luminance and scene contrast. It reveals that these neurons carry different information about scene luminance and contrast that gets distributed to ON and OFF selective pathways that guide behavior.

***For correspondence:** msilies@uni-mainz.de

†These authors contributed equally to this work

Competing interest: The authors declare that no competing interests exist.

Funding: See page 20

Received: 22 October 2021
Preprinted: 05 November 2021
Accepted: 03 March 2022
Published: 09 March 2022

Reviewing Editor: Damon A Clark, Yale University, United States

Introduction

Across species, contrast information forms the basis of visual computations. Contrast is the relative change in luminance, which can be computed across space or across time. For our perception to be stable, our eyes must compute contrast relative to the mean illumination of a scene. In natural environments, illumination changes by several orders of magnitude not only from dawn to dusk, but also at much faster timescales as our eyes saccade across a scene or we quickly move from sun to shade (***Frazor and Geisler, 2006***; ***Mante et al., 2005***; ***Rieke and Rudd, 2009***). Thus, the computation

of contrast needs to be invariant to rapid changes in luminance, such that visual perception of a given contrast remains constant. Invariant responses to contrast are accomplished by human perception, even when background luminance quickly changes (**Burkhardt et al., 1984**). At the circuit level, neuronal responses in the cat lateral geniculate nucleus (LGN) display luminance-invariant responses at rapid time scales (**Burkhardt et al., 1984**; **Mante et al., 2005**). Thus, robust contrast computation at rapid time scales appears to be a wide-spread phenomenon across visual systems. However, contrast encoding in photoreceptors is not luminance invariant when the stimulus changes more rapidly than photoreceptor adaptation (**Laughlin and Hardie, 1978**; **Normann and Werblin, 1974**), arguing for a common post-receptor corrective mechanism.

In most visual systems, information is split into two separate ON and OFF pathways, that process contrast increments (ON) or contrast decrements (OFF), respectively (**Behnia et al., 2014**; **Franceschini et al., 1989**; **Silies et al., 2014**; **Yang and Clandinin, 2018**). The visual OFF pathway in fruit flies drives luminance-invariant behavior (**Ketkar et al., 2020**). In the OFF pathway, luminance information itself is maintained postsynaptic to photoreceptors, and is crucial for the accurate estimation of temporal contrast, resulting in luminance-invariant behavior. Luminance serves as a corrective signal, leading to a luminance gain that adjusts temporal contrast computation when background luminance quickly changes (**Ketkar et al., 2020**). The requirement of such a corrective signal can be theoretically expected regardless of ON and OFF contrast polarities, since the adaptational constraints in dynamic environments challenge both contrast polarities. However, the ON and OFF pathways are not mere sign-inverted versions of each other since they face different environmental challenges (**Clark et al., 2014**; **Ruderman and Bialek, 1994**) and have evolved several structural and physiological asymmetries (**Chichilnisky and Kalmar, 2002**; **Jin et al., 2011**; **Leonhardt et al., 2016**; **Ratliff et al., 2010**). It is thus not clear if this luminance invariance is a general feature of both ON and OFF pathways, and how luminance and contrast information are distributed across visual pathways to establish luminance invariance.

The *Drosophila* visual system is composed of a columnar arrangement of 800 repeating units, carrying the same set of columnar neurons, together forming a retinotopic map. Different columnar neuronal cell types were assigned to distinct ON or OFF pathways based on physiological properties (**Molina-Obando et al., 2019**; **Serbe et al., 2016**; **Shinomiya et al., 2019**; **Silies et al., 2013**; **Strother et al., 2017**), anatomical connectivity (**Shinomiya et al., 2014**; **Takemura et al., 2015**; **Takemura et al., 2013**; **Takemura et al., 2017**), and behavioral function (**Clark et al., 2011**; **Silies et al., 2013**). ON and OFF contrast selectivity first arises two synapses downstream of photoreceptors, in medulla neurons (**Fischbach and Dittrich, 1989**; **Serbe et al., 2016**; **Silies et al., 2013**; **Strother et al., 2017**; **Yang et al., 2016**). In each visual column, these medulla neurons receive photoreceptor information through the lamina neurons L1-L3, together referred to as large monopolar cells (LMCs). LMCs project to specific medulla layers (**Meinertzhagen and O'Neil, 1991**; **Strother et al., 2014**). Although all LMCs show the same response polarity and hyperpolarize to light onset and depolarize to light offset, L1 projects to layers where it mostly connects to ON-selective medulla neurons. Similarly, L2 and L3 project to layers where OFF-selective medulla neurons get most of their inputs (**Shinomiya et al., 2014**; **Takemura et al., 2015**; **Takemura et al., 2013**). L1 is thus thought to be the sole major input of the ON pathway, whereas L2 and L3 are considered the two major inputs of the OFF pathway (**Figure 1A**; **Clark et al., 2011**; **Joesch et al., 2010**; **Shinomiya et al., 2019**). Among these, L2 is contrast sensitive, but cannot support luminance invariance alone when photoreceptor adaptation is insufficient. Instead, the stable computation of contrast at changing background luminance in OFF-motion guided behavior (OFF behavior) is ensured by a corrective signal from luminance-sensitive L3 neurons (**Ketkar et al., 2020**). It is not known whether ON-motion-driven behavior (ON behavior) also requires a post-receptor luminance gain and whether L1 can provide it along with its contrast signal (**Figure 1B**).

Contrast and luminance are encoded by the transient and sustained response components in both vertebrates and invertebrate photoreceptors, respectively (**Laughlin and Hardie, 1978**; **Normann and Perlman, 1979**; **Normann and Werblin, 1974**; **Shapley and Enroth-Cugell, 1984**), which are captured differentially by their downstream neurons. In the vertebrate retina, many different types of first order interneurons, bipolar cells, exist. Although they are generally thought to capture the contrast component of the photoreceptor response, luminance information has been shown to be preserved in visual circuitry postsynaptic to photoreceptors (**Awatramani and Slaughter, 2000**; **Ichinose and Hellmer,**

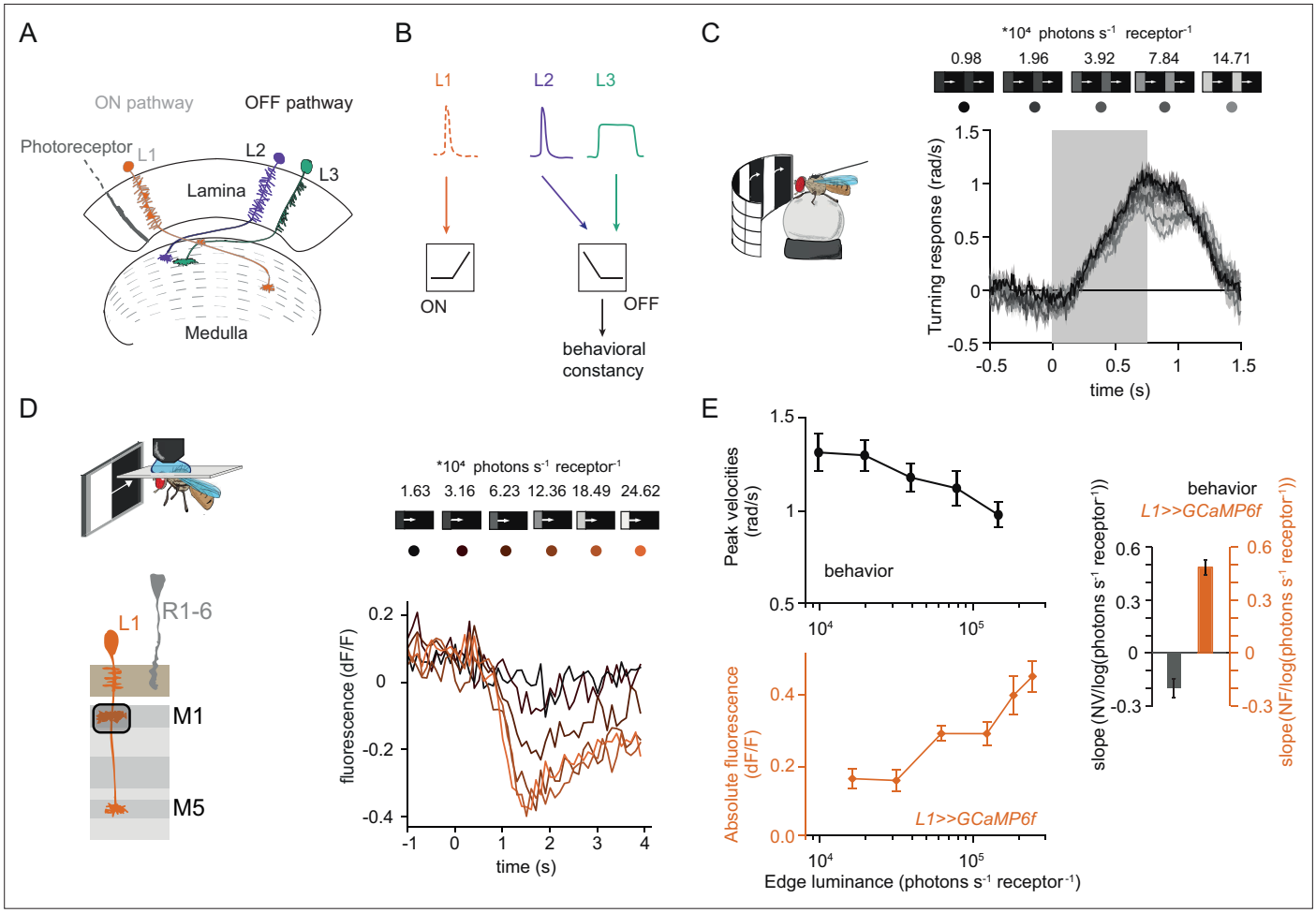

Figure 1. Fly behavioral responses to ON contrast do not co-vary with L1 responses. (**A**) Schematic of lamina neurons projecting from the lamina to the medulla. L1 is considered the main input to the ON-pathway, whereas L2 and L3 are thought to provide input to the OFF pathway. (**B**) Transient L2 and sustained L3 neurons provide contrast and luminance information, respectively, to the OFF pathway to guide contrast-constant behavior (***Ketkar et al., 2020***). L1 is thought to have physiological properties very similar to L2 (***Clark et al., 2011***) and provides contrast information to the ON selective pathway. (**C**) Turning response to multiple moving ON edges, moving at 160°/s, displayed on an LED arena that surrounds a fly walking on an air-cushioned ball. The edge luminance takes five different values, and the background is dark (~0 luminance), all resulting in 100% contrast. Turning responses are color-coded according to the edge luminance. The gray box indicates motion duration. n = 10 flies. (**D**) In vivo calcium signals of L1 axon terminal in medulla layer M1 in response to moving ON edges of six different luminances. Calcium responses of single L1 axon terminal are shown. (**E**) Top: peak turning velocities calculated from (**C**), bottom: absolute step responses of L1. Sample size for L1: n = 6 (15) flies(cells). Right: slope quantification of luminance dependency for normalized behavior and L1 fluorescence signals. NV = normalized peak velocity, NF = normalized fluorescent signal. Traces and plots in C and E show mean ± SEM.

2016; ***Ichinose and Lukasiewicz, 2007***; ***Odermatt et al., 2012***; ***Oesch and Diamond, 2011***). As suggested by their sustained response component, different degrees of luminance-sensitivity exist across bipolar cell types (***Baden et al., 2016***; ***Euler et al., 2014***). Furthermore, ON and OFF contrast selectivity emerges at the bipolar cell layer, where ON selectivity emerges through glutamatergic inhibition (***Masu et al., 1995***). These ON and OFF bipolar cells also split anatomically, as they innervate different layers (***Euler et al., 2014***).

Together, many parallels exist between the *Drosophila* visual system and the vertebrate retina, including the response properties of photoreceptors, the layered organization and the existence of ON and OFF pathways (***Clark and Demb, 2016***; ***Mauss et al., 2017***). However, in contrast to the vertebrate retina, fewer first-order interneuron types distribute contrast and luminance information, and contrast selectivity itself only occurs one synapse further downstream, where neurons postsynaptic to lamina neurons are either ON or OFF selective. Comparing the vertebrate retina with the

insect visual system, it is unclear how just three first-order interneurons distribute their different physiological properties across visual pathways.

Here, we show that luminance and contrast information are distributed to and are of behavioral relevance for both ON and OFF pathways. In vivo calcium imaging experiments reveal that each first-order interneuron is unique in its contrast and luminance encoding properties. Although L2 is purely contrast sensitive, L1 encodes both contrast and luminance in distinct response components. L1 linearly scales with luminance, whereas the luminance-sensitive L3 non-linearly amplifies dim light. Behavioral experiments further show that these differential luminance- and contrast- encoding properties translate into distinct behavioral roles. In the ON pathway, L1 and L3 both provide a luminance gain that scales behavioral responses to contrast. Furthermore, L2, known as the OFF-pathway contrast input, provides contrast information to the ON-pathway, in addition to L1. Surprisingly, both L1 and L3 neurons are necessary and sufficient for OFF behavior. These findings indicate that L1, L2, and L3 do not constitute ON- or OFF-specific inputs. Instead, the three first-order interneurons encode luminance and contrast differentially and contribute to computations in both ON and OFF pathways. Together, our data reveal how luminance and contrast information are distributed to both ON and OFF pathways to achieve stable visual behavior.

Results

L1 responses to contrast do not explain ON behavior

Luminance-invariant visual responses have been observed in multiple species (***Burkhardt et al., 1984***; ***Mante et al., 2005***), highlighting their relevance. In *Drosophila*, luminance-invariant behavior has been shown in response to moving OFF edges, where a dedicated luminance-sensitive pathway scales contrast-sensitive inputs to achieve luminance invariance in behavior (***Ketkar et al., 2020***). The ON pathway is thought to have just one prominent input, L1. We thus asked if luminance-invariant behavior is achieved in the ON pathway and if this can be accounted for by the contrast-sensitive input L1. For this purpose, we first compared turning behavior of walking flies with the responses of L1. Behavioral responses were measured in a fly-on-a-ball assay. Flies were shown moving ON edges of different luminance but the same 100% Michelson contrast (C_M = (I_{edge}-$I_{background}$) / (I_{edge} +$I_{background}$), where C stands for contrast and I stands for luminance). Consecutive motion epochs were separated by a dark interstimulus interval. Fly turning responses were similar across luminances, with low-luminance edges eliciting slightly larger turning responses than brighter edges (***Figure 1C***).

We wondered if the sole known ON-pathway input L1 can directly drive this behavior. To test this, we examined the contrast responses of L1 to moving ON edges with comparable parameters and overlapping luminance values as those used in the behavioral assay (***Figure 1D***). We recorded L1 in vivo calcium responses to visual stimuli from its axon terminals expressing GCaMP6f using two-photon microscopy. As described previously, L1 responded negatively to contrast increments, in line with the inverted response polarity of lamina neurons (***Figure 1D***; ***Clark et al., 2011***; ***Laughlin and Hardie, 1978***; ***Yang et al., 2016***). The absolute response amplitude of the L1 calcium signals scaled with luminance, showing smaller response in low as compared to high luminances, and did not co-vary with the behavioral response (***Figure 1E***). To extract the luminance dependency of the response, we performed linear regression across calcium signals at different luminances and quantified the slope. L1 signals and behavioral responses had opposite luminance dependencies (***Figure 1E***). Thus, the observed behavior cannot be explained solely by contrast inputs from L1, suggesting that the ON pathway additionally gets a luminance-sensitive input.

L1 neuronal responses carry a luminance-sensitive component

To explore the source of luminance information in first-order interneurons, we measured calcium signals in L1, L2, and L3. Flies were shown a staircase stimulus with luminance going sequentially up and down. L1 and L2 showed transient negative responses when luminance stepped up, and transient-positive responses when luminance stepped down (***Figure 2A***), consistent with the contrast sensitivity described for L1 and L2 (***Clark et al., 2011***; ***Silies et al., 2013***). L2 did not show any sustained component. L3 showed sustained responses to OFF steps and was non-linearly tuned to stimulus luminance, responding strongly to the darkest stimulus. Intriguingly, L1 showed a transient component followed by a sustained component, suggesting that it encodes luminance in addition to contrast (***Figure 2A***).

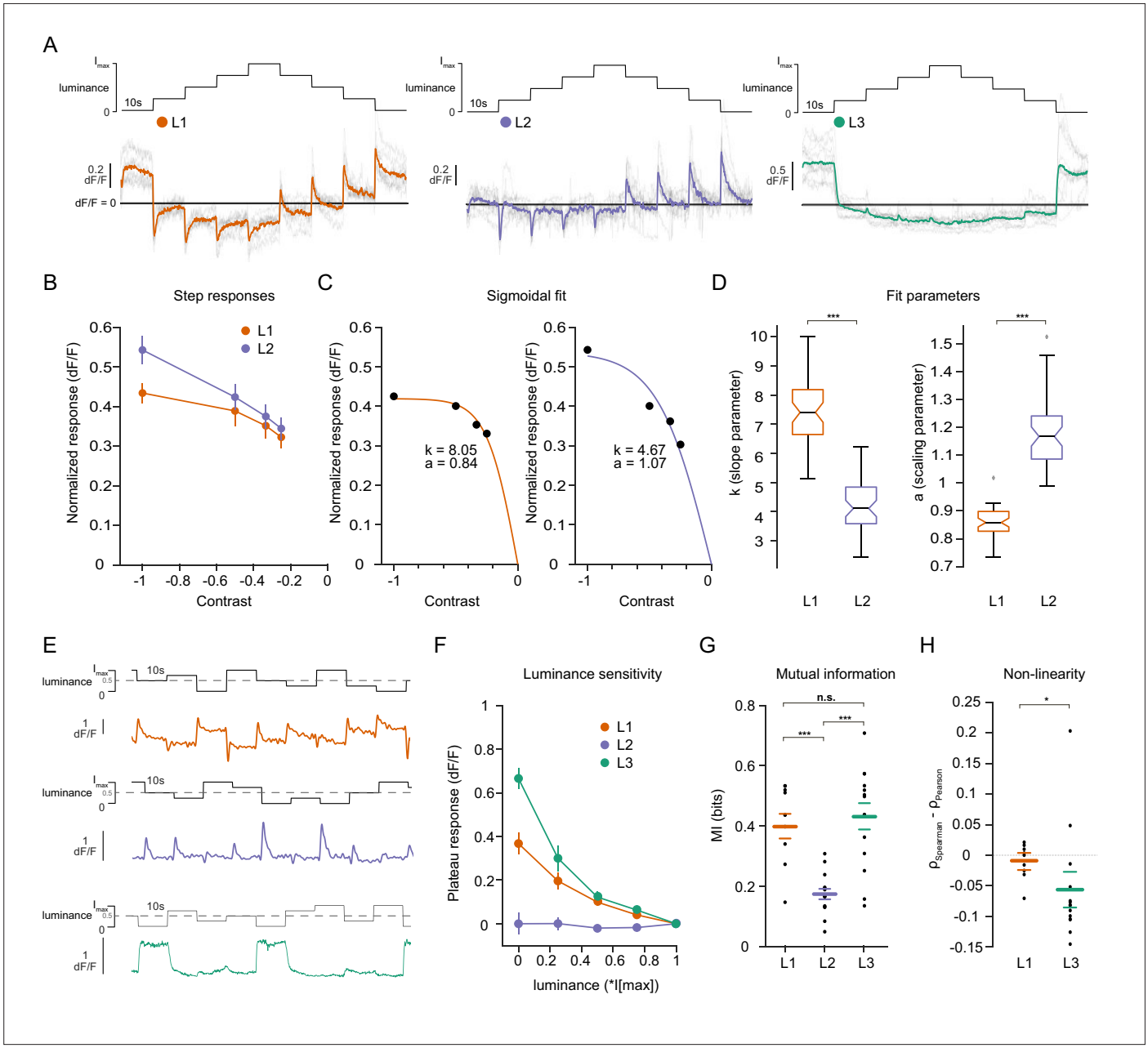

Figure 2. Lamina neuron types L1-L3 are differently sensitive to contrast and luminance. (**A**) Schematic of the 'staircase' stimulus, I_{max} = 2.17 × 10^5 photons s^{-1} $photoreceptor^{-1}$. Luminance sequentially steps up through five values and then sequentially steps down. Shown below are the calcium responses of L1 (orange), L2 (purple), and L3 (green) axon terminals. Colored traces show the mean response, grey traces show individual fly means. (**B**) Normalized step responses of L1 and L2 neurons to OFF contrasts of the staircase stimulus. (**C**) Individual bootstrapping examples of sigmoidal fits where k is the slope parameter and a is the scaling parameter. (**D**) Comparison of fit parameters between L1 and L2, Student t-test, ***p < 0.001 (**E**) Example calcium traces of single L1, L2, and L3 axon terminals to a stimulus comprising 10 s full-field flashes varying randomly between five different luminances. (**F**) Plateau responses of the three neuron types, quantified from the responses to the stimulus in (**E**). (**G**) Mutual information between luminance and calcium signal, ***p < 0.001, one-way ANOVA followed by multiple comparison test corrected with Bonferroni. (**H**) Non-linearity quantification of luminance-dependent signals of L1 and L3 in (**C**), *p < 0.05, tested by a wilcoxon rank sum test. Sample sizes for (**A and B**) L1: n = 8 (54), L2: n = 11(48), L3: n = 12(103), for (**D**) we used 50 times bootstrapping from the dataset in (**A**), and for (**E–H**) L1: n = 9 (71), L2: n = 14(74), L3: n = 14(88) flies(cells). Calcium traces show mean and quantification plots (**B, F, G, H**) show mean ± SEM. Boxplots in (**D**) show median, 25% and 75% percentiles and whiskers extend to the most extreme data points.

The online version of this article includes the following figure supplement(s) for figure 2:

Figure supplement 1. L1 has contrast and luminance-sensitive components.

The sustained components of L1 responses were negatively correlated with luminance, such that the baseline calcium signal at each step sequentially increased with decreasing stimulus luminance. We next used a stimulus that allows to systematically tease apart the contrast and luminance sensitivities of neurons (***Ketkar et al., 2020***; ***Oesch and Diamond, 2011***, ***Figure 2—figure supplement 1A***). Here, an adapting bright background was followed by two sequential OFF steps. The first step (A step) varied in its contrast and luminance values, whereas the second step (B step) always comprised 25% Weber contrast ($C_W = (I_B - I_A)/I_A$) but took on different luminance values. The transient peak responses of L1 neurons correlated positively with the A step contrast and were indistinguishable for the B steps. This suggests that L1, like L2, encodes contrast in its peak response (***Figure 2—figure supplement 1A, B***, tested with one-way ANOVA), (***Ketkar et al., 2020***). The sustained component of L1 responses negatively correlated with the luminance values of both A and B steps, indicating luminance encoding (***Figure 2—figure supplement 1A,C***). Together, L1 neurons encode contrast in their peak responses and luminance in their sustained responses.

We next explicitly compared contrast and luminance encoding between the input neurons. To look at the contrast encoding properties, we analyzed the step responses of L1 and L2 neurons to different OFF contrasts in the staircase stimulus (***Figure 2A and B***). Although L1 and L2 responded similarly to low-contrast stimuli, L2 responses tended to be higher for high contrasts (***Figure 2B***). We fitted sigmoidal contrast response functions (***Figure 2C***) and quantified contrast encoding properties in two ways: First, we used the slope parameter (k) of the sigmoid, indicating steepness of the contrast function, to analyze the encoding of different contrasts (see Materials and methods, ***Figure 2C and D***). Second, the scaling parameter (a) shows how much of the available response range is used to encode contrast (***Figure 2C and D***). L1 neuron contrast functions had steeper slopes and thus, L1 reached saturation at lower contrasts than L2, suggesting that L1 neurons encode contrasts with less resolution than L2 neurons do, especially in the high-contrast regimes. Furthermore, analysis of the scaling parameter revealed that L1 neurons dedicated less response range to encode contrast than L2 neurons (***Figure 2C and D***). These results show that L1 and L2 neurons have different contrast encoding properties, arguing that they might fulfill different roles in the circuitry. To look at luminance encoding properties, we measured responses to randomized luminance and calculated the mutual information between stimulus and the sustained response component (***Figure 2E–G***). As for the staircase stimulus, L2 transient responses returned to baseline within the 10 s of the stimulus presentation, whereas both L1 and L3 displayed sustained components that varied with luminance (***Figure 2E and F***). Sustained response components in L1 and L3 carried similar mutual information with luminance, and both were higher than L2 (***Figure 2G***). The luminance-sensitive response components of L1 and L3 scaled differently with luminance. We quantified non-linearity using the difference of Pearson's linear and Spearman's correlation between response and luminance. This value will approach zero if the relationship is linear and increase or decrease if non-linear, depending on the sign of correlation between luminance and response. L1 responses were more linear with respect to luminance than L3 responses, which selectively amplified low luminance (***Figure 2H***). Thus, the two luminance-sensitive neurons carry different types of luminance information.

L1 is not required but sufficient for ON behavior across luminances

Since the canonical ON-pathway input L1 is also found to carry luminance information, we hypothesized that it plays a role in mediating the observed behavior. To test this, we silenced L1 outputs while measuring ON behavior using Shibire^{ts} (***Kitamoto, 2001***). L1 silencing had little effect on responses to 100% contrast at varying luminance, suggesting the existence of other ON-pathway inputs (***Figure 3A and B***). This was initially surprising, considering that previous behavioral studies identified L1 as the major input to the ON pathway (***Clark et al., 2011***; ***Silies et al., 2013***). L1 silenced flies also turned normally to ON edges of fixed luminance, ruling out the possibility that changing luminance underlies this inconsistency (***Figure 3—figure supplement 1A, B***). However, L1 silencing severely reduced turning responses when a bright instead of a dark inter-stimulus interval was used, explaining the discrepancy between this and previous studies (***Figure 3—figure supplement 1C, D***). Thus, L1 is indeed a major but not the sole input to the ON pathway.

To explicitly test if and how L1 silencing changed the luminance dependence of behavioral responses, we quantified the slope of peak turning velocities across different background luminances (***Figure 3C***). The slopes were slightly negative for both the control and L1-silenced conditions, and did

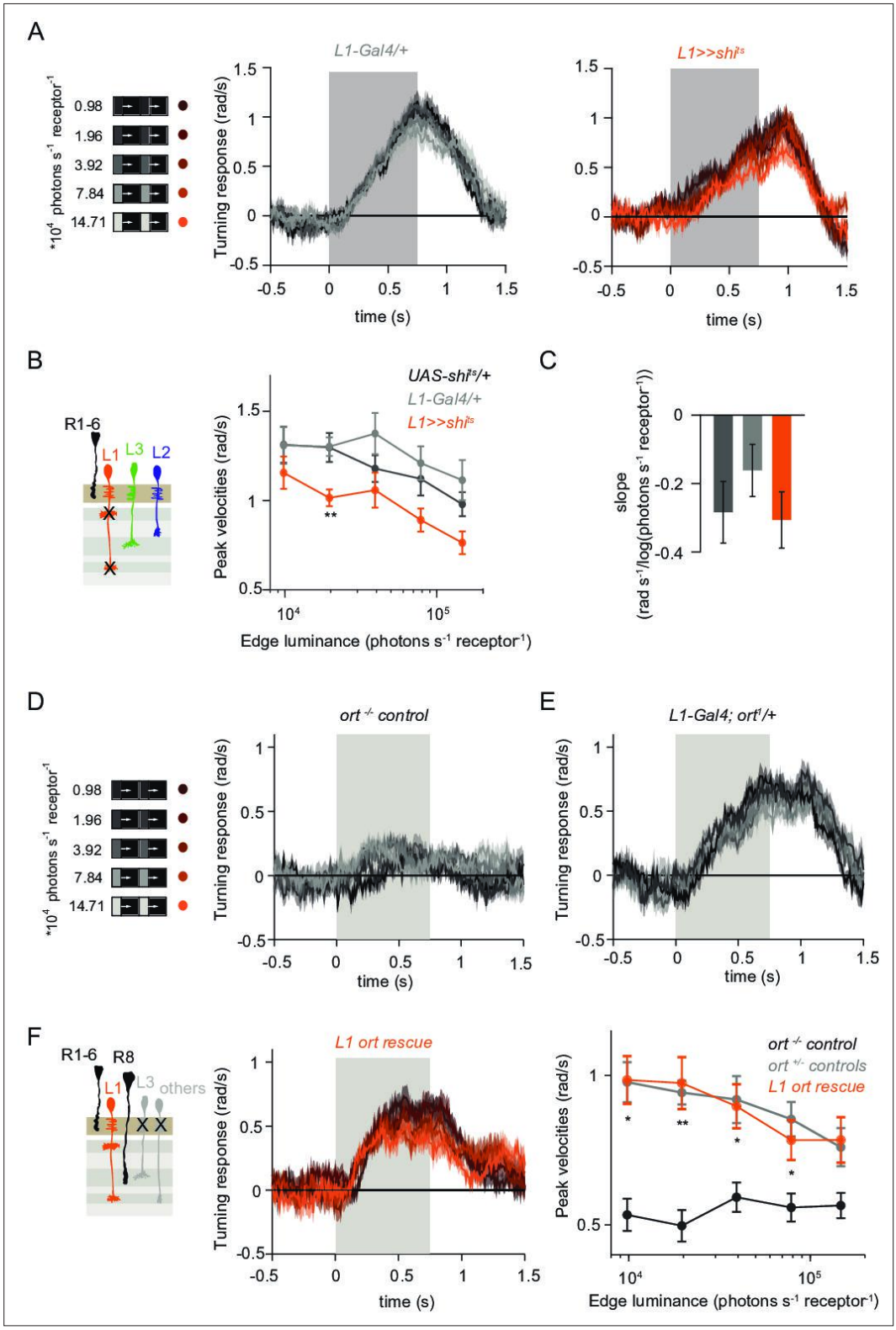

Figure 3. L1 is not required but sufficient for ON behavior across luminance. (**A**) Turning responses of L1-silenced flies (orange) and their specific Gal4 control (gray) to moving 100% contrast ON edges at five different luminances. (**B**) Peak velocities quantified for each of the five edges during the motion period, also including the control *UAS-shi^{ts}/+*, **p < 0.01, two-tailed Student's t-tests against both controls, with Bonferroni-Holm correction. (**C**) Relationship of the peak velocities with luminance, quantified as slopes of the linear fits to the data in (**B**). Sample sizes are n = 10 flies for each

Figure 3 continued on next page

Figure 3 continued

genotype. (**D–E**) Schematic of the stimulus (same as in A) and turning responses of the *ort* null mutant ($ort^{-/-}$ controls, **D**) and heterozygous *ort* controls ($ort^{+/-}$±, **E**). (**F**) Schematic of the L1 ort rescue genotype and turning responses of L1 ort rescue flies (left). Peak turning velocities of L1 ort rescue flies and the respective controls (right); *p < 0.05, **p < 0.01, two-tailed Student's t-tests against both controls, with Bonferroni-Holm correction. The gray box region in (**A,D,E,F**) indicates motion duration. Traces and plots show mean ± SEM.

The online version of this article includes the following figure supplement(s) for figure 3:

Figure supplement 1. L1 is required for ON behavior across a range of contrasts.

not differ significantly between conditions, suggesting another luminance input masking the L1 contribution. To test this possibility, we asked if L1 is sufficient to contribute to ON behavior in dynamically changing luminance conditions. We measured behavioral responses after functionally isolating L1 from other circuitry downstream of photoreceptors. To achieve this, we selectively rescued expression of the histamine-gated chloride channel Ort (Ora transientless) in *ort*-mutant flies, which otherwise lack communication between photoreceptors and their postsynaptic neurons. Behavioral responses of *ort* mutant control flies were absent, indicating that ON-motion behavior fully depends on Ort (***Figure 3D***). Heterozygous *ort* controls turned with the moving 100% contrast ON edges at all luminances (***Figure 3E***). Flies in which *ort* expression was rescued in L1 responded to ON motion at all luminances, and indistinguishable from controls (***Figure 3F***), showing that L1 can mediate normal turning behavior to ON edges at all luminances. This data confirms L1's general importance in the ON pathway.

L1 and L3 together provide luminance signals required for ON behavior

Our data suggest the existence of a second luminance input to the ON pathway. In the OFF pathway, the luminance-sensitive L3 neuron provides the necessary luminance-based correction to achieve contrast constancy (***Ketkar et al., 2020***). Connectomics data suggest that L3 could provide input to the ON pathway as well, as it makes direct synaptic contact with the major ON-pathway medulla neurons Mi1 and Mi9 (***Takemura et al., 2013***). To test the hypothesis that L3 also provides a luminance signal to the ON pathway, we measured behavioral responses to a set of 100% contrast ON edges at five different luminances while silencing L3 synaptic outputs (***Figure 4A–C***). Interestingly, unlike controls, L3-silenced flies responded stronger to all ON edges, revealing a potential, unexplored role of L3 in inhibiting behavioral responses to certain stimuli. However, the responses of L3-silenced flies were still similar across luminances (***Figure 4A and B***). Unlike controls, L3 silenced flies did not show a slight increase in turning amplitude at lower edge luminance, also reflected in the differences in their slopes (***Figure 4C***), suggesting that L3 inputs to the ON pathway also contribute to behavior in a luminance-dependent manner. To further explore if L3 indeed serves as an ON-pathway input, we next asked if L3 is sufficient for ON behavior and functionally isolated L3 from other circuitry. L3 ort rescue flies turned to ON edges at all luminances tested (***Figure 4D***) and significantly rescued turning behavior at low luminances compared to *ort* mutant flies (***Figure 4E***), showing that L3 is sufficient for ON behavior at low luminances. This further reflects L3's nonlinear preference for dim light seen at the physiological level (***Ketkar et al., 2020***, ***Figure 2F***).

We found that L3 is a second luminance input to the ON-pathway. To ask if L3, together with L1, provides a luminance gain to scale ON behavior, we simultaneously silenced the outputs of both L1 and L3 while measuring ON behavior across luminance. Flies still turned to the moving ON edges. However, unlike control responses which slightly deviated from luminance invariance by showing a negative correlation with luminance, turning responses of flies lacking both L1 and L3 functional outputs were positively correlated with luminance (***Figure 4F–H***). Intriguingly, behavioral responses of flies lacking both lamina neurons carrying luminance information underestimated dim stimuli (***Figure 4G***), and qualitatively recapitulated the LMC contrast-sensitive responses (***Ketkar et al., 2020***). Thus, L1 and L3 can together account for the luminance information available to the ON pathway. To analyze the extent of the individual contributions of L1 and L3, we compared L1 and L3 ort rescues by computing rescue efficiency, defined as the fraction of the difference between positive and negative control behaviors. Whereas L1 fully rescued turning behavior to ON edges at all luminances, L3 significantly rescued turning behavior selectively at low luminances (***Figure 4I***). Taken together, L3 is a functional input to the ON pathway, to which L1 and L3 both provide distinct types

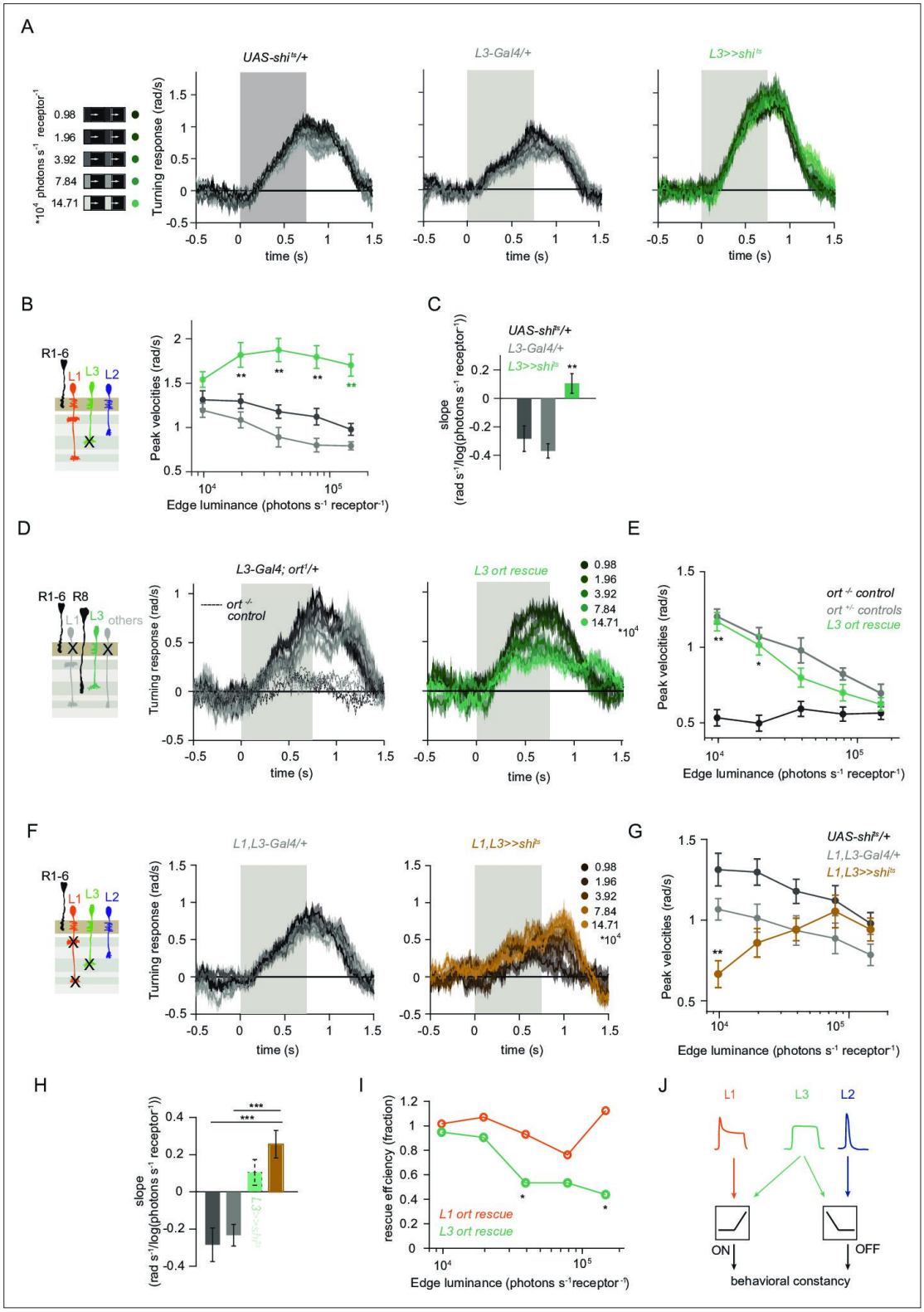

Figure 4. L1 and L3 together provide luminance signals required for ON behavior. (**A**) Turning velocities of the controls (gray) and L3-silenced flies (green) in response to five moving ON edges of 100% contrast. The gray box region indicates motion duration. (**B**) Peak turning velocities for five ON edges quantified during the motion period, **p < 0.01, two-tailed Student's t-tests against both controls, with Bonferroni-Holm correction. (**C**) Relationship of the peak velocities with luminance, quantified as slopes of the linear fits to the data in (**B**). Fitting was done for individual flies. Sample

Figure 4 continued on next page

Figure 4 continued

sizes are n = 10 (*UAS-shi^{ts}/+,L3 >>shi^{ts}*) and n = 8 (*L3^{0595}-Gal4/+*). **p < 0.01, two-tailed Student's t-tests against both controls, with Bonferroni-Holm correction. (**D**) Schematic of the L3 *ort* rescue genotype and turning responses of the heterozygous control (gray) and rescue (green) flies. (**E**) Peak turning velocities, *p < 0.05, **p < 0.01, two-tailed Student's t-tests against both controls, with Bonferroni-Holm correction. (**F**) Turning responses of flies where L1 and L3 were silenced together (golden brown) and their specific Gal4 control (gray), color-coded according to ON edge luminance. The same five moving ON edges of 100% contrast as in ***Figure 1C*** were shown. Responses of the other control *UAS-shi^{ts}/+* to these stimuli have been included in ***Figure 1C***. (**G**) Peak velocities quantified for each of the five edges during the motion period, also including the control *UAS-shi^{ts}/+*, **p < 0.01, two-tailed Student's t-tests against both controls, with Bonferroni-Holm correction (**H**) Relationship of the peak velocities with luminance, quantified as slopes of the linear fits to the data in (**G**). Slopes from the L3-silenced flies (green, dashed) responding to the same stimuli (***Figure 3C***) are included again for comparison. Fitting was done for individual flies. Sample sizes are n = 10 (*UAS-shi^{ts}/ +* and *L1,L3 >>shi^{ts}*) and n = 7 (*L1^{c2025}-Gal4/+;L3^{0595}-Gal4/+*). (**I**) Efficiency of the L1 and L3 behavioral rescue, calculated for each edge luminance as (*rescue - ort$^{-/-}$ control*) / (*ort$^{+/-}$ control - ort$^{-/-}$* control). ± < 0.05, permutation test with Bonferroni correction, 1,000 permutations over the *L1 ort rescue* and *L3 ort rescue* flies. (**J**) Summary schematic. The ON pathway in addition to the OFF pathway receives a prominent input from L3. Like the OFF pathway, the ON pathway drives contrast constant behavior. Traces and plots show mean ± SEM.

of luminance information (***Figure 4J***). Because flies lacking both neurons still respond to moving ON edges, our data suggest the existence of an unidentified contrast input.

The contrast-sensitive L2 neuron provides input to the ON-pathway

Besides L1 and L3, the remaining input downstream of photoreceptors is the contrast-sensitive L2 neuron, which provides strong inputs to OFF-pathway neurons (***Takemura et al., 2013***). To explore the possibility of L2 also being an ON-pathway input, we silenced L2 outputs either individually or together with L1. L2-silenced flies showed only slightly reduced turning to all ON edges as compared to controls (***Figure 5A and B***) similarly to silencing L1 alone (***Figure 3A and B***). However, when L1 and L2 were silenced together, fly turning responses were fully disrupted across conditions (***Figure 5C and D***). Moreover, these flies did not turn to moving ON edges of other contrasts either (***Figure 5—figure supplement 1***). This shows that L2, together with L1, is required for ON behavioral responses across different contrasts and luminances. Altogether, L1, L2, and L3 are all ON-pathway inputs.

L1 is also an OFF-pathway input

Given that three lamina neuron inputs encode visual stimuli differently and that all of them convey information to the ON-motion pathway, we next asked if L1 could also contribute to OFF-pathway function. To test if L1 contributes a luminance gain to the OFF pathway, we silenced L1 neurons while showing moving OFF edges, all of –100% contrast, and moving across five different background luminances. Although the two controls showed overall different response amplitudes, both controls showed luminance-invariant responses (***Figure 6A and B***). Previous work showed that L3 is required to achieve luminance invariance by scaling behavioral responses when background luminance turned dark (***Ketkar et al., 2020***). Similarly, when L1 was silenced, behavioral responses were no longer invariant across luminance, but flies turned less to –100% contrast at low luminance as compared to high luminance (***Figure 6A and B***). Underestimation of the dim OFF edges by L1-silenced flies was not as strong as by L3-silenced flies (***Ketkar et al., 2020***), again highlighting the specialized role of L3 in dim light (***Figure 6B***). These data demonstrate that L1 inputs provide a luminance gain to the OFF pathway. Since L1 carries both contrast and luminance information, it could also be sufficient to drive OFF behavior. To test this, we measured behavioral responses to OFF edges in L1 ort rescue flies. Heterozygous *ort* controls showed turning responses to –100% OFF edges at five different luminances (***Figure 6C***). As described previously (***Ketkar et al., 2020***), *ort* null mutants were not completely blind to this OFF-edge motion stimulus and responded especially at high luminance but very little at low luminances. L1 ort rescue flies responded similarly to positive controls at low luminances, rescuing responses to OFF edges at dim backgrounds (***Figure 6C and D***). Therefore, L1 is even sufficient to guide OFF behavior under the same conditions that were previously described for L3 (***Ketkar et al., 2020***). Taken together, these findings reveal that the lamina neurons L1 and L3 provide behaviorally relevant information to both ON and OFF pathways. In sum, our data uncover L1, L2, and L3 as important inputs for both ON and the OFF pathways, relevant for visually guided behaviors across luminances (***Figure 6E***).

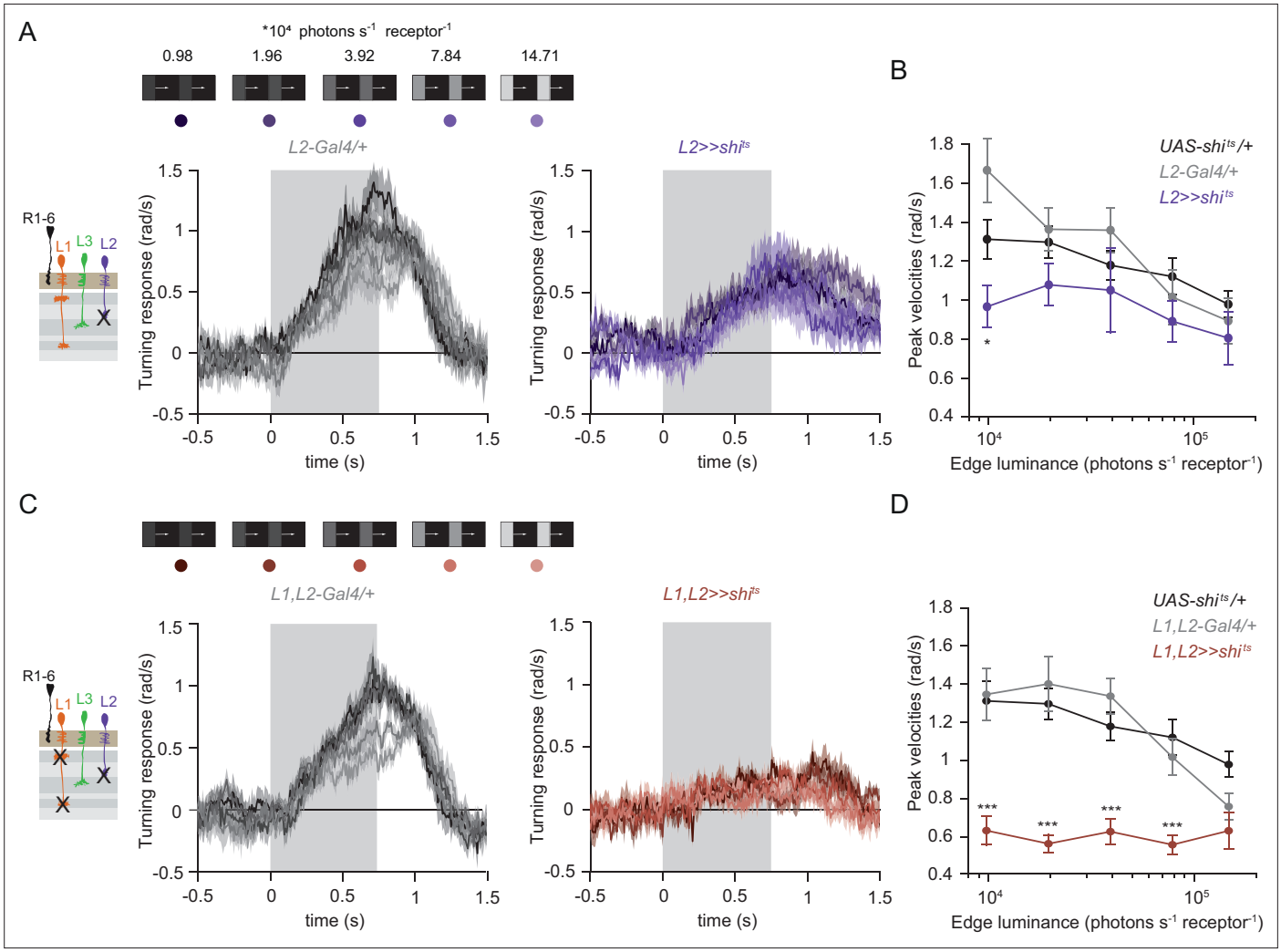

Figure 5. The contrast-sensitive L2 provides input to the ON-pathway. (**A**) Turning responses of flies where L2 was silenced (purple) and their specific Gal4 control (gray), color-coded according to 100% contrast ON edge at five different luminances. Sample sizes are n = 9 ($L2^{21Dhh}$ >> shi^{ts}) and n = 6 ($L2^{21Dhh}$-*Gal4/+*). (**B**) Peak velocities quantified for each of the five edges during the motion period, *p < 0.05, two-tailed Student's t tests against both controls, with Bonferroni-Holm correction. (**C**) Turning responses of flies where L1 and L2 were silenced together (brown) and their specific Gal4 control (gray), color-coded according to ON edge luminance. Sample sizes are n = 9 ($L1^{c2025}$,$L2^{21Dhh}$ >> shi^{ts}) and n = 8 ($L1^{c2025}$-*Gal4/+*;$L2^{21Dhh}$-*Gal4/+*). (**D**) Peak velocities quantified for each of the five edges during the motion period, ***p < 0.001, two-tailed Student's t-tests against both controls, with Bonferroni-Holm correction. Traces and plots show mean ± SEM.

The online version of this article includes the following figure supplement(s) for figure 5:

Figure supplement 1. L1 and L2 together are required for ON behavior across a range of contrasts.

Discussion

The present study establishes that contrast and luminance are basic visual features that interact with both ON and OFF pathways. In both pathways, the interaction between these features enables stable visual behaviors across changing conditions. The lamina neurons L1, L2, and L3 act as the circuit elements segregating both contrast and luminance information. Behavioral experiments show that luminance-sensitive input neurons scale behavioral responses to contrast in both ON and OFF pathways. While L1 and L2 provide distinct contrast inputs, L1 also encodes luminance, together with L3. Whereas L3 activity non-linearly increases with decreasing luminance, L1 shows a linear relationship with luminance. Input from both luminance-sensitive neurons is differently used in ON and OFF pathways. Thus, L1, L2, and L3 are not ON or OFF pathways specific inputs, but they instead distribute

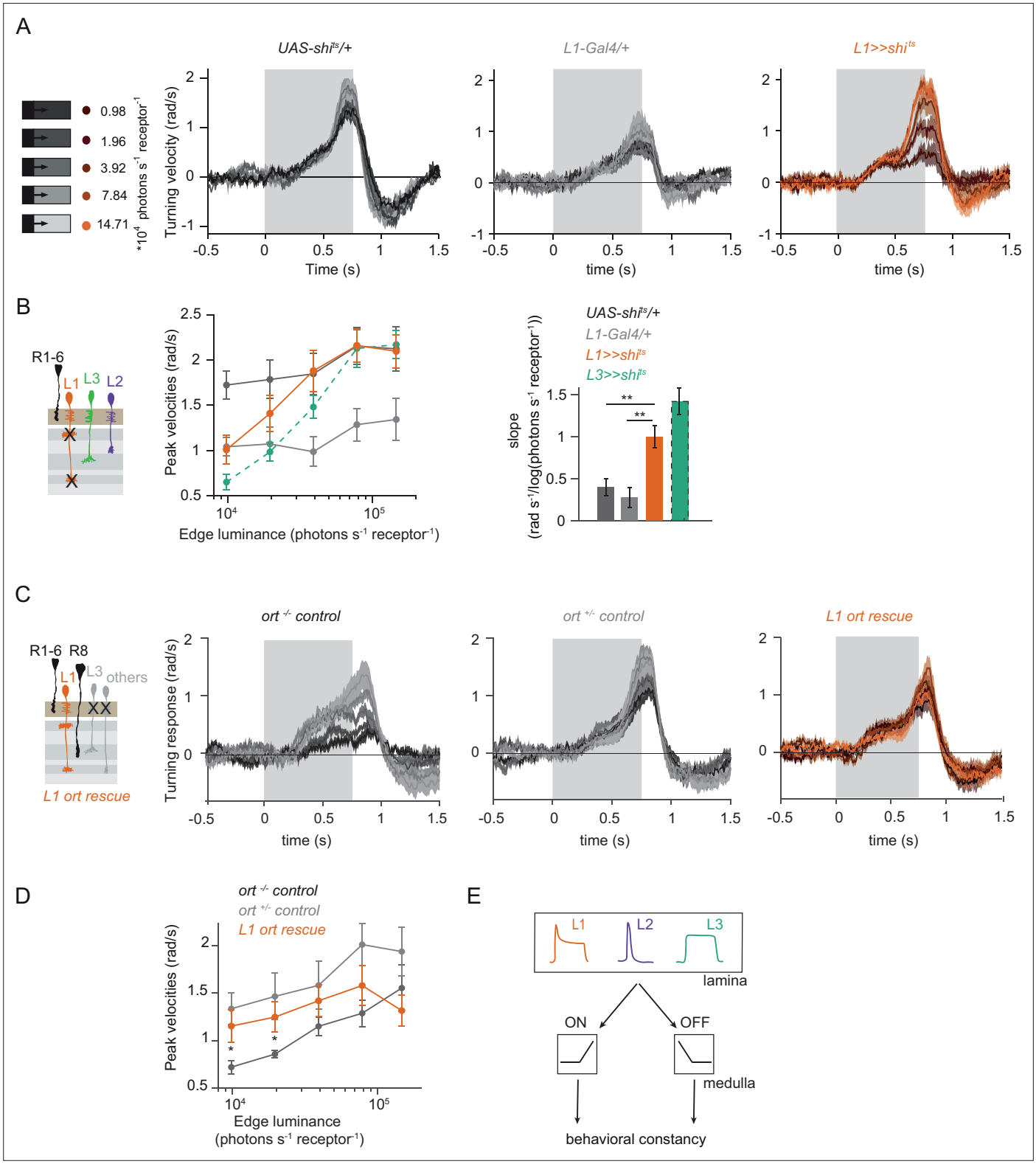

Figure 6. L1 function is required and sufficient for OFF behavior. (**A**) Turning responses of L1-silenced flies (orange) and the controls (gray) to five OFF edges moving onto different backgrounds. (**B**) Peak velocities quantified for each of the five edges during the motion period, also including the peak velocities of L3-silenced flies. Shown next to it is the relationship of the peak velocities with luminance, quantified as slopes of the linear fits to the data. **p < 0.01, two-tailed Student's t-tests against both controls, with Bonferroni-Holm correction (not significant against the *L3 >>shi^ts* slopes). *UAS-shi^ts*

Figure 6 continued on next page

Figure 6 continued

data in (**A**) and *ort*$^{-/-}$ data in (**C**) have been adapted from Figure 1B and 7C in ***Ketkar et al., 2020***, *L3 >>shi*^{ts} data in (**B**) have been re-quantified from data shown in Figure 4B in ***Ketkar et al., 2020***. Sample sizes are n = 7 (*L1-Gal4/+*) and n = 10 for other genotypes. (**C**) Schematics of the L1 ort rescue genotypes followed by its turning responses to the moving OFF edges. (**D**) Peak turning velocities of L1 ort rescue flies and the respective controls; *p < 0.05, two-tailed Student's t-tests against both controls, with Bonferroni-Holm correction. Sample sizes are n = 11 flies (*ort*$^{-/-}$control) and n = 10 for other genotypes. The gray box region in (**A**) and (**C**) indicates motion duration. (**E**) Summary schematic. Lamina neurons L1-L3 distribute different visual features necessary for both ON and OFF pathways to guide contrast-constant behavior. Traces and plots show mean ± SEM.

the two most basic visual features, contrast and luminance, across pathways to enable behaviorally relevant computations.

A post-receptor luminance gain is utilized in both ON and OFF visual pathways, but with distinct implementations

Changing visual environments impose a common challenge onto the encoding of both ON and OFF contrasts, namely the contrasts are underestimated in sudden dim light. Our work shows that visual behaviors guided by both ON and OFF pathways approach luminance invariance and are not susceptible to underestimation of contrast in sudden dim conditions. Similarly, luminance invariance has been shown in human perception of both ON and OFF contrasts, and in neural responses in cat LGN at fast time scales (***Burkhardt et al., 1984***; ***Mante et al., 2005***). This argues that the implementation of a rapid luminance gain is a common feature of all visual systems, which is relevant for any species that relies on visual information for its survival in changing visual environments. In *Drosophila*, luminance information from both L1 and L3 are required for rapid luminance gain control, but the impact of the two neurons on behavior is pathway dependent. In the OFF pathway, losing either L1 or L3 function leads to a strong deviation from luminance invariance, such that the dim light stimuli are underestimated. On the contrary, ON motion-driven behavior only underestimates dim stimuli if both L1 and L3 neuron types are not functional. Furthermore, L2 neurons, which were formerly thought to be OFF-pathway inputs, contribute contrast-sensitive information to ON behavior (***Clark et al., 2011***; ***Joesch et al., 2010***; ***Silies et al., 2013***). Notably, ON and OFF contrast constancy is not achieved symmetrically at every processing stage. For example, in the vertebrate retina, ON RGCs encode a mixture of luminance-invariant and absolute (i.e. luminance-dependent) contrast, whereas OFF RGCs encode predominantly absolute contrast (***Idrees and Münch, 2020***). Thus, asymmetrical implementation of contrast-corrective mechanisms can be common across visual systems, too.

All three lamina neurons are inputs to both ON and OFF pathways

Input from the three lamina neurons is differentially utilized across ON and OFF pathways. How does this fit with the established notion that L1 is an input to the ON and L2 and L3 are inputs to OFF pathways? The luminance-varying stimuli sets used here were able to pull out lamina neuron contributions that were not obvious with simpler stimuli. For example, our data show that L1 and L2 provide redundant contrast input to the ON pathway at 100% contrast and varying luminance. However, L1 is still strictly required for ON responses if different contrasts are mixed. This is consistent with a more complex ON-pathway input architecture and hints at a role for the L1 pathway in contrast adaptation. Interestingly, Mi1, an important post-synaptic partner of L1, shows an almost instantaneous and strong contrast adaptation (***Matulis et al., 2020***).

While all three lamina neuron types hyperpolarize to light onset and depolarize to light offset, contrast selectivity emerges downstream of these neurons: post-synaptic partners of L1 acquire ON contrast selectivity due to inhibitory glutamatergic synapses, whereas cholinergic L2 and L3 synapses retain OFF contrast selectivity (***Molina-Obando et al., 2019***; ***Yang et al., 2016***). L3 had furthermore mostly been considered an OFF-pathway neuron because the OFF-pathway neuron Tm9 receives its strongest input from L3 (***Fisher et al., 2015***; ***Shinomiya et al., 2014***; ***Takemura et al., 2013***). However, L3 itself actually makes most synaptic connections with the Mi9 neuron that plays a role in guiding behavioral responses to ON stimuli (***Strother et al., 2017***; ***Takemura et al., 2013***). Further synapses of L3 with the ON-selective Mi1 neuron are similar in number to those with Tm9 (***Takemura et al., 2013***). Finally, L3 can potentially also convey information to the chromatic pathway, as Tm20 is its second strongest postsynaptic connection (***Lin et al., 2016***). There, L3 luminance sensitivity might play a relevant role in achieving color constancy, that is color recognition irrespective of illumination

conditions. Altogether, anatomical and functional data indicate that it is time to redefine L3 as part of a luminance-encoding system rather than a mere OFF-pathway input. Other synaptic connections that link L2 to downstream ON-selective neurons still have to be investigated in detail.

A role of L1 beyond the ON pathway is supported by functional connectivity studies showing that Tm9 properties rely in part on L1 input (***Fisher et al., 2015***), and that Tm9 together with other OFF-pathway interneurons displays contrast-opponent receptive fields, showing the presence of ON information in the OFF pathway (***Ramos-Traslosheros and Silies, 2021***). Connectomics data did not identify any known OFF-pathway neurons postsynaptic to L1, but among the strongest postsynaptic partners of L1 are the GABAergic interneurons C2 and C3 that connect to the OFF pathway (***Takemura et al., 2013***). Intercolumnar neurons downstream of L1, such as Dm neurons (***Nern et al., 2015***), could further carry information to OFF-selective neurons, likely through disinhibition from ON-selective inputs. In the vertebrate retina, intercolumnar amacrine cells mediate interaction between ON and OFF bipolar cells, which has been shown to extend the operating range of the OFF pathway (***Manookin et al., 2008***; ***Odermatt et al., 2012***).

Altogether, it now becomes evident that a split in ON and OFF circuitry only truly exists in downstream medulla neurons and direction-selective cells. The luminance and contrast features encoded differently in L1, L2 and L3 lamina neurons are shared by both pathways. Importantly, the distinct features that are passed on by the specific inputs downstream of photoreceptors guide distinct behavioral roles.

Neurons postsynaptic to photoreceptors encode contrast and luminance differently

Despite being postsynaptic to the same photoreceptor input, L1, L2, and L3 all show different contrast and luminance sensitivities. L1 was previously considered the ON-pathway sibling of the contrast-sensitive L2, both with regard to its temporal filtering properties and at the transcriptome level (***Clark et al., 2011***; ***Tan et al., 2015***). However, L1 calcium signals show a transient and a sustained response component, which are contrast- and luminance-sensitive, respectively. Compared to photoreceptors, which also carry both contrast and luminance components, L1 still amplifies the contrast signals received from the photoreceptors, since its transient component is more pronounced than the one seen in the photoreceptor calcium traces (***Gür et al., 2020***). In other insect species, different types of lamina neurons have also been distinguished based on their physiological properties (***Rusanen et al., 2018***; ***Rusanen et al., 2017***), although their specific luminance and contrast sensitivities are yet unknown.

The two luminance-sensitive neurons L1 and L3 differ in their luminance-encoding properties. L1's initial transient contrast response might reduce the operating range of the subsequent luminance-sensitive baseline. L3's calcium responses show little adaptation and can utilize most of its operating range to encode luminance. L3 seems to invest this wider operating range into amplifying the darkest luminance values selectively and non-linearly. Thus, a predominantly luminance-sensitive channel among LMCs may have evolved to selectively process stimuli in the low luminance range. The different linear and non-linear properties of L1 and L3 might further increase the dynamic range of luminance signaling (***Odermatt et al., 2012***). Together with the pure contrast sensitivity of L2, the first-order interneurons in flies exhibit a wide range of sensitivities with respect to contrast and luminance, and different functional relevance. Diversifying feature encoding through distinct temporal properties of first-order interneurons is a strategy employed to reliably handle wide luminance ranges.

Similarities and differences of peripheral processing strategies across species

In flies, three first-order interneurons feed contrast and luminance information into downstream circuitry. In the mouse retina, more than 30 functionally distinct bipolar types show a spectrum of temporal filter properties rather than a strict transient-sustained dichotomy, thus capturing a larger diversity of temporal information in parallel channels (e.g. ***Baden et al., 2016***; ***Ichinose et al., 2014***; ***Odermatt et al., 2012***). Many bipolar cell types resemble L1, in that they have both luminance and contrast signals in distinct response components (e.g. ***Oesch and Diamond, 2011***). However, the degree of transiency varies from cell type to cell type, and some predominantly sustained bipolar cell types are also found, closely resembling the luminance-sensitive L3 (e.g. ***Awatramani and Slaughter,***

2000; Ichinose et al., 2014). Such diversification of feature extraction at the periphery has been shown to be computationally advantageous, especially when processing complex natural scenes (e.g. Odermatt et al., 2012; Rieke and Rudd, 2009). For example, during daylight, visual scenes can differ in intensity by 4–5 log units, whereas electrical signals in cone photoreceptors reach a dynamic range of only two orders of magnitude (Naka and Rushton, 1966; Normann and Perlman, 1979; Pouli et al., 2010; Schnapf et al., 1990).

Although the vertebrate retina apparently has a much larger diversity of cell types to handle the wide and complex statistics of the visual environments, there is only a single layer of processing between photoreceptors and the first direction-selective cells, whereas in insects, there are two: the lamina and the medulla. It seems as if the combined properties of bipolar cells are spread across these two processing stages in the fly visual system: whereas some properties, such as diversity of temporal filtering starts in LMCs, contrast selectivity only emerges in medulla neurons and not directly in the first-order interneurons as it happens in bipolar cells. In both vertebrates and invertebrates, the emergence of ON selectivity occurs through inhibitory glutamatergic synapses, but whereas this happens at the photoreceptor-to-bipolar cell synapse in vertebrates, it happens one synapse further down between lamina and medulla neurons in flies (Masu et al., 1995; Molina-Obando et al., 2019). Taken together, LMCs and downstream medulla neurons combined appear to be the functional equivalents of vertebrate bipolar cell layers. Given the size limitations of the fly visual system to encode the same complex environment effectively, one benefit of this configuration with an extra layer could be that it allows more combinations. Furthermore, the photoreceptor-to-lamina synapse in the fly superposition eye already serves to spatially pool information from different photoreceptors (Braitenberg, 1967;

Table 1. Genotypes used in this study.

Name	Genotype	Figure
Imaging		
L1 >>GCaMP6 f	*w+; L1^{c202a}-Gal4 /+; UAS-GCaMP6f /+*	**Figure 1**, **Figure 2—figure supplement 1**
L2 >>GCaMP6 f	*w+; UAS-GCaMP6f /+; L2^{21Dhh}-Gal4 /+*	**Figure 2**, **Figure 2—figure supplement 1**
L3 >>GCaMP6 f	*w+; L3^{MH56}-Gal4 /+; UAS-GCaMP6f /+*	**Figure 2**, **Figure 2—figure supplement 1**
Behavior		
UAS-shibire^{ts} control	*w+; +/+; UAS-shi^{ts} /+*	**Figures 1 and 3–6**, **Figure 2—figure supplement 2–1**, **Figure 5—figure supplement 5–1**
L3-Gal4 control	*w+; +/+; L3^{0595}-Gal4 /+*	**Figure 4**
L3 silencing	*w+; +/+; L3^{0595}-Gal4 / UAS- shi^{ts}*	**Figure 4**
L1-Gal4 control	*w+; L1^{c202a}-Gal4 /+; +/+*	**Figures 3 and 6**, **Figure 3—figure supplement 1**
L1 silencing	*w+; L1^{c202a}-Gal4 /+; +/UAS- shi^{ts}*	**Figures 3 and 6**, **Figure 3—figure supplement 1**
L1-Gal4, L3-Gal4 control	*w+; L1^{c202a}-Gal4 /+; L3^{0595}-Gal4/+*	**Figure 4**
L1, L3 silencing	*w+; L1^{c202a}-Gal4 /+; L3^{0595}-Gal4/UAS- shi^{ts}*	**Figure 4**
ort mutant	*w+; UAS-ort /+; ort^{1}, ninaE^{1}/Df(3 R)BSC809*	**Figures 3, 4 and 6**
L3 ort±control	*w+; +/+; L3^{0595}-Gal4, ort^{1}, ninaE^{1} /+*	**Figure 4**
L3 ort rescue	*w+; UAS-ort /+; L3^{0595}-Gal4, ort^{1}, ninaE^{1}/ Df(3 R)BSC809*	**Figure 4**
L1 ort±control	*w+; L1^{c202a}-Gal4/+, ort^{1}, ninaE^{1}/+*	**Figures 3 and 6**
L1 ort rescue	*w+; UAS-ort/+; L1^{c202a}; ort^{1},ninaE^{1}/Df(3 R) BSC809*	**Figures 3 and 6**
L2-Gal4 control	*w+; +/+; L2^{21Dhh}-Gal4/+*	**Figure 5**, **Figure 5—figure supplement 1**
L2 silencing	*w+; +/+; L2^{21Dhh}-Gal4/UAS- shi^{ts}*	**Figure 5**, **Figure 5—figure supplement 1**
L1-Gal4, L2-Gal4 control	*w+; L1^{c202a}-Gal4/+; L2^{21Dhh}-Gal4/+*	**Figure 5**, **Figure 5—figure supplement 1**
L1, L2 silencing	*w+; L1^{c202a}-Gal4/+; L2^{21Dhh}-Gal4/UAS- shi^{ts}*	**Figure 5**, **Figure 5—figure supplement 1**

Clandinin and Zipursky, 2002; *Kirschfeld, 1967*). In both visual systems, diversifying distinct information across several neurons could serve as a strategy to reliably respond to contrast when luminance conditions vary.

Materials and methods

Experimental model

All flies were raised at 25 °C and 65% humidity on standard molasses-based fly food while being subjected to a 12:12 hr light-dark cycle. Two-photon experiments were conducted at room temperature (20 °C) and behavioral experiments at 34 °C. Female flies 2–4 days after eclosion were used for all experimental purposes. Lamina neuron driver lines used for genetic silencing and *ort* rescue experiments were $L3^{0595}$-*Gal4* (*Silies et al., 2013*), $L2^{21Dhh}$-*Gal4* and $L1^{c202a}$-*Gal4* (*Rister et al., 2007*), and *UAS-shi[ts], ort*^{1},*ninaE*^{1} and *Df(3 R)BSC809* were from BDSC (# 44222, 1946 and 27380). Since the *ort*^{1} mutant chromosomes also carries a mutation in *ninaE*^{1} (*Drosophila rhodopsin1*), we used the *ort*^{1} mutation in trans to a deficiency that uncovers the *ort* but not the *ninaE* locus. *UAS-ort* was first described in *Hong et al., 2006*. For imaging experiments, GCaMP6f (BDSC #42747) was expressed using $L1^{c202a}$-*Gal4*, $L2^{21Dhh}$-*Gal4* (*Rister et al., 2007*), and $L3^{MH56}$-*Gal4* (*Timofeev et al., 2012*). Detailed genotypes are given in *Table 1*.

Behavioral experiments

Behavioral experiments were performed as described in *Ketkar et al., 2020*. In brief, all experiments were conducted at 34 °C, a restrictive temperature for *shibire*^{ts} (*Kitamoto, 2001*). Female flies were cold anesthetized and glued to the tip of a needle at their thorax using UV-hardened Norland optical adhesive. A 3D micromanipulator positioned the fly above an air-cushioned polyurethane ball (Kugel-Winnie, Bamberg, Germany), 6 mm in diameter, and located at the center of a cylindrical LED arena that spanned 192° in azimuth and 80° in elevation (*Reiser and Dickinson, 2008*). The LED panels arena (IO Rodeo, CA, USA) consisted of 570 nm LEDs and was enclosed in a dark chamber. The pixel resolution was ~2° at the fly's elevation. Rotation of the ball was sampled at 120 Hz with two wireless optical sensors (Logitech Anywhere MX 1, Lausanne, Switzerland), positioned toward the center of the ball and at 90° to each other (setup described in *Seelig et al., 2010*). Custom written C#-code was used to acquire ball movement data. MATLAB (Mathworks, MA, USA) was used to coordinate stimulus presentation and data acquisition. Data for each stimulus sequence were acquired for 15–20 min, depending on the number of distinct epochs in the sequence (see 'visual stimulation' for details).

Visual stimulation for behavior

The stimulation panels consist of green LEDs that can show 16 different, linearly spaced intensity levels. To measure the presented luminance, candela/m^2 values were first measured from the position of the fly using a LS-100 luminance meter (Konika Minolta, NJ, USA). Then, these values were transformed to photons incidence per photoreceptor per second, following the procedure described by *Dubs et al., 1981*. The highest native LED luminance was approximately 11.77 * 10^5 photons * s^{-1} * photoreceptor^{-1} (corresponding to a measured luminance of 51.34 cd/m^2), and the luminance meter read 0 candela/ m^2 when all LEDs were off. For all experiments, a 0.9 neutral density filter foil (Lee filters) was placed in front of the panels, such that the highest LED level corresponded to 14.71 *10^4 photons*s^{-1}*receptor^{-1}.

Fly behavior was measured in an open-loop paradigm where either ON or OFF edges were presented. For every set of ON or OFF edges, each epoch was presented for around 60–80 trials. Each trial consisted of an initial static pattern (i.e. the first frame of the upcoming pattern) shown for 500ms followed by 750ms of edge motion. Inter-trial intervals were 1 s. All edges from a set were randomly interleaved and presented in a mirror-symmetric fashion (moving to the right, or to the left) to account for potential biases in individual flies or introduced when positioning on the ball.

The ON edge stimuli comprised four edges, each covering 48° arena space. All ON edges moved with the angular speed of 160°/s. Thus, within a 750ms stimulus epoch, the edge motion repeated thrice: After each repetition, the now bright arena was reset to the pre-motion lower LED level, and the next repetition followed immediately, picking up from the positions where the edges terminated

in the first repetition. This way, each edge virtually moved continuously. The following sets of ON edges were presented:

1. 100% contrast edges: Here, the edges were made of 5 different luminance values (i.e. five unique epochs), moving on a complete dark background. Thus, the pre-motion LED level was zero, and the edges assumed the intensities 7%, 14%, 27%, 53%, or 100% of the highest LED intensity (corresponding to the luminances: 0.98, 1.96, 3.92, 7.84 or 14.71 *10^4 photons*s^{-1}*receptor^{-1} luminance). Thus, every epoch comprised 100% Michelson contrast. The inter-trial interval consisted of a dark screen.
2. Single-luminance edges: 100% contrast edges of a single luminance value (0.98*10^4 photons*s^{-1}*receptor^{-1} luminance) moved on a dark background. All epochs were identical. The inter-trial interval consisted of either a dark screen (***Figure 3—figure supplement 1A, B***) or a screen equally bright as the ON edges (***Figure 3—figure supplement 1C, D***).
3. Mixed-contrast edges: The set comprised of seven distinct epochs, each with a different Michelson contrast value (11%, 25%, 33%, 43%, 67%, 82%, and 100%). Here, the edge luminance was maintained constant at 67% of the highest LED intensity, across epochs, and the background luminance varied. The inter-trial interval showed a uniformly lit screen with luminance equivalent to the edge luminance.

For the experiments concerning OFF edges, a set of five OFF edges comprising 100% Weber contrast was used as described in ***Ketkar et al., 2020***. Epoch consisted of a single OFF edge presented at one of five different uniformly lit backgrounds. The edge luminance was always ~zero, whereas the five different background luminances were 7%, 14%, 27%, 54%, and 100% of the highest LED intensity (corresponding to five different background luminances: 0.98, 1.96, 3.92, 7.84, or 14.71 *10^4 photons*s^{-1}*receptor^{-1}). The inter-trial interval consisted of a dark screen.

Behavioral data analysis

Fly turning behavior was defined as yaw velocities that were derived as described in ***Seelig et al., 2010***, leading to a positive turn when flies turned in the direction of the stimulation and to a negative turn in the opposite case. Turning elicited by the same epoch moving either to the right or to the left were aggregated to compute the mean response of the fly to that epoch. Turning responses are presented as angular velocities (rad/s) averaged across flies ± SEM. Peak velocities were calculated over the stimulus motion period (750ms), shifted by 100ms to account for a response delay, and relative to a baseline defined as the last 200ms of the preceding inter-stimulus intervals. For the moving edges of 100% contrast and varying luminance, relation between peak velocities and luminance was assessed by fitting a straight line (V = a*log(luminance) + b) to the peak velocities of individual flies and quantifying the mean slope (a) ± SEM across flies. When comparing the slopes computed for behavior and L1 physiology, the two data types were first normalized for individual flies for behavior and individual regions of interest (ROIs) for L1 physiology (***Figure 1E***). For the *ort* rescue experiments, rescue efficiency was calculated at each stimulus luminance as

$$E_{rescue} = \frac{rescue - control^{-}}{control^{+} - control^{-}}$$

where E_{rescue} is the fractional rescue efficiency, *rescue* is the mean peak velocity of the rescue genotype such as L1 rescue, *control*$^{-}$ is the mean peak velocity of the *ort* null mutant negative control and *control*$^{+}$ + for the mean peak velocity of the positive heterozygous *ort*^{1} control (e.g. *L1-Gal4; ort*^{1}*/+*). Statistical significance of E_{rescue} differences was tested using a permutation test. Specifically, flies of the genotypes L1 ort rescue and L3 ort rescue were shuffled 1000 times and the difference between their rescue efficiencies was obtained each time. The difference values so obtained gave a probability distribution that approximated a normal distribution. The efficiency difference was considered significant when it corresponded to less than 5% probability on both tails of the distribution, after Bonferroni correction.

Mean turning of flies as well as the slopes from control and experimental genotypes were normal distributed as tested using a Kolmogorov-Smirnov test ($p > 0.05$). To test differences between these variables, pairwise t-tests considering Bonferroni-Holm correction for multiple comparisons were performed between genotypes. The experimental genotype was marked significantly different only when it differed from both genetic controls. Flies with a baseline forward walking speed of less than 2 mm/s were discarded from the analysis. This resulted in rejection of approximately 25% of all flies.

Two-photon imaging

Female flies were anesthetized on ice before placing them onto a sheet of stainless-steel foil bearing a hole that fit the thorax and head of the flies. Flies then were head fixated using UV-sensitive glue (Bondic). The head of the fly was tilted downward, looking toward the stimulation screen and their back of the head was exposed to the microscope objective. To optically access the optic lobe, a small window was cut in the cuticle on the back of the head using sharp forceps. During imaging, the brain was perfused with a carboxygenated saline-sugar imaging solution composed of 103 mM NaCl, 3 mM KCl, 5 mM TES, 1 mM NaH2PO4, 4 mM MgCl2, 1.5 mM CaCl2,10 mM trehalose, 10 mM glucose, 7 mM sucrose, and 26 mM NaHCO3. Dissections were done in the same solution, but lacking calcium and sugars. The pH of the saline equilibrated near 7.3 when bubbled with 95% O2 / 5% CO2. The two-photon experiments for ***Figure 2*** and ***Figure 2—figure supplement 1*** were performed using a Bruker Investigator microscope (Bruker, Madison,WI, USA), equipped with a 25 x/NA1.1 objective (Nikon, Minato, Japan). An excitation laser (Spectraphysics Insight DS+) tuned to 920 nm was used to excite GCaMP6f, applying 5–15 mW of power at the sample. For experiments in ***Figure 1***, a Bruker Ultima microscope, equipped with a 20 x/NA1.0 objective (Leica, Wetzlar, Germany) was used. Here the excitation laser (YLMO-930 Menlo Systems, Martinsried, Germany) had a fixed 930 nm wavelength, and a power of 5–15 mW was applied at the sample.

In both setups, emitted light was sent through a SP680 shortpass filter, a 560 lpxr dichroic filter and a 525/70 emission filter. Data was acquired at a frame rate of ~10–15 Hz and around 6–8 x optical zoom, using PrairieView software.

Visual stimulation for imaging

For the staircase stimuli and light flashes of different luminances, the visual stimuli were generated by custom-written software using C ++ and OpenGL and synchronized as described previously (***Freifeld et al., 2013***). The stimuli were projected onto an 8cm x 8cm rear projection screen placed anterior to the fly and covering 60° of the fly's visual system in azimuth and 60° in elevation. These experiments were performed with the Bruker Investigator microscope.

For ON-moving edges, the stimulus was generated by custom-written software using the Python package PsychoPy (***Peirce, 2008***), and then projected onto a 9cm x 9cm rear projection screen placed anterior to the fly at a 45° angle and covering 80° of the fly's visual system in azimuth and 80° in elevation. These experiments were performed with the Bruker Ultima microscope.

Both stimuli were projected using a LightCrafter (Texas Instruments, Dallas, TX, USA), updating stimuli at a frame rate of 100 Hz. Before reaching the fly eye, stimuli were filtered by a 482/18 band pass filter and a ND1.0 neutral density filter (Thorlabs). The luminance values are measured using the same procedure described above for the behavioral experiments. The maximum luminance value (I_{max}) measured at the fly position was $2.17*10^5$ photons s^{-1} $photoreceptor^{-1}$ for the staircase and random luminance stimulation, and $2.4*10^5$ photons s^{-1} $photoreceptor^{-1}$ for the ON-moving edge stimulation.

A and B contrast steps from the adapted background

The stimulus was adapted from ***Oesch and Diamond, 2011***. 30 s of bright adapting background luminance was followed by two consecutive 3 s OFF steps: the A and B steps. The A step took one of 7 decreasing luminance values, resulting in seven different contrast steps relative to the adapting step. The luminance of the B step was also composed of 7 decreasing luminance values, depending on the previous A step, resulting in 7 25% Weber contrast steps. The order of the A steps and their associated B steps was randomized.

Staircase stimulation

The stimulus consisted of 10 s full-field flashes of five different luminances (0, 0.25, 0.5, 0.75 and 1* of the maximal luminance I_{max}). The different luminance epochs were presented first in an increasing order (from darkness to full brightness) then in a decreasing order (full brightness to darkness). This sequence was repeated ~3–5 times.

Flashes of different luminances

The stimulus consisted of 10 s full-field flashes of five different luminances (0, 0.25, 0.5, 0.75 and 1* of the maximal luminance I_{max}). The order between the flashes was pseudo-randomized and the stimulus sequence was presented for ~300 s.

ON moving edges at different luminances

Here, the edges were made of 6 different luminance values (corresponding to 0.16, 0.31, 0.62, 1.2, 1.8, 2.4 *10^5 photons*s^{-1}*$receptor^{-1}$ luminance), moving on a dark background. The inter-stimulus interval was 4 seconds of darkness.

Two-photon data analysis

Staircase stimulation and randomized flashes of different luminances

Data processing was performed offline using MATLAB R2019a (The MathWorks Inc, Natick, MA). To correct for motion artifacts, individual images were aligned to a reference image composed of a maximum intensity projection of the first 30 frames. The average intensity for manually selected ROIs was computed for each imaging frame and background subtracted to generate a time trace of the response. All responses and visual stimuli were interpolated at 10 Hz and trial averaged. Neural responses are shown as relative fluorescence intensity changes over time (ΔF/F0). To calculate ΔF/F0, the mean of the whole trace was used as F0. In some recordings, a minority of ROIs responded in opposite polarity (positively correlated with stimulus), as described previously (***Fisher et al., 2015***). These ROIs have their receptive fields outside the stimulation screen (***Fisher et al., 2015***; ***Freifeld et al., 2013***). To discard these and other noisy ROIs, we only used ROIs that were negatively correlated (Spearman's rank correlation coefficient) with the stimulus.

To calculate the OFF-step responses to the staircase stimulus in ***Figure 2B***, we first normalized the traces of L1 and L2 to get comparable values (0–1). The OFF-step response then was the difference of the maximum response and the mean of the last two seconds of the previous luminance epoch. We then fitted a sigmoidal function

$$f(x) = a * \left(\frac{1}{1+e^{k*x}} - 0.5\right)$$

using 50 times bootstrapping with replacement to get the distribution of fit parameters (a and k).

In randomized flashes, plateau responses of neurons were calculated as the mean of the last 2 s within each luminance presentation. In the randomized flashes of different luminances, plateau response values of the highest luminance epoch were subtracted for each plateau response to get a comparable relationship between each neuron for visualization (this leads to 0 plateau response for each neuron in the highest luminance condition). Mutual information between luminance and response was calculated according to ***Ross, 2014***. To characterize the distinct luminance-response relationships of L1 and L3, the difference of Pearson correlation and Spearman's rank correlation was used as a Non-linearity index. This value will reach zero if there is a strict linear relationship between luminance and response.

A and B contrast steps from the adapted background

Data processing was performed offline using MATLAB R2019a (The MathWorks Inc, Natick, MA) following the same steps for the staircase stimulation. To calculate dF/F, the mean calcium response of the 30 s adaptation period was used as F0. Peak responses were calculated as the maximum response within each A and B steps compared to the mean baseline response in the last 2 s of the adapting period. Sustained responses were calculated as the mean response of the last 500ms of each step. We used One-way ANOVA to determine whether the peak responses to the B step were significantly different. The p-values are reported in Figure S1B.

ON moving edges at different luminances

Data processing was performed offline using Python 2.7 (Van Rossum 1995). Motion correction was performed using the SIMA Python package's Hidden Markov Model based motion correction

algorithm (***Kaifosh et al., 2014***). The average intensity for manually selected ROIs was computed for each imaging frame and background subtracted to generate a time trace of the response. To calculate ΔF/F0, the mean of the whole trace was used as F0. The traces were then trial averaged. Responses of ROIs for each epoch was calculated as the absolute difference between the mean of the full darkness background epoch and the minimum of the ON edge presentation (minimum values are chosen because L1 neurons respond to ON stimuli with hyperpolarization).

Statistics

Throughout the analysis procedure, mean of quantified variables were calculated first for all ROIs within a fly, and then between flies. All statistical analysis was performed between flies. For normally distributed data sets, a two-tailed Student *t* test for unpaired (independent) samples was used. For other data sets, Wilcoxon rank-sum was used for statistical analysis. Normality was tested using Lilliefors test ($p > 0.05$). One way ANOVA was used followed by multiple comparisons using the Bonferroni method for determining statistical significance between pairs of groups.

Analysis code is available at (https://github.com/silieslab/Ketkar-Gur-MolinaObando-etal2022, copy archived at swh:1:rev:392160a9f7e1336be1cb375cac53055f07620ddf; ***Ketkar et al., 2022a***) and source data can be found on Zenodo: https://doi.org/105281/zenodo6335347 ***Ketkar et al., 2022b***.

Acknowledgements

We thank members of the Silies lab for comments on the manuscript. We are grateful to Christine Gündner, Simone Renner, and Jonas Chojetzki for excellent technical assistance. This project has received funding from the European Research Council (ERC) under the European Union's Horizon 2020 research and innovation program (grant agreement No 716512), from the German Research Foundation (DFG) through the Emmy-Noether program (SI 1991/1-1) and the collaborative research center 1080 "Neural homeostasis" (project C06) to MS, as well as DFG grant MA 7804/2–1 to CM.

Additional information

Funding

Funder	Grant reference number	Author
European Commission	ERC Starting Grant No 716512	Marion Silies
Deutsche Forschungsgemeinschaft	CRC1080 project C06	Marion Silies
Deutsche Forschungsgemeinschaft	MA 7804/2-1	Carlotta Martelli

The funders had no role in study design, data collection and interpretation, or the decision to submit the work for publication.

Author contributions

Madhura D Ketkar, Conceptualization, Investigation, Methodology, Software, Visualization, Writing – original draft, Writing – review and editing; Burak Gür, Conceptualization, Investigation, Methodology, Software, Visualization, Writing – review and editing; Sebastian Molina-Obando, Conceptualization, Investigation, Software, Visualization, Writing – original draft, Writing – review and editing; Maria Ioannidou, Investigation, Writing – review and editing; Carlotta Martelli, Methodology, Supervision, Writing – review and editing; Marion Silies, Conceptualization, Funding acquisition, Supervision, Writing – original draft, Writing – review and editing

Author ORCIDs

Madhura D Ketkar http://orcid.org/0000-0002-0465-5616
Burak Gür http://orcid.org/0000-0001-8221-9767
Sebastian Molina-Obando http://orcid.org/0000-0003-1222-723X

Maria Ioannidou http://orcid.org/0000-0003-2869-5468
Carlotta Martelli http://orcid.org/0000-0002-5663-6580
Marion Silies http://orcid.org/0000-0003-2810-9828

Decision letter and Author response
Decision letter https://doi.org/10.7554/eLife.74937.sa1
Author response https://doi.org/10.7554/eLife.74937.sa2

Additional files

Supplementary files

- Transparent reporting form

Data availability

Analysis code is available at https://github.com/silieslab/Ketkar-Gur-MolinaObando-etal2022 (copy archived at swh:1:rev:392160a9f7e1336be1cb375cac53055f07620ddf), and source data can be found on Zenodo: https://doi.org/10.5281/zenodo.6335347.

The following dataset was generated:

Author(s)	Year	Dataset title	Dataset URL	Database and Identifier
Ketkar, Madhura Dinesh Johannes-Gutenberg University Mainz ; Gür, Burak; Molina-Obando, Sebastian; Ioannidou, Maria; Martelli, Carlotta; Silies, Marion	2022	First-order visual interneurons distribute distinct contrast and luminance information across ON and OFF pathways to achieve stable behavior	https://doi.org/10.5281/zenodo.6335347	Zenodo, 10.5281/zenodo.6335347

References

Awatramani GB, Slaughter MM. 2000. Origin of Transient and Sustained Responses in Ganglion Cells of the Retina *The Journal of Neuroscience* **20**:7087–7095. DOI: https://doi.org/10.1523/JNEUROSCI.20-18-07087.2000, PMID: 10995856

Baden T, Berens P, Franke K, Román Rosón M, Bethge M, Euler T. 2016. The functional diversity of retinal ganglion cells in the mouse *Nature* **529**:345–350. DOI: https://doi.org/10.1038/nature16468, PMID: 26735013

Behnia R, Clark DA, Carter AG, Clandinin TR, Desplan C. 2014. Processing properties of on and off pathways for *Drosophila* motion detection *Nature* **512**:427–430. DOI: https://doi.org/10.1038/nature13427, PMID: 25043016

Braitenberg V. 1967. Patterns of projection in the visual system of the fly I. Retina-lamina projections. *Experimental Brain Research* **3**:271–298. DOI: https://doi.org/10.1007/BF00235589

Burkhardt DA, Gottesman J, Kersten D, Legge GE. 1984. Symmetry and constancy in the perception of negative and positive luminance contrast *Journal of the Optical Society of America. A, Optics and Image Science* **1**:309–316. DOI: https://doi.org/10.1364/josaa.1.000309, PMID: 6716199

Chichilnisky EJ, Kalmar RS. 2002. Functional Asymmetries in ON and OFF Ganglion Cells of Primate Retina. *The Journal of Neuroscience* **22**:2737–2747., DOI: https://doi.org/20026215, PMID: 11923439

Clandinin TR, Zipursky SL. 2002. Making connections in the fly visual system *Neuron* **35**:827–841. DOI: https://doi.org/10.1016/s0896-6273(02)00876-0, PMID: 12372279

Clark DA, Bursztyn L, Horowitz MA, Schnitzer MJ, Clandinin TR. 2011. Defining the Computational Structure of the Motion Detector in *Drosophila Neuron* **70**:1165–1177. DOI: https://doi.org/10.1016/j.neuron.2011.05.023, PMID: 21689602

Clark DA, Fitzgerald JE, Ales JM, Gohl DM, Silies MA, Norcia AM, Clandinin TR. 2014. Flies and humans share a motion estimation strategy that exploits natural scene statistics *Nature Neuroscience* **17**:296–303. DOI: https://doi.org/10.1038/nn.3600, PMID: 24390225

Clark DA, Demb JB. 2016. Parallel Computations in Insect and Mammalian Visual Motion Processing *Current Biology* **26**:R1062–R1072. DOI: https://doi.org/10.1016/j.cub.2016.08.003, PMID: 27780048

Dubs A, Laughlin SB, Srinivasan MV. 1981. Single photon signals in fly photoreceptors and first order interneurones at behavioral threshold *The Journal of Physiology* **317**:317–334. DOI: https://doi.org/10.1113/jphysiol.1981.sp013827, PMID: 7310737

Euler T, Haverkamp S, Schubert T, Baden T. 2014. Retinal bipolar cells: Elementary building blocks of vision *Nature Reviews. Neuroscience* **15**:507–519. DOI: https://doi.org/10.1038/nrn3783, PMID: 25158357

Fischbach KF, Dittrich APM. 1989. The optic lobe of *Drosophila melanogaster* I. A Golgi analysis of wild-type structure. *Cell and Tissue Research* **258**:BF00218858. DOI: https://doi.org/10.1007/BF00218858
Fisher YE, Leong JCS, Sporar K, Ketkar MD, Gohl DM, Clandinin TR, Silies M. 2015. A Class of Visual Neurons with Wide-Field Properties Is Required for Local Motion Detection *Current Biology* **25**:3178–3189. DOI: https://doi.org/10.1016/j.cub.2015.11.018, PMID: 26670999
Franceschini N, Riehle A, Le Nestour A. 1989. Directionally Selective Motion Detection by Insect Neurons In. Stavenga DG, Hardie RC (Eds). *Facets of Vision*. Springer. p. 360–390. DOI: https://doi.org/10.1007/978-3-642-74082-4_17
Frazor RA, Geisler WS. 2006. Local luminance and contrast in natural images *Vision Research* **46**:1585–1598. DOI: https://doi.org/10.1016/j.visres.2005.06.038, PMID: 16403546
Freifeld L, Clark DA, Schnitzer MJ, Horowitz MA, Clandinin TR. 2013. GABAergic Lateral Interactions Tune the Early Stages of Visual Processing in *Drosophila Neuron* **78**:1075–1089. DOI: https://doi.org/10.1016/j.neuron.2013.04.024, PMID: 23791198
Gür B, Sporar K, Lopez-Behling A, Silies M. 2020. Distinct expression of potassium channels regulates visual response properties of lamina neurons in *Drosophila melanogaster Journal of Comparative Physiology. A, Neuroethology, Sensory, Neural, and Behavioral Physiology* **206**:273–287. DOI: https://doi.org/10.1007/s00359-019-01385-7, PMID: 31823004
Hong ST, Bang S, Paik D, Kang J, Hwang S, Jeon K, Chun B, Hyun S, Lee Y, Kim J. 2006. Histamine and Its Receptors Modulate Temperature-Preference Behaviors in *Drosophila The Journal of Neuroscience* **26**:7245–7256. DOI: https://doi.org/10.1523/JNEUROSCI.5426-05.2006, PMID: 16822982
Ichinose T, Lukasiewicz PD. 2007. Ambient Light Regulates Sodium Channel Activity to Dynamically Control Retinal Signaling *The Journal of Neuroscience* **27**:4756–4764. DOI: https://doi.org/10.1523/JNEUROSCI.0183-07.2007, PMID: 17460088
Ichinose T, Fyk-Kolodziej B, Cohn J. 2014. Roles of ON Cone Bipolar Cell Subtypes in Temporal Coding in the Mouse Retina *The Journal of Neuroscience* **34**:8761–8771. DOI: https://doi.org/10.1523/JNEUROSCI.3965-13.2014, PMID: 24966376
Ichinose T, Hellmer CB. 2016. Differential signalling and glutamate receptor compositions in the OFF bipolar cell types in the mouse retina: Temporal coding in the retinal OFF bipolar cells *The Journal of Physiology* **594**:883–894. DOI: https://doi.org/10.1113/JP271458, PMID: 26553530
Idrees S, Münch TA. 2020. Different contrast encoding in ON and OFF visual pathways (preprint)). *Neuroscience* **25**:398230. DOI: https://doi.org/10.1101/2020.11.25.398230
Jin J, Wang Y, Lashgari R, Swadlow HA, Alonso JM. 2011. Faster Thalamocortical Processing for Dark than Light Visual Targets *The Journal of Neuroscience* **31**:17471–17479. DOI: https://doi.org/10.1523/JNEUROSCI.2456-11.2011, PMID: 22131408
Joesch M, Schnell B, Raghu SV, Reiff DF, Borst A. 2010. ON and off pathways in *Drosophila* motion vision *Nature* **468**:300–304. DOI: https://doi.org/10.1038/nature09545, PMID: 21068841
Kaifosh P, Zaremba JD, Danielson NB, Losonczy A. 2014. SIMA: Python software for analysis of dynamic fluorescence imaging data, Frontiers in Neuroinformatics *Frontiers in Neuroinformatics* **8**:80. DOI: https://doi.org/10.3389/fninf.2014.00080, PMID: 25295002
Ketkar MD, Sporar K, Gür B, Ramos-Traslosheros G, Seifert M, Silies M. 2020. Luminance Information Is Required for the Accurate Estimation of Contrast in Rapidly Changing Visual Contexts *Current Biology* **30**:657-669.. DOI: https://doi.org/10.1016/j.cub.2019.12.038, PMID: 32008904
Ketkar MD, Gür B, Molina-Obando S, Ioannidou M, Martelli C, Silies M. 2022a. Code. 392160a. Github. https://github.com/silieslab/Ketkar-Gur-MolinaObando-etal2022
Ketkar MD, Gür B, Molina-Obando S, Ioannidou M, Martelli C, Silies M. 2022b. Data. Zenodo. https://doi.org/10.5281/zenodo.6335347DOI: https://doi.org/10.5281/zenodo.6335347
Kirschfeld K. 1967. Die projektion der optischen umwelt auf das raster der rhabdomere im komplexauge von Musca *Experimental Brain Research* **3**:248–270. DOI: https://doi.org/10.1007/BF00235588, PMID: 6067693
Kitamoto T. 2001. Conditional modification of behavior in *Drosophila* by targeted expression of a temperature-sensitiveshibire allele in defined neurons. *Journal of Neurobiology* **47**:81–92. DOI: https://doi.org/10.1002/neu.1018, PMID: 11291099
Laughlin SB, Hardie RC. 1978. Common strategies for light adaptation in the peripheral visual systems of fly and dragonfly *Journal of Comparative Physiology ? A* **128**:319–340. DOI: https://doi.org/10.1007/BF00657606
Leonhardt A, Ammer G, Meier M, Serbe E, Bahl A, Borst A. 2016. Asymmetry of *Drosophila* on and off motion detectors enhances real-world velocity estimation *Nature Neuroscience* **19**:706–715. DOI: https://doi.org/10.1038/nn.4262, PMID: 26928063
Lin TY, Luo J, Shinomiya K, Ting CY, Lu Z, Meinertzhagen IA, Lee CH. 2016. Mapping chromatic pathways in the *Drosophila* visual system: Chromatic Visual Circuits in the Fly's Lobula. *The Journal of Comparative Neurology* **524**:213–227. DOI: https://doi.org/10.1002/cne.23857
Manookin MB, Beaudoin DL, Ernst ZR, Flagel LJ, Demb JB. 2008. Disinhibition Combines with Excitation to Extend the Operating Range of the OFF Visual Pathway in Daylight *The Journal of Neuroscience* **28**:4136–4150. DOI: https://doi.org/10.1523/JNEUROSCI.4274-07.2008, PMID: 18417693
Mante V, Frazor RA, Bonin V, Geisler WS, Carandini M. 2005. Independence of luminance and contrast in natural scenes and in the early visual system *Nature Neuroscience* **8**:1690–1697. DOI: https://doi.org/10.1038/nn1556, PMID: 16286933

Masu M, Iwakabe H, Tagawa Y, Miyoshi T, Yamashita M, Fukuda Y, Sasaki H, Hiroi K, Nakamura Y, Shigemoto R. 1995. Specific deficit of the ON response in visual transmission by targeted disruption of the mGluR6 gene *Cell* **80**:757–765. DOI: https://doi.org/10.1016/0092-8674(95)90354-2, PMID: 7889569

Matulis CA, Chen J, Gonzalez-Suarez AD, Behnia R, Clark DA. 2020. Heterogeneous Temporal Contrast Adaptation in *Drosophila* Direction-Selective Circuits *Current Biology* **30**:222-236.. DOI: https://doi.org/10.1016/j.cub.2019.11.077, PMID: 31928874

Mauss AS, Vlasits A, Borst A, Feller M. 2017. Visual Circuits for Direction Selectivity *Annual Review of Neuroscience* **40**:211–230. DOI: https://doi.org/10.1146/annurev-neuro-072116-031335

Meinertzhagen IA, O'Neil SD. 1991. Synaptic organization of columnar elements in the lamina of the wild type in *Drosophila melanogaster The Journal of Comparative Neurology* **305**:232–263. DOI: https://doi.org/10.1002/cne.903050206, PMID: 1902848

Molina-Obando S, Vargas-Fique JF, Henning M, Gür B, Schladt TM, Akhtar J, Berger TK, Silies M. 2019. ON selectivity in the *Drosophila* visual system is a multisynaptic process involving both glutamatergic and GABAergic inhibition *eLife* **8**:e49373. DOI: https://doi.org/10.7554/eLife.49373, PMID: 31535971

Naka KI, Rushton WAH. 1966. S-potentials from luminosity units in the retina of fish (Cyprinidae) *The Journal of Physiology* **185**:587–599. DOI: https://doi.org/10.1113/jphysiol.1966.sp008003, PMID: 5918060

Nern A, Pfeiffer BD, Rubin GM. 2015. Optimized tools for multicolor stochastic labeling reveal diverse stereotyped cell arrangements in the fly visual system. *PNAS* **112**:E2967–E2976. DOI: https://doi.org/10.1073/pnas.1506763112, PMID: 25964354

Normann RA, Werblin FS. 1974. Control of Retinal Sensitivity I *Journal of General Physiology* **63**:37–61. DOI: https://doi.org/10.1085/jgp.63.1.37

Normann RA, Perlman I. 1979. The effects of background illumination on the photoresponses of red and green cones *The Journal of Physiology* **286**:491–507. DOI: https://doi.org/10.1113/jphysiol.1979.sp012633, PMID: 439037

Odermatt B, Nikolaev A, Lagnado L. 2012. Encoding of Luminance and Contrast by Linear and Nonlinear Synapses in the Retina *Neuron* **73**:758–773. DOI: https://doi.org/10.1016/j.neuron.2011.12.023, PMID: 22365549

Oesch NW, Diamond JS. 2011. Ribbon synapses compute temporal contrast and encode luminance in retinal rod bipolar cells *Nature Neuroscience* **14**:1555–1561. DOI: https://doi.org/10.1038/nn.2945, PMID: 22019730

Peirce JW. 2008. Generating stimuli for neuroscience using PsychoPy *Frontiers in Neuroinformatics* **2**:10. DOI: https://doi.org/10.3389/neuro.11.010.2008, PMID: 19198666

Pouli T, Cunningham D, Reinhard E. 2010. Statistical Regularities in Low and High Dynamic Range Images. Proceedings of the 7th Symposium on Applied Perception in Graphics and Visualization - APGV '10. . DOI: https://doi.org/10.1145/1836248.1836250

Ramos-Traslosheros G, Silies M. 2021. The physiological basis for contrast opponency in motion computation in *Drosophila Nature Communications* **12**:1–16. DOI: https://doi.org/10.1038/s41467-021-24986-w, PMID: 34404776

Ratliff CP, Borghuis BG, Kao YH, Sterling P, Balasubramanian V. 2010. Retina is structured to process an excess of darkness in natural scenes. *PNAS* **107**:17368–17373. DOI: https://doi.org/10.1073/pnas.1005846107, PMID: 20855627

Reiser MB, Dickinson MH. 2008. A modular display system for insect behavioral neuroscience *Journal of Neuroscience Methods* **167**:127–139. DOI: https://doi.org/10.1016/j.jneumeth.2007.07.019, PMID: 17854905

Rieke F, Rudd ME. 2009. The Challenges Natural Images Pose for Visual Adaptation *Neuron* **64**:605–616. DOI: https://doi.org/10.1016/j.neuron.2009.11.028, PMID: 20005818

Rister J, Pauls D, Schnell B, Ting CY, Lee CH, Sinakevitch I, Morante J, Strausfeld NJ, Ito K, Heisenberg M. 2007. Dissection of the Peripheral Motion Channel in the Visual System of *Drosophila melanogaster Neuron* **56**:155–170. DOI: https://doi.org/10.1016/j.neuron.2007.09.014, PMID: 17920022

Ross BC. 2014. Mutual information between discrete and continuous data sets. *PLOS ONE* **9**:e87357. DOI: https://doi.org/10.1371/journal.pone.0087357, PMID: 24586270

Ruderman DL, Bialek W. 1994. Statistics of natural images: Scaling in the woods. *Physical Review Letters* **73**:814–817. DOI: https://doi.org/10.1103/PhysRevLett.73.814, PMID: 10057546

Rusanen J, Vähäkainu A, Weckström M, Arikawa K. 2017. Characterization of the first-order visual interneurons in the visual system of the bumblebee (Bombus terrestris) *Journal of Comparative Physiology. A, Neuroethology, Sensory, Neural, and Behavioral Physiology* **203**:903–913. DOI: https://doi.org/10.1007/s00359-017-1201-9, PMID: 28741079

Rusanen J, Frolov R, Weckström M, Kinoshita M, Arikawa K. 2018. Non-linear amplification of graded voltage signals in the first-order visual interneurons of the butterfly Papilio xuthus *The Journal of Experimental Biology* **221**:jeb179085. DOI: https://doi.org/10.1242/jeb.179085, PMID: 29712749

Schnapf JL, Nunn BJ, Meister M, Baylor DA. 1990. Visual transduction in cones of the monkey Macaca fascicularis *The Journal of Physiology* **427**:681–713. DOI: https://doi.org/10.1113/jphysiol.1990.sp018193, PMID: 2100987

Seelig JD, Chiappe ME, Lott GK, Dutta A, Osborne JE, Reiser MB, Jayaraman V. 2010. Two-photon calcium imaging from head-fixed *Drosophila* during optomotor walking behavior *Nature Methods* **7**:535–540. DOI: https://doi.org/10.1038/nmeth.1468, PMID: 20526346

Serbe E, Meier M, Leonhardt A, Borst A. 2016. Comprehensive Characterization of the Major Presynaptic Elements to the *Drosophila* OFF Motion Detector *Neuron* **89**:829–841. DOI: https://doi.org/10.1016/j.neuron.2016.01.006, PMID: 26853306

Shapley R, Enroth-Cugell C. 1984. Chapter 9 Visual adaptation and retinal gain controls *Progress in Retinal Research* **3**:263–346. DOI: https://doi.org/10.1016/0278-4327(84)90011-7

Shinomiya K, Karuppudurai T, Lin TY, Lu Z, Lee CH, Meinertzhagen IA. 2014. Candidate neural substrates for off-edge motion detection in *Drosophila Current Biology* **24**:1062–1070. DOI: https://doi.org/10.1016/j.cub.2014.03.051, PMID: 24768048

Shinomiya K, Huang G, Lu Z, Parag T, Xu CS, Aniceto R, Ansari N, Cheatham N, Lauchie S, Neace E, Ogundeyi O, Ordish C, Peel D, Shinomiya A, Smith C, Takemura S, Talebi I, Rivlin PK, Nern A, Scheffer LK, et al. 2019. Comparisons between the ON- and OFF-edge motion pathways in the *Drosophila* brain. *eLife* **8**:e40025. DOI: https://doi.org/10.7554/eLife.40025

Silies M, Gohl DM, Fisher YE, Freifeld L, Clark DA, Clandinin TR. 2013. Modular Use of Peripheral Input Channels Tunes Motion-Detecting Circuitry *Neuron* **79**:111–127. DOI: https://doi.org/10.1016/j.neuron.2013.04.029, PMID: 23849199

Silies M, Gohl DM, Clandinin TR. 2014. Motion-Detecting Circuits in Flies: Coming into View *Annual Review of Neuroscience* **37**:307–327. DOI: https://doi.org/10.1146/annurev-neuro-071013-013931, PMID: 25032498

Strother JA, Nern A, Reiser MB. 2014. Direct observation of on and off pathways in the *Drosophila* visual system *Current Biology* **24**:976–983. DOI: https://doi.org/10.1016/j.cub.2014.03.017, PMID: 24704075

Strother JA, Wu ST, Wong AM, Nern A, Rogers EM, Le JQ, Rubin GM, Reiser MB. 2017. The Emergence of Directional Selectivity in the Visual Motion Pathway of *Drosophila Neuron* **94**:168-182.. DOI: https://doi.org/10.1016/j.neuron.2017.03.010, PMID: 28384470

Takemura S, Bharioke A, Lu Z, Nern A, Vitaladevuni S, Rivlin PK, Katz WT, Olbris DJ, Plaza SM, Winston P, Zhao T, Horne JA, Fetter RD, Takemura S, Blazek K, Chang L-A, Ogundeyi O, Saunders MA, Shapiro V, Sigmund C, et al. 2013. A visual motion detection circuit suggested by *Drosophila* connectomics *Nature* **500**:175–181. DOI: https://doi.org/10.1038/nature12450, PMID: 23925240

Takemura S, Xu CS, Lu Z, Rivlin PK, Parag T, Olbris DJ, Plaza S, Zhao T, Katz WT, Umayam L, Weaver C, Hess HF, Horne JA, Nunez-Iglesias J, Aniceto R, Chang LA, Lauchie S, Nasca A, Ogundeyi O, Sigmund C, et al. 2015. Synaptic circuits and their variations within different columns in the visual system of *Drosophila*. *PNAS* **112**:13711–13716. DOI: https://doi.org/10.1073/pnas.1509820112, PMID: 26483464

Takemura SY, Nern A, Chklovskii DB, Scheffer LK, Rubin GM, Meinertzhagen IA. 2017. The comprehensive connectome of a neural substrate for 'ON' motion detection in *Drosophila*. *eLife* **6**:e24394. DOI: https://doi.org/10.7554/eLife.24394, PMID: 28432786

Tan L, Zhang KX, Pecot MY, Nagarkar-Jaiswal S, Lee PT, Takemura SY, McEwen JM, Nern A, Xu S, Tadros W, Chen Z, Zinn K, Bellen HJ, Morey M, Zipursky SL. 2015. Ig Superfamily Ligand and Receptor Pairs Expressed in Synaptic Partners in *Drosophila Cell* **163**:1756–1769. DOI: https://doi.org/10.1016/j.cell.2015.11.021, PMID: 26687360

Timofeev K, Joly W, Hadjieconomou D, Salecker I. 2012. Localized netrins act as positional cues to control layer-specific targeting of photoreceptor axons in *Drosophila Neuron* **75**:80–93. DOI: https://doi.org/10.1016/j.neuron.2012.04.037, PMID: 22794263

Yang HHH, St-Pierre F, Sun X, Ding X, Lin MZZ, Clandinin TRR. 2016. Subcellular Imaging of Voltage and Calcium Signals Reveals Neural Processing In Vivo *Cell* **166**:245–257. DOI: https://doi.org/10.1016/j.cell.2016.05.031, PMID: 27264607

Yang HH, Clandinin TR. 2018. Elementary Motion Detection in *Drosophila*: Algorithms and Mechanisms *Annual Review of Vision Science* **4**:143–163. DOI: https://doi.org/10.1146/annurev-vision-091517-034153, PMID: 29949723

4 | Manuscript 2: Distinct expression of potassium channels regulates visual response properties of lamina neurons in *Drosophila melanogaster*

This manuscript is published as a research article in *Journal of Comparative Physiology A* and is available under DOI: https://doi.org/10.1007/s00359-019-01385-7

Authors and affiliations

Burak Gür[1,2,3], Katja Sporar[1,2,3], Anne Lopez Behling[2], Marion Silies[1,2,3,*]

1 - Institute of Developmental Biology and Neurobiology, Johannes Gutenberg-Universität Mainz, 55128 Mainz, Germany

2 - European Neuroscience Institute Göttingen a Joint Initiative of the University Medical Center Göttingen, and the Max Planck Society, 37077 Göttingen, Germany

3 - International Max Planck Research School and Göttingen Graduate School for Neurosciences, Biophysics, and Molecular Biosciences (GGNB) at the University of Göttingen, Göttingen, Germany

* - For correspondence: msilies@uni-mainz.de

Contribution statement

Marion Silies and I conceptualized and designed the study. Katja Sporar provided the photoreceptor imaging data in Figure 1. Anne Lopez Behling performed immunostainings in Figure 2 under my supervision as a rotation student. I performed the rest of the experiments and analyzed the data. I wrote the original draft of the manuscript, which was then edited and revised by Marion Silies and myself, with input from all authors.

Journal of Comparative Physiology A (2020) 206:273–287
https://doi.org/10.1007/s00359-019-01385-7

ORIGINAL PAPER

Distinct expression of potassium channels regulates visual response properties of lamina neurons in *Drosophila melanogaster*

Burak Gür[1,2,3] · Katja Sporar[1,2,3] · Anne Lopez-Behling[2] · Marion Silies[1,2]

Received: 15 August 2019 / Revised: 23 October 2019 / Accepted: 21 November 2019 / Published online: 10 December 2019

Abstract

The computational organization of sensory systems depends on the diversification of individual cell types with distinct signal-processing capabilities. The *Drosophila* visual system, for instance, splits information into channels with different temporal properties directly downstream of photoreceptors in the first-order interneurons of the OFF pathway, L2 and L3. However, the biophysical mechanisms that determine this specialization are largely unknown. Here, we show that the voltage-gated K_a channels Shaker and Shal contribute to the response properties of the major OFF pathway input L2. L3 calcium response kinetics postsynaptic to photoreceptors resemble the sustained calcium signals of photoreceptors, whereas L2 neurons decay transiently. Based on a cell-type-specific RNA-seq data set and endogenous protein tagging, we identified Shaker and Shal as the primary candidates to shape L2 responses. Using in vivo two-photon imaging of L2 calcium signals in combination with pharmacological and genetic perturbations of these K_a channels, we show that the wild-type Shaker and Shal function is to enhance L2 responses and cell-autonomously sharpen L2 kinetics. Our results reveal a role for K_a channels in determining the signal-processing characteristics of a specific cell type in the visual system.

Keywords Visual system · Potassium channels · Lamina · Visual processing · *Drosophila*

Introduction

Processing of information within sensory systems depends on the presence of neural circuits in which individual cell types perform specific computational tasks. For instance, in organisms ranging from insects to animals, neural circuits of the visual system need to process a wealth of information that can vary significantly in its spatiotemporal characteristics. Since the capacities of single neurons are constrained by their biophysical properties, specialized cell types are optimized for distinct signal-processing steps in the sequential extraction of relevant visual features (Laughlin 1994; Sanes and Zipursky 2010; Demb and Singer 2015). In early visual processing, a plethora of mechanisms, including the differences in biophysical membrane properties, vesicle release dynamics, neurotransmitter receptors, and circuit motifs, establish the diverse processing properties of more than 50 distinct cell types for parallel processing of the visual scenery (Demb and Singer 2015). Thus, understanding the mechanisms behind cell-type specialization in the visual system could provide useful insights into how information-processing strategies are established within neural circuits.

An elegant model to study the role of cell-type specialization for distinct visual processing steps is provided by the *Drosophila* visual system (Borst 2014; Silies et al. 2014; Yang and Clandinin 2018). With an extensive genetic toolkit combined with anatomical resources down to the synaptic level (Gohl et al. 2011; Jenett et al. 2012; Takemura et al. 2013, 2017; Shinomiya et al. 2019), cell types of core visual circuitry has been mapped (reviewed in Ramos-Traslosheros

Electronic supplementary material The online version of this article (https://doi.org/10.1007/s00359-019-01385-7) contains supplementary material, which is available to authorized users.

✉ Marion Silies
msilies@uni-mainz.de

[1] Institute of Developmental Biology and Neurobiology, Johannes Gutenberg-Universität Mainz, 55128 Mainz, Germany

[2] European Neuroscience Institute Göttingen a Joint Initiative of the University Medical Center Göttingen, and the Max Planck Society, 37077 Göttingen, Germany

[3] International Max Planck Research School and Göttingen Graduate School for Neurosciences, Biophysics, and Molecular Biosciences (GGNB) at the University of Göttingen, Göttingen, Germany

et al. 2018). For example, motion–detection circuitry harbors neurons with different spatiotemporal properties that fulfill distinct computational purposes (Clark et al. 2011; Silies et al. 2013; Tuthill et al. 2013; Behnia et al. 2014; Fisher et al. 2015; Serbe et al. 2016; Arenz et al. 2017). Although many molecular cascades have been revealed for the specification of cell types during development (Wernet et al. 2014), the molecular mechanisms underlying the signal-processing properties of distinct cell types is largely unknown.

In the *Drosophila* visual system, information flows from the retina to the lamina, medulla, lobula, and lobula plate. The retina is composed of 800 individual visual units, the ommatidia, which each contain eight photoreceptors. Downstream neuropils such as the lamina and medulla are organized in a columnar fashion, corresponding to the 800 retinal units. In the lamina, neighboring columns receive inputs from neighboring points in visual space, thus together forming a retinotopic image. The motion–detection circuitry starts with the achromatic R1–R6 photoreceptors in the retina, which connect to the lamina monopolar cells (LMC), where the circuitry splits into two pathways detecting contrast increments (ON) and decrements (OFF) (Joesch et al. 2010; Strother et al. 2014). Whereas the ON pathway contains one main input, the LMC L1, the OFF pathway has two distinct inputs, L2 and L3 (Joesch et al. 2010; Clark et al. 2011; Silies et al. 2013; Fisher et al. 2015). Despite L2 and L3 receiving the majority of their input synapses from R1 to R6 photoreceptors, L2 and L3 exhibit highly divergent characteristics. Calcium-imaging experiments from L2 to L3 axon terminals showed that L3 displays sustained responses to visual stimulation and has a nonlinear monophasic filter (Silies et al. 2013; Fisher et al. 2015), whereas L2 is characterized by transient responses with a biphasic linear filter (Reiff et al. 2010; Clark et al. 2011; Fisher et al. 2015). In the absence of genetic markers, L2- and L3-type neurons have been described in many other insect species based on anatomical and physiological features (Ribi 1975, 1987; Hardie and Weckström 1990; de Souza et al. 1992; Uusitalo et al. 1995; Stöckl et al. 2016). In blowflies, electrophysiological recordings also revealed slower response kinetics in L3-type LMCs, suggesting conserved signal-processing streams (Hardie and Weckström 1990; Uusitalo et al. 1995; Rusanen and Weckström 2016). Furthermore, anatomically and physiologically different LMC types have been described in different insect orders, suggesting that similar specializations might be present across insects (Arnett 1972; Laughlin 1974; Ribi 1987; Stöckl et al. 2016; Rusanen et al. 2017, 2018). However, how L2 and L3 neurons acquire their distinct physiologies remains an open question.

The biophysical properties of a neural membrane are crucial for determining the specific tasks a neuron has in information processing. A suite of different ion channels defines the membrane properties for the desired signal processing and the extraction of relevant features. Of these, potassium channels are the most diverse, and voltage-gated potassium channels (K_v) are known to regulate many neuronal properties (Coetzee et al. 1999; Hille 2001). K_v channels produce distinct currents that are specialized to differentially facilitate signal processing (Wei et al. 1990; Covarrubias et al. 1991). In insect photoreceptors, K_v channels are important for regulating gain and temporal response properties (Weckström et al. 1991; Hardie 1991; Anderson and Hardie 1996; Niven et al. 2003; Vahasoyrinki et al. 2006). Photoreceptors from different insects utilize different K_v channels depending on their ecology (Weckström and Laughlin 1995; Frolov et al. 2016). Electrophysiological studies in the blowfly have shown that L2- and L3-type neurons display different K_v currents. L2-type neurons have been shown to employ a rapidly inactivating, A-type (K_a) current, whereas L3-type neurons use a sustained delayed rectifier (K_d) current (Hardie and Weckström 1990; Rusanen and Weckström 2016). This was suggested to facilitate high-frequency transmission of the L2-type neurons (Rusanen and Weckström 2016). However, due to the different ecologies of blowflies and fruit flies, as reflected in the photoreceptor K_v currents (Weckström et al. 1991; Weckström and Laughlin 1995), the LMCs may also utilize K_v channels differently between species. Thus, K_v channels are interesting candidates to regulate differential L2 and L3 responses.

Here, we uncovered a role for K_a channels in shaping L2 visual response properties. Using in vivo two-photon calcium imaging, we measured axon terminal calcium responses of R1–R6, L2, and L3 neurons. Whereas L3 axon terminal calcium responses resemble R1–R6 calcium kinetics, L2 calcium responses to visual stimuli decay much faster. To identify candidate K_v channels that might shape the fast L2 kinetics, we compared K_v channel mRNA levels and identified two K_a channels, Shaker and Shal, as candidates to mediate L2 responses. We localized the endogenous Shal and Shaker proteins in the optic lobe and found that Shaker is broadly expressed in the optic lobe and Shal distinctly localizes to L2 but not L3 axon terminals. Acute pharmacological targeting of these channels showed that K_a channels enhance L2 visual responses to contrast and sharpen the transient property of L2. We then used cell-type-specific knockdown to investigate cell-autonomous roles of K_a channels and found that only the L2 temporal dynamics are mediated through K_a channels expressed specifically in L2 neurons. Our findings demonstrate that a specific subtype of K_v channels contributes to neuronal specialization for information processing in the visual system.

Materials and methods

Animals

Flies were raised on a standard molasses-based food at 25 °C and 55% humidity in a 12:12 h light:dark cycle. Only female

flies were used for experiments. Imaging experiments were performed at room temperature (RT, ~ 20 °C). The following fly strains were used for experiments: *L2*^{21Dhh}*-Gal4* (Rister et al. 2007), *L3*^{MH56}*-Gal4* (Timofeev et al. 2012), *UAS-GCaMP6f, UAS-Shal*^{dsRNA} (*UAS-Shal*$^{TRIP.J02154}$, BL 31879) (Feng et al. 2018), *UAS-Shaker*^{dsRNA} (*UAS-Shaker*$^{TRIP.JF01473}$, BL 31680), *Shal*$^{MI00446-GFSTF.1}$ (BL 60149), *Shaker*$^{MI10885-GFSTF.2}$ (BL 59423), and UAS-Shal (Ping and Tsunoda 2012). All effector and GFSTF lines were obtained from the Bloomington Drosophila Stock Center (Indiana University). Full genotypes are provided in Table 1.

RNA expression analysis, immunohistochemistry, and confocal imaging

RNA expression analysis

Published TPM tables were taken from Davis et al. (2018) (GSE116969). L2 K_v channel mRNA levels were summarized as fold change compared to L3 levels (also in TPM) in Python (Python Software Foundation, https://www.python.org/).

Immunohistochemistry

For immunohistochemistry experiments, female fly brains were dissected 2–5 days after eclosion in dissection solution (103 mM NaCl, 3 mM KCl, 5 mM TES, 1 mM NaH_2PO_4, 4 mM $MgCl_2$, 10 mM trehalose, 10 mM glucose, 7 mM sucrose, and 26 mM $NaHCO_3$) and fixed in 2% paraformaldehyde in phosphate-buffered lysine (PBL) for 50 min at RT. After fixation, brains were permeabilized in phosphate buffered saline containing 0.3% Triton X-100 (PBT) adjusted to pH 7.2 (3 × 5 min). Next, brains were blocked with 10% normal goat serum (NGS; Fisher Scientific GmbH, Schwerte, Germany) in PBT for 30 min at RT followed by 24 h incubation at 4 °C in primary antibody (diluted in blocking buffer). After primary antibody incubation, brains were washed with PBT (3 × 5 min) and incubated overnight at 4 °C in secondary antibody (diluted in blocking buffer). After secondary antibody incubation, the brains were washed in PBT (3 × 5 min) and mounted in Vectashield (Vector Laboratories, Burlingame). The brains were stained with the following primary antibodies: anti-GFP (chicken 1:2000, Abcam), anti-dsRed (rabbit, 1:400, Clontech), Brp (mouse monoclonal nc82 1:25, DSHB), and the following secondary antibodies diluted at 1:200: anti-chicken Alexa 488, anti-rabbit Alexa 594, and anti-mouse Alexa 647 (Dianova).

Confocal imaging and data analysis

After preparation, samples were imaged on a Zeiss LSM710 microscope (Carl Zeiss Microscopy GmbH, Germany) equipped with oil immersion Plan-Apochromat 40×/1.3 or 63×/1.4 objectives. Size, contrast, and brightness of images were adjusted using Fiji (Schindelin et al. 2012). Figures were assembled using Affinity Designer (Serif Ltd, United Kingdom).

To quantify the Shal- or Shaker-reporter signal within L2 or L3 axon terminals, we first manually selected single axon terminals for either L2 or L3 based on the tdTomato signal, using Fiji. We then calculated the mean signals in the GFP channel. Signals of single axon terminals were divided to the mean GFP signal within the medulla section (determined from the nc82 neuropil staining) of that image to normalize between experiments. The mean and the standard error of

Table 1 Genotypes used in this study

Figure	Name	Full genotype	Sources
Figure 1	*ninaE-GCaMP6f*	*w+; ninaE-GCaMP6f; +/+*	Asteriti et al. (2017)
Figures 1, 3, 4, S2	*L2 ≫ GCaMP6f*	*w+;UAS-GCaMP6f/+;L2*^{21Dhh}*-Gal4/+*	Rister et al. (2007), BDSC (BL 42747)
Figure 1, S2, S3	*L3 ≫ GCaMP6f*	*w+; L3*^{MH56}*-Gal4/+;UAS-GCaMP6f/+*	Timofeev et al. (2012), BDSC (BL 42747)
Figure 2	*Shal::GFP*	*y[1] w[*]; +/+; Shal*$^{MI00446-GFSTF.1}$*/+*	BDSC (BL 60149)
Figure 2	*Sh::GFP*	*y[1] w[*] Shaker*$^{MI10885-GFSTF.2}$*/+; +/+; +/+*	BDSC (BL 59423)
Figure 2, S1	*L2 ≫ tdTomato,Shal::GFP*	*w+; UAS-tdTomato/+; Shal*$^{MI00446-GFSTF.1}$*/L2*^{21Dhh} *-Gal4*	
Figure 2, S1	*L3 ≫ tdTomato,Shal::GFP*	*w+; UAS-tdTomato/L3*^{MH56}*-Gal4; Shal*$^{MI00446-GFSTF.1}$*/+*	
Figure 4	*L2 ≫ GCaMP6f,Sh*^{dsRNA}	*w+;UAS-GCaMP6f/+; L2*^{21Dhh} *-Gal4/UAS-Sh*^{dsRNA}	BDSC (BL 31680)
Figure 4	*L2 ≫ GCaMP6f,Shal*^{dsRNA}	*w+;UAS-GCaMP6f/+; L2*^{21Dhh} *-Gal4/UAS-Shal*^{dsRNA}	BDSC (BL 31879)
Fig. S1	*Wild Type*	*w+; +/+; +/+*	
Fig. S1	*L2 ≫ tdTomato,Sh::GFP*	*Shaker*$^{MI10885-GFSTF.2}$*; UAS-tdTomato/+; L2*^{21Dhh} *-Gal4/+*	
Fig. S1	*L3 ≫ tdTomato,Sh::GFP*	*Shaker*$^{MI10885-GFSTF.2}$*; UAS-tdTomato/L3*^{MH56}*-Gal4; +/+*	
Fig. S3	*UAS-Shal*	*w+; L3*^{MH56}*-Gal4/+;UAS-GCaMP6f/UAS-Shal*	Ping and Tsunoda (2012)

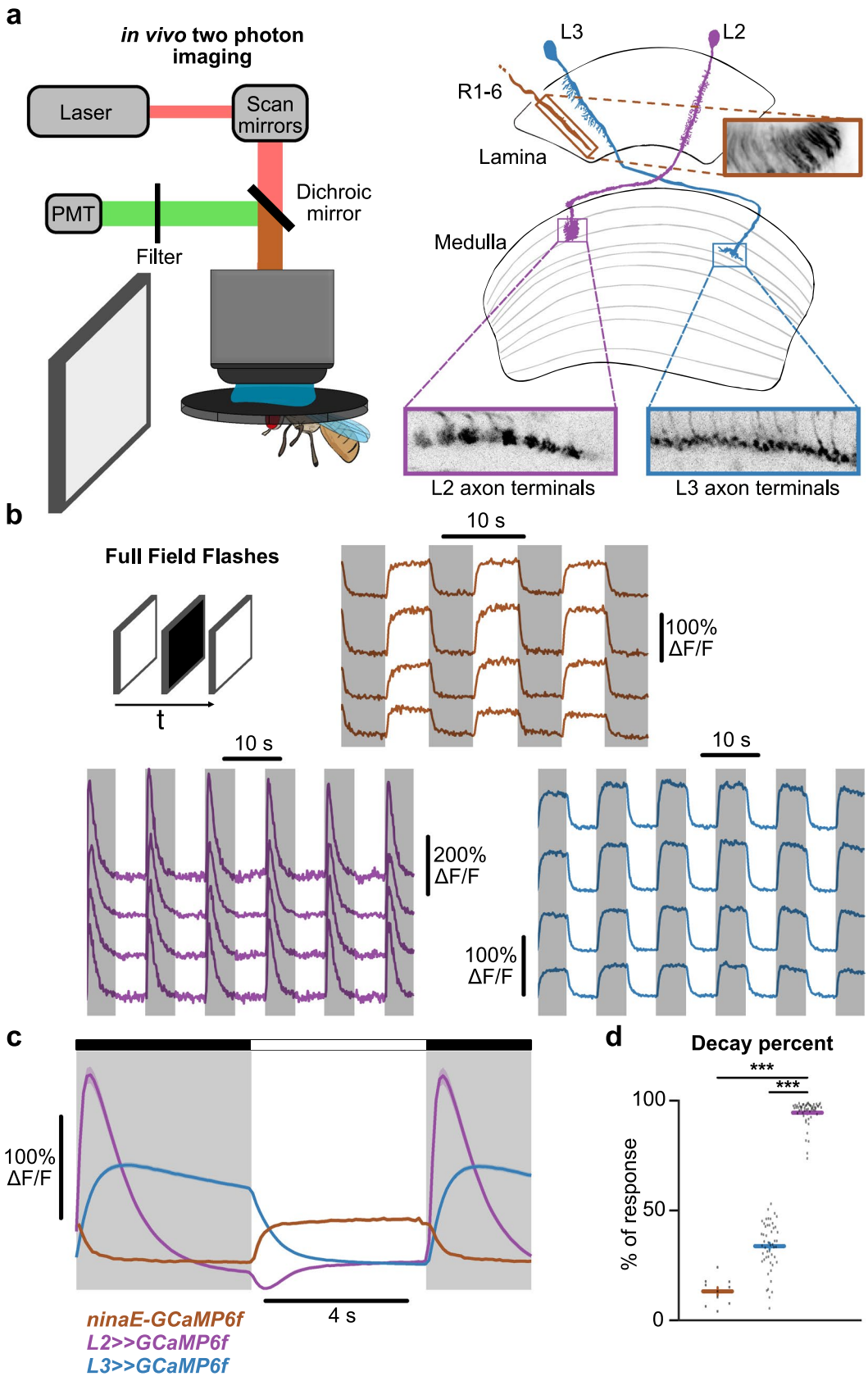
a
in vivo two photon imaging
Laser
Scan mirrors
PMT
Filter
Dichroic mirror
L3
L2
R1-6
Lamina
Medulla
L2 axon terminals
L3 axon terminals
b
Full Field Flashes
t
10 s
100% ΔF/F
10 s
200% ΔF/F
10 s
100% ΔF/F
c
100% ΔF/F
4 s
ninaE-GCaMP6f
L2>>GCaMP6f
L3>>GCaMP6f
d
Decay percent
***
***
100
50
0
% of response

Fig. 1 OFF pathway inputs L2 and L3 show differences in temporal calcium dynamics. **a** (Left) schematic of the two-photon imaging paradigm, where a fly is placed in a holder in front of a screen used for visual stimulation. (Right) the first two neuropils of the optic lobe: the lamina and the medulla. The lamina monopolar cells L2 (magenta) and L3 (blue) receive inputs from photoreceptor R1–R6 projections (brown) in the lamina. L2 and L3 outputs project to distinct layers of the medulla. Single neurons from one column are represented. Insets show in vivo two-photon images of axon terminals from R1 to R6, L2 and L3 neurons from several neighboring columns or cartridges, expressing the genetically encoded calcium indicator GCaMP6f that is used for calcium imaging. **b** Examples of calcium signals (ΔF/F) of single R1-R6, L2 and L3 axon terminals to 5 s full-field flashes of 100% contrast. **c** Calcium signals averaged over ROIs and flies (L2, $N=50$ flies [586 cells]; L3, $N=50$ [757 cells]; R1–R6, $N=10$ [86 cells]). Traces and shaded areas denote mean ± SEM. **d** Distribution plots showing the quantification of the change in the OFF response as a percentage of the maximum response for L2 and L3, and the minimum response for R1–R6 until the last second. In addition to individual flies, mean ± SEM is shown. $***p<0.001$ according to Kruskal–Wallis test followed by multiple comparisons using Dunn's test. Normality of samples was assessed using Lilliefors test

the mean (SEM) were calculated across flies after averaging over axon terminals for each brain. For normally distributed data sets, a two-tailed Student *t* test for unpaired (independent) samples was used. For other data sets, Wilcoxon rank-sum was used for statistical analysis. Normality was tested using Lilliefors test. Statistical analysis was done using MATLAB R2019a (The MathWorks Inc., Natick, MA).

In vivo two-photon calcium imaging

Fly preparation, experimental setup, and data acquisition

Up to 5-day-old female flies were used for imaging experiments. Dissection and experiments were performed at RT in a dark room. Flies were anaesthetized by cooling them on ice and mounted onto a custom-made stainless-steel microscope holder. The thorax and the head of the fly were fixed with a UV-sensitive glue (Bondic), such that the fly's eye was below the steel foil and faced the stimulation screen while exposing the back of the head for imaging experiments. The cuticle was removed using breakable razor blades and fine forceps were used to remove fat bodies and trachea. During imaging, the flies were perfused with a carboxygenated saline (103 mM NaCl, 3 mM KCl, 5 mM TES, 1 mM NaH_2PO_4, 4 mM $MgCl_2$, 1.5 mM $CaCl_2$, 10 mM trehalose, 10 mM glucose, 7 mM sucrose, and 26 mM $NaHCO_3$). Dissections were done in the same solutions lacking sugars and $CaCl_2$. Imaging experiments were performed on a Bruker Investigator 2-photon microscope (Bruker, Madison, WI, USA) equipped with a 25×/1.1 objective (Nikon, Minato, Japan). The excitation laser (Spectraphysics Insight DS +) was set to 920 nm to excite GCaMP6f, applying 5–15 mW of power to the sample. Emitted light was filtered using a SP680 short-pass filter, a 560 lpxr dichroic filter, and a 525/70 emission filter. Data were acquired using Prairie View software at a frame rate of ~ 10–15 Hz and around 6–8× optical zoom.

Pharmacology

All pharmacological agents were stored, handled, and disposed of as indicated in the corresponding SDS and/or information sheets. Agitoxin-2 and Phrixotoxin-2 were purchased from Alomone Labs (STA-420, STP-710). All agents were first dissolved in water and kept as stock solutions (Agitoxin-2 at 24 µM, Phrixotoxin-2 at 25 µM) at − 20 °C for a maximum duration of 1 month. For experiments, toxin stock solutions were allowed to equilibrate to RT for at least 1 h before dilution to the working concentrations in the imaging solution. This working solution was used for a maximum of 3 days, stored at 4 °C. Agitoxin-2 was used at 0.2 µM and Phrixotoxin-2 was used at 0.5 µM. All toxins were bath applied. No perfusion was used before or after toxin application. The toxin was allowed to penetrate for 5 min before the start of experiments. For sham experiments, imaging solution was used instead of toxin-containing solution. The same medulla layers of a fly were imaged before and after toxin applications to allow for paired comparisons.

Visual stimulation

Visual stimuli were generated using custom-written software using C++ and OpenGL and presented using a LightCrafter 4500 (Texas Instruments, Texas, USA) running at a frame rate of 100 Hz. The imaging and the visual stimulus presentation were synchronized as described previously (Freifeld et al. 2013). Stimulus light was filtered by a 482/18 bandpass and ND1.0 neutral density filter and projected onto an 8 cm × 8 cm rear projection screen that was positioned in front of the fly and spanning a visual angle of 60° in azimuth and elevation. Periodic, alternating full contrast (100% Weber contrast) ON and OFF flashes covering the whole screen, each lasting 5 s, were presented to the flies. Each stimulus epoch was presented for ~ 7 trials. Before each stimulus presentation, neurons were imaged for 5 s to measure the dark-adapted calcium levels, which were quantified as the baseline calcium signal in L2 and L3 neurons.

Data analysis

All data processing was performed offline using MATLAB R2019a (The MathWorks Inc., Natick, MA). To correct for motion artifacts, individual images were aligned to a reference image composed of a maximum intensity projection of the first 30 frames. The average intensity for manually selected regions of interests (ROIs) was computed for each

imaging frame and background subtracted to generate a time trace of the response. All responses and visual stimuli were interpolated at 10 Hz and trial averaged. Neural responses are shown as relative fluorescence intensity changes over time ($\Delta F/F_0$). The mean and the standard error of the mean (SEM) were calculated across flies after averaging over ROIs for each fly. For normally distributed data sets, a two-tailed Student *t* test for paired or unpaired (independent) samples was used. For other data sets, Wilcoxon signed-rank for paired and Wilcoxon rank-sum for unpaired samples were used for statistical analysis. Normality was tested using Lilliefors test. For multiple comparisons (Fig. 1d), a Kruskal–Wallis test was used followed by Dunn's test for comparing pairs of samples.

To calculate $\Delta F/F_0$, the mean of the whole trace was used as F_0. In some recordings, a minority of ROIs responded in opposite polarity (positively correlated with stimulus), as described previously (Fisher et al. 2015). These ROIs were referred to as "inverted" and have their receptive fields outside the stimulation screen (Freifeld et al. 2013; Fisher et al. 2015). To discard the "inverted" and other noisy ROIs, we applied a threshold consisting of an amplitude threshold and a correlation threshold. The amplitude threshold was defined as 2× the standard deviation of the ON epoch and applied to the maximum response within the OFF epoch. Pearson's correlation coefficient was used to discard ROIs that had a positive correlation with the stimulus. A further absolute threshold of 0.1 ΔF/F was used to discard non-responding ROIs. This thresholding method discarded similar amounts of ROIs before and after toxin conditions (Online Resource 1). For photoreceptors R1–R6, ROIs that had a positive correlation (> 0.3) were taken for further analysis.

OFF-step responses were calculated as the difference between the ΔF/F value one frame before the contrast step and the maximum value after the step. The ON-step response was calculated similarly but using the minimum value. Baseline calcium signal was calculated as the mean of the pre-stimulus period that lasted for 5 s. Decay percentages were calculated as the ratio between mean ΔF/F value during the last second of the OFF stimulation and the maximum OFF response (L2 and L3) or the minimum OFF response (R1–R6). Decay rates for L2 neurons were estimated by fitting an exponential function in the form of $N_t = N_0 e^{-\lambda t}$ to the OFF responses (starting from 200 ms after the peak until the 3rd second of the OFF epoch). This was done to ensure that the exponential decay part of the L2 is captured. Goodness of fit was assessed by calculating the R-squared value and a threshold of R-squared > 0.8 was used to select ROIs.

All data values as mean, standard deviation and SEM along with the *p* values are reported in Online Resource 2.

Results

L2 and L3 exhibit different decay times in their calcium response to visual stimuli

Previous studies showed that L2 and L3 responses are transient and sustained, respectively (Reiff et al. 2010; Clark et al. 2011; Silies et al. 2013; Fisher et al. 2015). To determine how L2 and L3 calcium dynamics relate to the calcium signal of their major inputs, photoreceptors R1–R6, we used in vivo two-photon imaging in combination with visual stimulation. We measured calcium signals in R1–R6, L2, and L3 axon terminals under the same imaging and stimulus conditions (Fig. 1a, b). To measure R1–R6 calcium responses, we expressed the genetically encoded calcium indicator GCaMP6f (Chen et al. 2013) using a *ninaE-GCaMP6f* fusion (Asteriti et al. 2017), and specific Gal4-driver lines were used to express GCaMP6f in either L2 or L3 neurons (Fig. 1b).

Previous studies showed that invertebrate photoreceptors respond to visual stimuli with fast and slow response components. The fast component is composed of a transient peak lasting from tens to hundreds of milliseconds, whereas the slow component is a sustained response that is present throughout the stimulation (Laughlin and Hardie 1978). When we presented flies with full-field contrast flashes of 5 s each, as expected from the voltage responses of the photoreceptors, calcium signals in R1–R6 axon terminals increased following brightness increments (ON step) and decreased following brightness decrements (OFF step) (Fig. 1b, Laughlin and Hardie 1978; Kohn et al. 2015; Asteriti et al. 2017). R1–R6 calcium signals were sustained and thus captured the steady-state component of the photoreceptor response. Calcium responses of L2 and L3 axon terminals increased during the OFF step (Fig. 1b, see also Fisher et al. 2015), consistent with a sign inversion mediated by the histaminergic photoreceptor–LMC synapse (Hardie 1987, 1989). Single neurons responded very robustly to stimulation, and responses of single axon terminals within one cell type were highly similar (Fig. 1b). L3 calcium dynamics showed only limited decay after the initial calcium increase in response to the OFF step, which resembles photoreceptor calcium signals (Fig. 1b, c). In contrast, calcium signals in L2 neurons decayed rapidly back to baseline levels (Fig. 1b, c). Analysis of the response decay during a 5 s presentation of the visual stimulus (OFF epoch) revealed that sustained L3 and R1–R6 neurons decayed significantly less than L2 neurons (Fig. 1d, L2 94%, L3 34%, PR 13%). Taken together, our results highlight a distinct signal transformation step between R1–R6 and L2 neurons, suggesting that L2 properties are mediated by distinct, L2-specific membrane properties.

The K_a channels Shaker and Shal are strongly expressed in L2

To identify candidates that mediate transient L2 responses, we focused on K_v channels, because they regulate active membrane properties and are critical for counteracting depolarization (Hille 2001). Numerous studies have shown important roles for K_v channels in neurons of the insect visual system, especially photoreceptors and LMCs (Hardie and Weckström 1990; Weckström et al. 1991; Hardie 1991; Weckström et al. 1992; Uusitalo et al. 1995; Anderson and Hardie 1996; Niven et al. 2003; Juusola et al. 2003; Vahasoyrinki et al. 2006; Frolov et al. 2016; Rusanen and Weckström 2016). Studies in blowfly LMCs showed that L2-type neurons exhibit a fast-inactivating K_a current, whereas L3-type neurons display a delayed rectifier K_d current (Hardie and Weckström 1990; Rusanen and Weckström 2016). However, the roles of these currents have not been investigated in the LMCs of *Drosophila* which differs ecologically from blowflies. Thus, we took an unbiased approach to find candidate K_v channels that are responsible for L2 transient responses in *Drosophila*.

In *Drosophila melanogaster*, there are nine K_v channels that have been shown to regulate different aspects of neural and muscle membranes (Frolov et al. 2012). Using a cell-type-specific RNA-seq data set, we compared mRNA expression levels for these channels in L2 and L3 (Fig. 2a, Davis et al. 2018). We found that the two most differentially expressed K_v channel genes were *Shaker (Sh)* and *Shal*, arguing that they might play a role in specializing L2 responses. Sh and Shal are the only K_v channels that mediate K_a currents in *Drosophila* (Wei et al. 1990; Covarrubias et al. 1991). This is in line with blowfly LMC properties, where L2-type neurons use K_a currents, further suggesting a conserved property of signal processing (Rusanen and Weckström 2016). To determine where endogenous Sh and Shal channels are expressed in the *Drosophila* optic lobe, we used a protein tagging approach based on recombinase-mediated cassette exchange. A genetic cassette containing EGFP (GFSTF) flanked by a splice acceptor and a donor was inserted into the intronic regions of the coding domains of the *Shaker* and *Shal* genes (Fig. 2b, Nagarkar-Jaiswal et al. 2015). In $Sh^{MI10885-GFSTF.2}$ flies, the Sh::GFP signal was broadly present throughout the visual system, including the lamina, parts of the medulla, and the lobula plate (Fig. 2c, Fig. S1b,c). However, it was not possible to resolve individual cell types. We then quantified the relative Sh::GFP signal within either L2 or L3 axon terminals by additionally expressing the red fluorescent protein tdTomato in L2 or L3 neurons (see "Materials and methods"). We did not observe a significant difference between L2 and L3 (Fig. S1d). However, the $Sh^{MI10885-GFSTF.2}$ insertion does not cover all *Sh* transcripts and this might explain the discrepancy between the RNA-seq data set and protein tagging approaches. In $Shal^{MI00446-GFSTF.1}$ flies, there was diffuse expression throughout the visual system (Fig. 2d). Strikingly, the Shal::GFP signal was strongest in the lamina, as well as in the medulla layer M2. The signal in the M2 layer resembled the bulb-like shape of L2 axon terminals (Fig. 2d, arrows). When we expressed the red fluorescent protein tdTomato in L2 or L3 neurons, L2 axon terminals and axons co-localized with the GFP signal, confirming that Shal is strongly expressed in L2 (Fig. 2e, Fig. S1e). In contrast, L3 axon terminals did not co-localize with the GFP signal, arguing against a prominent role for Shal in L3 (Fig. 2f, Fig. S1f). The quantification of the relative Shal::GFP signal revealed a significant increase for L2 relative to L3 axon terminals, further supporting Shal enrichment in L2 (Fig. S1g). Taken together, these data suggest that Sh and Shal are strong candidates for mediating L2 response properties.

K_a channels enhance L2 contrast responses and sharpen L2 kinetics

To test whether Sh and Shal play a functional role in L2 physiological properties, we acutely targeted Shaker and Shal using pharmacological agents. While imaging GCaMP6f responses, we applied specific blockers of Sh or Shal and imaged L2 and L3 responses to visual stimulation before and after toxin application. When we applied agitoxin, a specific blocker for Shaker channels (Garcia et al. 1994; Gross and MacKinnon 1996; Gutman et al. 2005) (Fig. 3a), we observed a significant decrease in response to the OFF step and a significant increase in the downward response to the ON step (Fig. 3ai, Fig. S2a). The same effect was also visible when we applied phrixotoxin, a Shal-specific blocker (Diochot et al. 1999; Gasque et al. 2005) (Fig. 3b, bi). These data suggest that K_a channels are involved in regulating the amplitude of L2 responses to contrast. Since both the OFF and ON step responses were modulated, we hypothesized that K_a channels might regulate baseline levels and shift the dynamic range of L2 neurons, so that OFF stimuli have a large gain. We thus assessed the effects of blocking K_a channels on the calcium baseline levels of L2 neurons by measuring the GCaMP6f signal before stimulation, in a period of darkness lasting for 5 s (Fig. 3c). Importantly, GCaMP baseline could be measured within the same flies and even the same imaging planes, before and after toxin application (Fig. 3c). Baseline calcium levels in L2 axon terminals were significantly higher when either of the K_a channels was blocked (Fig. 3ci, cii), suggesting a shift in L2 dynamic range.

Since a prominent feature of L2 responses is their transient nature, we investigated whether K_a channels alter the temporal dynamics of *Drosophila* L2 neurons. After applying either the Shaker blocker agitoxin or the Shal blocker

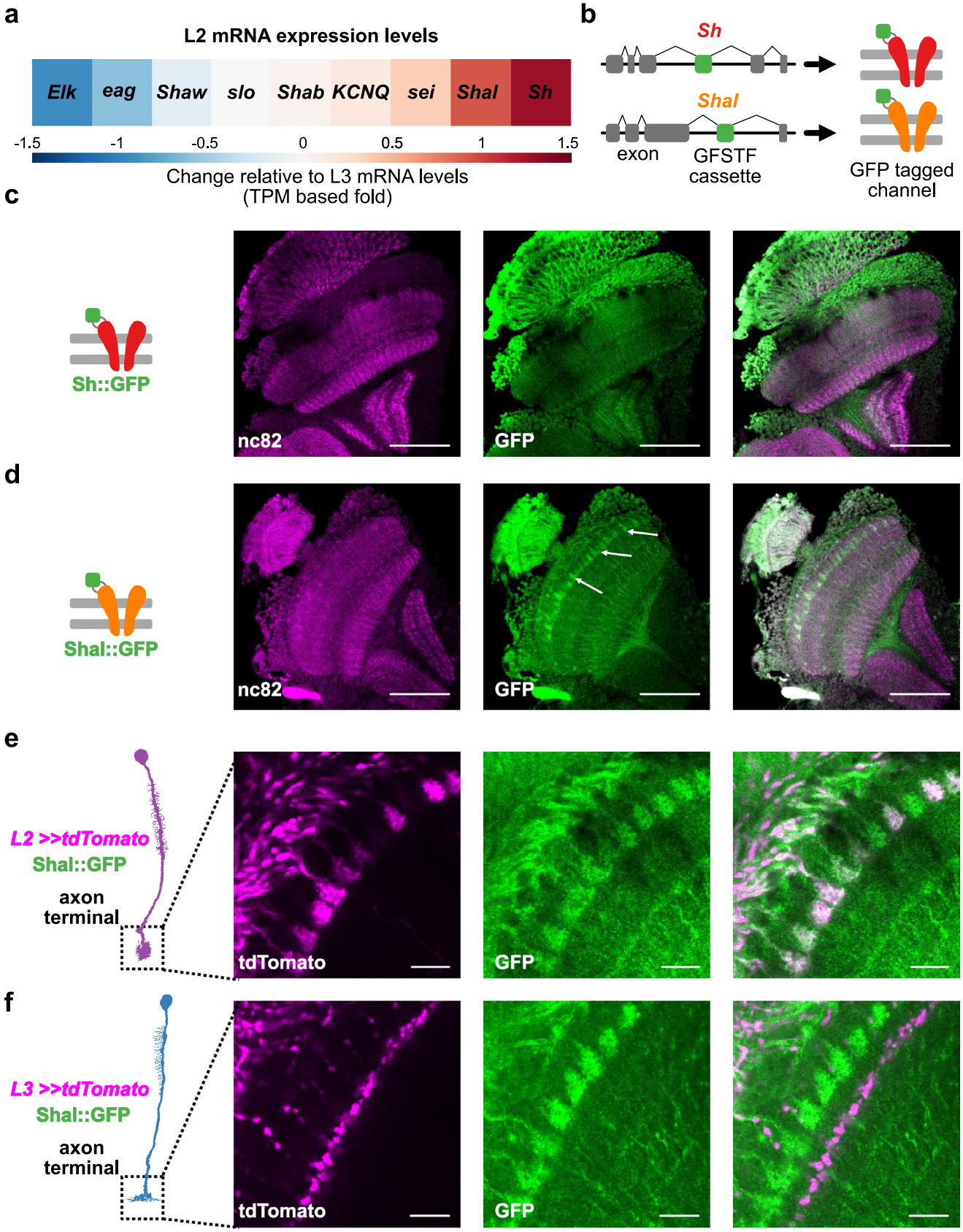
a
L2 mRNA expression levels
Elk
eag
Shaw
slo
Shab
KCNQ
sei
Shal
Sh
-1.5
-1
-0.5
0
0.5
1
1.5
Change relative to L3 mRNA levels
(TPM based fold)
b
Sh
Shal
exon
GFSTF
cassette
GFP tagged
channel
c
Sh::GFP
nc82
GFP
d
Shal::GFP
nc82
GFP
e
L2 >>tdTomato
Shal::GFP
axon
terminal
tdTomato
GFP
f
L3 >>tdTomato
Shal::GFP
axon
terminal
tdTomato
GFP

Fig. 2 K_a channels Shal and Shaker (Sh) are primary candidates to mediate L2 specialization. **a** K_V channel mRNA expression levels represented as fold change in L2 relative to L3 (based on TPM levels). RNA-seq data from Davis et al. (2018) (GEO accession number: GSE 116969). **b** GFP exon trapping of *Sh* and *Shal* genes to label the endogenous proteins. (**c**, **d**) Confocal section of a fly visual system expressing **c** endogenously tagged Sh::GFP ($Shaker^{MI10885-GFSTF.2}$) or **d** Shal::GFP ($Shal^{MI00446-GFSTF.1}$). The brain is labeled with nc82 (magenta) to label the neuropil, and anti-GFP (green). Scale bars are 50 µm. (**e**, **f**) Confocal section of a medulla region showing the expression pattern of Shal::GFP (green) along with the expression of a red fluorescent marker (tdTomato, magenta) expressed specifically in **e** L2 neurons or in **f** L3 neurons. Scale bars are 10 µm

phrixotoxin, the decay rate of L2 responses to the OFF step was significantly reduced (Fig. S2b, Fig. 3aii, bii). Sham controls did not show any change in L2 properties, and neither of the two toxins influenced the response properties of L3 (Fig. S2c–e), arguing that the phenotypes are specific. After the K_a channel manipulations, L2 neurons did not become fully sustained, arguing that additional mechanisms contribute to L2 specialization. In summary, our data indicate that K_a channels enhance L2 responses to OFF stimuli and are involved in sharpening L2 responses, thus contributing to the specialization of L2 neurons.

K_a channels sharpen the decay kinetics of L2 neuron cell-autonomously

The effects of pharmacological manipulation of L2 neuron properties could be non-cell-type specific and arise anywhere within the visual system. Therefore, we assessed the cell-autonomous role of K_a channels in L2 neurons by expression of dsRNA targeting either *Sh* or *Shal* in L2 cells (Fig. 4a, b). In $L2 \gg Sh^{dsRNA}$ flies, the response amplitude to either the ON or OFF step did not differ from control L2 neurons, contrasting with the results obtained in the toxin experiments (Figs. 3, 4a, ai). When we expressed $Shal^{dsRNA}$ in L2, the responses to the OFF or ON step were again unchanged, unlike in the phrixotoxin experiments (Figs. 3bi, 4bi). This suggests that K_a channels expressed in visual circuitry other than L2 neurons themselves are responsible for controlling L2 response amplitudes.

When we assessed the temporal response properties of L2 neurons, we observed that knockdown of *Sh* led to a longer decay of the L2 calcium signal (Fig. 4a). Quantification of the decay rate showed that this effect was significant compared to control L2 responses (Fig. 4aii). This is the same phenotype that was observed when Sh was pharmacologically blocked using agitoxin (Fig. 3aii). The same phenotype was observed upon cell-type specific expression of $Shal^{dsRNA}$ in L2 neurons (Fig. 4b, bii). Decay rates of L2 OFF responses were significantly lower than control responses, again resembling the pharmacological block of Shal (Figs. 3bii, 4bii). To ask if K_a channels are alone sufficient to generate more transient responses in sustained L3 neurons, we expressed *Shal* in L3 neurons using an overexpression construct (*UAS-Shal*, Ping and Tsunoda 2012). This did not change L3 responses to light, showing that Shal alone is not sufficient for transient responses (Fig. S3). Taken together, our results show that the K_a channels Sh and Shal enhance L2 contrast responses within visual circuitry, and Sh and Shal channels cell-autonomously sharpen the transient L2 response.

Discussion

Here, we identified a role for the K_a channels Shal and Shaker in specializing *Drosophila* first-order visual interneurons. The L2 and L3 inputs to the OFF pathway exhibit calcium signals with different temporal dynamics, suggesting distinct roles in visual circuitry. Transient responses in L2 differ strikingly from photoreceptor calcium signals, indicating that distinct mechanisms regulate L2 properties. Using an existing single-cell RNA-seq data set (Davis et al. 2018), we identified *Shaker* and *Shal* as the most highly expressed *Drosophila* K_v channels in L2. Shal protein can be clearly visualized in the axons and axon terminals of L2 neurons. Physiologically, both K_a channels are involved in modulating baseline levels and enhancing OFF contrast responses of L2 neurons. Furthermore, both Shaker and Shal cell-autonomously sharpen L2 kinetics. Taken together, our data demonstrate a role for the K_a-type potassium channels Shaker and Shal in refining distinct neuronal properties within a defined circuit.

The K_a channels Shaker and Shal mediate different L2 visual response properties

Our work demonstrates that K_a channels enhance the OFF responses of L2 neurons, change their baseline calcium signal, and sharpen their transient responses. While a reduction in *K* currents is normally associated with increased excitability, our data revealed a smaller dynamic range for OFF responses when K_a currents are absent. Here, a shift in calcium baseline can lead to a shift in dynamic range. Similarly, a shift in resting potential or dynamic range has been associated with K_v currents, since a fraction of these channels can be found open in resting potentials (Hille 2001; Niven et al. 2003; Abou Tayoun et al. 2011). In L2 neurons, K_a channels can thus facilitate transmission of OFF information to the fly visual circuitry. Interestingly, under dynamic light conditions, L2 neurons provide information about both brightness decrements and increments (Clark et al. 2011), suggesting

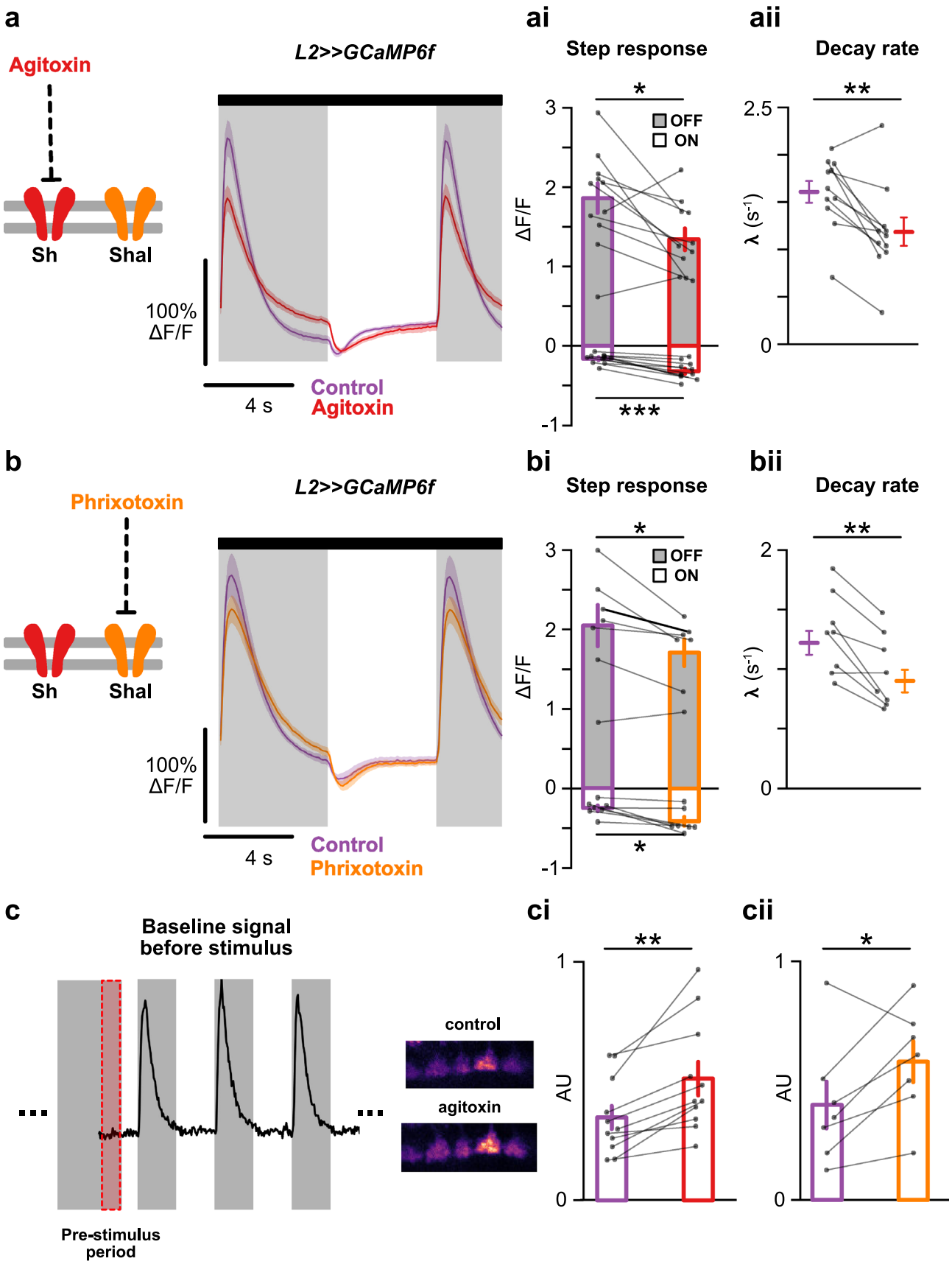
a
Agitoxin
Sh
Shal
L2>>GCaMP6f
100%
ΔF/F
4 s
Control
Agitoxin
ai
Step response
OFF
ON
ΔF/F
aii
Decay rate
λ (s⁻¹)
b
Phrixotoxin
Sh
Shal
L2>>GCaMP6f
100%
ΔF/F
4 s
Control
Phrixotoxin
bi
Step response
OFF
ON
ΔF/F
bii
Decay rate
λ (s⁻¹)
c
Baseline signal
before stimulus
Pre-stimulus
period
control
agitoxin
ci
AU
cii
AU

Fig. 3 K_a channels enhance OFF responses, modulate baseline and increase decay rates of L2 neurons. **a** Agitoxin was used to selectively block Shaker (Sh) channels. In vivo imaging of L2 axon terminal calcium responses (ΔF/F) before (magenta, $N=11$ flies [121 cells]) and after (red, $N=11$ [99 cells]) toxin application. (ai) Bar plots showing the quantification of OFF (gray filled bars) and ON (white filled bars) step responses; (aii) OFF response decay rates. These data were acquired in the same fly before and after toxin application. **b** Phrixotoxin was used to selectively block Shal channels. In vivo imaging of L2 axon terminal calcium responses before (magenta, $N=7$ [96 cells]) and after (orange, $N=7$ [96 cells]) toxin application. (bi, bii) Bar and distribution plots showing the quantification of data. **c** Determination of the baseline signal levels during the pre-stimulus period within the same imaging planes, before and after (ci) agitoxin and (cii) phrixotoxin application. Example of L2 axon terminal calcium signals during this interval are shown. All traces and plots show mean ± SEM. $*p<0.05$, $**p<0.01$ according to paired Student t test if data was normally distributed, otherwise Wilcoxon signed-rank test was used. Normality of samples was assessed using Lilliefors test

that regulation of the dynamic range might depend on the context.

Time constants of neural membranes are important in determining the signaling bandwidth of neurons. K_a channels give L2 neurons high-pass filtering characteristics by reducing the time constant of the OFF response. This reduction in time constant could be a specific property of K_a channels in regulating the temporal properties of neurons, and the fact that L2 specific knockdown of K_a affects decay rate, but not response amplitude argues in favor of that idea. However, unlike for the pharmacological experiments (which were done in paired samples), we did not compare baseline calcium signal in control and knockdown flies. Thus, the altered decay rate might also be a consequence of a changed resting state, which then can lead to a change in the driving force of calcium. The signal-processing properties regulated by K_a channels might be important for L2 to convey information about fast changes in the visual scenery, one of the described roles of L2 neurons (Tuthill et al. 2013). Similarly, blowfly L2-type neurons utilize K_a channels to facilitate high-frequency transmission (Rusanen and Weckström 2016). Whereas the different visual ecologies of these species have driven differential expression of K_v channels to evolve in their photoreceptors (Weckström et al. 1991; Hardie 1991; Weckström and Laughlin 1995), the neurons downstream thus seem to conserve K_a expression across species. This suggests a common role of L2-type LMCs, irrespective of ecologies (Laughlin and Weckström 1993). K_a currents in L2-type neurons in other flies have prominent roles in regulating the hyperpolarizing response to the onset of light, but they also regulate a so-called "light-off spike" by modulating its falling phase and increasing the frequency response of the signal (Hardie and Weckström 1990; Rusanen and Weckström 2016). While no such light-off spike has been found in *Drosophila* LMCs (Zheng et al. 2006, 2009), K_a channels still appear to modify graded L2 responses.

Shaker and Shal have both cell-autonomous and non-cell-autonomous roles

Cell-type-specific downregulation of K_a channels showed that Shal and Shaker cell-autonomously regulate the kinetics of the L2 response, but not its amplitude. One possibility is that knockdown of the K_a channels was partial and thus resulted in a milder phenotype than using pharmacological agents. However, the $Shal^{dsRNA}$ line was previously shown to reproduce Shal null mutant phenotypes (Bergquist et al. 2010; Feng et al. 2018). The discrepancy between cell-type-specific and broad effects on L2 function can also be explained by the role of K_a channels in circuitry outside of L2. Previous studies have identified a Shaker-mediated K_a current in R1–R6 (Hardie 1991), the major L2 input, which is involved in amplifying photoreceptor light responses for optimized usage of their voltage range (Niven et al. 2003). Calcium signals at the R1–R6 presynapse would, therefore, also very likely be reduced. R1–R6 also exhibit two other types of potassium currents, one of which is a rapidly inactivating delayed rectifier that highly resembles Shal properties (Hardie 1991; Vahasoyrinki et al. 2006). These observations provide a possible explanation for the toxin effects on response amplitude of L2 neurons. As an alternative explanation, chronic manipulations of ion channels might trigger homeostatic mechanisms that provide robustness to changing ion channel levels (Marder and Goaillard 2006; Davis 2006). Consistent with this possibility, Shal and Shaker were found to be transcriptionally coupled in *Drosophila* (Bergquist et al. 2010). Interestingly, Shaker and Shal channels were also found to be co-expressed in other systems, such as *Drosophila* mushroom body neurons and flight motor neurons, where Shaker and Shal together constitute the total K_a current (Gasque et al. 2005; Ryglewski and Duch 2009). Furthermore, Shaker and Shal show different temporal kinetics when expressed in Xenopus oocytes (Wei et al. 1990; Covarrubias et al. 1991), arguing that they might regulate neuronal response properties in different temporal regimes.

K_v channels in fly LMCs

RNA expression data suggest that K_a-type channels are much more strongly expressed in L2 cells harboring transient calcium signals than in sustained L3 neurons. In blowfly LMCs, the combination of identified K_v conductances is also one of the factors that distinguish L2-type from L3-type neurons (Hardie and Weckström 1990; Rusanen and Weckström 2016). L2-type neurons exhibit a prominent K_a current (Hardie and Weckström 1990)

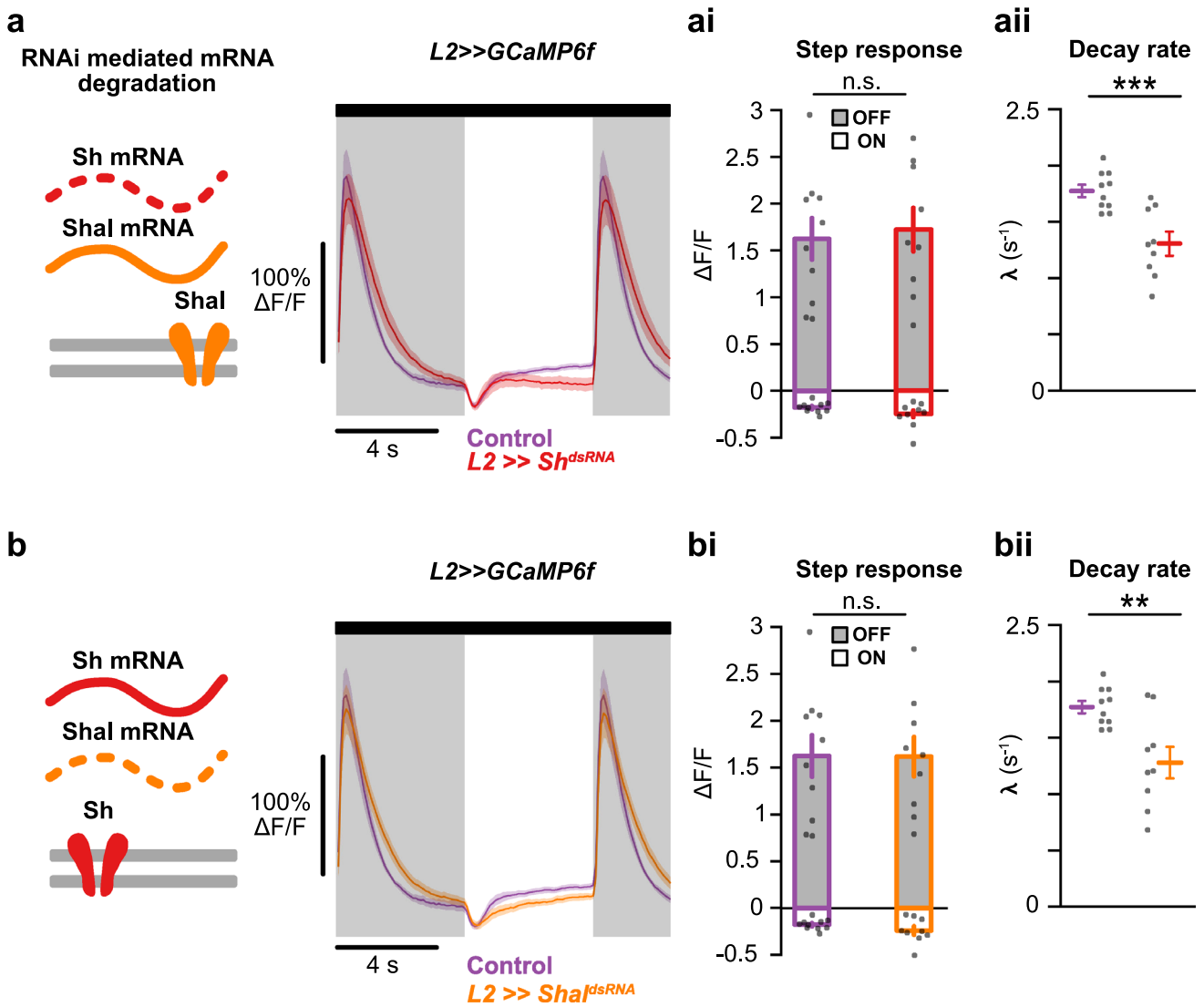

Fig. 4 K_a channels Shaker (Sh) and Shal cell-autonomously sharpen kinetics of L2 neurons **a** RNAi-mediated knockdown of the *Sh* gene in L2 neurons. In vivo imaging of L2 axon terminal calcium responses (ΔF/F) of control (magenta, $N=10$ flies [134 cells]) and $L2 \gg Sh^{dsRNA}$ (red, $N=8$ [103 cells]). (ai) Bar plots showing the quantification of OFF (gray filled) and ON (white filled) step responses, and (aii) distribution plots showing the OFF response decay rates. **b** RNAi-mediated knockdown of the *Shal* gene in L2 neurons. Calcium responses of control (magenta, $N=10$ [134 cells]) and $L2 \gg Shal^{dsRNA}$ (orange, $N=9$ (125 cells]). (bi, bii) Bar and distribution plots showing the quantification of data. All traces and plots show mean ± SEM. $^*p<0.05$, $^{**}p<0.01$, $^{***}p<0.001$ according to two-tailed Student *t* test. Normality of samples was assed using Lilliefors test

that is pronounced in axonal compartments (Rusanen and Weckström 2016). Together with the data presented here, this argues for a conserved mechanism in early visual processing of flies. Endogenous protein tagging even showed that the K_a channel Shal localizes to L2 axons and axon terminals, arguing for active signal processing that can prevent the attenuation of fast signals in LMCs (Rusanen and Weckström 2016), rather than purely passive transmission (van Hateren and Laughlin 1990). Our calcium-imaging approach allowed us to investigate the roles of K_a channels after any such signal processing has taken place. Although in vivo calcium recordings will miss fast aspects of the neuronal response that can be captured in electrophysiological recordings, it is interesting to see that we isolated distinct roles for the K_a channels Shaker and Shal that are consistent with previous voltage recordings in other species.

Finally, blowfly LMCs also display a small K_d current in L2 and a strong K_d current in L3 responsible for additional high-pass filtering of signals (Rusanen and Weckström 2016). RNA-seq data suggest that Shaw channels are expressed in both L2 and L3 and highly expressed in

L3, making Shaw a molecular candidate for K_d currents present in LMCs (Davis et al. 2018).

Additional factors mediating transient L2 responses

Neither blocking Shal nor Shaker produced fully sustained responses, indicating that additional mechanisms play a role in L2 transient responses. L2-type LMCs from blowflies and fruit flies display an antagonistic center-surround receptive field that shapes temporal response properties of LMCs, arguing that circuit mechanisms might play further roles in regulating the kinetics of the L2 response (Arnett 1972; Mimura 1976; Dubs 1982; Laughlin and Osorio 1989; Freifeld et al. 2013). In fruit flies, surround inhibition is mainly mediated by GABAergic mechanisms that act both presynaptically in photoreceptors and outside the photoreceptor-L2 synapse (Freifeld et al. 2013). In addition, extracellular field potentials in the blowfly are involved in shaping LMC responses (Weckstrom and Laughlin 2010). Thus, a multiplex of mechanisms including K_v channels, center-surround receptive fields, and extracellular mechanisms may specialize a distinct LMC cell type to fulfill its specific role in visual processing.

Acknowledgements We are grateful to Christine Gündner for excellent technical assistance and to all members of the Silies lab for helpful discussion and comments on the manuscript. This work was supported by the Deutsche Forschungsgemeinschaft (DFG) through the Emmy Noether Program, grant SI1991/1-1, to MS.

Author contributions Burak Gür and Marion Silies conceptualized and designed the study. Burak Gür, Katja Sporar, and Anne Lopez-Behling performed experiments, and Burak Gür and Katja Sporar analyzed the data. Burak Gür and Marion Silies wrote the manuscript with input from all authors.

Compliance with ethical standards

Conflict of interest The authors declare no conflict of interests.

Ethical standards Experiments on *Drosophila* are not subject to the approval of ethics committee.

References

Abou Tayoun AN, Li X, Chu B, Hardie RC, Juusola M, Dolph PJ (2011) The *Drosophila* SK channel (dSK) contributes to photoreceptor performance by mediating sensitivity control at the first visual network. J Neurosci 31:13897–13910. https://doi.org/10.1523/JNEUROSCI.3134-11.2011

Anderson J, Hardie RC (1996) Different photoreceptors within the same retina express unique combinations of potassium channels. J Comp Physiol A. https://doi.org/10.1007/BF00190181

Arenz A, Drews MS, Richter FG, Ammer G, Borst A (2017) The temporal tuning of the *Drosophila* motion detectors is determined by the dynamics of their input elements. Curr Biol 27:929–944. https://doi.org/10.1016/j.cub.2017.01.051

Arnett DW (1972) Spatial and temporal integration properties of units in first optic ganglion of dipterans. J Neurophysiol 35:429–444. https://doi.org/10.1152/jn.1972.35.4.429

Asteriti S, Liu C-H, Hardie RC (2017) Calcium signalling in *Drosophila* photoreceptors measured with GCaMP6f. Cell Calcium 65:40–51. https://doi.org/10.1016/j.ceca.2017.02.006

Behnia R, Clark DA, Carter AG, Clandinin TR, Desplan C (2014) Processing properties of ON and OFF pathways for *Drosophila* motion detection. Nature 512:427–430. https://doi.org/10.1038/nature13427

Bergquist S, Dickman DK, Davis GW (2010) A Hierarchy of cell intrinsic and target-derived homeostatic signaling. Neuron 66:220–234. https://doi.org/10.1016/j.neuron.2010.03.023

Borst A (2014) Neural circuits for motion vision in the fly. Cold Spring Harb Symp Quant Biol 79:131–139. https://doi.org/10.1101/sqb.2014.79.024695

Chen T-W, Wardill TJ, Sun Y, Pulver SR, Renninger SL, Baohan A, Schreiter ER, Kerr RA, Orger MB, Jayaraman V, Looger LL, Svoboda K, Kim DS (2013) Ultrasensitive fluorescent proteins for imaging neuronal activity. Nature 499:295–300. https://doi.org/10.1038/nature12354

Clark DA, Bursztyn L, Horowitz MA, Schnitzer MJ, Clandinin TR (2011) Defining the computational structure of the motion detector in *Drosophila*. Neuron 70:1165–1177. https://doi.org/10.1016/j.neuron.2011.05.023

Coetzee WA, Amarillo Y, Chiu J, Chow A, Lau D, McCormack T, Morena H, Nadal MS, Ozaita A, Pountney D, Saganich M, Miera EV-S, Rudy B (1999) Molecular diversity of K + channels. Ann N Y Acad Sci 868:233–255. https://doi.org/10.1111/j.1749-6632.1999.tb11293.x

Covarrubias M, Wei A, Salkoff L (1991) Shaker, Shal, Shab, and Shaw express independent K + current systems. Neuron 7:763–773. https://doi.org/10.1016/0896-6273(91)90279-9

Davis GW (2006) Homeostatic control of neural activity: from phenomenology to molecular design. Annu Rev Neurosci 29:307–323. https://doi.org/10.1146/annurev.neuro.28.061604.135751

Davis FP, Nern A, Picard S, Reiser MB, Rubin GM, Eddy SR, Henry GL (2018) A genetic, genomic, and computational resource for exploring neural circuit function. bioRxiv. https://doi.org/10.1101/385476

de Souza J, Hertel H, Ventura DF, Menzel R (1992) Response properties of stained monopolar cells in the honeybee lamina. J Comp Physiol A 170:267–274. https://doi.org/10.1007/BF00191414

Demb JB, Singer JH (2015) Functional circuitry of the retina. Annu Rev Vis Sci 1:263–289. https://doi.org/10.1146/annurev-vision-082114-035334

Diochot S, Drici M-D, Moinier D, Fink M, Lazdunski M (1999) Effects of phrixotoxins on the Kv4 family of potassium channels and implications for the role of I_{to1} in cardiac electrogenesis. Br J Pharmacol 126:251–263. https://doi.org/10.1038/sj.bjp.0702283

Dubs A (1982) The spatial integration of signals in the retina and lamina of the fly compound eye under different conditions of luminance. J Comp Physiol A 146:321–343. https://doi.org/10.1007/BF00612703

Feng G, Zhang J, Li M, Shao L, Yang L, Song Q, Ping Y (2018) Control of sleep onset by Shal/K_v4 channels in *Drosophila* circadian neurons. J Neurosci 38:9059–9071. https://doi.org/10.1523/JNEUROSCI.0777-18.2018

Fisher YE, Leong JCS, Sporar K, Ketkar MD, Gohl DM, Clandinin TR, Silies M (2015) A class of visual neurons with wide-field properties is required for local motion detection. Curr Biol 25:3178–3189. https://doi.org/10.1016/j.cub.2015.11.018

Freifeld L, Clark DA, Schnitzer MJ, Horowitz MA, Clandinin TR (2013) GABAergic lateral interactions tune the early stages of visual processing in *Drosophila*. Neuron 78:1075–1089. https://doi.org/10.1016/j.neuron.2013.04.024

Frolov RV, Bagati A, Casino B, Singh S (2012) Potassium channels in *Drosophila*: historical breakthroughs, significance, and perspectives. J Neurogenet 26:275–290. https://doi.org/10.3109/01677063.2012.744990

Frolov R, Immonen E-V, Weckström M (2016) Visual ecology and potassium conductances of insect photoreceptors. J Neurophysiol 115:2147–2157. https://doi.org/10.1152/jn.00795.2015

Garcia ML, Garcia-Calvo M, Hidalgo P, Lee A, MacKinnon R (1994) Purification and characterization of three inhibitors of voltage-dependent K + channels from *Leiurus Quinquestriatus var. hebraeus* venom. Biochemistry 33:6834–6839. https://doi.org/10.1021/bi00188a012

Gasque G, Labarca P, Reynaud E, Darszon A (2005) Shal and shaker differential contribution to the K + currents in the *Drosophila* mushroom body neurons. J Neurosci 25:2348–2358. https://doi.org/10.1523/JNEUROSCI.4384-04.2005

Gohl DM, Silies MA, Gao XJ, Bhalerao S, Luongo FJ, Lin C-C, Potter CJ, Clandinin TR (2011) A versatile in vivo system for directed dissection of gene expression patterns. Nat Methods 8:231–237. https://doi.org/10.1038/nmeth.1561

Gross A, MacKinnon R (1996) Agitoxin footprinting the shaker potassium channel pore. Neuron 16:399–406. https://doi.org/10.1016/S0896-6273(00)80057-4

Gutman GA, Chandy KG, Grissmer S, Lazdunski M, Mckinnon D, Pardo LA, Robertson GA, Rudy B, Sanguinetti MC, Stühmer W, Wang X (2005) International union of pharmacology. LIII. nomenclature and molecular relationships of voltage-gated potassium channels. Pharmacol Rev 57:473–508. https://doi.org/10.1124/pr.57.4.10

Hardie RC (1987) Is histamine a neurotransmitter in insect photoreceptors? J Comp Physiol A 161:201–213. https://doi.org/10.1007/BF00615241

Hardie RC (1989) A histamine-activated chloride channel involved in neurotransmission at a photoreceptor synapse. Nature 339:704–706. https://doi.org/10.1038/339704a0

Hardie R (1991) Voltage-sensitive potassium channels in *Drosophila* photoreceptors. J Neurosci 11:3079–3095. https://doi.org/10.1523/JNEUROSCI.11-10-03079.1991

Hardie RC, Weckström M (1990) Three classes of potassium channels in large monopolar cells of the blowfly *Calliphora vicina*. J Comp Physiol A. https://doi.org/10.1007/BF00189763

Hille B (2001) Ion channels of excitable membranes, 3rd edn. Sinauer, Sunderland

Jenett A, Rubin GM, Ngo T-TB, Shepherd D, Murphy C, Dionne H, Pfeiffer BD, Cavallaro A, Hall D, Jeter J, Iyer N, Fetter D, Hausenfluck JH, Peng H, Trautman ET, Svirskas RR, Myers EW, Iwinski ZR, Aso Y, DePasquale GM, Enos A, Hulamm P, Lam SCB, Li H-H, Laverty TR, Long F, Qu L, Murphy SD, Rokicki K, Safford T, Shaw K, Simpson JH, Sowell A, Tae S, Yu Y, Zugates CT (2012) A GAL4-driver line resource for *Drosophila* neurobiology. Cell Rep 2:991–1001. https://doi.org/10.1016/j.celrep.2012.09.011

Joesch M, Schnell B, Raghu SV, Reiff DF, Borst A (2010) ON and OFF pathways in *Drosophila* motion vision. Nature 468:300–304. https://doi.org/10.1038/nature09545

Juusola M, Niven JE, French AS (2003) *Shaker* K^+ channels contribute early nonlinear amplification to the light response in *Drosophila* photoreceptors. J Neurophysiol 90:2014–2021. https://doi.org/10.1152/jn.00395.2003

Kohn E, Katz B, Yasin B, Peters M, Rhodes E, Zaguri R, Weiss S, Minke B (2015) Functional cooperation between the IP3 receptor and phospholipase C secures the high sensitivity to light of *Drosophila* photoreceptors *In Vivo*. J Neurosci 35:2530–2546. https://doi.org/10.1523/JNEUROSCI.3933-14.2015

Laughlin SB (1974) Neural integration in the first optic neuropile of dragonflies: III. The transfer of angular information. J Comp Physiol 92:377–396. https://doi.org/10.1007/BF00694708

Laughlin SB (1994) Matching coding, circuits, cells, and molecules to signals: general principles of retinal design in the fly's eye. Prog Retin Eye Res 13:165–196. https://doi.org/10.1016/1350-9462(94)90009-4

Laughlin SB, Hardie RC (1978) Common strategies for light adaptation in the peripheral visual systems of fly and dragonfly. J Comp Physiol A 128:319–340. https://doi.org/10.1007/BF00657606

Laughlin SB, Osorio D (1989) Mechanisms for neural signal enhancement in the blowfly compound eye. J Exp Biol 144:113–146

Laughlin SB, Weckström M (1993) Fast and slow photoreceptors–a comparative study of the functional diversity of coding and conductances in the *Diptera*. J Comp Physiol A 172:593–609. https://doi.org/10.1007/BF00213682

Marder E, Goaillard J-M (2006) Variability, compensation and homeostasis in neuron and network function. Nat Rev Neurosci 7:563–574. https://doi.org/10.1038/nrn1949

Mimura K (1976) Some spatial properties in the first optic ganglion of the fly. J Comp Physiol A 105:65–82. https://doi.org/10.1007/BF01380054

Nagarkar-Jaiswal S, Lee P-T, Campbell ME, Chen K, Anguiano-Zarate S, Gutierrez MC, Busby T, Lin W-W, He Y, Schulze KL, Booth BW, Evans-Holm M, Venken KJ, Levis RW, Spradling AC, Hoskins RA, Bellen HJ (2015) A library of MiMICs allows tagging of genes and reversible, spatial and temporal knockdown of proteins in *Drosophila*. eLife 4:e05338. https://doi.org/10.7554/eLife.05338

Niven JE, Vähäsöyrinki M, Kauranen M, Hardie RC, Juusola M, Weckström M (2003) The contribution of shaker K + channels to the information capacity of *Drosophila* photoreceptors. Nature 421:630–634. https://doi.org/10.1038/nature01384

Ping Y, Tsunoda S (2012) Inactivity-induced increase in nAChRs upregulates Shal K + channels to stabilize synaptic potentials. Nat Neurosci 15:90–97. https://doi.org/10.1038/nn.2969

Ramos-Traslosheros G, Henning M, Silies M (2018) Motion detection: cells, circuits and algorithms. Neuroforum 24:A61–A72. https://doi.org/10.1515/nf-2017-A028

Reiff DF, Plett J, Mank M, Griesbeck O, Borst A (2010) Visualizing retinotopic half-wave rectified input to the motion detection circuitry of *Drosophila*. Nat Neurosci 13:973–978. https://doi.org/10.1038/nn.2595

Ribi WA (1975) The first optic ganglion of the bee: I. Correlation between visual cell types and their terminals in the lamina and medulla. Cell Tissue Res. https://doi.org/10.1007/BF00222803

Ribi WA (1987) Anatomical identification of spectral receptor types in the retina and lamina of the Australian orchard butterfly, *Papilio aegeus aegeus D*. Cell Tissue Res. https://doi.org/10.1007/BF00218321

Rister J, Pauls D, Schnell B, Ting C-Y, Lee C-H, Sinakevitch I, Morante J, Strausfeld NJ, Ito K, Heisenberg M (2007) Dissection of the peripheral motion channel in the visual system of *Drosophila melanogaster*. Neuron 56:155–170. https://doi.org/10.1016/j.neuron.2007.09.014

Rusanen J, Weckström M (2016) Frequency-selective transmission of graded signals in large monopolar neurons of blowfly *Calliphora vicina* compound eye. J Neurophysiol 115:2052–2064. https://doi.org/10.1152/jn.00747.2015

Rusanen J, Vähäkainu A, Weckström M, Arikawa K (2017) Characterization of the first-order visual interneurons in the visual system of the bumblebee (*Bombus terrestris*). J Comp Physiol A 203:903–913. https://doi.org/10.1007/s00359-017-1201-9

Rusanen J, Frolov R, Weckström M, Kinoshita M, Arikawa K (2018) Non-linear amplification of graded voltage signals in the first-order visual interneurons of the butterfly *Papilio xuthus*. J Exp Biol 221:jeb179085. https://doi.org/10.1242/jeb.179085

Ryglewski S, Duch C (2009) *Shaker* and *Shal* mediate transient calcium-independent potassium current in a *Drosophila* flight motoneuron. J Neurophysiol 102:3673–3688. https://doi.org/10.1152/jn.00693.2009

Sanes JR, Zipursky SL (2010) Design principles of insect and vertebrate visual systems. Neuron 66:15–36. https://doi.org/10.1016/j.neuron.2010.01.018

Schindelin J, Arganda-Carreras I, Frise E, Kaynig V, Longair M, Pietzsch T, Preibisch S, Rueden C, Saalfeld S, Schmid B, Tinevez J-Y, White DJ, Hartenstein V, Eliceiri K, Tomancak P, Cardona A (2012) Fiji: an open-source platform for biological-image analysis. Nat Methods 9:676–682. https://doi.org/10.1038/nmeth.2019

Serbe E, Meier M, Leonhardt A, Borst A (2016) Comprehensive characterization of the major presynaptic elements to the *Drosophila* off motion detector. Neuron 89:829–841. https://doi.org/10.1016/j.neuron.2016.01.006

Shinomiya K, Huang G, Lu Z, Parag T, Xu CS, Aniceto R, Ansari N, Cheatham N, Lauchie S, Neace E, Ogundeyi O, Ordish C, Peel D, Shinomiya A, Smith C, Takemura S, Talebi I, Rivlin PK, Nern A, Scheffer LK, Plaza SM, Meinertzhagen IA (2019) Comparisons between the ON- and OFF-edge motion pathways in the *Drosophila* brain. eLife 8:e40-025. https://doi.org/10.7554/eLife.40025

Silies M, Gohl DM, Fisher YE, Freifeld L, Clark DA, Clandinin TR (2013) Modular use of peripheral input channels tunes motion-detecting circuitry. Neuron 79:111–127. https://doi.org/10.1016/j.neuron.2013.04.029

Silies M, Gohl DM, Clandinin TR (2014) Motion-detecting circuits in flies: coming into view. Annu Rev Neurosci 37:307–327. https://doi.org/10.1146/annurev-neuro-071013-013931

Stöckl AL, Ribi WA, Warrant EJ (2016) Adaptations for nocturnal and diurnal vision in the hawkmoth lamina: visual adaptations in the Hawkmoth Lamina. J Comp Neurol 524:160–175. https://doi.org/10.1002/cne.23832

Strother JA, Nern A, Reiser MB (2014) Direct observation of ON and OFF pathways in the *Drosophila* visual system. Curr Biol 24:976–983. https://doi.org/10.1016/j.cub.2014.03.017

Takemura S, Bharioke A, Lu Z, Nern A, Vitaladevuni S, Rivlin PK, Katz WT, Olbris DJ, Plaza SM, Winston P, Zhao T, Horne JA, Fetter RD, Takemura S, Blazek K, Chang L-A, Ogundeyi O, Saunders MA, Shapiro V, Sigmund C, Rubin GM, Scheffer LK, Meinertzhagen IA, Chklovskii DB (2013) A visual motion detection circuit suggested by *Drosophila* connectomics. Nature 500:175–181. https://doi.org/10.1038/nature12450

Takemura S, Nern A, Chklovskii DB, Scheffer LK, Rubin GM, Meinertzhagen IA (2017) The comprehensive connectome of a neural substrate for 'ON' motion detection in *Drosophila*. eLife 6:e24394. https://doi.org/10.7554/eLife.24394

Timofeev K, Joly W, Hadjieconomou D, Salecker I (2012) Localized netrins act as positional cues to control layer-specific targeting of photoreceptor axons in *Drosophila*. Neuron 75:80–93. https://doi.org/10.1016/j.neuron.2012.04.037

Tuthill JC, Nern A, Holtz SL, Rubin GM, Reiser MB (2013) Contributions of the 12 neuron classes in the fly lamina to motion vision. Neuron 79:128–140. https://doi.org/10.1016/j.neuron.2013.05.024

Uusitalo RO, Juusola M, Weckstrom M (1995) Graded responses and spiking properties of identified first-order visual interneurons of the fly compound eye. J Neurophysiol 73:1782–1792. https://doi.org/10.1152/jn.1995.73.5.1782

Vahasoyrinki M, Niven JE, Hardie RC, Weckström M, Juusola M (2006) Robustness of neural coding in *Drosophila* photoreceptors in the absence of slow delayed rectifier K + channels. J Neurosci 26:2652–2660. https://doi.org/10.1523/JNEUROSCI.3316-05.2006

van Hateren JH, Laughlin SB (1990) Membrane parameters, signal transmission, and the design of a graded potential neuron. J Comp Physiol A 166:437–448. https://doi.org/10.1007/BF00192015

Weckstrom M, Laughlin S (2010) Extracellular potentials modify the transfer of information at photoreceptor output synapses in the blowfly compound eye. J Neurosci 30:9557–9566. https://doi.org/10.1523/JNEUROSCI.6122-09.2010

Weckström M, Laughlin SB (1995) Visual ecology and voltage-gated ion channels in insect photoreceptors. Trends Neurosci 18:17–21. https://doi.org/10.1016/0166-2236(95)93945-T

Weckström M, Hardie RC, Laughlin SB (1991) Voltage-activated potassium channels in blowfly photoreceptors and their role in light adaptation. J Physiol 440:635–657. https://doi.org/10.1113/jphysiol.1991.sp018729

Weckström M, Juusola M, Laughlin SB (1992) Presynaptic enhancement of signal transients in photoreceptor terminals in the compound eye. Proc R Soc Lond B Biol Sci 250:83–89. https://doi.org/10.1098/rspb.1992.0134

Wei A, Covarrubias M, Butler A, Baker K, Pak M, Salkoff L (1990) K + current diversity is produced by an extended gene family conserved in *Drosophila* and mouse. Science 248:599–603. https://doi.org/10.1126/science.2333511

Wernet MF, Huberman AD, Desplan C (2014) So many pieces, one puzzle: cell type specification and visual circuitry in flies and mice. Genes Dev 28:2565–2584. https://doi.org/10.1101/gad.248245.114

Yang HH, Clandinin TR (2018) Elementary motion detection in *Drosophila*: algorithms and mechanisms. Annu Rev Vis Sci 4:143–163. https://doi.org/10.1146/annurev-vision-091517-034153

Zheng L, de Polavieja GG, Wolfram V, Asyali MH, Hardie RC, Juusola M (2006) Feedback network controls photoreceptor output at the layer of first visual synapses in *Drosophila*. J Gen Physiol 127:495–510. https://doi.org/10.1085/jgp.200509470

Zheng L, Nikolaev A, Wardill TJ, O'Kane CJ, de Polavieja GG, Juusola M (2009) Network adaptation improves temporal representation of naturalistic stimuli in *Drosophila* eye: i dynamics. PLoS One 4:e4307. https://doi.org/10.1371/journal.pone.0004307

5 | Manuscript 3: Implementation of stable contrast computation in the visual circuits

The following manuscript is under preparation.

Authors and affiliations

Burak Gür[1,2], Jacqueline Cornean[1], Marion Silies[1,*]

1 - Institute of Developmental Biology and Neurobiology, Johannes-Gutenberg University Mainz, Mainz, Germany

2 - Göttingen Graduate School for Neurosciences, Biophysics, and Molecular Biosciences (GGNB) and International Max Planck Research School (IMPRS) for Neurosciences at the University of Göttingen, Göttingen, Germany

* - For correspondence: msilies@uni-mainz.de

Contribution statement

Marion Silies and I conceptualized and designed the study. I conducted the investigation, developed stimulation and analysis software, visualized the data, and wrote the manuscript draft. Jacqueline Cornean conducted the imaging experiments in Figure5.5D, E and Figure5.6.

Abstract

A major challenge for the brain is to keep stable neural representations of stimulus features while facing a wide range of sensory inputs. Visual systems handle slow changes in luminance, spanning up to ten orders of magnitude throughout the day, using photoreceptor gain control mechanisms. However, the same mechanisms are not sufficient to accommodate rapid luminance changes encountered when viewing or navigating natural scenes. Thus, a rapid post-receptor luminance gain must be implemented to keep luminance-invariant contrast representations. Here we reveal the visual circuits and mechanisms that implement such rapid post-receptor gain. In the *Drosophila* visual system, the first neurons that exhibit stable contrast representation are the second order interneurons Tm1 and Tm9. These two OFF pathway neurons exhibit a luminance gain that leads to distinct contrast representations, such that Tm1 has luminance-invariant representations, whereas Tm9 boosts the representation of contrasts at low luminance. We show that spatial pooling underlies the luminance gain and accommodates the local differences in luminance within visual scenes. Both neurons receive wide glutamatergic inputs along with their columnar cholinergic inputs. Finally, we reveal that the luminance gain in the two pathways is implemented via distinct molecular mechanisms. Tm9 neurons utilize the glutamate-gated chloride channel GluClα to implement luminance gain control in its dendrites. Together, our results demonstrate the circuit and biophysical implementation of a novel, rapid gain mechanism vital for dynamic and stable vision in natural scenes. Since visual systems of animals evolved to process similar natural scenes, such mechanisms likely generalize across species.

Introduction

Animals encounter a vast magnitude of sensory information as they navigate changing environments. For example, visual systems face changes in ambient light levels that span up to ten orders of magnitude (Rieke et al. 2009). Individual sensory neurons encoding these natural scenes do not have the signaling range to cover these values simultaneously. Gain control mechanisms that adjust input-output relationships are thus essential, especially in the periphery of the sensory systems. They match the neural signaling range to the immense range of natural inputs coming from the environment (Laughlin 1981). One primary purpose of peripheral visual gain control is to keep the processing of contrast stable, the earliest and most fundamental feature extracted by visual systems. It is the relative difference in light intensities, for example, the normalized difference between the light reflected from a tree and its background. Many downstream computations rely on contrast computation, such as edge detection and motion processing, spatial localization, and object and pattern recognition. Stable contrast processing across vast illumination differences is thus vital for behavior. Because the absolute differences in light intensities between a given object and a background change massively throughout the day, the visual systems must compute contrast relative to the mean illumination levels. Visual responses that accurately compute contrast, and report this information to downstream circuits, are called luminance invariant.

One prime location of gain control that is well understood is the light-capturing photoreceptor cells that transform ten orders of magnitude of visual information into limited neural signals. Luminance gain control enables photoreceptors to achieve luminance-invariant contrast representations that follow Weber's law (Normann et al. 1974; Laughlin et al. 1978; Burkhardt 1994). Decades-long research revealed various adaptation mechanisms implemented in the photoreceptors that underlie gain control (Pugh et al. 1999; Burns et al. 2001; Fain et al. 2001; Katz et al. 2009). These mechanisms are implemented in multiple timescales ranging from milliseconds to minutes to hours, making photoreceptor luminance gain control sensitive to a history of luminance inputs.

However, significant variations in the illumination conditions also happen on rapid timescales. For example, many mammals explore visual scenery by performing saccades leading to 2-3 orders of magnitude changes in local luminance occurring at around 200-300ms (Mante et al. 2005; Binda et al. 2018; Frazor et al. 2006). Similarly, insects perform sharp head and body movements while navigating their environments (Wehrhahn et al. 1982; Tammero et al. 2002; Geurten et al. 2014). Despite the challenges imposed by the rapid luminance changes, visual systems of animals ranging from humans to fruit flies can achieve luminance invariant contrast representations (Burkhardt et al. 1984; Shapley et al. 1984; MacEvoy et al. 2001; Mante et al. 2005; Ketkar et al. 2020). As such, human perception accurately estimates the contrast changes following different luminance backgrounds after 300-400ms (Burkhardt et al. 1984; Kilpeläinen et al. 2011). Downstream of the retinal circuitry, neurons in the cat lateral geniculate nucleus (LGN) respond similarly to fixed contrast gratings, invariant to rapidly changing luminance (Mante et al. 2005). Similarly, this rapid change in gain was observed in cat Y retinal ganglion cells (RGC) in low light levels (Shapley et al. 1984), arguing post-photoreceptor (post-receptor) gain mechanisms are already implemented in the retina. However, the exact circuitry that implements fast luminance gain control is not known in any system.

So far the post-receptor gain mechanisms discovered all explain the stable contrast processing in dim light when photoreceptor adaptation fails (Green et al. 1975; Green et al. 1982; Purpura et al. 1990; Lee et al. 1990). For example, a post-receptor gain in the synapses between cone bipolar cells and RGCs ensure the scaling of RGC responses to contrast in dim light (Dunn et al. 2007). However, the gain mechanisms responsible for other light conditions that keep contrast processing stable in rapidly changing luminances are mostly unknown.

Recently, causal insights about how visual systems estimate contrast in rapidly changing conditions have been gained from in the fruit fly *Drosophila melanogaster*. Both ON and OFF motion-driven behavior of the fly depends on a luminance gain that leads to stable contrast responses in rapidly changing conditions (Ketkar et al. 2020; Ketkar et al. 2022). In the fly visual system, photoreceptors first transmit their signals to different types of first-order neurons, the so-called Lamina Monopolar Cells (LMCs) L1-L3. The luminance-invariant behavior of the fly depends on the interactions of LMCs, especially on a rapid luminance gain provided by the luminance-sensitive L1

and L3 neurons (Ketkar et al. 2020). However, the downstream circuitry that establishes the rapid luminance gain and its mechanisms are unknown. Given the cell-type specific genetic access and tools to manipulate genes, the fly visual system offers the opportunity to reveal both the location of post-receptor luminance gain and the underlying mechanisms and properties.

Here we first reveal the circuitry that implements the luminance gain responsible for ensuring stable contrast responses. Whereas none of the LMC types encode contrasts stably in rapidly changing luminances, OFF direction-selective T5 cells display luminance-invariant direction-selective responses. An investigation of the major inputs to T5 cells, the medulla neurons, reveal that Tm1 and Tm9 neurons are the first neurons to implement the rapid luminance gain. This rapid luminance gain generalizes over contrasts but shows distinct properties in Tm1 and Tm9 neurons, forming two parallel channels with luminance gain. We then show that this luminance gain depends on spatial pooling of luminance, and identify wide-glutamatergic inputs onto both Tm1 and Tm9 dendrites that can form the basis of the rapid luminance gain. Next, we investigate the biophysical mechanisms underlying rapid luminance gain control. Cell-type specific gene loss-of-function shows that the ionotropic glutamate-gated chloride channel GluClα is required for the luminance gain in Tm9 neurons, possibly via shunting inhibition. Together, our data reveal the cellular and molecular implementation of rapid luminance gain control and its spatial properties in a well-defined visual circuit.

Results

Direction selective cells exhibit luminance gain in rapidly changing conditions

The fidelity of contrast signals are challenged by rapid changes in illumination levels occurring due to eye, head or body movements that lead to changes in neuron receptive fields (Figure 5.1A, left). Luminance information in the newly viewed region can be used to scale contrast signals and preserve contrast representation (Figure 5.1A, right). In the OFF pathway of the fly, estimation of contrast in rapidly changing luminances depends on the interaction of contrast and luminance sensitive first-order interneurons, L2 and L3 (Ketkar et al. 2020). To localize the circuit implementation of the rapid luminance gain, we started by recording the LMC responses via *in vivo* two-photon imaging (Figure 5.1B). We expressed the genetically encoded calcium indicator GCaMP6f specifically in either L2 or L3 and and imaged their axon terminals while presenting the fly with visual stimuli. To assess for a rapid luminance gain we used moving sinusoidal gratings with a constant contrast (100% Michelson contrast) at changing luminances (Figure 5.1C). Both L2 and L3 neuron responses oscillated with the temporal frequency of the sinusoidal grating (1 Hz). The amplitude of these response oscillations in both L2 and L3 axon terminals were lower in lower luminances showing that the responses depended on the mean luminance of the gratings. Our data shows that LMCs cannot achieve stable contrast estimation in rapidly changing luminances and thus luminance gain is absent in the first-order neurons of the fly visual system.

Then we asked if the outputs of the motion circuitry, the direction selective T4-T5 neurons, have already implemented a luminance gain and exhibit luminance-invariant responses. We imaged the axon terminals of T4 and T5 neurons located in the lobula plate and presented the same 100% Michelson gratings, this time moving in two opposite directions to capture more types of T4 and T5 cells. The amplitude of the T4 and T5 response oscillations were similar when luminances changed rapidly (Figure 5.1C). To quantify the contrast response of the neurons we calculated the F1 amplitude of the 1Hz response component upon fast Fourier transformation (Figure 5.1D), see Materials and Methods). Unlike L2 and L3, whose responses changed with changing luminance, T4 and T5 neurons encoded contrasts invariantly in rapidly changing luminances. We then quantified the luminance dependence of each neuron by using the slopes of the contrast responses curves. T4 and T5 luminance dependence was significantly lower than L2 and L3 neurons indicating that the luminance gain leads to luminance-invariant responses in DS cells (Figure 5.1E). This comes as no surprise because luminance-invariant contrast signals are essential for reliable DS signals in rapidly changing luminances.

Focusing on the OFF pathway, We next stimulated only OFF T5 cells using OFF stimuli and also imaged L2 and L3 neurons in the same conditions. We presented flies -100% contrast OFF edges

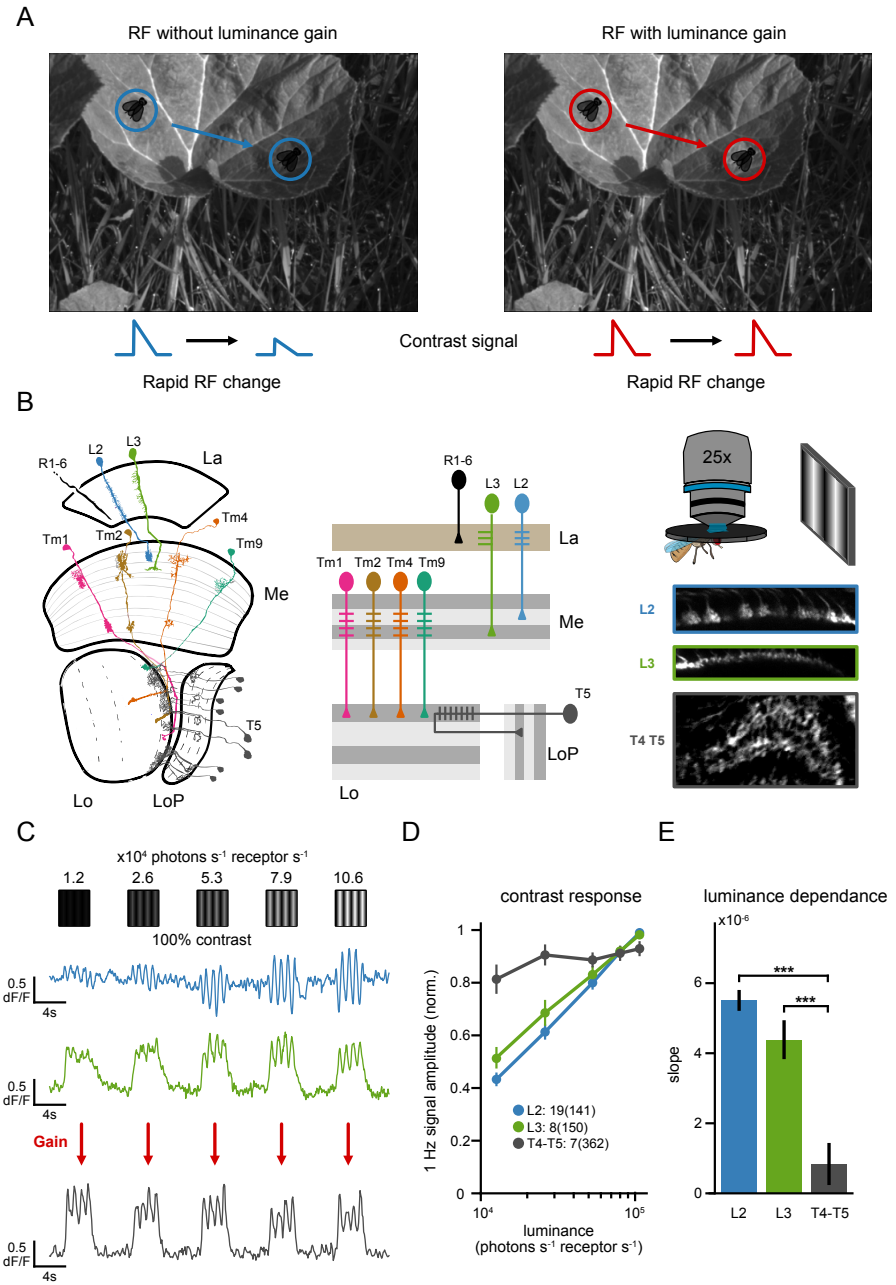

Figure 5.1: Rapid luminance gain occurs after first-order neurons and leads to luminance invariant DS responses. **(A)** Rapid luminance gain ensures stable contrast representation when luminance changes rapidly. (Left) Upon a fast change of a neuron's receptive field (RF) to a low luminance region, a neuron without luminance gain will represent the contrast between the leaf and a fly by a lower signal, resulting in luminance-dependent representations. (Right) With a luminance gain implemented, the neuron adjusts the contrast responses according to local luminance, keeping contrast representations stable across luminance. **(B)** (Left, Middle) Schematic of the fly OFF visual circuits. Photoreceptors give inputs to lamina (La) neurons L2 and L3 which give inputs to the major OFF medulla (Me) neurons Tm1, Tm2, Tm4 and Tm9 that converge onto the dendrites of the first direction-selective cell T5 located in the lobula complex composed of lobula (Lo) and lobula plate (LoP). (Right) *in vivo* two photon images of axon terminals of L2, L3 and T4, T5 neurons expressing GCaMP6f. **(C)** Calcium signals of single axon terminals of L2 (blue), L3 (green) and DS neurons (gray) to drifting 1Hz gratings of constant 100% Michelson contrast and changing luminances. Mean luminance is given on top. **(D)** Contrast responses of each neuron across luminances. **(E)** Slopes of the contrast responses depicting the luminance dependence for each neuron. ***p<0.001, one way ANOVA with post-hoc Tukey HSD test. Sample sizes are given on the plots as flies(cells). Quantification plots in **(D,E)** show mean±SEM.

moving onto backgrounds of different luminances (Figure 5.2A) similar to previous behavioral experiments that tested luminance invariance in Ketkar et al. 2020. L2 and L3 neuron responses again dependent heavily on luminance (Figure 5.2A,B). T5 neurons on the other hand, showed invariant responses (Figure 5.2C). Thus, OFF motion pathway outputs are luminance-invariant across stimulus conditions. We further checked if luminance-invariancy generalized over different temporal scales. T4 and T5 responses exhibited a luminance gain for all temporal frequencies tested (Figure 5.2D). Our results suggest that luminance gain is implemented in diverse conditions, making contrast representations stable.

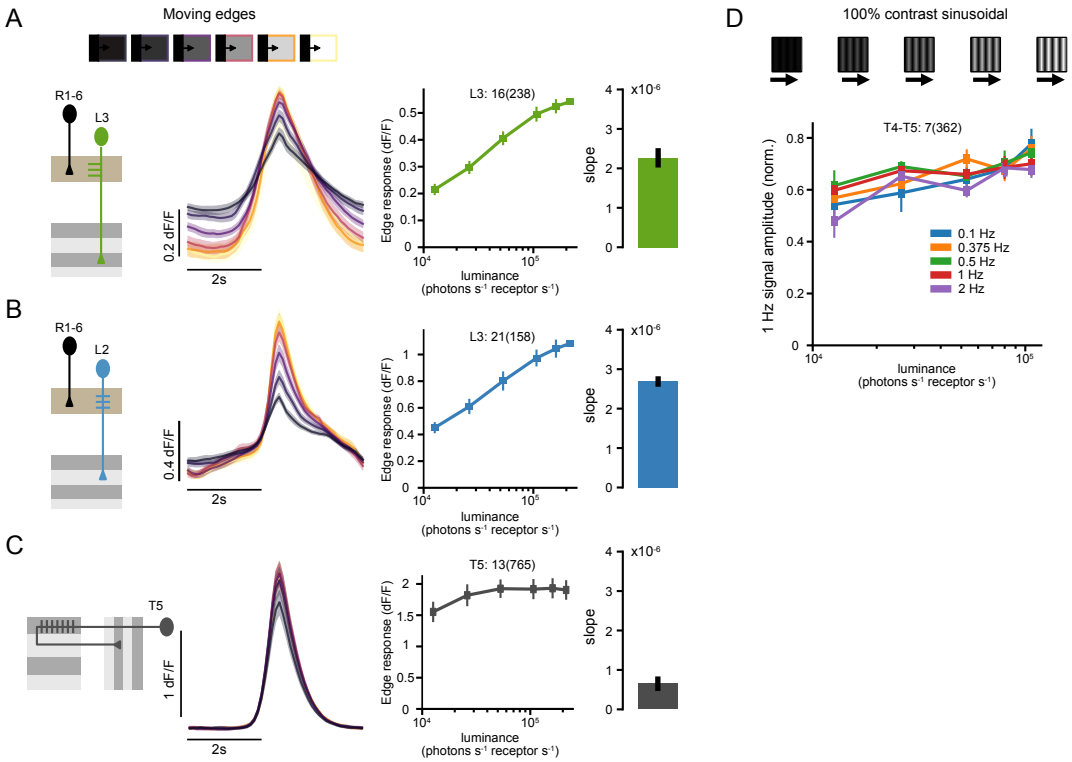

Figure 5.2: Direction selective cells are luminance invariant in diverse stimulus conditions. (A) Calcium signals of L3 neurons (green) to moving -100% contrast OFF edges of six different luminances with the quantification of edge responses and slope of the edge responses depicting luminance sensitivity. **(B)** Same as (A) but for L2 (blue) and **(C)** T5 (gray) neurons. **(D)** Contrast responses of T4 and T5 neurons to drifting gratings of constant contrast and changing luminances across different grating temporal frequencies. Sample sizes are given on the plots as flies(cells). All time traces and quantification plots show mean±SEM.

Together, our data suggests a signal transformation downstream of first-order interneurons of the *Drosophila* visual system, but upstream of DS cell axon terminals, by which a luminance gain scales neuronal contrast responses.

Luminance gain arises pre-synaptically to direction selective cells in distinct medulla neurons

The L2 and L3 lamina neurons connect to DS cells via second order medulla interneurons. To pinpoint the origins of the rapid luminance gain, we thus next measured *in vivo* calcium signals in the four major OFF pathway medulla neurons, Tm1, Tm2, Tm4 and Tm9 (Serbe et al. 2016). Since the fast luminance gain is mediated by luminance-sensitive L3 neurons, we first asked which of these medulla OFF pathway neurons contain luminance information. We presented flies full field flashes of changing luminances lasting for 7 seconds and imaged axon terminals of L3, Tm1, Tm2, Tm4 and Tm9 neurons. L3 neurons exhibited sustained responses that were higher in lower luminances (Figure 5.3A) as reported previously (Ketkar et al. 2020). All Tm neurons showed an increase in calcium signals in response to OFF stimuli. Tm2 and Tm4 neurons responded to OFF changes with transient responses, suggesting that they do not contain luminance information (Figure 5.3C, D). Tm1 and Tm9 neurons responses were sustained throughout the stimulation

period and, similar to L3 neurons, lower luminances elicited higher responses (Figure 5.3B, E). Our data thus suggests that Tm1 and Tm9 neurons receive luminance information and are prime candidates for exhibiting the luminance gain.

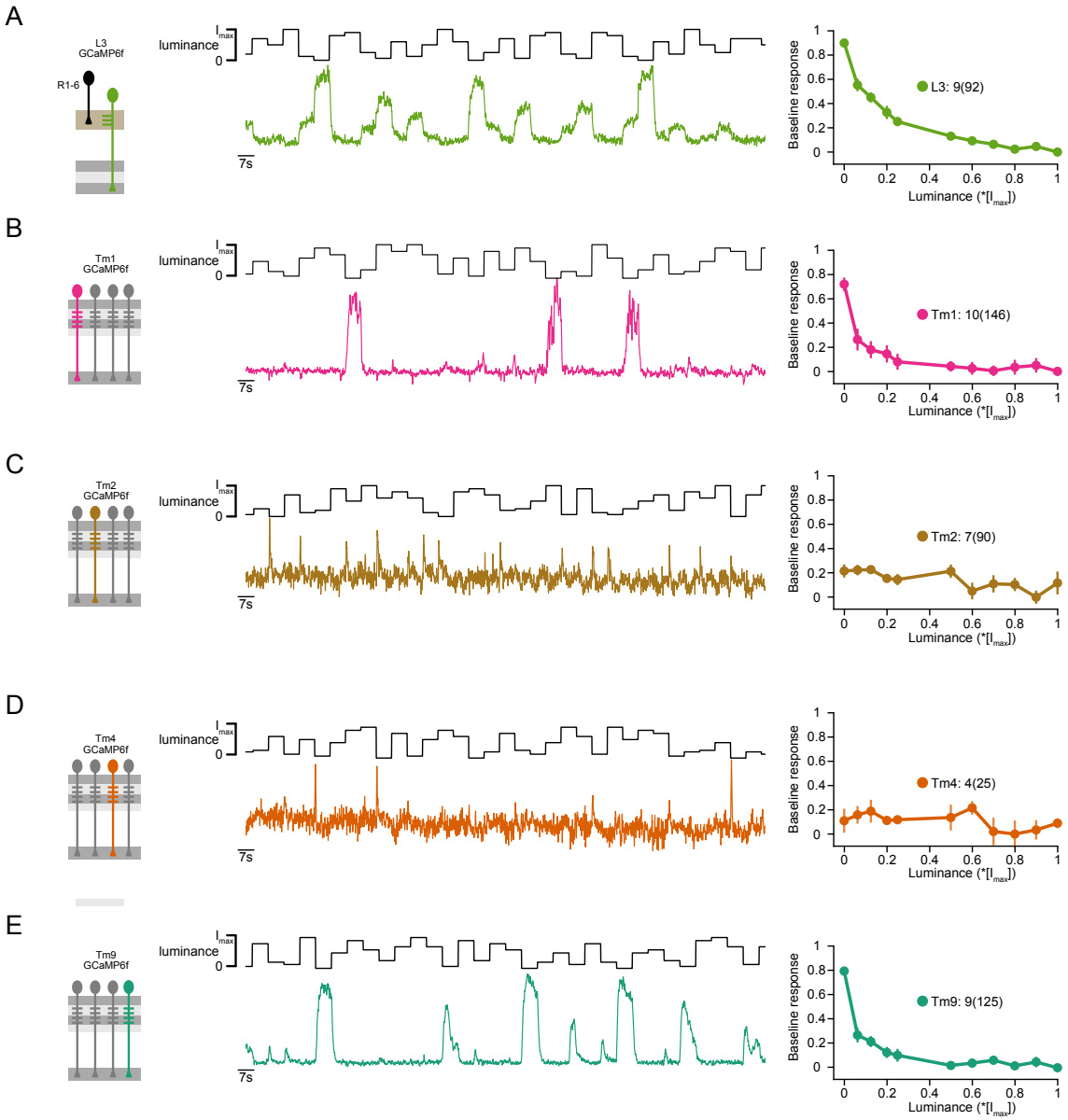

Figure 5.3: Tm1 and Tm9 responses have a luminance sensitive plateau. Example calcium traces of single **(A)** L3 (green), **(B)** Tm1 (magenta), **(C)** Tm2 (brown), **(D)** Tm4 (orange), **(E)** Tm9 (dark green) axon terminals to a stimulus comprising 7 s full-field flashes varying randomly between eleven different luminances. To the right of each panel, the plateau responses (mean of the last 1 second of the response) are quantified. Sample sizes are given on the plots as flies(cells). All plots show mean±SEM.

To test if specific types of medulla neurons indeed implement luminance gain control presynaptic to DS cells, we then investigated the medulla neurons using the moving sinusoidal grating with a constant contrast (100% Michelson contrast) and changing luminances (Figure 5.4). All medulla neurons showed oscillatory responses that followed the temporal frequency of the grating (Figure 5.4A, B, C, D). The contrast responses of Tm4 neurons varied with grating luminance and thus were similar to L2 neurons. (Figure 5.4C) suggesting that rapid luminance gain was absent in Tm4 neurons. Tm2 neuron responses were also dependent on luminance but there was a slight reduction of dependency as compared to L2 neurons (Figure 5.4B), yet this reduction was not significantly different than L3 neurons. This suggests a possible minor rapid luminance gain implemented in Tm2 neurons. Tm1 neurons responses were very similar in different luminances and had a major reduction of luminance dependency compared to L2 and L3 neurons (Figure 5.4A). Similar to Tm1

neurons, Tm9 neuron responses were luminance-invariant with even a slight tendency for higher responses in lower luminances (Figure 5.4D).

The luminance dependencies of contrast responses in Tm1 and Tm9 differed slightly such that Tm9 neurons seemed to boost selectively low luminance regimes. To further investigate this, we quantified the luminance gain for each neuron by dividing their responses to L2 contrast responses (Figure 5.4E, see Materials and Methods). Tm1 neurons implemented a high gain as the luminances went lower, starting from the brightest luminance. Interestingly, Tm9 neurons applied a gain reduction in high luminances and selectively boosted lower luminances. This thus leads to over-representation of contrasts in lower luminance regimes.

Our results show that the rapid luminance gain that leads to luminance-invariant contrasts representations first arises in the second-order medulla neurons of the fly visual system, Tm1 and Tm9 and possibly underlie the luminance-invariant direction selective responses in the T5 neuron terminals (Figure 5.4F). Furthermore, Tm2 and Tm4 neurons lack a clear luminance gain indicating that parallel pathways without luminance gain might be necessary for other computations.

Luminance gain generalizes across contrasts

Natural scenes contain a wide range of contrasts that needs to be processed in a luminance-invariant fashion. We thus assessed if the rapid luminance gain generalizes to different contrasts. To do this, we presented moving sinusoidal gratings with 5 changing luminances and 5 different contrasts of 20%, 40%, 60%, 80% and 100% (Figure 5.5). We imaged Tm1 and Tm9 neuron axon terminals as well as all lamina neurons for comparison. All lamina neuron responses were similar: increasing with grating contrast and decreasing with grating luminance. This is reflected in the contour lines of the contrast-luminance maps as the contour lines extend while luminance and contrast changes (Figure 5.5A, B, C - right panels). This confirms that lamina neurons, including L1, are unable to achieve stable contrast representations in different luminances over different contrasts (Figure 5.5A, B, C - left panels).

The responses of the medulla neuron Tm1 exhibited a prominent luminance gain for all contrasts (Figure 5.5D - left). The contours lines of the contrast-luminance maps were flatter in given contrast regimes (Figure 5.5D - right). Tm9 responses also exhibited a luminance gain for all contrasts but in a distinct way: the responses were higher in lower luminance regimes similar to the effect observed for the previous 100% contrast experiments (Figure 5.5E - left). The contours of the contrast-luminance maps had an inversion of the slope of the contour lines compared to the lamina neurons (Figure 5.5E - right). Thus, the luminance gain lead to over-representation of contrasts in lower luminance regimes. Our data shows that the rapid luminance gain is implemented across different contrasts and leading to luminance-invariant contrast representation in Tm1 neurons and an over-representation of contrast in low luminances in Tm9 neurons.

To understand where these luminance gain properties arise, we also imaged dendrites Tm1 and Tm9 responses. The luminance gain properties of Tm1 and Tm9 dendrites were similar to the responses of the respective axon terminals of each neuron (Figure 5.6A, B) arguing for a mechanism to be already implemented in the dendritic levels of each neuron.

Spatial pooling is necessary for luminance gain

Adjusting contrast responses according to the nearby scene luminance requires reliable estimation of luminance levels in a given space. This can be done by spatial pooling of upstream neuron responses However, pooling also has its trade-offs since natural scenes contain substantial variability in luminance statistics over space (Frazor et al. 2006), meaning that the correlation between local luminances falls rapidly with the distance indicating a problem of estimating luminance over large spatial extents. Local contrast estimation will not be reliable if a large and thus highly variable area of luminance is selected for the gain control mechanisms. We thus investigated if and to what extend Tm1 and Tm9 luminance gain depends on spatial pooling to achieve reliable contrast encoding.

To probe for spatial pooling, we developed an online stimulation paradigm where we centered gratings of different sizes on single neuron receptive fields (Figure 5.7A). We first estimated the

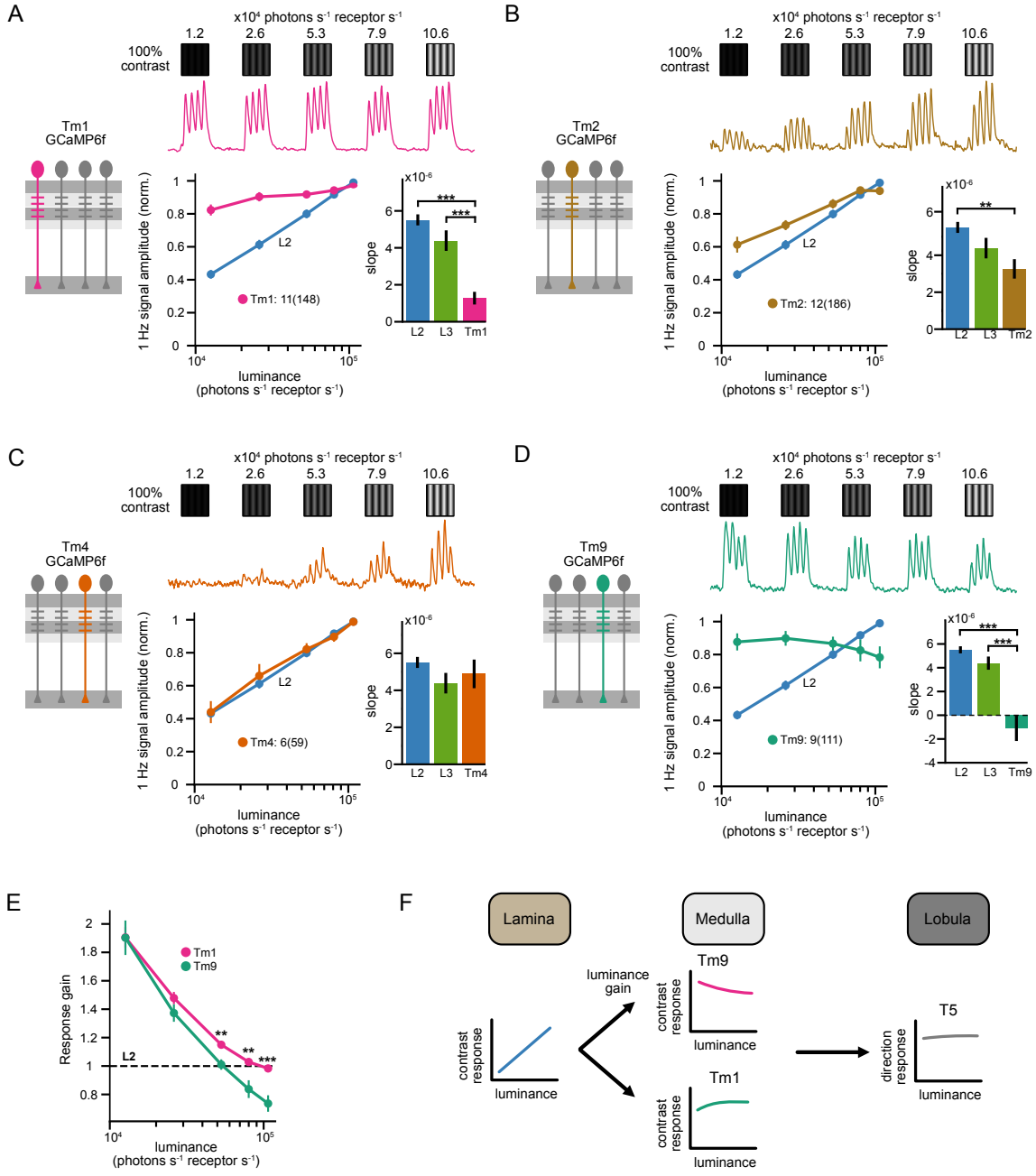

Figure 5.4: Luminance gain arises in Tm1 and Tm9 neurons (A) Above, calcium signals of a single Tm1 neuron example (magenta) to drifting 1Hz gratings of constant contrast (100% Michelson) and changing luminances. Below, quantification of contrast responses compared to L2 neurons (blue) and Tm1 slope compared to L2 and L3 (green) neurons. **(B)** Same for Tm2 (brown) **(C)** Tm4 (orange) and **(D)** Tm9 (dark green) neurons. *****p<0.005, ***p<0.001, one way ANOVA with post-hoc Tukey HSD test. **(E)** Quantification of the response gain between L2 and Tm1 (magenta) and L2 and Tm9 (dark green) neurons. **p<0.005, ***p<0.001, one way ANOVA followed by multiple comparisons corrected with Bonferroni. Sample sizes are given on the plots as flies(cells). Quantification plots show mean±SEM. **(F)** Summary schematic of the contrast representations throughout the OFF pathway. Postsynaptic to lamina neurons, two distinct luminance gain channels arise in Tm1 and Tm9 neurons and possibly ensure luminance-invariant direction-selective responses in the T5 neurons.

receptive fields of neurons using a white noise stimuli followed by a reverse correlation analysis. After finding a neuron with a suitable receptive field located in the center of the stimulus screen, we stimulated it using moving sinusoidal gratings with different mean luminances and the same contrast (Figure 5.8). We assessed the neuron responses over different grating sizes. Tm1 neuron responses depended highly on luminance when the grating size was 5 degrees (Figure 5.7B, ma-

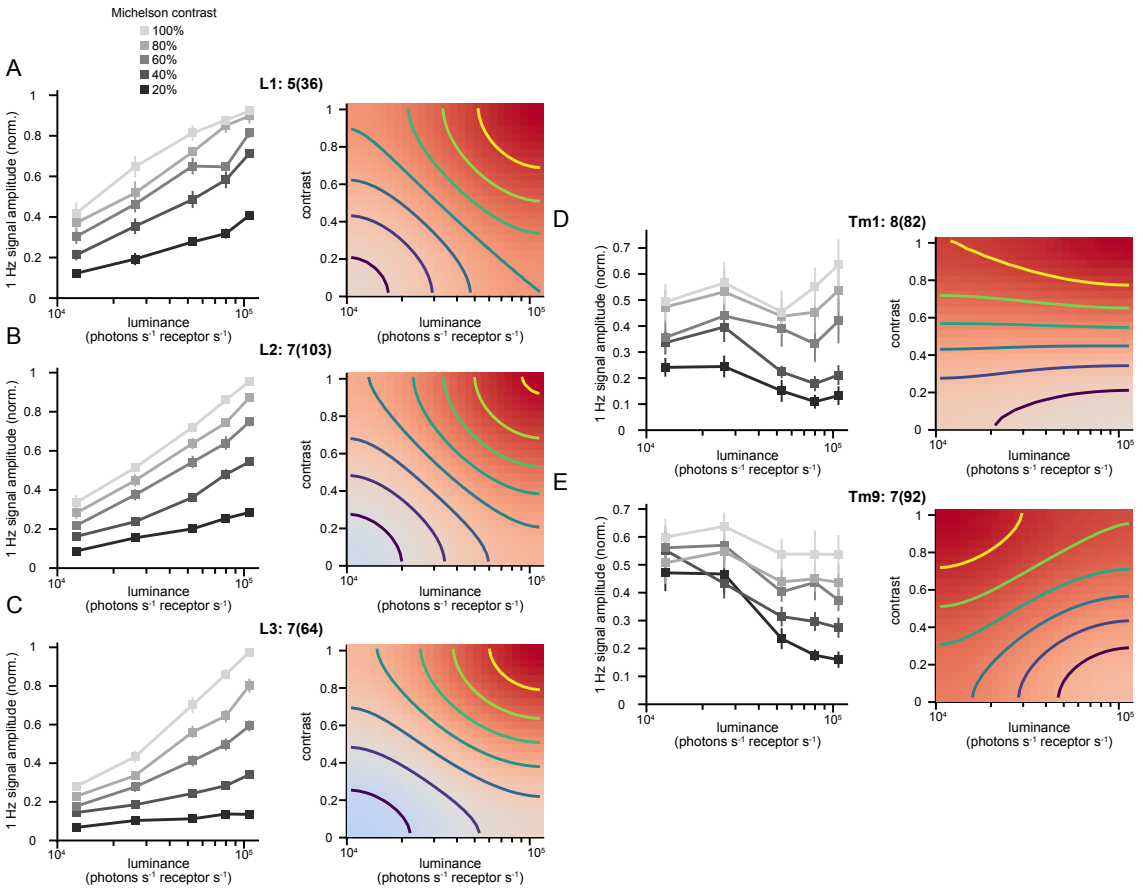

Figure 5.5: Rapid luminance gain generalizes across contrasts. The left panels show contrast responses of **(A)** L1, **(B)** L2, **(C)** L3, **(D)** Tm1 and **(E)** Tm9 neurons to drifting 1 Hz gratings of different contrast and luminance. The right panels show contrast-luminance maps of contrast responses where contours represent equal response lines. Sample sizes are given in the plots as flies(cells). Quantification plots show mean±SEM.

genta traces), leading to similar contrast responses as L2 neurons (Figure 5.1C). The luminance dependency of Tm1 contrast responses gradually decreased with increasing grating size suggesting that the luminance gain depends on spatial pooling mechanisms (Figure 5.7B,C). For Tm9 neurons we saw an underestimation of contrast only in the very low luminance regime for small grating sizes of 5 degrees. This effect disappeared upon increasing the size of the grating and the reverse luminance dependence of Tm9 appeared starting at a grating size of 15-20 degrees (Figure 5.7C). Furthermore, for both Tm1 and Tm9 neurons, the response amplitudes to contrasts at high luminances did not change with the increasing grating size suggesting that the gain mechanism mainly operates in the low luminance regimes by boosting the responses (Figure 5.7C).

In summary, our data reveals that the rapid luminance gain in second-order visual neurons depends on spatial pooling mechanisms. Furthermore, the spatial pooling achieves two different goals in these neurons: whereas Tm1 neurons reach a similar representation of the same contrast in changing luminances and thus achieve luminance-invariancy, Tm9 neurons over-represent the contrast happening in low luminances.

Tm1 and Tm9 neurons receive OFF glutamatergic inputs that do not show luminance gain

After identifying that rapid luminance gain control is implemented at the dendrites of Tm1 and Tm9 neurons, we wanted to investigate the underlying mechanisms on how this is implemented. The main columnar inputs to Tm1 and Tm9 neurons are L2 and L3 neurons, respectively, which are cholinergic (Takemura et al. 2013; Davis et al. 2020). We hypothesized that a convergence of cholinergic and an additional wide-field input that provides the spatial pooling may explain the luminance gain occurring in Tm1 and Tm9 neurons. Main candidates to provide these wide-field

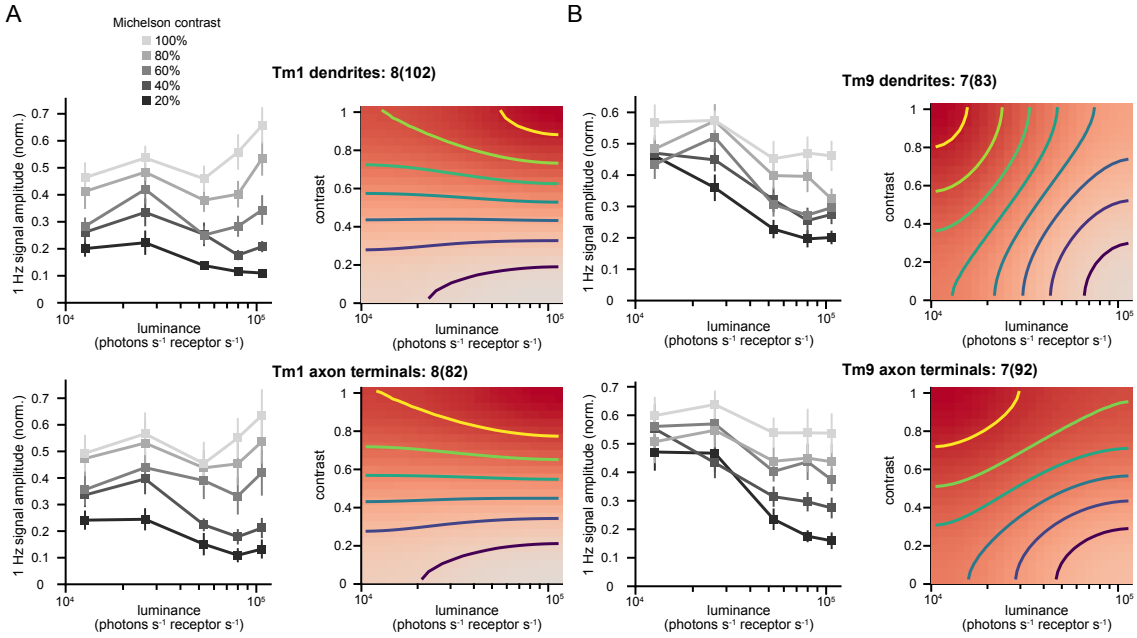

Figure 5.6: The rapid luminance gain is already implemented in medulla neuron dendrites Left panels show contrast responses of **(A)** Tm1 dendrites (upper) and axon terminals (lower), **(B)** Tm9 dendrites (upper) and axon terminals (lower) to drifting 1Hz gratings of different contrasts and luminance. Right panels show contrast-luminance maps of contrast responses where contours represent equal responses lines. Sample sizes are given on the plots as flies(cells). Quantification plots show mean±SEM.

inputs to medulla neurons are wide-field Distal Medulla (Dm) neurons which have glutamatergic and GABAergic properties (Nern 2015). We thus started by checking if Tm1 and Tm9 neurons receive glutamatergic inputs by expressing the glutamate sensor iGluSnFR (Marvin et al. 2018) in Tm1 and Tm9 neurons and imaging iGluSnFR signals from their dendrites (Figure 5.9). We first stimulated the neurons using full field ON and OFF flashes and saw that both neurons responded positively at the onset of the OFF flash (Figure 5.9A). This suggests that both of these neurons receive OFF glutamatergic inputs that can be used to implement luminance gain. We then assessed if these inputs are already luminance invariant since this would eliminate a need for a mechanism to be implemented in the neurons themselves. We measured iGluSnFR responses to the same moving sinusoidal gratings as in previous experiments and saw that both Tm1 and Tm9 neuron iGluSnFR signals depended on the luminance of the grating (Figure 5.9B, C). Both neurons received glutamate signals that had higher luminance dependency than their calcium responses (Figure 5.9D) confirming that the luminance gain is not implemented solely with these inputs. Together, our data showed that both Tm1 and Tm9 neurons receive OFF glutamate signals which can underlie the mechanism behind the implementation of luminance gain. Our data supports the idea that a glutamatergic and cholinergic dendritic integration happening on Tm1 and Tm9 neurons leads to luminance gain.

We then assessed the RF properties of the glutamatergic inputs. We used white noise stimulation followed by reverse correlation analysis to extract the linear spatio-temporal receptive fields of both neurons' dendritic glutamatergic inputs and calcium signals of the axon terminals (Figure 5.9E, F). Tm1 calcium signals at the axon terminals had a biphasic temporal filter and Tm9 calcium signals had a monophasic temporal filter (Figure 5.9E). The spatial extend of the filter calculated as the full-width-half-maximum (FWHM) measured around 10 degrees for both neurons (Figure 5.9E, F). These spatial and temporal properties are in line with the previous measurements of Tm1 and Tm9 neurons (Serbe 2016). The glutamate inputs onto Tm1 neurons also exhibited a biphasic filter but due to iGluSnFR expression levels, the recordings were noisier and resulted in lower filter amplitudes. The spatial filter of Tm1 glutamate inputs were around 15 degrees, one column wider than the Tm1 receptive field (Figure 5.9E). Tm9 glutamate inputs were both temporally and spatially different than Tm9 calcium signals (Figure 5.9F). The temporal filter was biphasic contrasting the Tm9 monophasic calcium temporal filter. Furthermore the spatial filter had a FWHM around 22 degrees, and thus roughly two columns wider than its calcium

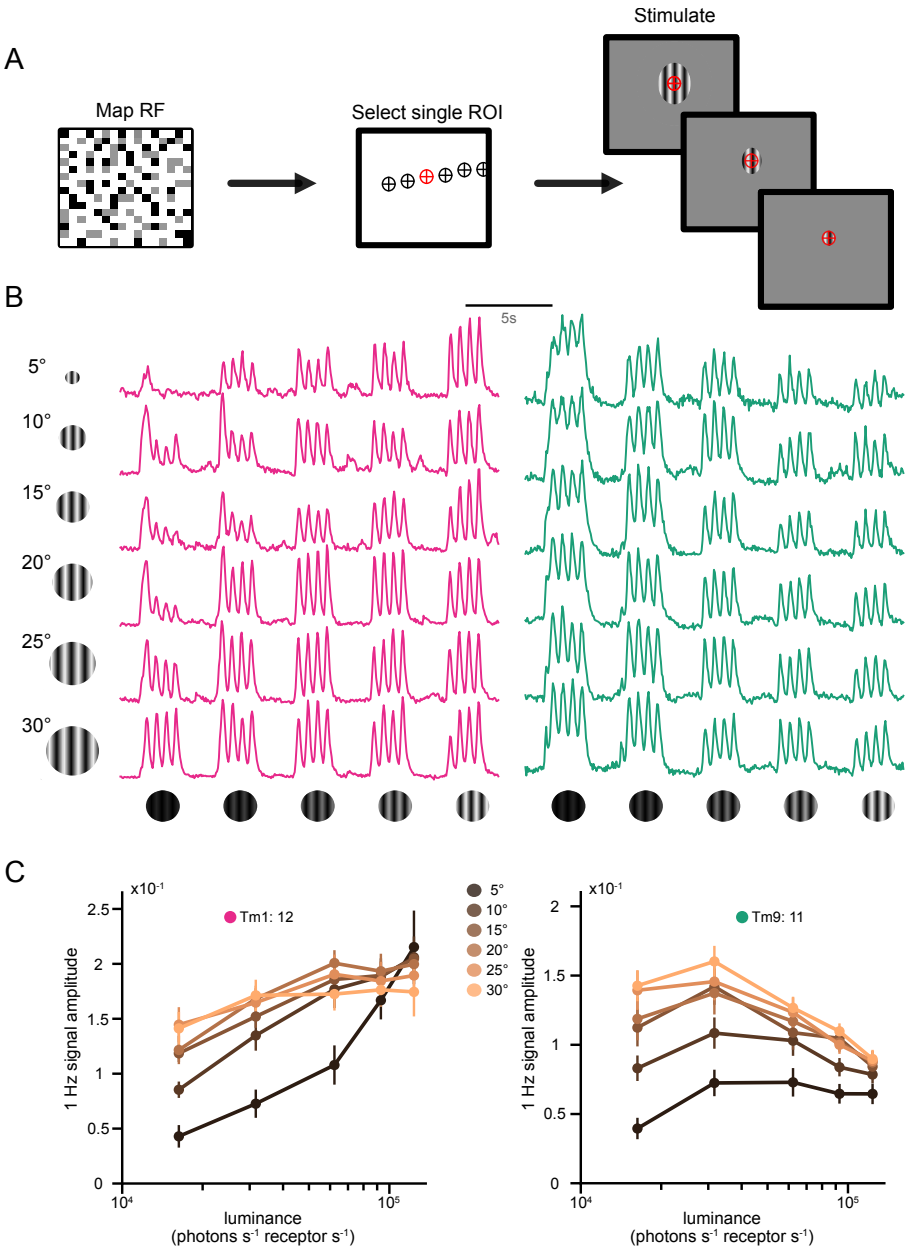

Figure 5.7: Spatial pooling is necessary for the rapid luminance gain. (A) Schematic of the online RF mapping and single neuron stimulation paradigm. First RFs of individual axon terminals were mapped and based on their location a suitable one was selected for further stimulation with drifting gratings centered at the RF center with constant contrast and changing luminances at varying sizes. **(B)** Calcium traces from single axon terminals of Tm1 (magenta) and Tm9 (dark green) neurons. **(C)** Quantification of contrast responses in different luminance and varying grating sizes. Gratings vary from 5° (dark lines) to 30° (bright lines) with 5° increments. Sample sizes are given on the plots as number of axon terminals. Quantification plots show mean±SEM.

temporal filter (Figure 5.9F). Our results showed that both Tm1 and Tm9 neurons receive wide-field glutamatergic inputs. These inputs can underlie the spatial pooling mechanism observed in Tm1 and Tm9 neurons and a convergence with cholinergic inputs may explain the scaled contrast representations of Tm1 and Tm9 neurons.

GluClα is required for luminance gain in Tm9

After identifying that Tm1 and Tm9 neurons receive wide-field glutamate signals that can underlie luminance gain, we asked, what could mediate the coincidence detection of glutamate and acetylcholine at the Tm neuron dendrites to produce the rapid luminance gain. Since the luminance gain

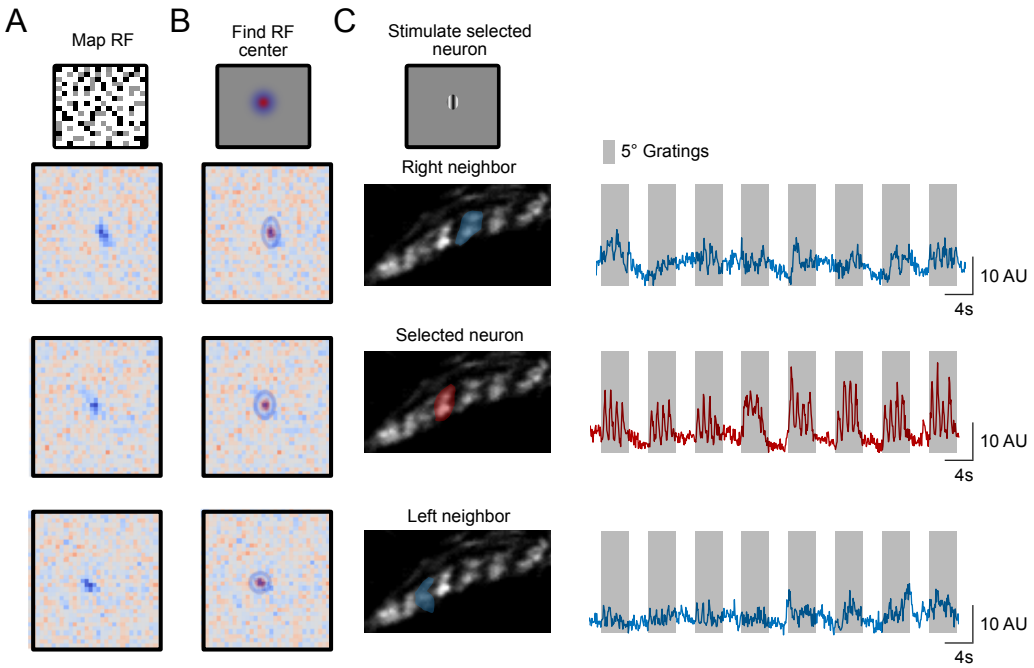

Figure 5.8: Online RF mapping and stimulation paradigm. (A) A white noise stimulus was used to map receptive fields of single axon terminals of Tm1 and Tm9 neurons. **(B)** The center of the receptive fields was identified by fitting a 2D Gaussian function and taking its center. **(C)** At the central panel, calcium signal trace from an axon terminal whose RF center was used as the position for a 5° drifting grating of constant contrast and changing luminances. Neighboring axon terminals (upper and lower panels) had slightly shifted RFs and thus did not respond to the stimulation confirming the accuracy of the online RF mapping-stimulation method.

leads to luminance-invariant representations of contrast, it can be considered as a normalization method. A common model to explain normalization based gain mechanisms relies on shunting inhibition (Carandini et al. 1994; Carandini et al. 1997; Carandini 2012). A recent study suggested that a glutamate-gated chloride channel, GluClα, implements a part of the multiplicative step in motion computation algorithms via a shunting mechanism (Groschner et al. 2022). GluClα is also broadly expressed in the medulla neurons (Molina-Obando et al. 2019; Davis et al. 2020). Since glutamatergic dendritic inputs of Tm1 and Tm9 neurons increased with increasing luminance (Figure 5.9B,C,D), we hypothesized that a shunting input that acts primarily in higher luminances can mediate a rapid luminance gain control. We thus tested GluClα as a molecular candidate mediating normalization via shunting inhibition.

To test if GluClα is involved in mediating the luminance gain in Tm1 and Tm9 neurons, we set out to knock down GluClα in a cell-type specific manner from Tm1 and Tm9 neurons. To do so, we used a fly line with a FlpStop exon inserted into the endogenous GluClα locus GluCl$\alpha^{FlpStop-ND}$ (Figure 5.10A, Molina-Obando et al. 2019). The FlpStop exon in the GluCl$\alpha^{FlpStop-ND}$ is inverted with respect to the GluClα gene and thus causes no disruption. Only upon expression of a Flp recombinase, the FlpStop cassette is inverted and stops the transcription and translation of the protein (Figure 5.10A). To achieve cell-type specific disruption of GluClα, we expressed Flp recombinase specifically in Tm1 or Tm9 neurons. A tdTomato marker, which is only expressed upon inversion, confirmed the inversion event in both neurons (Figure 5.10B, C). We then recorded calcium signals from Tm1 and Tm9 axon terminals. Control flies of Tm9 experiments exhibited luminance gain in their responses 5.10D). In the flies where GluClα was cell-type specifically disrupted in Tm9 neurons responses were less to the gratings with lower mean luminances (Figure 5.10D). The luminance dependence of Tm9 neurons increased significantly showing that the rapid luminance gain was gone or reduced in the absence of GluClα channels in Tm9 neurons (Figure 5.10F). Tm1 neuron responses showed no differences between control and GluClα loss of function conditions (Figure 5.10E) and the luminance dependency was not altered (Figure 5.10G) suggesting that the luminance gain mechanism in Tm1 neurons is not mediated by GluClα channels. Our data reveals that distinct molecular mechanisms underlie the distinct luminance gains observed in

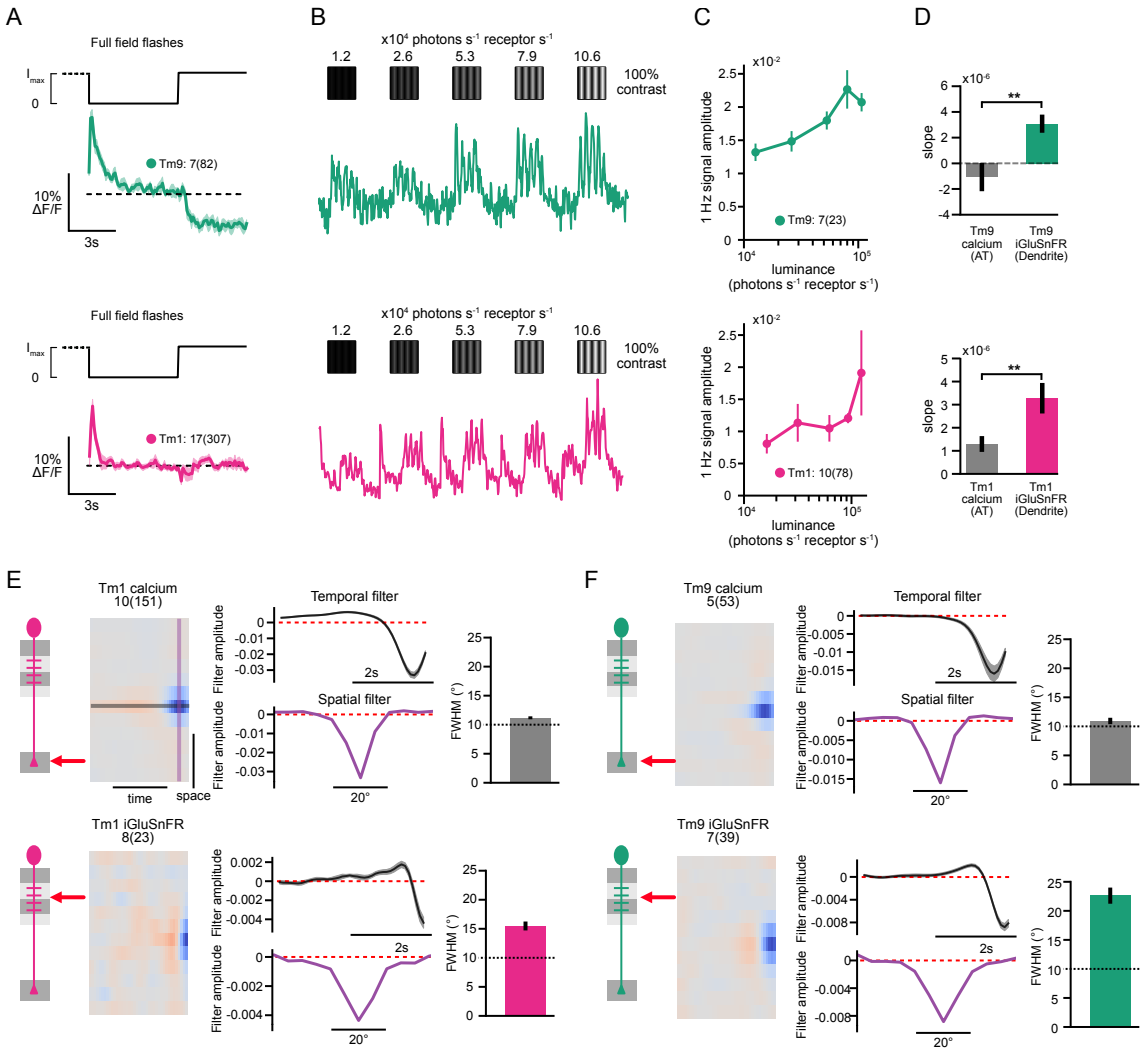

Figure 5.9: Tm1 and Tm9 neurons receive wide OFF glutamate signals that do not show luminance gain. (A) iGluSnFR signals recorded from Tm9 (dark green) and Tm1 (magenta) dendrites upon presentation of full field ON and OFF flashes. $I^{max} = 2.17 \times 10^5$ photons s^{-1} photoreceptor^{-1}. Traces show mean±SEM. **(B)** iGluSnFR signals of single Tm1 and Tm9 neuron dendrites to drifting 1Hz gratings of constant contrast and different luminances. **(C)** Quantification of contrast responses across luminances. **(D)** Slope of contrast responses of iGluSnFR signals compared to axon terminal calcium responses (gray) of each respective neuron. **p<0.005, Student's t-test. Sample sizes are given on the plots as flies(cells). Quantification plots **(C),(D)** show mean±SEM. **(E), (F)** Spatio-temporal receptive fields (STRF) of **(E)** Tm1 and **(F)** Tm9 neurons extracted using reverse correlation analysis upon ternary white-noise stimulation. Upper panels show axon terminal calcium STRF and lower panels show iGluSnFR STRF from dendrites. Black traces show the temporal filter extracted from the STRF center and magenta traces show the spatial filters. FWHM is calculated to quantify the extend of the spatial filters. Sample sizes are given on the plots as flies(cells). Temporal filters and FWHM quantification show mean±SEM.

Tm1 and Tm9 neurons, and reveals a novel function for GluClα in mediating rapid luminance gain control, likely via divisive normalization.

Discussion

A rapid luminance gain facilitates stable contrast estimation when visual systems are exposed to fast luminance differences, such as those encountered when viewing natural scenes. In this study, we reveal the cellular and molecular implementation of a rapid luminance gain in the OFF pathway of the fly visual system. In post-photoreceptor circuitry, this luminance gain first emerges in distinct third-order neurons and is propagated to downstream directions-selective cells. Whereas Tm1 and

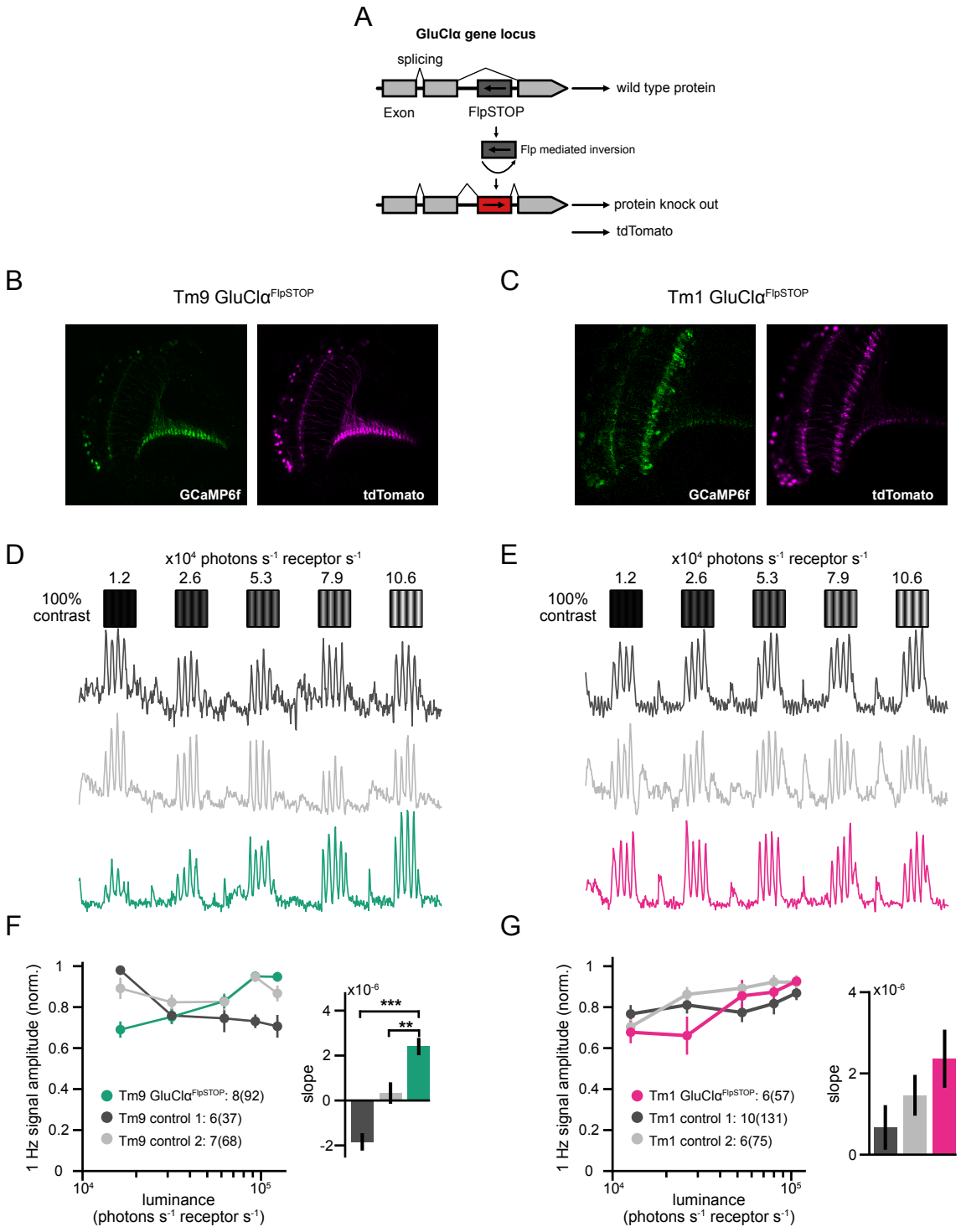

Figure 5.10: GluClα is required for luminance gain in Tm9 (A) The FlpSTOP exon in the non-disrupting orientation is flipped cell-type specifically in Tm1 and Tm9 neurons using cell-type specific expression of Flp recombinase. The flipping event is visualized by the expression of tdTomato. **(B)** tdTomato expression (magenta) confirms flipping in Tm9 experimental group and **(C)** Tm1 experimental group. **(D)** Calcium response traces to drifting sinusoidal gratings of constant contrast with changing luminances from example axon terminals of Tm9 control conditions (dark and light gray) and Tm9 experimental condition (dark green). **(E)** Calcium traces from example axon terminals of Tm1 control conditions (dark and light gray) and Tm1 experimental condition (magenta). **(F)** Quantification of contrast responses and slopes depicting luminance sensitivity of responses for Tm9 neurons and **(G)** Tm1 neurons. **p<0.005 ***p<0.001, one way ANOVA with post-hoc Tukey HSD test. Sample sizes are given on the plots as flies(cells). Quantification plots show mean±SEM.

Tm9 exhibit the rapid luminance gain, others do not, suggesting the presence of computations independent of luminance invariant contrast estimation. Both Tm1 and Tm9 neurons utilize spatial pooling mechanisms to implement the luminance gain. Yet, the properties of luminance gain in these neurons differ: whereas Tm9 neuronal properties favor contrasts in low luminance regimes, Tm1 neurons achieve a constant representation of contrasts in different luminances. Biophysically, the Tm9 luminance gain is achieved via glutamate-gated chloride channels, possibly through shunting inhibition that normalizes the contrast responses in different luminance regimes. Taken together, our data reveal the circuitry and properties of rapid luminance gain control in visual circuitry, and establish causal links to molecular mechanisms underlying its implementation.

First-order visual neurons fail to estimate contrast stably in rapidly changing conditions

L1, L2 and L3 type LMCs are the first-order neurons located in the lamina that receive direct inputs from photoreceptors and guide the stable contrast-driven behavior of the fly in both ON and OFF pathways (Ketkar et al. 2020; Ketkar et al. 2022). Yet, contrast responses of these neurons depend on the luminance levels in rapidly changing conditions, and thus these neurons are unable to provide a constant, luminance invariant estimation of contrast. This shows that even though photoreceptors use a plethora of adaptation mechanisms to encode contrast throughout the day (Pugh et al. 1999; Burns et al. 2001; Fain et al. 2001; Katz et al. 2009), these mechanisms are not sufficient to establish stable responses in rapidly changing conditions.

Why is implementing a rapid-luminance gain more suitable in post-receptor sites? Photoreceptor responses are more susceptible to noise than the downstream neurons (Laughlin et al. 1989). A higher noise will fluctuate the gain and can lead to distortions of contrast representations within the same mean luminance levels (Rieke et al. 2009). Postsynaptic to photoreceptors, noise reduction steps can be applied through synaptic and spatial pooling mechanisms and thus provide a better location for a rapid gain to operate (Laughlin 1981; Shapley et al. 1984). In line with this, post-receptor gain observed in the vertebrate retina was suggested to benefit from the pooling of BPC signals in retinal ganglion cells (Dunn et al. 2007). In this study, we have shown that spatial pooling underlies the post-receptor gain in *Drosophila*, supporting this idea.

Why is post-receptor gain not implemented already at the LMC level? Several explanations might account for the downstream location of the post-receptor gain. Inter-columnar interactions (e.g., spatial pooling) are required for post-receptor gain and neurons mediating horizontal processing also exist at the LMC level. However, these interactions are restricted by the low number of horizontal neurons available whereas numerous types of horizontal neurons exist in medulla such as Dm and Pm neurons (Fischbach et al. 1989; Nern et al. 2015). The major spatial processing done in lamina is the creation of the antagonistic center-surround which benefits the extraction and sharpening of contrast signals (Srinivasan et al. 1982; Laughlin 1989; Freifeld et al. 2013). Furthermore, not all third-order neurons exhibit a luminance gain, which suggests that some pathways require luminance-dependent representations of contrast. To ensure this, it might be beneficial to not implement luminance gain in the few LMCs existing downstream of the photoreceptors. Similar to *Drosophila* third-order neurons without luminance gain, some RGCs in the vertebrate retina exhibit luminance-dependent contrast responses (Idrees et al. 2020).

A rapid luminance gain arises in distinct third-order visual neurons

Previous neural silencing experiments showed that interactions between pathways receiving inputs from distinct LMCs lead to stable contrast representations in fly behavior (Ketkar et al. 2020; Ketkar et al. 2022). Here, we pinpointed the site of interaction to medulla neurons downstream of LMCs: The neurons Tm1 and Tm9 show a luminance gain that scales the upstream contrast signals coming from the second-order neurons located in the lamina. Thus, the convergence of distinct LMC signals onto medulla neuron dendrites is required to achieve the luminance gain observed in Tm1 and Tm9 neurons. LMC signals encode luminance and contrast of the visual scenes differently. L1 and L3 neurons have sustained response components that encode the luminance of the visual scenery (Ketkar et al. 2022). These luminance signals then might be providing the scaling to the contrast signals coming mainly from L1 and L2 neurons. The interaction of the two channels will then achieve a stable representation of contrast. Similarly to LMCs, in the vertebrate retina, bipolar

cells (BPCs) located downstream of the photoreceptors exhibit diverse temporal properties which suggests that they have distinct contrast and luminance encoding (Euler et al. 2014). In line with these observations, a type of luminance gain that operates in dim light happens in the BPC output synapses (Dunn et al. 2007). This suggests that downstream of second-order neurons is an optimal site for implementing various types of luminance gain mechanisms across species.

Interestingly, the luminance gain in Tm1 and Tm9 neurons is not identical. Tm1 luminance gain ensures stable contrast representations across luminances, vital for luminance-invariant downstream feature encoding such as direction-selectivity that arise in the T5 neurons. On the other hand, Tm9 luminance gain leads to an over-representation of contrasts in low contextual luminances. Estimating contrast in low luminances is particularly challenging due to low signal-to-noise levels but vital since predators use contextual dim light as a strategy for prey capture. Additionally dark regions dominate in natural scenes (Ratliff et al. 2010; Odermatt et al. 2012; Dyakova et al. 2017). Thus it might be beneficial to use a dedicated pathway for boosting contrasts in low luminance regimes. The major inputs to Tm9 neurons come from the first-order luminance-sensitive L3 neurons that non-linearly amplify their responses in low luminances (Fisher et al. 2015; Ketkar et al. 2020; Ketkar et al. 2022), providing a possible explanation for the differences in Tm9 and Tm1 properties. The Tm9 luminance gain channel may be predominantly using the L3 inputs to selectively boost contrasts encountered in low luminance regimes.

Different uses for post-receptor gain mechanisms

Although the phenomenological needs for a rapid luminance gain can be derived from experiments in insects (Ketkar et al. 2020), cats (Mante et al. 2005) and humans (Burkhardt et al. 1984), this is the first study to address the circuit basis for a post-receptor luminance gain in rapidly changing light conditions. So far, in vertebrates, only post-receptor luminance gain mechanisms that are utilized in absolute dim light conditions were discovered (Green et al. 1982; Shapley et al. 1984; Dunn et al. 2007). For example, the gain location switches from cones to the synapses between bipolar cells and retinal ganglion cells in low light levels (Green et al. 1975; Dunn et al. 2007). Similarly invertebrates also have post-receptor strategies to handle dim light conditions such as spatial and temporal summation (Stöckl et al. 2016). Our experiments were conducted in illumination conditions where fruit flies have peak activity during the day (Rieger et al. 2007; Spitschan et al. 2016), so the mechanisms we discovered do not necessarily translate to the gain mechanisms in absolute dim light conditions but rather contextual changes in luminance levels that can be also encountered in high light levels. Thus, the retina employs different post-receptor gain mechanisms according to the changing demands of the environment. Since the vertebrate retina is also subjected to similar contextual changes in luminance as the fly visual system (Mante et al. 2005; Rieke et al. 2009), it should also possess luminance gain strategies similar to the fly. If the implementation of the gain observed in absolute dim light conditions and contextual conditions overlap will be revealed with further studies covering wider ranges of luminance.

A rapid luminance gain arises through a combination of circuit and molecular mechanisms

Spatial pooling underlies the luminance gain in Tm1 and Tm9 neurons. Tm1 and Tm9 neurons are columnar meaning that their dendritic regions span only a single medulla column. For spatial pooling to occur, Tm1 and Tm9 neurons both require horizontal inputs besides their columnar direct cholinergic inputs mainly from L2 and L3 neurons (Takemura et al. 2013; Davis et al. 2020). We showed that Tm1 and Tm9 receive receive wide-field glutamatergic inputs onto their dendrites. Thus, convergence of columnar cholinergic and wide-field glutamatergic inputs is the prime candidate for underlying the implementation of luminance gain. In line with this, the glutamate receptor GluClα is required for the luminance gain in Tm9 neurons. Accordingly, GluClα expression data shows that it is expressed broadly in the medulla neurons (Molina-Obando et al. 2019).

Which neurons underlie the spatial pooling in Tm neurons? The wide-field inter-columnar Dm neurons are the prime candidates for mediating horizontal processing at the distal medulla where Tm neuron dendrites are located (Fischbach et al. 1989; Nern et al. 2015). Furthermore, based on the expression of genes required in neurotransmitter synthesis, Dm neurons can be glutamatergic (Davis et al. 2020), in line with the wide-field glutamate signals coming onto Tm1 and Tm9 den-

drites. Dm9 for example, has its neurites in the medulla layer M3 where Tm1 and Tm9 dendrites are located. Furthermore it is glutamatergic and its neurites extend to 5-7 columns of the medulla (Nern et al. 2015; Davis et al. 2020) similar to the pooling sizes we observed in our experiments. Other glutamatergic Dm neurons with their neurites in layer M3, such as Dm4, Dm12 or Dm20 can also provide narrower glutamatergic signals. Their arborizations span more medulla columns, but horizontal neuron dendrites can act as independent units (Grimes et al. 2010; Meier et al. 2019) and unpublished work from the lab suggests that at least some of them signal locally (Lopez et al. 2020). Assessing the physiology of Dm neurons and silencing them while assessing Tm neuron contrast representations will reveal the roles of distinct Dm neurons for rapid luminance gain control.

How can a combination of spatial pooling and GluClα lead to luminance gain in Tm9 neurons? Luminance gain is a normalization process where contrast responses are scaled by local luminance levels. Normalization in the brain can be achieved by various network and molecular mechanisms (Carandini et al. 2011). A common mechanism for normalization in the visual system involves shunting inhibition (Reichardt et al. 1983; Carandini et al. 1994; Carandini et al. 1997). Shunting inhibition requires the expression of channels that have reversal potentials close to the resting state such as channels that are permeable to chloride. Activation of such channels leads to membrane conductance changes which scale other incoming inputs. A recent study showed that GluClα mediates shunting inhibition for enhancing motion computation in T4 dendrites (Groschner et al. 2022). Thus GluClα could be scaling the cholinergic direct inputs on Tm9 with a shunting mechanism. However, this does not exclude other mechanisms supplementing the rapid luminance gain. GABA receptors are also permeable to chloride and can underlie normalization as discovered in the fly olfactory system where lateral GABAergic inhibition acts to normalize responses (Olsen et al. 2008b). Furthermore, some Dm neurons are GABAergic (Davis et al. 2020), and the $GABA_A$ receptor Rdl is broadly expressed in Tm neurons (Molina-Obando et al. 2019). GluClα was not required for luminance gain in Tm1 neurons and thus Tm1 neurons could be utilizing a GABAergic mechanism.

The extent of spatial pooling is crucial for reliable and accurate estimation of luminance. Pooling over wide extents reduces the noise in the signal and thus makes it more reliable. However, a trade-off between reliability and accuracy arises since natural scene luminance correlations fall rapidly with the distance indicating a problem of estimating luminance over large spatial extents (Frazor et al. 2006). Local contrast estimation will not be accurate if a large and thus highly variable area of luminance is selected for the gain control mechanisms. In line with this, at the level of perception, brightness constancy is achieved in spatially non-uniform illumination, suggesting that the luminance gain control is local (Davidson et al. 1965). We showed that Tm neuron pooling extends around 20° of the fly visual field revealing the local estimation of luminance at the neuronal level. Matching the pooling extent with the luminance correlations in natural scenes encountered by the fly will reveal if the pooling extend is optimal for processing natural scenes.

Visual gain mechanisms operate independently and ensure higher-order sensory processing

Changes in luminance can be confounding with the other dimensions of visual stimuli. For example, an object with a given velocity could elicit different signals in motion detectors if these detectors do not receive luminance-invariant signals. By achieving luminance-invariance at multiple timescales, the peripheral visual neurons greatly simplify consecutive processing steps. In accordance with this idea, our data showed that local direction-selective T5 cells exhibit luminance-invariant responses to edges moving at the same velocity. Inputs from the luminance gain exhibiting neurons Tm1 and Tm9 spatially cover all the dendritic region of the T5 neurons (Shinomiya et al. 2019a). This architecture ensures that T5 neurons receive luminance-invariant inputs throughout their dendritic region which is important for motion computation since it depends on spatially separated inputs.

Amongst the four major OFF medulla neurons that convergence onto T5 dendrites, only Tm1 and Tm9 exhibited the rapid luminance gain whereas Tm2 and Tm4 show a luminance-dependent representations of contrast. What are the roles of Tm2 and Tm4 signals on the downstream processing? Recent studies showed that another form of rapid gain in the medulla, contrast gain, ensure

stable velocity estimation in direction-selective cells (Drews et al. 2020; Matulis et al. 2020). Tm2 and Tm4 neurons both exhibit temporal contrast gain. Thus, the circuitry in the medulla processes the variances of contrast and luminance in parallel. In vertebrates, contrast and luminance gain operate independently which reflects the natural scene statistics where contrast and luminance are independent features (Mante et al. 2005). The separation of luminance and contrast gain in the fly medulla could thus arise due to the need to operate these processes independently.

A combination of parallel gain mechanisms ensures stable extraction of downstream visual features. Similarities between vertebrates and invertebrates for the location and implementation of the post-receptor luminance gain suggests convergent evolution. Thus our findings provide a widely-applicable detailed understanding of how visual systems handle rapid luminance changes that occur in natural scenes.

Methods

Drosophila strains and fly husbandry

Flies used for confocal and two photon imaging were raised in plastic vials on molasses-based food on a 12:12 hr light:dark cycle at 25°C in an incubator with 65% humidity. Parental crosses were flipped every 2-3 days into new vials and dry food was watered regularly to keep the vial conditions optimal. *Drosophila* strains used are provided in Table 5.1.

Two photon imaging

Before imaging, flies were anesthetized by incubating them shortly on ice and placed into a stainless-steel custom-made fly holder. The fly heads were tilted to expose the head cuticle for further dissection. Left side of the head was fixed to the holder using a UV-sensitive glue (Bondic) and legs and proboscis were fixed to the body using a low temperature melting wax to prevent brain motion during recordings. The cuticle on the right side of the head was removed using a razor and sharp forceps to provide optical access. Fat bodies and trachea were also removed. The dissection procedure was done in saline containing 103 mM NaCl, 3 mM KCl, 5 mM TES, 1 mM NaH2PO4, 4 mM MgCl2, and 26 mM NaHCO3. During imaging a similar saline solution with additional calcium and sugars (1.5 mM CaCl2, 10 mM trehalose, 10 mM glucose, 7 mM sucrose) was perfused to the fly brain and carboxygenated to achieve a constant pH 7.3. Two photon experiments for figures 5.1, 5.2, 5.3, 5.4, 5.5, 5.9-Tm9 experiments were done using a Bruker Investigator microscope (Bruker, Madison, WI, USA) that is equipped with a 25 x/NA1.1 objective (Nikon, Minato, Japan). An excitation laser (Spectraphysics Insight DS+) tuned to 920 nm was used to excite GCaMP6f, using 5–15 mW of power measured at the sample. tdTomato expression in 5.10B, C was checked using the 1040 nm laser in the same microscope. For figures 5.7, 5.8, 5.10 we used a Bruker Ultima microscope with a 20 x/NA1.0 objective (Leica, Wetzlar, Germany). A fixed excitation laser of 930 nm (YLMO-930 Menlo Systems, Martinsried, Germany) was used with the same power applied to the sample.

For both setups we used a SP680 shortpass filter, a 560 lpxr dichroic filter and a 525/70 emission filter for the emitted light. To acquire the data, PrairieView software was used. Images were acquired at a frame rate of 10-15 Hz and an optical zoom level of 6-8x was used.

Visual stimulation

For both setups, stimulation and imaging was synchronized using custom-written software written in either Python (Bruker Ultima setup) or C++ (Bruker Investigator setup). Stimuli were projected using a DLP LightCrafter(Texas Instruments, Dallas, TX, USA), working at a frame rate of 100 Hz. The stimuli were filtered using a 482/18 band pass filter and a ND1.0 neutral density filter (Thorlabs) placed on the projector. For stimulus generation in the Bruker Ultima setup, I developed and used PyStim (https://github.com/bgur123/PyStim) which is based on the Python package PsychoPy (Peirce, 2008). The stimulus was projected onto a 9 x 9 cm rear projection screen placed in front of the fly at a 45° angle spanning 80° of visual space in both azimuth and elevation. For stimulus generation in the Bruker Investigator setup, I used custom-written C++ and OpenGL

Table 5.1: Genotypes used in this study.

Name	**Genotype**	**Figure**
L1	w+; *L1^{c202}Gal4 /+; UAS-GCaMP6f /+*	5.5
L2	*w+; UAS-GCaMP6f /+; L2^{21Dhh}-Gal4 /+*	5.1, 5.2, 5.4, 5.5
L3	*w+; L3^{MH56}-Gal4 /+; UAS-GCaMP6f /+*	5.1, 5.2, 5.3, 5.4, 5.5
Tm1	*w+; UAS-GCaMP6f /+; GMR74G01-Gal4 /+*	5.3, 5.4, 5.5, 5.6, 5.7, 5.9, 5.10
Tm2	*w+; R28D05-p65ADZp^{attP40} /UAS-GCaMP6f; R82F12-ZpGdbd^{attP2} /+*	5.3, 5.4
Tm4	*w+; R53C02-p65ADZp^{attP40} /UAS-GCaMP6f; R60H04-ZpGdbd^{attP2} /+*	5.3, 5.4
Tm9	*w+; Tm9-lexAp65attP40,lexAop-GCaMP6f^{attP5}/+ ; + /+*	5.3, 5.4, 5.5, 5.6, 5.7, 5.8, 5.9, 5.10
T4-T5	*w+; R59E08-LexA^{attP40}, lexAop-GCaMP6f-p10$^{su(Hw)attP5}$/+ ; +/+*	5.1, 5.2
Tm1-iGluSnFR	*w+; + /+; GMR74G01-Gal4 / UAS-iGluSnFR A184A^{attP2}*	5.9
Tm9-iGluSnFR	*w+; + /+; GMR42C08-Gal4^{attP2} / UAS-iGluSnFR A184A^{attP2}*	5.9
Tm9, GluCl$\alpha^{FlpStop-D}$	*w+; UAS-GCaMP6f,UAS-Flp /+; GluCl$\alpha^{FlpStop-ND}$/GMR42C08-Gal4^{attP2},GluCl$\alpha^{MI14426}$*	5.10
Tm9, Flp control	*w+; UAS-GCaMP6f /+; GluCl$\alpha^{FlpStop-ND}$/GMR42C08-Gal4^{attP2},GluCl$\alpha^{MI14426}$*	5.10
Tm9, GluCl$\alpha^{FlpStop-D}$ heterozygous control	*w+; UAS-GCaMP6f,UAS-Flp /+; GluCl$\alpha^{FlpStop-ND}$/GMR42C08-Gal4^{attP2}*	5.10
Tm1, GluCl$\alpha^{FlpStop-D}$	*w+; UAS-GCaMP6f,UAS-Flp /+; GluCl$\alpha^{FlpStop-ND}$/GMR74G01-Gal4^{attP2},GluCl$\alpha^{MI14426}$*	5.10
Tm1, Flp control	*w+; UAS-GCaMP6f /+; GluCl$\alpha^{FlpStop-ND}$/GMR74G01-Gal4^{attP2},GluCl$\alpha^{MI14426}$*	5.10
Tm1, GluCl$\alpha^{FlpStop-D}$ heterozygous control	*w+; UAS-GCaMP6f,UAS-Flp /+; GluCl$\alpha^{FlpStop-ND}$/GMR74G01-Gal4^{attP2}*	5.10

software (Freifeld 2013) and stimuli were projected onto 8x8cm rear projection screen covering 60° of visual space in both azimuth and elevation. The maximum luminance value (I^{max}) measured at the fly position was 2.17*10^5 photons s^{-1} $photoreceptor^{-1}$ for the Bruker Investigator, and 2.4*10^5 photons s^{-1} $photoreceptor^{-1}$ for the Bruker Ultima setup.

Drifting sinusoidal gratings Drifting sinusoidal gratings moving at 1 Hz (speed 30°s^{-1}, spatial wavelength 30°) with a constant 100% Michelson contrast at changing mean luminances

were used. The mean luminance of gratings were 1.2, 2.6, 5.3, 7.9 and 10.6 *10^4 photons s^{-1} photoreceptor^{-1}. The drifting epochs lasted 4 seconds and interleaved by 4 seconds of full field mean luminance. Epochs were presented in a randomized fashion and repeated at least 3 times for trial averaging of noise. The gratings moved to two opposing horizontal directions for stimulating layer A and B of T4 and T5 neurons whereas for other neurons only a single direction was used. For Figure 5.2, 5 temporal frequencies were used by changing the speed of the grating. The temporal frequencies were 0.1, 0.375, 0.5, 1, 2Hz. For Figures 5.5 and 5.6, 5 different contrast values were used on top of the above mentioned mean luminance values. These were 20, 40, 60, 80 and 100% Michelson contrast.

OFF moving edges The stimuli consisted of a 1 second full field presentation of a given luminance which was followed by a moving dark edge at a constant 100% Weber contrast ($\frac{I_{edge}-I_{background}}{I_{background}}$). The full field luminance levels before the OFF edges were 1.2, 2.6, 5.3, 10.6, 16, 21.4 *10^4 photons s^{-1} photoreceptor^{-1}. The edge epochs were interleaved by 4 seconds of darkness.

Ternary white noise for online RF mapping-stimulation paradigm The frames of the white noise consisted of squares with edges of 2.5° spanning the whole 80° x 80° screen. Each square changed its brightness value at 20 Hz, becoming either fully dark, intermediate brightness (0.5*I^{max}) or full brightness (I^{max}). The changes happened with equal probability. Before the white noise, 4 seconds of full field intermediate brightness was presented to acquire the baseline signal of neurons. The stimulation lasted around 3-4 minutes which enabled extraction of a RF with good signal-to-noise ratio for estimating the RF centers.

Drifting gratings with various sizes for online RF mapping-stimulation paradigm Above mentioned drifting gratings at 100% Michelson contrast and different luminances were used with varying the size of the gratings. The diameter ranged from 5° to 30° with 5° increments. The grating was placed at the center of the mapped receptive field.

Flashes of different luminances The stimulus consisted of epochs with full-field flashes lasting 7s at 11 different luminances: 0, 0.0625, 0.125, 0.2, 0.25, 0.5, 0.6, 0.7, 0.8, 0.9, 1 *I^{max}. The epochs were randomized and repeated at least 3 times.

Periodic full-field flashes The stimulus consisted of two epochs with full-field ON (I^{max}) and OFF flashes lasting 5s. The epochs were repeated at least 8 times.

Ternary white noise of stripes The frames of the white noise consisted of vertical stripes with a width of 5° spanning the 60°x60° (Investigator setup) or 80°x80° (Ultima setup) screen. Each stripe changed its brightness value at 20Hz, becoming either fully dark, intermediate brightness (0.5*I^{max}) or full brightness (I^{max}). The changes happened with equal probability. Before the white noise, 4 seconds of full field intermediate brightness was presented to acquire the baseline signal of neurons. The stimulation lasted around 10 minutes.

Data analysis

Python 2.7 was used to perform data processing (Van Rossum 1995). Pre-processing steps consisted of motion correction using the Hidden Markov Model from the SIMA Python package (Kaifosh et al., 2014), ROI selections were either performed manually (for all neurons except T4 and T5) or using the spatiotemporal ICA segmentation algorithm of the SIMA package (for T4 and T5 neurons). The time traces for each ROI was extracted by averaging the signal within the delimited space followed by background subtraction. Relative changes in signal ($\Delta F/F0$) were calculated using the mean of the trace as F0. This was followed by trial averaging and stimulus specific analyses. Stimulus specific analyses were done for each individual ROI and then averaged across flies.

Drifting gratings Since the drifting gratings moved at a given temporal frequency (1Hz except Figure 5.2D), contrast responses were calculated as the amplitude of the signal at the grating temporal frequency following a Fourier transformation of the signal using FFT. The contrast responses were normalized by maximum for each ROI for facilitating comparisons of luminance dependency between different types of neurons. Furthermore, luminance dependency was calculated by fitting a linear regression line at contrast response vs luminance values and extracting the slope. Gain was calculated by dividing the normalized contrast responses of each ROI of Tm1 and Tm9 neurons to the mean normalized L2 response.

The contrast-luminance heat maps were generated by using linear spline interpolation via the SciPy function scipy.ndimage.zoom() on the original data (mean across flies) from grating contrast responses to 5 contrasts and 5 luminances (The original data is a 5x5 matrix depicting the amplitudes for each contrast-luminance pair). The used zoom value was 5 (increasing the resolution 5 times from 5x5 to 25x25), interpolation order was 1 (linear). The interpolated maps were then smoothened with a Gaussian filter with a sigma 10 before plotting the contour lines. This method facilitates the visualization of the contrast-luminance space to explore how responses vary with contrast and luminance.

OFF moving edges Edge responses of ROIs for each epoch was calculated as the difference between the mean of the preceding 1 s luminance presentation and the maximum response elicited to the OFF edge. Similar to drifting gratings, the luminance dependency was calculated by fitting a linear regression line at edge response vs luminance values and extracting the slope.

Flashes of different luminances Plateau responses were calculated using the mean of the ROI calcium signal at the last 500ms for each luminance epoch. In order to create a value that depicts the level of plateau within the operating range of a given neuron, we calculated the plateau response as:

$$F_{Plateau} = \frac{F_{last500ms} - F_{min}}{F_{max} - F_{min}}$$

Ternary white noise analysis First the time traces of ROIs were extrapolated to 20Hz matching the update rate of the white noise stimulation paradigm. Here relative changes in signal ($\Delta F/F0$) were calculated using the mean of the first 4 seconds of full field intermediate brightness stimulation as F0. The trace was centered around the mean as the stimulus was centered around 0. Reverse correlation analysis was used to extract the STRFs. Briefly, a backwards sliding window of 2 seconds was propagated through the stimulus and for each slide, the stimulus values were scaled with the neuron's response at the beginning of the window (r_t). Given the total time of the stimulus presentation (T) stimulus time window (τ), cell response at time point t (r_t) and the stimulus values during the time window ($s(t-\tau)$), the equation of the STRF is as follows:

$$STRF = \frac{1}{T-\tau}\sum_{t=\tau}^{T} r_t s(t-\tau)$$

To filter out noisy STRFs we used a absolute filter threshold of 0.008. Since iGluSnFR Tm1 recordings were noisier than other experiments, the threshold here was reduced to 0.003. To further get rid of noisy STRFs in iGluSnFR Tm1 recordings, we used a SNR threshold of 10 where SNR is determined as the absolute maximum value of the STRF divided by the mean of the STRF. These thresholds were determined upon visual inspection of STRFs. Temporal filters were extracted by picking the time trace of the spatial location where filter produced its minimum response. Spatial filters were extracted by picking the space trace of temporal location with the minimum response. Minimum was used since STRF amplitudes of OFF cells grow in the negative direction. To calculate the full-width-at-half-maximum (FWHM) we fitted a single Gaussian:

$$f(x) = a * e^{-\frac{(x-\mu)^2}{2\sigma^2}}$$

where μ is the mean and σ is the standard deviation. FWHM was then calculated as $2.355 * \sigma$.

Online RF mapping-stimulation paradigm First, the neurons the STRFs were extracted using reverse correlation analysis (mentioned above). To get the center location of the STRFs, a two dimensional Gaussian was fitted to the spatial receptive field at the time where minimum filter amplitude is reached (minimum since our neurons are OFF cells). A two dimensional Gaussian is defined as:

$$f(x,y) = h * e^{-\frac{(\frac{center_x - x}{width_x})^2 + (\frac{center_y - y}{width_y})^2}{2}}$$

$center_x$ and $center_y$ values were then used to place the drifting grating center in the stimulus screen. We tested the method accuracy by comparing adjacent axon terminal responses to a 5° test grating that only stimulated the selected neuron (Figure 5.8).

Statistics

Quantified variables were first calculated for each ROI and then averaged within and across flies. Statistical tests are reported in each figure.

Acknowledgements

We thank Christine Gündner, Simone Renner, and Jonas Chojetzki for excellent technical assistance in the Silies lab. This project has received funding from the European Research Council (ERC) under the European Union's Horizon 2020 research and innovation program (grant agreement No 716512) and the collaborative research center 1080 "Neural homeostasis" (project C06) to MS.

6 | Manuscript 4: STAB: A versatile genetic tool for the synapse-specific analysis of circuit function

The following manuscript is under preparation.

Authors and affiliations

Burak Gür[1,2], Jonas Peper[1], Marion Silies[1,*]

1 - Institute of Developmental Biology and Neurobiology, Johannes-Gutenberg University Mainz, Mainz, Germany

2 - Göttingen Graduate School for Neurosciences, Biophysics, and Molecular Biosciences (GGNB) and International Max Planck Research School (IMPRS) for Neurosciences at the University of Göttingen, Göttingen, Germany

* - For correspondence: msilies@uni-mainz.de

Contribution statement

Marion Silies and I conceptualized and designed the study, reviewed and edited the original draft. I conducted the investigation, developed analysis software, visualized the data, wrote the original draft. Jonas Peper conducted experiments for Figure6.2H, Figure6.5A, Figure6.6.

Abstract

A causal understanding of how neural circuits drive behavior is a major goal of neuroscience. Manipulation methods such as optogenetics are used to activate or inhibit neural activity down to the cell-type level. However, neural circuits are intricate networks where single cell-types can simultaneously receive inputs from or feed into different information processing streams. In this complex architecture, synaptic connections of a given cell-type can specialize in processing information differently via synaptic specializations ranging from neurotransmitter and receptor differences to learning-induced synaptic weight changes. Thus, the elementary unit of neural information processing lies in the synaptic connections between two partners. However, no method exists to manipulate distinct synaptic connections, hindering a detailed causal understanding of neural circuits. Here, using *Drosophila melanogaster* as a platform, we are developing a versatile genetic tool, Synapse Targeted Activity Block (STAB), that allows the manipulation of neural circuits at the level of individual synaptic connections. STAB is a strategy based on TEV protease-mediated disruption of endogenous synaptic proteins. We generated TEV protease fusion proteins for usage in pre- and post-synapses of *Drosophila* neurons and generated a strategy to conditionally tag endogenous proteins with a TEV cleavage site. As a proof or principle, we tested STAB by targeting glutamate-gated chloride channel GluClα and GABA$_A$ receptors. TEVp can cleave GluClα *in vitro* yet *in vivo* cleavage is not sufficient to lead to a full LOF. Thus we improved TEVp activity using mutagenesis and showed that the mutated TEVp can cleave more GluClα. STAB with new TEVp still needs to be validated *in vivo*. The STAB approach provides the first example of synapse-specific manipulation system and can also be flexibly used to achieve protein-specific synaptic disruptions. STAB can be in principle be applied in any *Drosophila* circuit and in other model organisms with binary expression systems. Once successful, STAB will thus open a high-resolution window to obtain a detailed causal understanding of neural circuit function.

Introduction

One of the principal aims of neuroscience is to elucidate the architectural and functional principles of neural networks that allow them to perform sophisticated computational tasks to elicit behavior. Recent years have seen significant advances in genetic methods for manipulating neural activity which is instrumental to a detailed causal understanding of neural processing (Sternson et al. 2014; Deisseroth 2015; Owald et al. 2015). Genetic tools now allow different levels of analyses down to specific cell-types. Consequently, cells or cell types are considered the fundamental units of neural computation. However, neural circuits are intricate networks where single neurons can simultaneously receive input from, and feed into, different pathways through distinct synaptic partners.

Electron microscopy techniques allowed precise reconstruction of circuits in diverse organisms and revealed the complex wiring diagrams of neural circuits (Chen et al. 2006; Briggman et al. 2011; Takemura et al. 2013; Schlegel et al. 2017; Lee et al. 2016; Takemura et al. 2017; Horne et al. 2018; Shinomiya et al. 2019a; Scheffer et al. 2020). These diagrams show that divergence and convergence happen at many stages within neural processing streams, also shown at the functional level (Cohen et al. 1990; Jeanne et al. 2015; Takagi et al. 2017; Luo 2021). This architecture suggests that the boundaries between the processing of different types of information are not clearly defined between specific cell-types. An essential property of this circuit architecture is that a diverging cell type can affect its post-synaptic partners differentially (e.g., depending on the connection strength or the neurotransmitter profile) and thus contribute to neural processing in a complex way through this synaptic heterogeneity. Synaptic heterogeneity is found in many sensory (Baden et al. 2010; Euler 2001; Taylor et al. 2011; Euler et al. 2014; Gaudry et al. 2013) and motor systems (Guerrero et al. 2005). In the *Drosophila* olfactory system the first order olfactory receptor neurons (ORNs), for example, project bilaterally to both hemispheres of the fly brain. Ipsilateral projections from the same ORN release 40% more neurotransmitters suggesting transmission of different information from the same ORN to downstream circuits (Gaudry et al. 2013). To understand the role of ORNs olfactory computation, one would need to separately investigate the causes of these two phenomena on further processing or behavior. Additionally, in the second processing layer of the vertebrate retina, the synapses formed between bipolar and RGCs are differently modulated by amacrine cells leading to individual bipolar-RGC synapses acquiring distinct transfer functions expanding the computational capabilities of RGCs (Asari et al. 2012). These examples and many more suggest that instead of an individual neuron or cell type, one should rather consider the specific connection between two cell types a computationally relevant unit. Thus, understanding the fundamentals of neural computations requires tools to manipulate neural activity with synaptic resolution.

The genetics, the short generation time, a relatively small nervous system, a wide repertoire of quantifiable behaviors and the most extensive genetic toolbox among all model organisms make the fruit fly a versatile platform for studying neuronal function and developing cutting-edge genetic tools (Venken et al. 2011a). Binary expression systems, such as Gal4-UAS can be used to drive the expression of transgenes in a cell type of interest and vast libraries of Gal4 lines exist and give access to in principle every single neuron or cell type in the fly brain (Jenett et al. 2012; Gohl et al. 2011). Other binary expression systems exists and enable independent expression of genetic constructs simultaneously in several cell-types (Lai et al. 2006; Potter et al. 2010). Transgenesis is time and cost efficient Venken et al. 2005. Recombination methods such as Flp-FRT, Cre-loxP and attB-phiC31 provide site-specificity and directionality in the manipulation of the genome (Venken et al. 2005). The fly genome is of course also amenable to very specific genome editing methods such as CRISPR-Cas9 (Gratz et al. 2015a). Currently, there are numerous methods for neural manipulations, all can be used with a resolution down to cell-type level (Owald et al. 2015). So far, no manipulation method achieves targeting of synaptic partners but the recently developed trans-synaptic tracing methods activate only in synaptic partners opening up possibilities for developing other synapse-specific methods (Macpherson et al. 2015; Talay et al. 2017; Huang et al. 2017; Cachero et al. 2020).

Here we developed a novel genetic tool, Synapse Targeted Activity Block (STAB), in order to manipulate neural activity with synaptic resolution. STAB is a TEV protease-based synapse disruption method where extracellular TEV protease (TEVp) is expressed on one side of the synapse and

cleaves an essential protein on the other side of the synapse leading to disruption of the synapses only between two defined cell types. STAB depends on two components, a pre- or post-synaptically expressed TEVp and a TEV cleavage site (TEVcs) integrated into post- or pre-synaptic protein. Both TEVp and TEVcs can be expressed or exposed in a cell-type specific way. First, we developed and tested TEVp fusion proteins *in vitro* and successfully targeted them to pre- or post-synaptic sites *in vivo*. Then we designed a strategy to conditionally integrate TEVcs into synaptic proteins (flp-TEV) and generated flp-TEV versions of the glutamate gated chloride channel GluClα and the GABA$_A$ receptor Rdl. Endogenous protein function was preserved upon TEVcs integration. We then showed that TEVp can cleave the TEVcs integrated GluClα and cleavage leads to the degradation of protein *in vitro*. However, the cleavage was not sufficient for recapitulating LOF phenotypes *in vivo*. Thus we improved the TEVp activity by introducing mutations that facilitated protein folding and stability and showed that a TEVp with 3 point mutations had increased cleavage and lead to a higher degradation of GluClα *in vitro*. STAB needs to be further validated *in vivo* with the improved TEVp before it can be applied to study circuit function at synaptic resolution.

Results

Synapse Targeted Activity Block (STAB) strategy

With Synapse Targeted Activity Block (STAB) we aim to achieve disruption of specific synaptic connections between two cell types within a neural circuit (Figure 6.1A). Our strategy is based on the disruption of synaptic communication via proteolytic cleavage of an essential synaptic protein. On one side of the synapse, the Tobacco Etch Virus protease (TEVp) is fused to a synapse-enriched trans-membrane molecule and spans the synaptic cleft. On the other side of the synapse, an essential synaptic protein is modified at its endogenous locus with an artificially inserted TEV cleavage site (TEVcs). To achieve synapse-specific disruption of function, both components require cell-type specificity which is achieved by using established binary expression systems (Gal4-UAS and LexA-lexAop) for their expression (TEVp) or exposure (TEVcs). The choice of TEVp relies on several factors. First, TEVp is widely used in *in vitro* and *in vivo* studies including recent genetic methods developed in the *Drosophila* system enabling us to utilize the wide knowledge to design and optimize the protease components of STAB (Harder et al. 2008; Pauli et al. 2008; Urban et al. 2014; Politi et al. 2014; Cachero et al. 2020; Byri et al. 2015; Brankatschk et al. 2010). Second, the *Drosophila* proteome doesn't contain any essential protein that the TEVp targets (Harder et al. 2008).

We designed two versions of STAB that either disrupt synaptic function of the pre- and the post-synaptic site. For disruption of the pre-synapse we used a post-synaptic TEVp fusion protein that targets the endogenously modified pre-synaptic voltage gated calcium channels (Figure 6.1B). For disruption of the post-synapse, a pre-synaptic TEVp targets an essential post-synaptic receptor with a TEV cleavage site (Figure 6.1C).

TEV protease fusion proteins are active *in vitro*

To achieve synaptic disruption, the TEVp has to be present in the extracellular side of either the post- or the pre- synapse. If a post-synaptic receptor is targeted, the TEVp must be present in the pre-synaptic side of the synaptic partner and vice versa if a pre-synaptic molecule is targeted (Figure 6.1). To localize TEVp to pre-synapses we attached it to the extracellular side of vesicular SNARE protein Synaptobrevin (nSyb) which has previously been widely used to target proteins to the pre-synapse (Gandhi et al. 2003; Wienisch et al. 2006; Huang et al. 2017). For post-synaptic targeting of TEVp we chose two synaptically expressed proteins that tolerate fusion on the extracellular site: 1) The murine intercellular adhesion molecule (ICAM5) has been previously used for post-synaptic targeting of fluorescent molecules in *Drosophila* and does not interfere with synaptic morphology or function (Nicolaï et al. 2010). 2) The post-synaptic adhesion molecule Neuroligin has also previously been shown to tolerate extracellular fusion proteins (Tsetsenis et al. 2014; Huang et al. 2017). Using optimized *Drosophila* expression vectors (Pfeiffer et al. 2010; Pfeiffer et al. 2012) we first tested the TEVp expression and activity in *Drosophila* S2 cells (Figure 6.2).

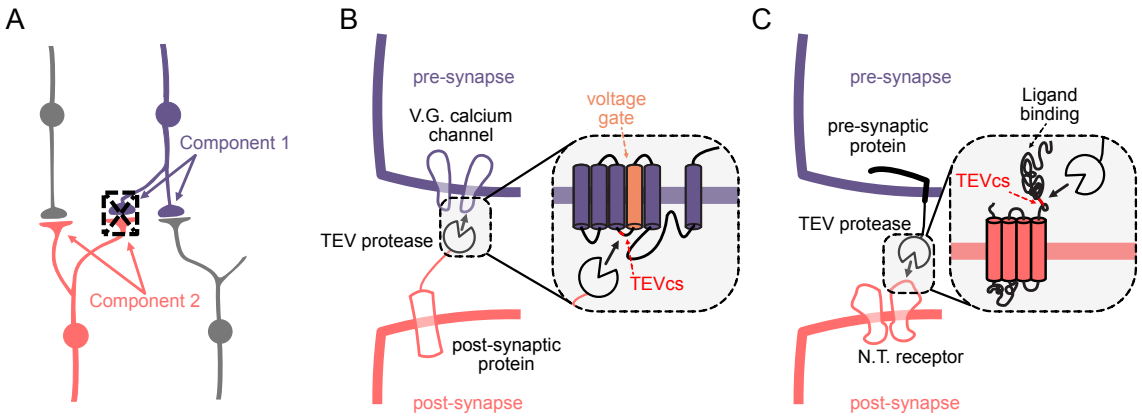

Figure 6.1: STAB Strategy. (A) STAB consists of two components that are expressed in distinct synaptic partners. Only when these two components meet in the synapses, STAB leads to synaptic disruption between just these two cell types (blue and red), leaving connections to other partners (other cell types, grey) functional. **(B)** To achieve pre-synaptic disruption, TEV protease (TEVp) is expressed on the post-synaptic site and targets an endogenous pre-synaptic protein modified with an integrated TEV cleavage site (e.g., voltage-gated calcium channels) to disrupt synaptic function. **(C)** For post-synaptic disruption, TEVp is expressed on the pre-synaptic site and targets a post-synaptic protein (e.g., a neurotransmitter receptor) to disrupt synaptic function.

All TEVp fusion proteins could be expressed in S2 cells. nSyb fused TEVp (nSyb-TEVp) exclusively localized to the cell membrane (Figure 6.2A) and the post-synaptic TEVp (TEVp-ICAM, TEVp-Nlg) fusion proteins showed localization throughout the cell (Figure 6.2B, C). To check TEVp activity, we generated a cleavage probe consisting of a synaptobrevin protein and a GFP separated by the TEVcs (Figure 6.2D). We first validated the cleavability of the probe by expressing it in S2 cells and adding synthesized TEVp to the bath solution (Figure 6.2D). Bath application of TEVp led to a rapid loss of GFP in the membrane, confirming the accessibility of the TEV cleavage site in the probe and its suitability for checking the activity of our TEVp constructs (Figure 6.2D).

We then expressed the TEVp fusion proteins together with the cleavage probe in S2 cells. We saw a loss of membrane GFP when expressing the cleavage probe together with the nSyb-TEVp suggesting that membrane localized nSyb-TEVp cleaved the TEVcs leading to the separation of GFP from the nSyb (Figure 6.2E). The post-synaptic TEVp fusion proteins did not show evidence of successful cleavage since the cleavage probe GFP was still present in the membrane of the cell (Figure 6.2F, G). This could be due to the insufficient extracellular localization of the fusion proteins (ER arrest etc.) in the cultured cells which could arise because of the differences between neuronal and S2 cell types.

To confirm the cleavage biochemically, we performed Western blots with the cells expressing the nSyb-TEVp and the cleavage probe (Figure 6.2H). We took different approaches to probe for protein cleavage. First, we used a TEV cleavage site antibody that specifically recognizes the sequence only when it is cleaved. This antibody gave signal at the expected molecular weight only when we expressed the nSyb-TEVp and the cleavage probe, confirming the cleavage at the protein level (Figure 6.2H). Furthermore, we checked for the GFP signal of the cleavage probe and saw a substantial reduction indicating that the GFP was separated from the cell after the cleavage of the TEVcs (Figure 6.2H).

Together, our data shows that TEVp is active *in vitro* in *Drosophila* cells.

TEV protease fusion proteins function *in vivo*

Next we tested our TEV protease fusion proteins in adult flies. Using the GAl4-UAS system we expressed the fusion proteins in the first-order visual system neurons L2 or L3 and assessed for expression and localization (Figure 6.3A). We expressed the pre-synaptic TEVp fusion protein, nSyb-TEVp, in L2 neurons which have their dendrites in the lamina and axon terminals as bulbs in the medulla M2 layer (Figure 6.3B). nSyb-TEVp strongly localized to L2 axon terminals, suggesting that nSyb-TEVp was well processed and transported to the desired location within the cells (Figure

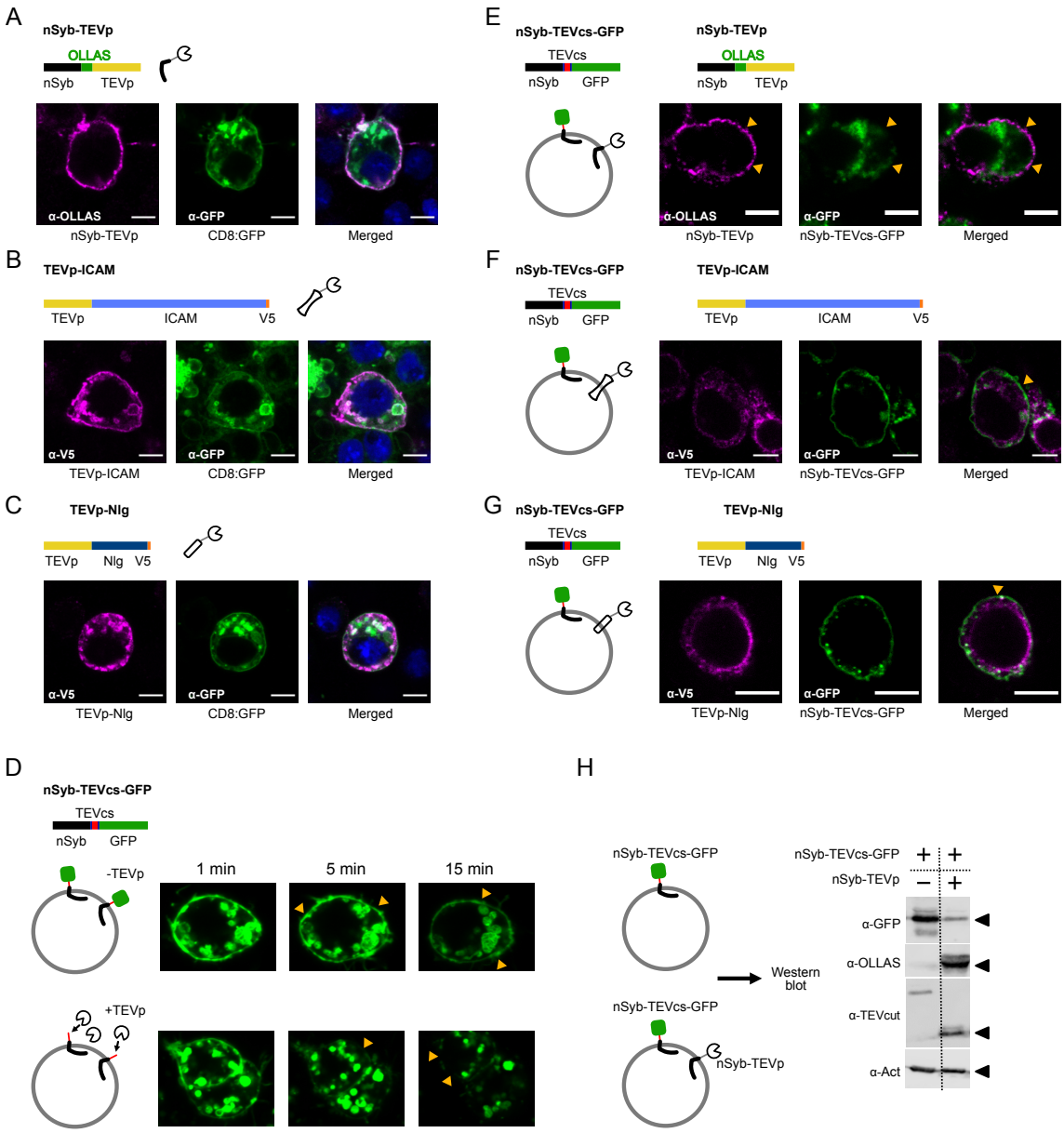

Figure 6.2: TEV protease is activate *in vitro*. S2 cells expressing a membrane-targeted GFP (CD8::GFP) construct (green) along with **(A)** nSyb-TEVp (magenta) **(B)** TEVp-ICAM **(C)** TEVp-Nlg. DAPI staining is used for nuclei (blue). **(D)** S2 cells expressing the TEV cleavage probe nSyb-TEVcs-GFP incubated in a control solution (upper row) and with bath application of TEVp after 1, 5 and 15 minutes. Membrane GFP signal disappears in cells incubated with a solution with TEVp (arrowheads) whereas the GFP signal is still present across the membrane for the cells incubated in control solution. **(E)** S2 cells expressing both the cleavage probe (green) and the nSyb-TEVp (magenta) have no membrane GFP signal (arrowheads). **(F)** S2 cells expressing both the cleavage probe (green) and the TEVp-ICAM (magenta) still have membrane GFP signal (arrowheads) **(G)** S2 cells expressing both the cleavage probe (green) and the TEVp-Nlg (magenta) still have membrane GFP signal (arrowheads). Scale bars show 5μm. **(H)** Western blot analysis from S2 cells expressing the cleavage probe together with nSyb-TEVp. Arrowheads show the expected size of the bands.

6.3B).

Then we tested our post-synaptic TEVp fusion proteins using L3 neurons since their dendrites are easily distinguishable. L3 neuron dendrites extend into a single direction from the main neurite, unlike L2 neuron dendrites which extend to both directions and make it harder for clearly differentiating signals between axons and dendritic sections (Figure 6.3A). Both post-synaptic TEVp fusion proteins expressed well in L3 neurons. TEVp-ICAM signal was present in L3 dendrites suggesting post-synaptic localization (Figure 6.3C). TEVp-Nlg failed to localize to the dendritic regions (Fig-

ure 6.3D) and thus we excluded this fusion protein from further usage. Together, we generated TEVp fusion proteins that localize to either pre- and post-synaptic regions.

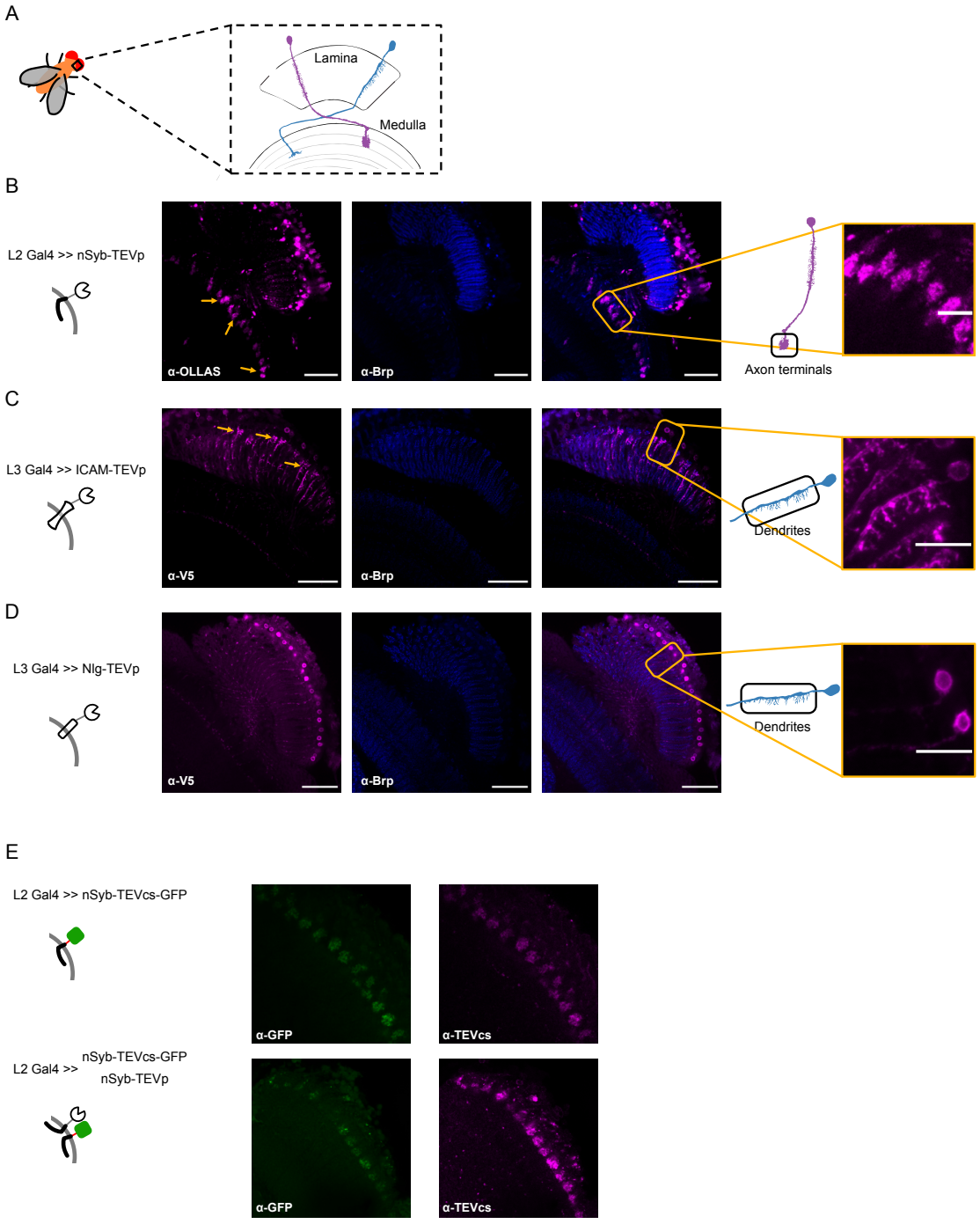

Figure 6.3: TEVp is active *in vivo*. **(A)** To check the expression of constructs, expression in L2 and L3 neurons located in the visual system of the fly was chosen. L2 and L3 dendrites are located in the lamina and they project their axon terminals to the medulla. **(B)** L2 neurons expressing the OLLAS tagged nSyb-TEVp (magenta). anti-Brp (nc82) staining (blue) marks the neuropil. Arrowheads point to L2 axon terminals located in the medulla M2 layer. In the right panel, a magnified image shows axon terminals of L2 neurons. **(C)** L3 neurons expressing V5 tagged TEVp-ICAM (magenta). Arrowheads point to the L3 dendritic regions located in the medulla. In the right panel a magnified image shows the dendrites of single L3 neurons showing their stereotypical orientation into the neuropil. **(D)** L3 neurons expressing V5 tagged TEVp-Nlg (magenta). Scale bars of images in the first 3 columns show 50μm and magnified image scale bars show 5μm (in B) and 10μm (in C, D). **(E)** L2 neurons expressing either only the cleavage probe with GFP (nSyb-TEVcs-GFP, upper row) or both the cleavage probe and the nSyb-TEVp (lower row). α-TEVcs antibody targets the cleaved TEVcs with higher affinity.

We then wanted to probe for TEVp activity *in vivo*. We expressed the cleavage probe together with the nSyb-TEVp transgene in L2 neurons (Figure 6.3E). We used the TEV cleavage site antibody which recognizes the cleaved TEVcs with higher-affinity. We compared brains under identical experimental conditions (including experimental procedure, microscope settings etc.) and observed an increased signal for the TEV cleavage site antibody when expressing the probe and the nSyb-TEVp together compared to when the probe was expressed alone (Figure 6.3E). This suggests that TEVp is active *in vivo* and TEVcs cleavage is successful.

In summary, TEVp is localized to the desired synaptic regions and is able to cleave an expressed TEVcs *in vivo*.

Integration of a TEV cleavage site into crucial synaptic proteins does not disrupt protein function

The TEVp should only target essential synaptic molecules of a single cell type to achieve synapse-specific cleavage. For this, the endogenous target protein has to be cleaved in a cell-type-specific way (Figure 6.4A). To achieve this, we designed a cell-type specifically integratable TEV cleavage site cassette (flp-TEV). This cassette contains an exon containing a TEV cleavage site flanked by the Flp-recombinase Recognition Target (FRT) sites (Figure 6.4B). When introduced into an intronic site in an inverted orientation (flpTEV-NI, non-integrated orientation), the TEV site will not be integrated into the protein and the wild type channel to be tested should be able to fulfill its normal function (Figure 6.4C). Only upon expression of a Flp recombinase, this sequence will undergo cell-type specific inversion and will be integrated into the molecule (flpTEV-I, integrated orientation) (Figure 6.4C). Cell type specificity is achieved by expressing the Flp recombinase using the binary expression systems (e.g., Gal4-UAS). This results into a protein harboring the TEVcs in a functionally critical domain only in a certain cell type but not others. By the action of extracellular synaptic TEV protease expressed in a synaptic partner this protein should go undergo proteolytic cleavage and should be functionally disrupted.

We chose several crucial synaptic proteins as candidate molecules to integrate the flp-TEV cassette. We started by post-synaptic targeting and chose the glutamate-gated chloride channel GluClα and the *Drosophila* $GABA_A$ receptor Rdl. STAB targeting these proteins won't be applicable to every synapse like when for example targeting pre-synaptic voltage-gated calcium channels but will give us protein specific disruption of synaptic communication. Since GluClα and Rdl are both essential for neural circuit function, and their mutants are associated with well-described and easily quantifiable phenotypes, STAB targeting these proteins gives us a reliable way to validate STAB (Ffrench-Constant et al. 1991; Kane et al. 2000; Molina-Obando et al. 2019). We created transgenic flies using the Recombinase Mediated Cassette Exchange method. This allowed us to introduce the flp-TEV cassette into an intronic region of the gene, using available MiMIC sites of each gene (Venken et al. 2011a). These sites were chosen such that a peptide encoded by an additional exon will be located in an extracellular domain of the protein. For GluClα we used the MI14426 landing site since a peptide encoded in this location will be located close to the glutamate-binding domain of the protein. For Rdl, we used MI02620 which will also result in an extracellular TEVcs peptide sequence.

For our tool to function properly, the introduced TEVcs should not disrupt the function of the protein in the absence of TEVp-mediated cleavage. We next confirmed this by using the insertions with flpTEV-I orientation where the TEVcs is integrated into all the proteins of the fly. We did complementation assays with the corresponding knock-out lines and probed for phenotypes associated with mutants. Specifically, we crossed the rdl^1 mutant flies with the Df ED4421 flies which contain a deficiency for the *rdl* gene. In the F1 generation, no flies were of the *Rdl^1/Df ED4421* genotype confirming the lethality phenotype of *rdl* disruption (Figure 6.4D). We then crossed rdl^1 mutant with $rdl^{flpTEV-I}$. We observed the expected number of flies with $rdl^{flpTEV-I}/rdl^1$ genotype (33%) in the F1 generation suggesting that TEVcs insertion does not disrupt endogenous protein function (Figure 6.4D). We then also tested if GluClα TEVcs insertion disrupts the protein function. GluClα null alleles are associated with motor problems (Kane et al. 2000). To quantify these, we used a climbing assay where flies perform negative geotaxis upon gently tapping them down to the bottom of a vial. We used two GluClα null alleles: Df ED6025 and GluCl$\alpha^{flpSTOP-D}$ (Molina-Obando et al. 2019). Flies with *GluCl$\alpha^{flpSTOP-D}$/GluClα-Df* failed to climb up the vial

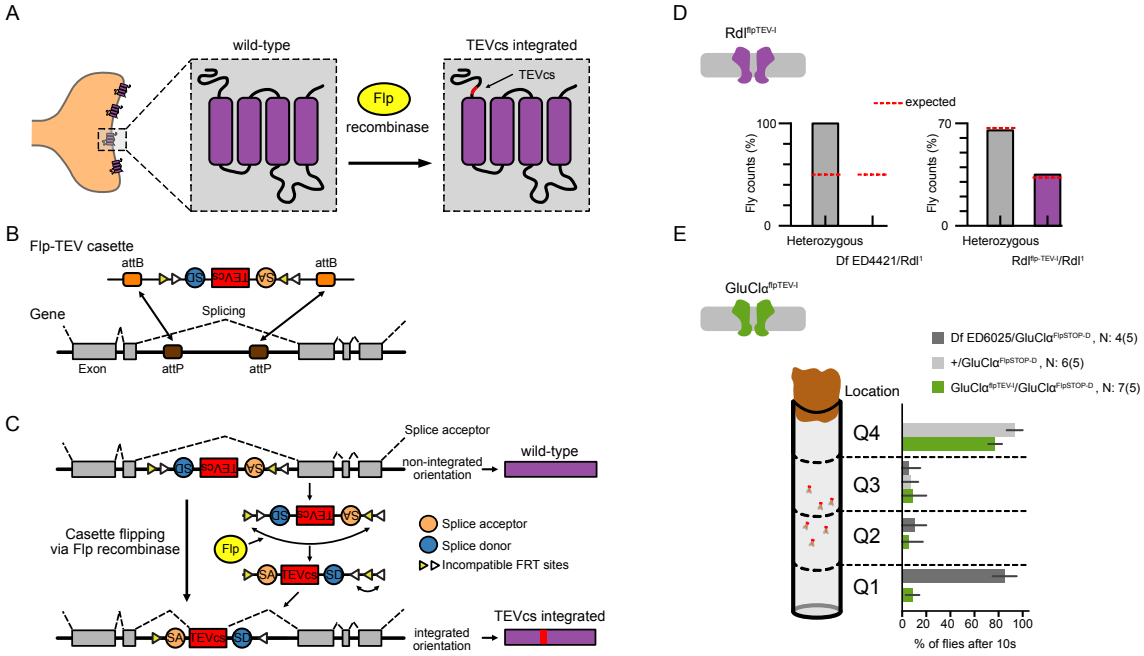

Figure 6.4: TEV cleavage site integration does not disrupt endogenous protein function. (A) Only upon the expression of cell-type specific Flp recombinase, the TEV cleavage site (TEVcs) will be conditionally integrated into the synaptic molecule which can be cleaved by the action of TEV protease. **(B)** An inverted Flp- TEV cassette will be integrated into an intronic region of the gene-of interest. This cassette harbors the TEVcs flanked by two pairs of incompatible Flp-recombinase Recognition Target (FRT) that are recognized by the same Flp recombinase. **(C)** Upon integration the TEVcs is not integrated in the transcription product and wild-type protein sequence is unaltered (non-integrated orientation). Upon the expression of Flp recombinase the cassette is inverted and locked in the non-inverted (integrated) orientation. Due to the splice acceptor and donor sites, Flp-TEV in integrated orientation will lead to the integration of the TEV site in a distinct region of the protein. **(D)** Fly counts upon TEVcs integration into the Rdl protein (magenta). The dashed line (red) shows the expected counts of flies assuming no lethality in an experimental fly cross. **(E)** Climbing assay to measure the motor abilities of the flies. Percentage of flies crossing the quartiles are quantified after 10 seconds from the start of the assay. Flies harboring TEVcs integrated GluClα (green), GluClα LOF (dark gray) and heterozyougs control flies (light gray). Sample sizes are given on the plots as flies(trials). Quantification plots show mean$\pm$SEM.

and remained mostly at the bottom quarter of the vial (Figure 6.4E). Positive control flies of the *GluCl*$\alpha^{flpSTOP-D}$/+ genotype climbed rapidly after tapping and most of them reached the top quarter of the vial within 10 seconds (Figure 6.4E). Similar to the positive controls, the majority of the flies with the *GluCl*$\alpha^{flpTEV-I}$/*GluCl*$\alpha^{flpSTOP-D}$ were found in the top quartile of the vial suggesting that GluClα is not majorly disrupted upon TEVcs integration (Figure 6.4E). For both postsynaptic proteins with TEVcs integration, our data shows that integrating the TEVcs does not disrupt the protein function and can be used for targeting these proteins.

TEVp cleavage leads to loss of GluClα but does not recapitulate LOF phenotypes *in vivo*

After developing and testing each of the STAB components separately, we combined them for function validation tests. Initially, we went back to S2 cells to probe for cleavage of GluClα with integrated TEVcs. For this, we generated a version of the GluCl$\alpha^{flpTEV-I}$ with an additional V5 tag (GluCl$\alpha^{TEVcs-V5}$) for probing protein presence after cleavage (Figure 6.5A). We transfected one S2 cell population with GluCl$\alpha^{TEVcs-V5}$ and another cell population with the nSyb-TEVp. Afterwards mixing these two cell lines, we performed western blot analysis to probe for GluClα presence. When we expressed the GluCl$\alpha^{TEVcs-V5}$ we observed a strong band around 260 kD corresponding to the pentameric state of the GluClα protein (Figure 6.5A). Mixing with the cell population expressing the nSyb-TEVp lead to a decrease of signal in the V5 band suggesting that the our TEVp could access the TEVcs and cleave it, possibly leading to the degradation of the protein (Figure 6.5B).

Next, we proceeded to *in vivo* tests. We performed experiments for *rdl* by expressing TEVp pan-neuronally in a *rdl*$^{flpTEV-I}$*/rdl-Df* background and probing for lethality. We used both nSyb-TEVp and TEVp-ICAM for our experiments. Our experimental genotypes (expressing the TEVp in *rdl*$^{flpTEV-I}$*/rdl-Df* background) were not lethal further suggesting that the TEVp fusion proteins were not able to disrupt Rdl function (Figure 6.5C). We also tested cleavage of GluClα aiming to recapitulate GluClα knock-out phenotypes upon pan-neuronal expression of TEVp fusion proteins in a *GluCl*$\alpha^{flpTEV-I}$*/GluCl*α*-Df* background. In the climbing assay neither expressing the nSyb-TEVp nor the TEVp-ICAM in a *GluCl*$\alpha^{flpTEV-I}$*/GluCl*α*-Df* background resulted in a clear motor deficit suggesting that GluClα disruption was not complete (Figure 6.5D). We then proceeded to check protein function at the neuronal level. Disrupting GluClα leads to loss of responses in the second-order visual system neuron Mi1 Molina-Obando et al. 2019. We thus also checked Mi1 function with two-photon calcium imaging experiments. We selectively expressed GCaMP6f in Mi1 neurons and imaged calcium signals in their axon terminals. We presented 5 second full-field ON and OFF flashes and found no alteration upon expression of the TEVp-ICAM in a *GluCl*$\alpha^{flpTEV-I}$*/GluCl*α*-Df* background (Figure 6.5E, F). Combined, our data show that panneuronal TEVp targeting does not lead to LOF phenotypes for both Rdl and GluClα suggesting that STAB with its current components do not lead to silencing of synaptic function.

Mutations enhance TEV protease activity

After observing that STAB was not efficient enough *in vivo*, we implemented troubleshooting steps. Our previous experiments showed that TEVp could cleave both a cleavage probe and the GluClα in cell-mixing experiments (Figure 6.2H, 6.3E, 6.5A). These observations suggest that TEVp is functional and reaching the TEVcs even when expressed in different cells. The loss of GluCl$\alpha^{TEVcs-V5}$ upon cleavage suggests that cleavage can destabilize the protein and possibly lead to protein degradation. However, the signal decrease was not drastic, hinting at insufficient TEVp activity (Figure 6.5D). Failed *in vivo* validation experiments could thus be due to the insufficient loss of proteins leading to remaining synaptic activity.

We then set out to improve TEVp by introducing mutations that are thought to enhance activity. A previous study developed an improved TEVp by mutating residues that are subjected to post-translational modification, N-glycosylation and cysteine oxidation, in the secretory pathway which in turn may lead to protein inactivation (Cesaratto et al. 2015). One of these mutations, T173V, improved trans-synaptic TEVp activity in the recently developed synaptic tracing tool BAcTrace (Cachero et al. 2020). We engineered three versions of TEVp: the single mutant used also in BAcTrace, T173V (TEVp^{V}), the double mutant N23Q-T173V (TEVp^{QV}), and the triple mutant N23Q-C130S-T173V (TEVp^{QSV}) (Figure 6.6A) (Cesaratto et al. 2015).

To first test activity *in vitro* (Figure 6.6A), we expressed the three TEVp mutants in S2 cells along with the cleavage probe and analyzed the change in cleavage using western blots. We first observed an increase in OLLAS signal in all mutants compared to our original TEVp construct suggesting enhanced protein stability (Figure 6.6B, C). The highest OLLAS signal was observed in the triple mutant (Figure 6.6C) in line with their previous characterization (Cesaratto et al. 2015). We then assessed cleavage using the anti-TEVcs antibody and similarly observed the strongest signal in TEVp^{QSV}, more than doubled from the initial TEVp we started with (Figure 6.6B, D). Furthermore, the GFP signal from the cleavage probe was almost completely absent (Figure 6.6B). We then performed cell-mixing followed by western blot experiments with cells expressing GluCl$\alpha^{TEVcs-V5}$ and cells expressing TEVp^{QSV} (Figure 6.6D, E). The triple mutant led to a further reduction in GluCl$\alpha^{TEVcs-V5}$ signal compared to the initial TEVp showing that more GluClα proteins were disrupted (Figure 6.6E, F). In summary, by introducing mutations to prevent N-glycosylation and cysteine oxidation we significantly improved the TEVp activity and achieved higher levels of protein disruption.

We then generated transgenic flies with the nSyb-TEVp^{QSV}. We will test STAB activity with the new TEVp *in vivo*.

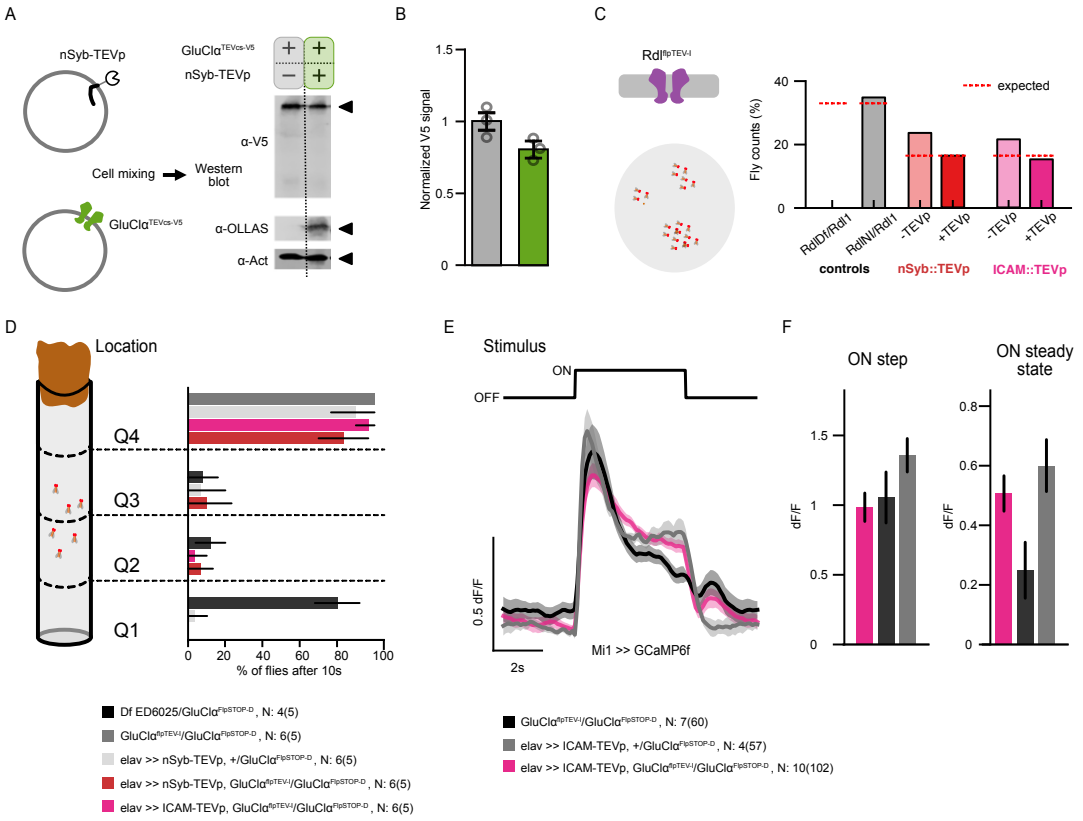

Figure 6.5: TEVp cleavage leads to loss of GluClα but does not recapitulate LOF phenotypes *in vivo* **(A)** Western blot analysis after cell mixture experiments with S2 cells expressing a TEVcs and V5 tagged GluClα with cells expressing the nSyb-TEVp. **(B)** Quantification of the V5 signal depicting the change in GluClα$^{TEVcs-V5}$ protein levels. Three biological replicates were used for quantification of Western blot signals. Quantification plots show mean±SEM. **(C)** Fly counts upon expression of nSyb-TEVp (red bar) and TEVp-ICAM (magenta bar) in a *Rdl*$^{flpTEV-I}$*/Rdl-Df* background (dark bars) and controls (light bars and gray bars).The expected line (red) shows the expected counts of flies for each genotype assuming no lethality in an experimental fly cross. **(D)** Climbing assay to measure the motor abilities of the flies. Percentage of flies crossing the quartiles are quantified after 10 seconds from the start of the assay. Flies expressing nSyb-TEVp (red) or TEVp-ICAM (magenta) in a *GluClα*$^{flpTEV-I}$*/GluClα-Df* background and controls (shades of gray). Sample sizes are given on the plots as flies(trials). **(E)** *in vivo* calcium signals from axon terminals of Mi1 neurons expressing TEVp-ICAM in a *GluClα*$^{flpTEV-I}$*/GluClα-Df* background (magenta) and controls (shades of gray). The stimulus used is a periodic full field OFF and ON flashes lasting 5 seconds each. **(F)** Quantification of the ON step and ON steady state extracted from Mi1 calcium signals. Sample sizes are given on the plots as flies(cells). Quantification plots show mean±SEM.

Discussion

Heterogeneity in synaptic connections allows a given cell-type to contribute differentially to neural computations within neural circuits. Here, we developed a trans-synaptic genetic neural manipulation method, Synapse Targeted Activity Block (STAB), to target the activity of synaptic connections between defined synaptic partners. STAB is composed of two main components: a pre- or post-synaptic TEV protease (TEVp) which trans-synaptically cleaves the second component, an endogenously TEV cleavage site (TEVcs) tagged essential synaptic protein. Upon cleavage, the synaptic protein function is disrupted, disrupting synaptic function. We first showed that our initially designed TEVp functions *in vitro* and *in vivo* and also can be preferentially targeted to pre- and post-synaptic sites . We integrated the TEVcs to post-synaptic neurotransmitter receptors GluClα and Rdl and showed that TEVcs integration does not interfere with protein function *in vivo*. The TEVp can reach and cleave the TEVcs integrated in GluClα in S2 cell mixing experiments. However, we failed to observe sufficient STAB activity *in vivo* and thus implemented optimization steps.

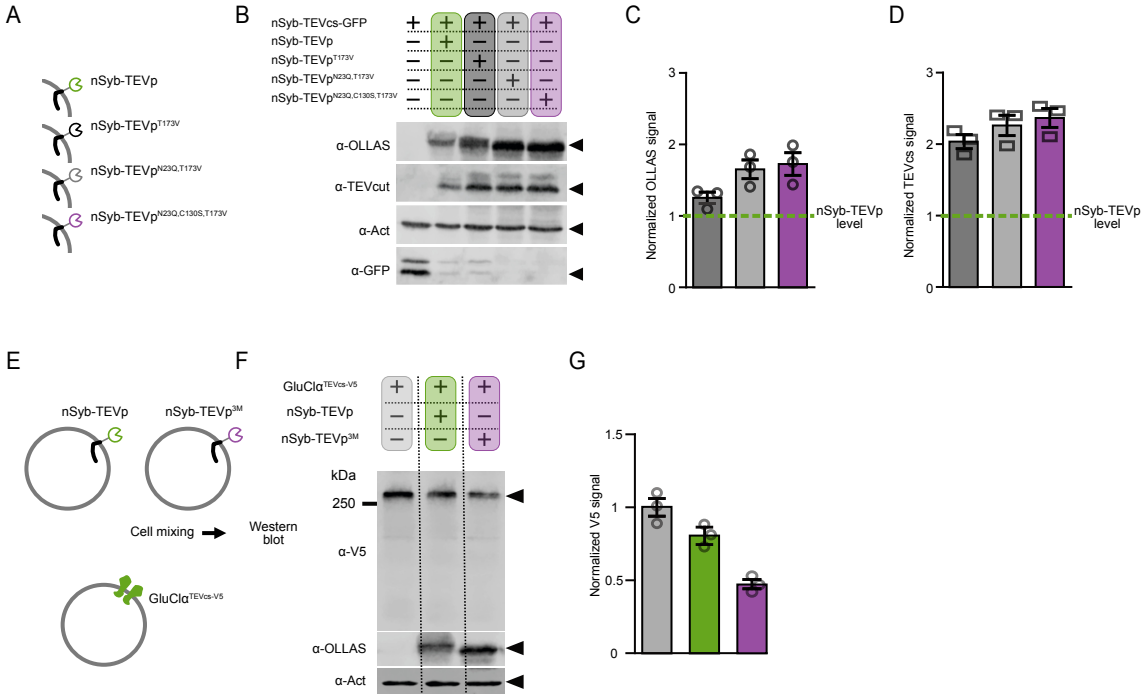

Figure 6.6: Mutations enhance TEVp activity (A) Three additional TEVp variants were generated by mutagenesis of residues affecting post-translational modifications. The original nSyb-TEVp (green) construct, a mutant TEVp with T173V (TEVp^{V}, black), double mutant with N23Q-T173V (TEVp^{QV}, gray) and a triple mutant with N23Q-C130S-T173V (TEVp^{QSV}, magenta) was used. **(B)** Western blot analysis of S2 cell extracts upon expression of the TEV cleavage probe along with the newly generated TEVp fusion proteins. **(C)** Quantification of the OLLAS signal normalized to nSyb-TEVp levels (green dashed line). **(D)** Quantification of the TEVcut signal normalized to nSyb-TEVp levels (green dashed line). **(E, F)** Western blot analysis after cell mixture experiments with S2 cells expressing GluClα$^{TEVcs-V5}$ with cells expressing the TEVp variants nSyb-TEVp (green) and nSyb-TEVp^{QSV}. **(G)** Quantification of the normalized V5 signal depicting the change in GluClα$^{TEVcs-V5}$ protein levels. Three biological replicates were used for quantification of Western blot signals. Quantification plots show mean±SEM.

Modifying the TEVp enhanced protein stability and lead to enhanced cleavage and degradation of GluClα *in vitro*. Next, STAB with new TEVp will be validated *in vivo*.

In the current version of STAB, the TEVp can cleave the TEVcs in GluClα and this possibly leads to the degradation of the protein, showed by *in vitro* experiments. The integrated TEVcs (genomic site MI14426) is located nearby the glutamate binding domain and might explain why cleavage leads to protein degradation. However, we have also seen that *in vitro* cell mixing experiments that the protein signal was not drastically reduced which could explain why *in vivo* GluClα targeting did not lead to LOF phenotypes associated with GluClα. Improving TEVp activity by adding three point mutations that prevent post-translational modifications (Cesaratto et al. 2015) increased the TEVp levels and also TEVcs cleavage *in vitro*. The improved TEVp (TEV^{QSV}) lead to degradation of more GluClα protein in cell mixing experiments. Expressing TEV^{QSV} in a GluClα$^{flpTEV-I}$/GluClα-Df background will reveal if STAB works with the optimized components.

Once STAB can be made efficient enough to disrupt synaptic function, STAB will be a versatile tool at three levels: first, using binary systems, synapses between any cell type that can be accessed via driver lines can be manipulated. This allows the investigation of synapses between almost all cell-types in the *Drosophila* system (Gohl et al. 2011; Jenett et al. 2012). Second, STAB can be used to abolish synaptic activity by targeting essential synaptic proteins such as pre-synaptic voltage-gated calcium channels. This can be applied in principle to any synapses, even the ones with unknown neurotransmitter or receptor profiles. In our validation assays, we used post-synaptic receptors GluClα and Rdl which only achieves synaptic disruption in synapses where they're used as the sole receptor. Still, LOF of these proteins leads to phenotypes that are easily quantifiable and thus suitable for our validation experiments. STAB targeting of GluClα and Rdl highlights another major aspect of STAB: it can achieve protein specific synaptic manipulations since the

TEVcs can be integrated into any desired protein of interest. One major application of this is that it allows investigations of co-release from individual cell-types (Nässel 2018; Svensson et al. 2019). Another application is when the release of a given neurotransmitter from the pre-synaptic partners is differentially transduced via different post-synaptic receptors in the same post-synaptic cell-type. Thus, STAB offers a high-resolution manipulation technique with wide-ranging applications.

Several important points are necessary to consider for using STAB. TEVp needs to be targeted to the synaptic regions. The pre-synaptically enriched nSyb-TEVp can be used when targeting post-synaptic proteins whereas post-synaptic ICAM-TEVp can be used when pre-synaptic proteins are targeted. Since nSyb is a panneuronal pre-synaptic protein (Broadie et al. 1995; Wu et al. 1997), nSyb-TEVp can be used in any neuronal type of interest for pre-synaptic TEVp expression. Similarly, ICAM protein has been used as a dendritic marking strategy in *Drosophila* neurons (Nicolaï et al. 2010; Rohwedder et al. 2016; Min et al. 2021) making ICAM-TEVp applicable for post-synaptic TEVp expression in any neuronal cell-type. Furthermore, integration of TEVcs should only disrupt protein function upon cleavage. Indeed, in this study, neither the TEVcs integrated GluClα nor the Rdl lead to disruption suggesting that TEVcs integration is not problematic for proteins. Furthermore the integrated TEVcs should be accessible and protein disruption should be achieved upon cleavage. Thus to use STAB, one must confirm first that the the targeted protein LOF phenotypes can be phenocopied upon TEVp mediated cleavage of the protein so that STAB with this particular protein can be reliably used to discover the functional importance of specific synapses.

A potential shortcoming of chronic neural activity manipulations such as STAB is the homeostatic compensatory mechanisms acting in neural circuits that can restore synaptic activity levels (Marder et al. 2006; Davis 2006). The homeostatic compensations broadly occur in two different ways: one involves the restoring of neural activity through restoring the activity of the original ion channel or receptor that was targeted whereas the other one involves restoring neural activity by using alternative ion channels or receptors. To counteract the first one STAB needs very high levels of activity such that it can disrupt all the ion channels or receptors of a given type, so that even the changes of protein numbers or the changes in neurotransmitter numbers that bind to the protein does not restore activity. We already increased the STAB activity by introducing mutations within the TEVp that enhance its folding and stability based on a previous study (Cesaratto et al. 2015). Further mutations can be incorporated in TEVp to improve its catalytic activity (Sanchez et al. 2020). For the second type of homeostatic compensation mechanism, which happens when a similar ion channel or receptor replaces the activity of the targeted protein, one can integrate the TEVcs to multiple proteins. For example while disrupting the synaptic activity by targeting a pre-synaptic voltage-gated calcium channel, other similar type of channels can compensate for the targeted channel activity. In *Drosophila* there are 3 types of voltage gated calcium channels (Littleton et al. 2000) which can lead to compensation when one type is targeted. In these conditions, STAB robustness can increase if TEVcs is integrated into all 3 types of channels.

Once validated, STAB can be applied in many different contexts to investigate neural function in high-resolution that was never done before. For example, the complex circuitry in the first olfactory processing center, the insect antennal lobe, the analog of the mammalian olfactory bulb, can be investigated in detail. Olfactory receptor neurons (ORNs) respond to odorants and project to one of the many distinct glomeruli in the antennal lobe (Masse et al. 2009). Here intra and inter-glomerular processing is achieved via various types of lateral neurons. Inhibiting ORN-later neuron partners would thus provide a very detailed causal understanding of the information processing going within the antennal lobe. Another big question within olfactory processing is the distinct roles of projection neurons (PNs) that take inputs from the glomeruli and send them to two areas of the brain: the lateral horn, the insect analog of the mammalian cortical amygdala, and the mushroom body the insect analog of the mammalian piriform cortex (Masse et al. 2009). Lateral horn is responsible for innate behavior whereas mushroom body is a center of associative memory. Thus, same PN type can contribute to very distinct functions in the brain and isolating these using STAB would give important insights about distinct roles of PNs in information processing. Another candidate of STAB application is in the visual system. Second-order visual neurons of the *Drosophila* give their inputs to downstream ON and OFF pathways which process brightness increments and decrements, respectively (Ramos-Traslosheros et al. 2018). Interestingly, these contributions can be asymmetric suggesting that diverging synapses from the second-order visual neurons have distinct behavioral functions (Ketkar et al. 2022). Isolating these functions of second-order neurons is

especially important for understanding their roles in natural scenes which are composed of mixed ON and OFF stimuli.

Genetic manipulation methods are instrumental for obtaining a causal understanding of the brain. STAB is a fully-genetic approach which can be extended to other model species with available driver lines such as mouse and zebrafish. Along with the RMCE method that we used in STAB, the well established CRISPR-Cas9 methods in all 3 model organisms (Yang et al. 2013; Gratz et al. 2015b; Albadri et al. 2017) can be used to rapidly modify endogenous proteins for introducing the TEVcs. STAB has thus immense potential to reveal the role of individual synaptic connections between given partners in various organisms.

Methods

Molecular cloning and transgenic flies

DNA for nSyb-TEVcs-GFP, nSyb-TEVcp, ICAM-TEVp and dNlg-TEVp was synthesized and codon optimized for *Drosophila* expression by Integrated DNA Technologies (IDT, Iowa, USA). These were cloned into the pJFRC7, pJFRC12, pJFRC81 (UAS) and pJFRC19 (lexAop) (Pfeiffer et al. 2010; Pfeiffer et al. 2012) backbones using *Not*I and *Xba*I restriction digestion (R3189 and R0145S, NEB).

Mutations within the TEVp were introduced by site directed mutagenesis according to the manufacturer's instructions (Q5® Site-Directed Mutagenesis Kit, E0554S, NEB). Mutagenesis primers were designed with the NEBaseChanger™ tool (http://nebasechanger.neb.com). Used primers are shown in Table 6.2.

GluClα_{for}-TEVcs-V5 was generated by amplifying GluCLα by PCR, using cDNA from the wild type strain isoD1 (2057, Bloomington) with primers shown in Table 6.3.

GluCLα PCR construct was cloned into the pJFRC7 using NotI and XbaI restriction digest (R3189 and R0145S, NEB). TEVcs-V5 was inserted by site directed mutagenesis according to the manufacturer's instructions (Q5® Site-Directed Mutagenesis Kit, E0554S, NEB). Mutagenesis Primers were designed with the NEBaseChanger™ tool (http://nebasechanger.neb.com). Used primers in Table 6.4.

The flippable TEV construct (flp-TEV) contains 3 times the TEV cleavage site (TEVcs) composed of the peptide sequence ENLYFQG. A splice acceptor and donor site was placed before and after the 3xTEVcs respectively (Fisher et al. 2017). This sequence was then flanked by two pairs of incompatible FRT sites to facilitate Flp recombinase mediated inversion, as done in the FlpStop method (Fisher et al. 2017). The 3xTEVcs sequence was generated in 3 different phases to ensure correct integration to the protein sequence according to the site of insertion regardless of the reading frame. DNA was synthesized and codon optimized for *Drosophila* expression by IDT. flp-TEV was cloned into the pGDY-attB-UAS-2.1-tdTom backbone (Fisher et al. 2017) upon digestion using *Not*I and *EcoR*I and using the 3294bp part of pGDY-attB-UAS-2.1-tdTom that lacks the flpSTOP casette, tdTomato sequence and the transcription termination sites. This plasmid was then integrated into the GluClalpha MI14426 (flp-TEV phase 1 into BL 59515) and Rdl MI02957 (flp-TEV phase 1 into BL 37777) using recombinase mediated cassette exchange done via phiC31 mediated transgenesis.

All transgenic flies were generated by BestGene (CA, USA) or FlyORF (Zurich, Switzerland).

S2 cell culture

Drosophila Schneider 2 (S2) cells were acquired from Thermo Fisher Scientific (R69007) and cultured at 25°C (HeraTherm, Thermo Fisher) in T25 flasks with Schneider´s Insect Medium (21720024, Gibco) supplemented with 10 % heat inactivated FBS (F9665-50ML, Sigma Aldrich) and 1 % Penicillin-Streptomycin (P4333-20ML, Sigma Aldrich). For immunohistochemistry assays, the cells were cultured in 6 well-plates (10536952, Greiner). Transfection of S2 cells was performed in 6-well plates, with each well containing 2 ml of 1×106 cells/ml. Cells amount was determined by mixing 0.1 mL cell suspension with 0.1 mL trypan blue (15250061, Greiner), followed by cell counting in Neubauer chamber (1310000, Optik Labor). Plasmid DNA for transfect-

Table 6.1: Plasmids used in this study.

Name	Source
pJFRC7-20XUAS-IVS-mCD8::GFP	Addgene, 26220
pJFRC12-10XUAS-IVS-myr::GFP	Addgene, 26222
pJFRC81-10XUAS-IVS-Syn21-GFP-p10	Addgene, 36432
pJFRC19-13XLexAop2-IVS-myr::GFP	Addgene, 26224
pJFRC7-20XUAS-IVS-TEVp-dNLG2-V5	This study
pJFRC7-20XUAS-IVS-TEVp-ICAM5-V5	This study
pJFRC7-20XUAS-IVS-nSyb-Ollas-TEVp	This study
pJFRC12-10XUAS-IVS-TEVp-dNLG2-V5	This study
pJFRC12-10XUAS-IVS-TEVp-ICAM5-V5	This study
pJFRC12-10XUAS-IVS-nSyb-Ollas-TEVp	This study
pJFRC81-10XUAS-IVS-TEVp-dNLG2-V5	This study
pJFRC81-10XUAS-IVS-TEVp-ICAM5-V5	This study
pJFRC81-10XUAS-IVS-nSyb-Ollas-TEVp	This study
pJFRC19-13XLexAop2-IVS-TEVp-dNLG2-V5	This study
pJFRC19-13XLexAop2-IVS-TEVp-ICAM5-V5	This study
pJFRC19-13XLexAop2-IVS-nSyb-Ollas-TEVp	This study
pJFRC7-20XUAS-IVS-nSyb-Ollas-TEVp-T173V	This study
pJFRC7-20XUAS-IVS-nSyb-Ollas-TEVp-N23Q-T173V	This study
pJFRC7-20XUAS-IVS-nSyb-Ollas-TEVp-N23Q-C130S-T173V	This study
pJFRC7-20XUAS-IVS-nSyb-TEVcs-sfGFP	This study
pJFRC7-20XUAS-IVS-GluClalpha-TEVcs-V5	This study
pUAST-CD8-GFP	Addgene, 17746
pAC-GAL4	Addgene, 24344

Table 6.2: Primers used for TEVp mutagenesis

Name	Sequence
T173V$_{for}$	GGAGTTGCTCgtAAATCAAGAAGC
T173$_{rev}$	ATAAAGTTCTTAGGTACGC
N23Q$_{for}$	TCATCTCACTCAAGAGTCCGATG
N23Q$_{rev}$	CATATTGTGCTACTAATTGG
C130S$_{for}$	CGACACTAGTAGCACTTTTCC
C130S$_{rev}$	GATACCATGCTCGACATC

Table 6.3: Primers used for GluClα isolation

Name	Sequence	Overhang
GluClα_{for}	cggccgcatgggcagcggacactat	NotI
GluClα_{rev}	tctagattactcatcctcctcctccctg	XbaI

Table 6.4: Primers used for GluClα-TEVcs-V5

Name	Sequence
TEVcs-V5$_{for}$	attcggaatgggcttgcccattaggtaccCACCGGTGTTGGTTTTAC
TEVcs-V5$_{rev}$	ccgctgctgggactcgatagcacaggtgAATACAGTTGCCTCAAAG

ing S2 cells was prepared using a Midiprep DNA purification kit according to the manufacturer's instructions (Qiagen, 12143). A total of 1 μg per plasmid DNA was diluted with supplemented Schneider's Insect Medium to a volume of 100 μl. For transfection we added Effectene Transfection Reagent (301425, Quiagen) according to the manufacturer's instructions to the diluted DNA, mixed gently and incubated for 15 min at room temperature (HeraSafe KS, Thermo Fisher). The DNA/Effectene mixture was added dropwise to the well, and the plate was incubated at 25°C for 48 h (HeraTherm, Thermo Fisher). Plasmids used are in Table 6.1.

Immunoblotting and protein analysis

Transfected *Drosophila* Schneider 2 (S2) cells were washed thrice with ice cold PBS (pH 7.4, without Ca2+ and Mg2+, Gibco), scraped (Cell Scraper 25 cm, Sarstedt), and collected in 250 μL ice-cold RIPA buffer (Table I). S2 cells were homogenized by passing through a 20 gauche needle assembled with a 10 mL syringe 15 times at 4°C. The homogenate was centrifuged at 10,000 x g for 10 min at 4°C to pellet insoluble materials and protein concentration was determined (ROTI®Quant; Carl Roth). For immunoblotting cleared homogenate was mixed 1:1 with 2x SDS buffer (Table I) and 25 μg of homogenate was loaded per lane onto a 10 % Tris-Glycine gel and resolved by SDS gel electrophoresis (Mini Trans-Blot, Bio-Rad) at constant 120 V. Proteins were transferred onto PVDF membranes (0.45 mm, Immobilon-FL, Merck Millipore) using an electrophoretic transfer cell (Mini Trans-Blot Electrophoretic Transfer Cell, Bio-Rad) at constant 40 V over night in transfer buffer (Table I) at 4°C. PVDF membranes were blocked for 1 h in 5 % w/v non-fat milk (Milkpowder, Roth) in Tris-buffered saline with 0.05 % v/v Tween (Tween 20, Sigma Aldrich). PVDF membranes were incubated with the primary antibodies at a dilution of 1:1,000 in 5 % w/v non-fat milk (the antibodies are reported in Table 6.5.) at 4 °C overnight, washed thrice with PBS (pH 7.4, without Ca2+ and Mg2+, Gibco) and incubated with fluorescent anti-mouse or anti-rabbit secondary antibodies at a dilution of 1:10.000 in 5 % w/v non-fat milk for a minimum period of 3 h at RT (P/N 926-32212, P/N 926-32213, P/N: 926-68076, P/N: 926-32218, IRDye LI-COR). Fluorescence signals were captured with the Odyssey CLx imaging system (LI-COR) and band intensities analyzed with Image Studio Lite Version 5.2 (LI-COR). All samples were first normalized to the respective actin levels before further quantifications. For the quantification, three technical replicates were averaged for each sample and used as one of the three biological replicates shown in the bar plots.

Fly husbandry and strains

Flies used for confocal and two photon imaging were crossed and grown in plastic vials on molasses-based food on a 12:12 hr light:dark cycle at 25°C in an incubator with 65% humidity. Parental crosses were flipped every 2-3 days into new vials and dry food was watered regularly to keep the vial conditions optimal. *Drosophila* strains used for experiments are provided in Table 6.6.

Table 6.5: Antibodies used in this study.

Antibody	Company	Dilution
Primary antibodies		
$\alpha - \beta$-Actin mouse	CST, 3700T	1:1000 (Blotting)
α-CD2 mouse	GeneTex, GTX75123	1:1000 (Blotting)
α-GFP rabbit	Abcam, ab290	1:1000 (Blotting)
α-GFP chicken	Abcam	1:2000 (Immunohisto)
α-OLLAS rat	Novus, NBP1-06713	1:1000 (Blotting), 1:500 (S2 Immunohisto), 1:300 (Adult fly Immunohisto)
α-TEVcut rabbit	Synaptic Systems, 265003	1:1000 (Blotting) 1:600 (Immunohisto)
α-V5 mouse	Thermo Fisher Scientific, R960-25	1:1000 (Blotting)
α-V5 conjugated 549 rabbit		1:1500 (Adult fly Immunohisto), 1:2000 (S2 Immunohisto)
α-brp nc82 mouse	DSHB	1:25 (Immunohisto)
Secondary antibodies		
α-chicken Alexa 488	Dianova (Cambridgeshire, UK)	1:200 (Immunohisto)
α-mouse Alexa 647	Dianova (Cambridgeshire, UK)	1:200 (Immunohisto)
α-rabbit Alexa 594	Dianova (Cambridgeshire, UK)	1:200 (Immunohisto)
α-rat Alexa 594	Dianova (Cambridgeshire, UK)	1:200 (Immunohisto)

Immunohistochemistry and Confocal imaging

S2 cells

For immunohistochemistry in S2 cells, the cells were cultured on 6 well plates and used 48 hours after transfection. Initially, cells were detached from 6 well plates (by scratching) and put in 1.5 ml tubes followed by centrifugation at 100g for 7.5 minutes. Then they were resuspended and 200μl was put in a single well of an 8-well plate (μ-Slide-8 well, Ibidi). After 1h of room temperature (RT) incubation for cell attachment, the medium was gently removed and cells were fixed in 1% paraformaldehyde (PFA) in phosphate-buffered lysine with 0.1% Triton X-100 (PBT) at RT for 10 minutes. The medium was removed and the cells were washed with phosphate-buffered saline (PBS) 2 times. Then cells were blocked with BSA in PBT (0.1% Triton X-100, 1% w/v BSA) for 1 hour at RT followed by incubation with the primary antibodies diluted in blocking solution (1:1000) over night at 4°C. After primary incubation, the cells were washed in PBT 3 times for 10 minutes each and incubated in the secondary antibody diluted in blocking solution at RT for 1 hour. The cells were then washed in PBT 3 times for 10 minutes each and prepared for mounting by dropping a Vectashield containing DAPI staining. The antibodies are reported in Table 6.5.

Confocal imaging was done on a Zeiss LSM710 microscope (Carl Zeiss Microscopy GmbH, Germany) equipped with an oil immersion Plan-Apochromat 40x (NA = 1.3) objective. Z-stacks and single images were recorded using the Zen 2 Blue Edition software (Carl Zeiss Microscopy, LLC, United States). Images were processed and rendered using Fiji (Schindelin et al., 2012). The

Table 6.6: Genotypes used in this study.

Name	Genotype	Figure	Source
L2 Gal4	*w+; + /+; $L2^{21Dhh}$-Gal4 /+*	6.3	
L3 Gal4	*w+; $L3^{MH56}$-Gal4 /+; + /+*	6.3	
Nlg-TEVp	*w+; + /+; UAS20x-TEVp-dNlg2-$V5^{VK27}$ /Tm6B*	6.3	This study
ICAM-TEVp	*w+; + /+; UAS20x-ICAM-TEVp-$V5^{VK27}$ /Tm6B*	6.3, 6.5	This study
nSyb-TEVcs-GFP	*w+; + /+; UAS20x-nSyb-GFP^{VK27} /Tm6B*	6.3	This study
nSyb-TEVp	*w+; + /+; UAS20x-nSyb-OLLAS-$TEVp^{VK27}$ /Tm6B*	6.3, 6.5	This study
GluClα Df ED6025	*w+; + /+; Df(3R)ED6025 /Tm6B*	6.4, 6.5	BL 8964
GluClαFlpSTOP-D	*w+; + /+; GluCl$\alpha^{FlpStop-D}$ /Tm6B*	6.4, 6.5	Molina-Obando et al. 2019
GluClαflpTEV-I	*w+; + /+; GluCl$\alpha^{FlpTEV-I}$ /Tm6B*	6.4, 6.5	This study
Df ED4421	*w+; + /+; DfED4421 /Tm6B*	6.4, 6.5	BL 8066
Rdl1	*w+; + /+; Rdl^{1} /Tm6B*	6.4, 6.5	
Rdlflp-TEV-I	*w+; + /+; $Rdl^{FlpTEV-I}$ /Tm6B*	6.4, 6.5	This study
elav	*w+; +/+ ; elavGal4/Tm6B*	6.4, 6.5	
Mi1 GCaMP6f	*w +; R19F01-LexAattP40, lexAop2-IVS-GCaMP6f-p10su(Hw)attP5 / CyO; +/ +*	6.5	

images were arranged into figures using Affinity Designer (Serif Europe).

Experiments to test the TEV cleavage probe was conducted by transfecting the cells with nSyb-TEVcs-GFP construct and then adding either 1% DTT and 60U AcTEV^{TM}-Protease (Invitrogen, 12575015) to 200μl culture medium or just 1% DTT as control. Using the Zeiss LSM710 microscope, the GFP signal was recorded as time-series taking frames every minute after the application of TEVp.

Adult flies

For immunohistochemistry in adult flies, 3-5 days old female flies were used. Brains were dissected in a solution containing 103 mM NaCl, 3 mM KCl, 5 mM TES, 1 mM NaH2PO4, 4 mM MgCl2, and 26 mM NaHCO3 and later fixed for 50 min at RT in 2% PFA in phosphate-buffered lysine (PBL). Then brains were then permeabilized in PBT (0.3% Triton X-100, pH 7.2) at RT for 5 minutes repeated 3 times. Afterwards, brains were incubated in the blocking solution of 10% normal goat serum in PBT at RT for 30 minutes. Then brains were incubated with primary antibodies diluted in blocking buffer at 4°C for 24 hours. This was followed by 3 times 5 minutes washing in PBT and overnight incubation in the secondary antibodies diluted in blocking buffer. After secondary incubation, brains were washed 3 time 5 minutes in PBT and mounted in Vectashield (Vector Laboratories, Burlingame). The antibodies are reported in Table 6.5.

Samples were imaged on a Zeiss LSM 800 confocal microscope (Carl Zeiss Microscopy GmbH, Jena, Germany) equipped with an EC Plan-Neofluar 40x/1.30 M27 (oil) objective. Stacks and single images were acquired using the Zen 2 Blue Edition (Carl Zeiss Microscopy GmbH, Jena, Germany). Images were processed and rendered using Fiji (Schindelin et al., 2012). The images were arranged into figures using Affinity Designer (Serif Europe).

Behavioral climbing assay

We used a climbing assay to quantify possible motor deficits of the fly based on (Madabattula et al. 2015). Female flies aged 2-5 was put in an empty vial where quartiles were marked. To start the assay, all flies were tapped to the bottom of the fly where they immediately started a negative geotaxis. The fly behavior was filmed using a mobile phone that was put in the a constant distance from the vial. Each experiment was repeated for 5 trials. After filming, the amount of flies located in each quartile at 5th, 10th, 15th and 20th second was quantified through manual inspection of videos.

Two-photon imaging, stimulation and data analysis of Mi1 neuron responses

Flies were anesthetized on ice before imaging and placed into a custom-made fly holder. The heads were tilted to expose the head cuticle for dissection and then fixed using a UV-sensitive glue (Bondic). The cuticle on the right hemisphere of the head was removed via sharp forceps and trachea and fat bodies were removed. Dissection was done in a solution with 103 mM NaCl, 3 mM KCl, 5 mM TES, 1 mM NaH2PO4, 4 mM MgCl2, and 26 mM NaHCO3. Calcium and sugars were added to this saline during imaging (1.5 mM CaCl2, 10 mM trehalose, 10 mM glucose, 7 mM sucrose) and carboxygenated to achieve a constant pH 7.3 druing perfusion. A Bruker Investigator microscope (Bruker, Madison, WI, USA) that is equppied with a 25 x/NA1.1 objective (Nikon, Minato, Japan) was used. A 920nm excitation laser (Spectraphysics Insight DS+) was used for exciting GCaMP6f, with 5–15 mW of power measured at the fly position.

Stimulation and imaging was synchronized using custom-written software written in C++ (Freifeld et al. 2013). Stimulus projection was done using a DLP LightCrafter(Texas Instruments, Dallas, TX, USA), at a frame rate of 100 Hz onto a 8x8cm rear projection screen covering 60° of visual space in both azimuth and elevation. Filtering of the stimuli was done using a 482/18 band pass filter and a ND1.0 neutral density filter (Thorlabs) on the projector. Stimuli were generated via a custom-written C++ and OpenGL software (Freifeld et al. 2013). The stimulus consisted of two epochs with full-field ON and OFF flashes lasting 5s. The epochs were repeated at least 7 times. We used Python 2.7 for data processing (Van Rossum 1995) starting with motion correction using the Hidden Markov Model from the SIMA Python package (Kaifosh et al., 2014). Afterwards, time traces from manually selected region of interests (ROIs) were extracted by averaging the signal within the delimited space followed by background subtraction. Relative changes in the fluorescent signal ($\Delta F/F0$) were calculated using the mean of the trace as F0. This was followed by trial averaging and calculation of ON step as the difference between the maximum response of the ON epoch and the mean of the last 500ms of the OFF epoch. ON steady state was calculated as the mean response of the last 500ms of the ON epoch. The quantifications were done for each individual ROI and then averaged across flies.

Acknowledgements

We thank Christine Gündner, Simone Renner, and Jonas Chojetzki for excellent technical assistance. This project has received funding from the European Research Council (ERC) under the European Union's Horizon 2020 research and innovation program (grant agreement No 716512) awarded to MS.

7 | General discussion

Extraction and stable estimation of contrast is instrumental in all visual systems since the majority of downstream feature extractions rely on this basic feature of the visual scenery. Contrast signals are present starting from the photoreceptors and are further refined in downstream parallel pathways. Each of these pathways consist of distinct cell-types that apply different spatiotemporal signal transformation steps. Thanks to the signal processing happening in the visual circuits, animals can handle the complex and ever changing visual sceneries that contain changes happening in various spatiotemporal scales. In this thesis, I investigated the molecular and cellular basis of how visual systems extract contrast and estimate it stably during the rapid luminance changes happening in the visual world. I used the *Drosophila* system as its genetic toolbox can be used get a causal understanding of neural computations from molecular to circuit to behavioral levels. In the first study, me and my colleagues revealed that the second order visual neurons, LMCs, encode luminance and contrast in different ways and segregate distinct types of contrast and luminance information to both ON and OFF pathways. L1 and L3 LMCs provide a rapid luminance gain to scale behavioral ON and OFF contrast representations to achieve robust behavior in changing luminances. However, their different functional role in the ON and OFF pathways reveal pathway asymmetries. In the second study, I investigated the molecular basis of LMC specializations. Contrast-sensitive L2 neurons utilize rapidly inactivating K_v channels to sharpen their contrast responses and for signal amplification. In the third study, I investigated the cell types involved in stable contrast estimation in the OFF pathway downstream of LMCs. The rapid luminance gain that is vital for stable contrast behavior of the fly is implemented in the medulla neuropile in two distinct channels, Tm1 and Tm9 neurons. Tm9 neuron responses boost contrast representations at lower luminances whereas Tm1 neurons reach a constant representation of contrast. Both neurons utilize spatial pooling to implement a luminance gain. Consistent with this, they receive wide glutamate signals which may provide the biophysical basis of implementing the luminance gain along with columnar cholinergic inputs. In line with this, the Tm9 luminance gain depends on a dendritic mechanism implemented via glutamate gated chloride receptors. In summary, we revealed that the contrast and luminance signals are extracted in distinct LMCs and used for a rapid luminance gain which is first implemented in distinct medulla neurons and drives robust behavior of the fly in rapidly changing luminance conditions.

Studies in this PhD thesis added to many others in showing the complex wiring of neural circuits where divergence and convergence is common. Within this circuit architecture specific synaptic partners become the units of information processing since a single cell-type contribute into distinct pathways through different synaptic partners. In the fourth study, I developed a tool to manipulate specific synaptic connections for enabling a detailed causal understanding of neural circuits. Synapse Targeted Activity Block (STAB) is a genetic tool based on protease-mediated disruption of essential synaptic proteins. As protease, we used the viral TEV protease (TEVp) since it cleaves a very specific cleavage sequence (TEVcs) and does not cause unspecific effects. We developed pre- or post-synaptic TEVp fusion proteins and showed TEVp is active *in vitro* and *in vivo*. We developed a strategy to introduce a TEVcs into endogenous proteins and showed that TEVcs integration in the absence of TEVp does not disrupt protein function *in vivo* for two crucial post-synaptic receptors, the glutamate gated chloride channel GluClα and the $GABA_A$ receptor Rdl. While *in vivo* STAB activity with initial TEVp variants was not sufficient, we improved TEVp activity using point mutations by enhancing its folding and stability. STAB with improved components can next be tested in *in vivo*. After successfully establishing STAB, we will be able to use STAB for discovering the role of specific synapses in highly interconnected neural circuits.

7.1 Contrast processing requires specializations downstream of photoreceptors

Even though a form of contrast is already extracted in photoreceptors (Laughlin et al. 1978; Normann et al. 1974; Normann et al. 1979), it needs further refinement and transformations to enable downstream feature extractions and accommodate the constrains imposed on the animal in rapidly changing conditions.

7.1.1 LMCs provide key features for downstream neurons but fail to encode stable contrast

Fly LMCs specialize to distribute key features that form the building blocks of further visual computations. They receive similar photoreceptor inputs but show different tuning to the visual features contrast and luminance. L1 and L2 both exhibit an initial transient response to light decrements (Laughlin et al. 1987; Juusola et al. 1995). Furthermore, L1 and L2 neurons were thought to serve identical purposes in parallel ON and OFF pathways, respectively (Joesch et al. 2010; Clark et al. 2011; Eichner et al. 2011; Joesch et al. 2013). Our work now revealed that these transient responses encode contrast in different manners such that L1 neurons saturate faster in higher contrasts and provide better resolution in lower contrasts than L2 neurons. Additionally, L1 neurons also exhibit luminance-sensitive sustained responses whereas L2 neurons adapt rapidly to baseline following their contrast response. These differences in L1 and L2 neurons were not captured by the linear filters of the neurons (Clark et al. 2011). This means, L1 and L2 specializations are partly dependent on non-linear processes and might elude the linear analysis methods to characterize neurons. In our first study, L3 responses only had a sustained component arguing that it discards contrast information. However, there is still evidence that L3 neurons might be relaying additional contrast signals. Voltage recordings in other flies and voltage imaging in *Drosophila* has shown transient responses in L3 neurons (Uusitalo et al. 1995; Rusanen et al. 2016; Ketkar et al. 2020). Through the slower dynamics of calcium imaging, these small contrast encoding components of L3 might be missed since the responses are dominated by large sustained signals. Our third study also captured a transient component of L3 responses to moving edges. The differences between stimulation paradigms, for example spatial filling of RF or the dynamic nature of the latter stimulation, can also be shaping L3 encoding.

Since L1 was thought to be an ON pathway input and luminance-invariance had only been studied in the OFF pathway, the luminance encoding of L1 was not investigated before (Ketkar et al. 2020). Now we show that L1 neurons have a luminance sensitive baseline that depends linearly on luminance changes. L3 on the other hand encodes luminance non-linearly, favoring the low luminance regimes. This highlights another diversification in luminance encoding in the lamina. A combination of linear and non-linear processes can increase the range of luminances sent to downstream circuitry (Odermatt et al. 2012).

In the vertebrate retina, typically more than 10 types of bipolar cells (BPCs) further refine and transform the photoreceptors signals. Similar to the fly LMCs, these bipolar cells also exhibit different temporal dynamics ranging from sustained to transient or a combination of both (Euler et al. 2014). These distinct temporal filtering properties thus enable BPCs to encode contrast and luminance differently (Ichinose et al. 2014). However, how these distinct features causally relate to animal behavior is not known in vertebrate systems.

The interaction of luminance and contrast features extracted in the lamina then leads to stable contrast representations in fly behavior as shown in the first study and Ketkar et al. 2020. However, the interactions do not happen directly in the lamina since our third study showed that none of the LMCs exhibit stable representations of contrast in rapidly changing luminances. This property generalized over stimuli (edges and gratings) and different contrasts. Since LMCs inherit photoreceptor adaptation properties, this adds to the evidence that photoreceptors are unable to counteract rapid luminance changes and thus visual systems need a post-receptor luminance gain to achieve stable representations of contrast. This necessity should generalize to different luminance regimes since the amplification of the contrast signals between photoreceptors and LMCs remain constant (Laughlin et al. 1978).

7.1.2 LMCs provide key features to both ON and OFF pathways

Even though ON and OFF selectivity arises in the medulla neurons, ON and OFF pathways of the *Drosophila* visual circuits were thought to split already at the lamina level with L1 being the sole input to the ON pathway whereas L2 and L3 were considered the inputs to the OFF pathway (Joesch et al. 2010; Clark et al. 2011; Silies et al. 2013; Clark et al. 2016). Still, silencing experiments in combination with behavioral and physiological read-outs in medulla neurons showed hints of L1 contribution to the OFF pathways (Silies et al. 2013; Fisher et al. 2015). Here we showed that the latter is true, and that in fact, all lamina neurons contribute to both ON and OFF behavior. This was possible because we investigated a defined computation with stimuli having higher complexity than what was done before for assigning the roles of these neurons. Especially for L3, considering that some of its major outputs based on connectomics studied include the ON pathway neurons Mi9 and Mi1 (Takemura et al. 2013), it is not surprising that it affects both pathways, and our work provides the first functional evidence for this. Our data suggests that the ON and OFF pathway split only happens downstream of lamina and lamina serves as a region that segregates distinct features for the downstream computations. In the vertebrate retina, ON and OFF pathways are already split at the level of second-order neurons, the BPCs. In contrast to three distinct LMC types of the fly, BPCs contain up to at least 13 different types that exhibit different temporal characteristics (Euler et al. 2014) providing more functional channels to enhance contrast processing. Thus the circuitry might already have sufficient channels to use for different features and also for contrast polarity simultaneously. This architecture can be beneficial since it immediately can shape contrast signals according to the asymmetric demands of ON and OFF processing in distinct ON and OFF channels for downstream processing. In line with this, direction selectivity arises already in the third-order neurons in vertebrates whereas it arises in the fourth-order neurons in the invertebrates. Due to the size restrictions of the small fly brains, fly visual systems may invest on an additional layer rather than many more number of cell-types since adding a layer allows the network to represent more complex, more non-linear functions compared to adding more units in a single layer, shown in deep-learning approaches (Poggio et al. 2017).

7.1.3 A rapid luminance gain arises in distinct medulla neurons

Downstream of the lamina, contrast and luminance information are then combined to achieve luminance-invariant behavior. The medulla neurons Tm1 and Tm9 transform lamina contrast signals with a rapid luminance gain. Thus, both neurons achieve reduced dependency on luminance indicating that contrast representations become stable through the signal transformation happening in these neurons.

What makes post-receptor sites better for a rapid luminance gain than the photoreceptor level? From an efficient coding point of view, the luminance information should be discarded since it does not reflect the changes happening in a given environment, thus contain no useful information (Laughlin 1981). Optimizing neural code, especially at the initial stages of sensory processing, requires balancing the cost-benefit trade-offs of individual processes. At the photoreceptor level, noise is a major obstacle to visual processing, especially when luminance levels decrease (Laughlin et al. 1989; Laughlin et al. 1987). With noise, an ideal match between the input and neural signals is challenging since noise will fluctuate this gain over time even if the input's statistical properties do not change. This is especially important considering luminance estimation in rapidly changing contexts since temporal noise reduction techniques (e.g., averaging over time) have to be very limited. Even when there is sufficient signal in photopic conditions, contextual dim luminances can create problems since photoreceptor operating curves are centered at the mean luminance levels to maximize information (Normann et al. 1979; Laughlin 1981) and thus will have minimal responses in changes occurring in contextual dim light. Signal amplification steps are employed in circuitry postsynaptic to photoreceptors in many animals, providing a better location for rapid mechanisms to operate. For example, in flies, photoreceptor to lamina monopolar cell synapses are high-gain and amplify signals up to ten times (Laughlin 1981). Furthermore, another advantage of post-receptor sites is the possibility of pooling signals, leading to a reduction of noise. Pooling is additionally important for estimating luminance levels since single points in space do not represent local luminance individually but are used to estimate contrast. Spatial pooling is present in macaques where ganglion cells receive inputs from hundreds of cones and implement a post-receptor luminance gain (Dunn et al. 2007).

Considering that there is signal amplification in LMC neurons, why then is the post-receptor gain not already implemented at this stage? LMCs extract distinct features given the same photoreceptor signal and the interactions of these features are key for computing contrast in rapidly changing luminances. Compared to the medulla, the lamina contains very few inter-columnar neurons that can provide these interactions (Fischbach et al. 1989). Thus, spatial pooling which is a necessary mechanism for the rapid luminance gain would also be restricted in the lamina. Even though horizontal circuit mechanisms like lateral inhibition affect LMC responses, these are aimed at extracting and sharpening contrast signals (Srinivasan et al. 1982; Laughlin 1989; Freifeld et al. 2013). Another possibility is that some computations benefit luminance-dependent representations of contrasts. For example, in contrast to Tm1 and Tm9, the medulla neurons Tm2 and Tm4 do not exhibit a luminance gain and instead exhibit luminance-dependent contrast representations. Accordingly, some vertebrate RGCs represent absolute contrast information which depends on the luminance (Idrees et al. 2020). Which computations require luminance-dependent representations of contrast remains yet to be explored. Additionally, the medulla has 60 columnar cell types suitable for many independent computations to take place (Fischbach et al. 1989). Similar to our observations, the post-receptor gain control in primates arises two synapses downstream of photoreceptors, at the synapses between cone bipolar cells and RGCs (Dunn et al. 2007).

One interesting distinction between Tm1 and Tm9 neurons is that Tm9 neurons responses have a disproportional gain for lower luminances leading to enhanced representations of contrasts in lower luminances. The detection of contrast in dim light is especially challenging due to low signal to noise ratios. However, essential salient features can still linger in dim light, such as a predator lurking in the shadows to ambush its prey. Thus assigning higher importance to contrast happening in dim light in a dedicated visual channel could be evolutionary advantageous. Interestingly, our first study revealed that ON behavior also has a tendency to increase representations of contrast in low light conditions which might indicate a link between the OFF pathway neuron Tm9 and ON motion behavior. In line with this idea, Tm9 neurons also contain ON information (Ramos-Traslosheros et al. 2021) and receive major inputs from the ON pathway neuron Mi4 (Takemura et al. 2013). Tm1 neurons on the other hand, represent contrast signals stably across changing conditions similar to the OFF behavior (Ketkar et al. 2020). Stable contrast representation then is crucial for all downstream feature extractions, such as the observed T5 direction-selective signals.

7.1.4 Further feature extraction is reliable once stable contrast processing is achieved

T4 and T5 neurons are the first direction-selective cells in the fly visual pathway. OFF pathway medulla neurons converge onto the dendrites of T5 neurons where motion is computed based on the spatial and temporal differences in its inputs. Tm1 provides fast input at the center of T5 dendrites whereas Tm9 gives slow direct inputs at the tip of T5 dendrites and slow indirect inputs at the base of the dendrite (Shinomiya et al. 2019a; Ramos-Traslosheros et al. 2021). Thus during changing luminances, all T5 dendritic spatial locations receive stable representations of contrast. This is critical for computing motion in changing luminances since otherwise direction signals would be confounded by luminance dependent contrast signals (same object moving at the same velocity but at different luminances would elicit different DS responses). Accordingly, T5 responses to a given contrast are equally represented across changing luminances. Similarly in vertebrates, post-receptor luminance gain mechanisms are implemented before the direction-selective starburst amacrine cells and direction-selective RGCs (Cicerone et al. 1980; Green et al. 1982; Dunn et al. 2007; Freeman et al. 2010). This highlights the need for a stable contrast signal before further extraction of features across species.

Two other parallel medulla neuron pathways via Tm2 and Tm4 neurons do not exhibit a luminance gain raising the question of their purpose for further signal processing such as motion detection. Two recent studies showed that another form of rapid gain, contrast gain, is important for stable and efficient visual processing (Drews et al. 2020; Matulis et al. 2020). Contrast gain ensured contrast-invariant velocity calculations in direction-selective cells which can explain the spatially overlapping inputs of Tm1 and Tm2/4 neurons at the T5 neuron dendrites. Tm2 and Tm4 both show temporal contrast gain whereas Tm1 and Tm9 neurons lack temporal contrast gain. This suggests that parallel streams implement either rapid luminance or contrast gains. In line with this, luminance and contrast are independent features of natural scenes (Mante et al. 2005; Frazor

et al. 2006) and luminance and contrast gain mechanisms also operate independently in vertebrate neural circuits (Mante et al. 2005).

7.1.5 Molecular and circuit mechanisms underlying contrast computations in visual circuits

Contrast-sensitive LMC responses depend on K_v channel expression profiles

Despite receiving the same histaminergic inputs from the photoreceptors and using the same receptors to transduce these inputs (Hardie 1989; Gengs et al. 2002), LMCs show different tuning to visual features of contrast and luminance. How does the specialization of these neurons arise?

In the second manuscript, I showed that L2 neuron contrast encoding is shaped by the fast-inactivating K_a channels, Shaker and Shal. Shaker and Shal cell-autonomously sharpen L2 transient responses and modulate L2 baseline to enhance its dynamic range. The sharpening of L2 responses is mediated by the reduced time-constant giving L2 neurons high-pass filtering properties facilitating transmission of rapid signals. Accordingly, L2 neurons were described as conveying information about the rapid changes to downstream circuits (Tuthill et al. 2013). However, Shal and Shaker can not explain the full dynamics of L2 responses indicating additional mechanisms for contrast processing in L2 neurons. Studies from *Drosophila* and other fly species showed that L2 responses are shaped by lateral interactions such as lateral inhibition which further contributes to their sharp transient responses and thus contrast encoding (Mimura 1976; Dubs 1982; Laughlin et al. 1989; Freifeld et al. 2013).

Similar to our observations, blowfly L2 neurons also utilize K_a channels to transmit high-frequency signals (Rusanen et al. 2016). In vertebrates, voltage-gated K channels also shape bipolar cell properties and contribute to extending dynamic range and generating fast and transient responses (Klumpp et al. 1995; Joselevitch et al. 2020). Even though a causal relationship between cell-autonomous mechanisms and neural responses is not achieved in other studies, K_a channels seem to be an evolutionary conserved mechanism to shape contrast signals.

What then could shape other LMC responses to achieve their distinct feature encoding? Differential expression of voltage-gated channels is definitely a prime candidate. L3 neurons in other fly species express a delayed rectified K_d current (Rusanen et al. 2016) which could also be responsible for shaping L3 luminance-encoding responses. In line with this, *Drosophila* RNA-seq data comparisons between L2 and L3 neurons showed that K_a channels are upregulated in L2 neurons whereas K_d channels are enriched in L3 neurons (Davis et al. 2020). Furthermore, all LMCs get lateral inputs (Mimura 1976; Dubs 1982; Laughlin et al. 1989; Freifeld et al. 2013). Lateral inputs can be mediated by the amacrine cells which make synapses with all LMCs (Rivera-Alba et al. 2011). Lamina dendrites also receives feedback centrifugal inputs from neurons such as C2, C3, Lawf and T1 (Fischbach et al. 1989; Rivera-Alba et al. 2011). A difference in lateral or centrifugal inputs could underlie some differences between LMC properties.

Since L1 neurons exhibit both transient contrast responses and sustained luminance responses, it might be employing a combination of mechanism implemented by L2 and L3 neurons. L1 neurons form lateral connections with L2 neurons using both chemical and electrical connections and thus can inherit some signaling properties of L2 neurons (Joesch et al. 2010; Rivera-Alba et al. 2011). RNA-seq data can further be used to narrow down molecular candidates for L1 specialization (Davis et al. 2020).

A combination of circuit and dendritic molecular mechanisms underlies the rapid luminance gain

Spatial pooling in fly medulla neurons Tm1 and Tm9 leads to stable estimation of contrast in rapidly changing luminances. Similarly in vertebrates, spatial mechanisms are shown to mediate post-receptor gain between second and third order neuron synapses (Dunn et al. 2007). However, pooling also has its trade-offs since natural scenes contain substantial variability in luminance statistics over space (Frazor et al. 2006), meaning that the correlation between local luminances falls rapidly with the distance indicating a problem of estimating luminance over large spatial extents. Local contrast estimation will not be reliable if a large and thus highly variable area of

luminance is selected for the gain control mechanisms. In line with this, psychophysical studies have observed that brightness constancy works under conditions of spatially non-uniform luminance, suggesting that the gain control based on luminance operates locally rather than globally (Davidson et al. 1965). We showed that the fly luminance gain required an estimation of luminance around 15-20° of the visual field, a size bigger than a single photoreceptor acceptance angle (5°) but still fairly local considering the whole visual span of the fly eye. An analysis of the natural scenes that the fly eye encounters will reveal how the extent of the luminance gain matches the luminance correlations within natural scenes.

Besides their columnar direct cholinergic inputs from L2 and L3 neurons (Davis et al. 2020), we showed that Tm1 and Tm9 receive dendritic glutmatergic OFF inputs that vary with luminance. In both neurons, these inputs originate from a wider range than their calcium linear RFs and thus can form the molecular basis of the spatial pooling mechanism required for luminance gain. Accordingly, Tm9 neurons use the glutamate gated chloride channel GluClα to achieve their contrast representations. In line with this, GluClα is broadly expressed in the medulla (Molina-Obando et al. 2019). GluClα mediated luminance gain is implemented already in the Tm9 dendrites located in medulla layer M3 since the rapid luminance gain is already visible in Tm9 dendrites. The wide-field inter-columnar Dm neurons are the candidates for the glutmatergic signal onto Tm9 dendrites. Accordingly, functional connectivity experiments using optogenetics showed that several Dm neurons give OFF inputs to Tm9 (Lopez et al. 2020).

Algorithmically, the rapid luminance gain observed in Tm9 and Tm1 neurons can not be explained by a simple spatial summation mechanism since this will lead to proportional increase of responses at all luminances. Furthermore the use of an inhibitory glutamate receptor argues against simple summation. A divisive normalization mechanism that follows a summation was previously used to explain response properties of primate visual neurons (Carandini et al. 1994). Normalization leads to scaling of responses by a common factor and can be achieved by numerous network and molecular mechanisms (Carandini et al. 2011). For achieving stable contrast responses, luminance could be the common factor that is scaling the contrast signals, or luminance-dependent representations of contrast could be scaling each other. Several early molecular implementations of normalization were suggested to be achieved by shunting inhibition (Reichardt et al. 1983; Carandini et al. 1994; Carandini et al. 1997). Shunting inhibition changes the membrane conductance without eliciting depolarizing or hyperpolarizing currents. Shunting can be achieved by Cl- channels (Reichardt et al. 1983; Carandini et al. 1997). A recent study showed GluClα as mediating a shunting inhibition in motion detection in the T4 dendrites (Groschner et al. 2022). In Tm9 dendrites, GluClα could also be mediating a shunting inhibition to normalize luminance-dependent contrast responses which are provided by the cholinergic columnar inputs from LMCs. At the same time, this does not exclude other mechanisms supplementing the rapid luminance gain. For example, a GABA-based lateral pre-synaptic inhibition causes normalization of responses in fly olfactory circuits (Olsen et al. 2008b). Especially for Tm1 neurons where the luminance gain does not depend on GluClα GABA-based mechanisms could be in place. Tm9 and Tm1 neurons also express GABA receptors and some Dm neurons are GABAergic, raising the possibility of GABAergic mechanisms implementing or contributing to the rapid luminance gain observed in Tm neuron dendrites (Nern et al. 2015; Davis et al. 2020; Lopez et al. 2020). However we showed that Tm1 neurons also get wide-field glutamatergic inputs so another type of glutamate receptor could be mediating Tm1 luminance gain.

What can be the mechanisms underlying these differences in Tm1 and Tm9 neurons? Tm9 neurons receive major inputs from L3 neurons and our first study and Ketkar et al. 2020 showed that L3 neurons non-linearly favor dark luminances. Tm1 neurons on the other hand receive major inputs from L2 neurons (Takemura et al. 2013) which are purely contrast sensitive (Ketkar et al. 2020). Thus, Tm1 neurons might be receiving indirect luminance inputs through wide-field Dm neuron inputs. To establish Tm1 contrast representations, L1 luminance inputs could be utilized. L1 luminance inputs vary linearly with scene luminance and might achieve a stable contrast representation instead of favoring dim light conditions like Tm9 neurons do. Other major synaptic input to Tm1 neurons comes from the proximal medulla neuron Pm2 (Takemura et al. 2013). The Pm2 neuron covers multiple columns and could also provide a spatially wide luminance input to Tm1 neurons to scale incoming L2 contrast signals. However, Pm2 connections are in the proximal layers of the medulla where Tm1 neurites make a "stop over" on their way to the lobula to connect

T5 neurons (Fischbach et al. 1989). Our recordings suggested that Tm1 luminance gain already arises in its dendrites located in the distal layers of the medulla contradicting the notion that Pm2 neurons are required for the luminance gain in Tm1 neurons.

The early visual system is composed of parallel pathways that first encode distinct features as in LMCs, then implement distinct types of gain, contrast and luminance gain seen in medulla to further ensure reliable downstream computations. A plethora of molecular and circuit mechanisms underlie the specialization of each pathway and thus enable distinct computations. These computations then ensure stable animal behavior in an ever-changing environment.

7.2 Synapse specific manipulations to get insight into the complex functional connectivity of neural circuits

7.2.1 Convergence and divergence of information highlights the role of specific synapses in computations implemented in neural circuits

Both functional and anatomical studies showed that neural circuits are highly inter-connected. Single neurons receive inputs from multiple synaptic partners and send outputs to multiple synaptic partners. This architecture allows distinct signal transformations happening in individual synaptic connections which leads to a synaptic heterogeneity, also referred to as multiplexing. Multiplexing increases the computational capabilities of neural circuits by allowing multiple transformations happening in a given cell-type.

In manuscript 1, we found that all LMCs provide inputs to both ON and OFF pathways. A divergence of information thus highlights lamina to medulla connectivity. This functional architecture is in line with the anatomical connectivity revealed by EM reconstructions (Takemura et al. 2013). Furthermore, genetic silencing experiments showed that the behavioral relevance of LMCs inputs is not symmetrical in ON and OFF pathways (Ketkar et al. 2022). In the manuscript 3, we show that convergence of distinct lamina features leads to the luminance gain. Some of lamina inputs arrive to medulla neurons via direct synapses and some arrive indirectly via e.g., horizontal wide-field Dm neurons. We showed that horizontal inputs mediate spatial pooling to implement luminance gain and to understand the computational role of these inputs it is necessary to differentiate between LMC direct synapses to columnar medulla neurons and LMC synapses to horizontal neurons. One synapse downstream of medulla neurons, another convergent circuit motif is visible where T5 neurons integrate inputs of distinct medulla neurons to compute DS signals. In summary, our studies add to numerous others showing that multiplexing is a common feature of neural circuits (Baden et al. 2010; Euler 2001; Taylor et al. 2011; Euler et al. 2014; Gaudry et al. 2013; Guerrero et al. 2005; Asari et al. 2012). To understand the role of individual connections, we need manipulation methods of higher resolution.

7.2.2 STAB aims to achieve disrupting specific synaptic connections

A genetic approach is advantageous

STAB aims to address the above issue and thus provide important insights into computations happening within neural circuits. STAB is a genetic manipulation approach which depends on binary expression systems to drive its components in defined cell-types. Thus, it ensures reproducible manipulations that can be combined with various read-outs spanning the cellular, circuit or behavioral level including population imaging, high-throughput behavioral assays and electrophysiology.

Furthermore, it only consists of genetic elements which enables its usage in different species that are amenable to genetic modifications. With the recent developments in endogenous gene modifications (e.g., CRISPR-Cas9) STAB can be theoretically applied in any organism. However it is much easier to develop and apply first in genetic organisms with existing expression systems, such as *Drosophila*, mice and zebrafish.

Protease approach makes STAB flexible and gives specificity on targeted molecules

Our protease approach can be modified to address different types of questions. Silencing synapse-wide activity can be achieved by integrating the TEVcs in essential synaptic molecules like pre-synaptic calcium channels (in combination with postsynaptic TEVp) or post-synaptic neurotransmitter receptors (in combination with presynaptic TEVp). STAB targeting pre-synaptic calcium channels can flexibly applied to any synaptic connection since calcium-mediated vesicle release is a universal neuronal mechanism. Furthermore, STAB targeting post-synaptic receptors can be used to investigate specific types of neurotransmission. It is now widely known that in some synapses, pre-synaptic partners release a combination of different neurotransmitters or neuropeptides which are recognized by multiple types of receptors (Svensson et al. 2019). In these cases, our protease approach might not achieve synapse silencing but will then allow more specific investigations of the synaptic connections by providing molecule specific silencing. This will, for example, allow studying of specific variants of a given post-synaptic receptor family. Furthermore, in a pathway where neurotransmitters GABA and Glycine are co-released (Nicoll et al. 1998; Jonas et al. 1998) one can specifically get rid of either post-synaptic receptor and assess their computational relevance. Thus STAB can be used as a flexible genetic tool to manipulate synaptic activity in all given synaptic partners or achieve manipulations with molecular specificity.

Cleaving targeted molecules depends on the integrated region of the TEVcs and TEVp activity

Depending on the site of the TEVcs within the protein, TEVcs alone can cause protein dysfunction, TEVcs sequence might be within the complex structure of the protein and thus out of reach for the TEVp or cleavage might not cause a major problem for the protein and thus the protein can preserve its function. If it is not possible to find a suitable MiMIC site that fulfills all these conditions for TEVcs integration one can use specific gene editing methods such as CRISPR-Cas9 to integrate the TEVcs into the desired point within the protein sequence. TEVp activity can also be improved by further mutagenesis using the mutations that increased its catalytic activity in vitro (Sanchez et al. 2020).

If protease mediated approach fails, alternative approaches can be used to implement STAB. A recently developed genetic tool, BAcTrace, achieves trans-synaptic labeling in *Drosophila* with an inactivated version of the botolinum toxin (Cachero et al. 2020). Here a pre-synaptic protease cleaves and frees the post-synaptically expressed toxin which is then taken up by the pre-synapses. This approach can be easily modified for our purposes with an active toxin that leads to synapse specific disruption.

STAB is a fully genetic tool to target specific synapses. STAB will be applicable in any neural circuit in *Drosophila* and also can be modified for application in other model organisms. As for any genetic tool, further studies will improve and modify STAB to optimize for their purposes. STAB will allow a causal understanding of neural computations down to a detail that has not existed before.

8 | Conclusions and outlook

In this thesis, I characterized the molecular and circuit properties of several neuronal layers in the peripheral visual system of the fly. These characterizations were predominantly targeted to understand contrast encoding (Manuscript 2) and how contrast computation incorporates a rapid luminance gain to achieve stability towards dynamically changing luminance conditions (Manuscript 1, Manuscript 3). I furthermore set out to develop a novel genetic tool that will allow an unprecedented level of circuit analysis by achieving synapse-specific manipulation of neural activity (Manuscript 4). In the following paragraphs, I will briefly summarize the key findings and highlight the subsequent emerging questions with suggesting experiments to address these questions.

This work showed that all lamina neurons have distinct physiologies and encode contrast and luminance differently. For example, L1 and L3 neurons have different luminance sensitivities. L1 neurons cover the luminance range linearly whereas L3 neurons non-linearly amplify the dark regimes. Why are these specializations in feature encoding useful for the fly? To investigate this, one can use modeling approaches and test if these specializations provide a more efficient neural code in downstream circuits. Specific silencing of L1 or L3 neurons while imaging downstream motion-sensitive cell responses to natural scenes containing luminance changes could also be useful in recovering their distinct roles. A recent study, for example, revealed that fly motion behavior and motion-sensitive neuronal responses to natural scenes are more robust than the contrast-based motion detector predictions indicating a role for contrast and luminance gain control (Drews et al. 2020). A statistical analysis of luminance distribution and variations in natural scenes, ideally specifically targeted to the specific scene statistics that flies encounter, could be useful in making hypotheses about how a non-linearly dark-sensitive channel can be utilized for visual processing. Similar specializations are present in other species and systems. For example, bipolar cells exhibit distinct temporal properties (Euler et al. 2014). Furthermore, the fly offers the possibility to perform measurements and manipulations *in vivo*, in behaving animals (Olsen et al. 2008a), allowing to link peripheral visual computation to the ultimate goal of the visual system: guiding behavior. Thus, the fly offers a unique causal understanding of how feature specializations in cell-types shape neural computations and behavior.

Distinct cell-types use a plethora of molecular and circuit mechanisms to achieve their specialization. Postsynaptic to the same photoreceptors in the lamina, first order interneurons encode fundamentally different features of the visual scene. L2 neurons use a specific sub-type of K_v channels, the K_a, to acquire their contrast encoding properties. However, these channels alone do not explain the full temporal dynamics of L2 neurons. It is known that lateral inhibition is additionally involved in shaping L2 responses (Freifeld et al. 2013). To test if K_v channels and lateral inhibition fully explain the L2 contrast responses, channel manipulations and spatial stimulation of L2 neurons (center and surround) can be combined. Our study did not reveal the specialization of L1 and L3 neurons. Similar to L2 neurons, L1 neurons also encode contrast and thus could benefit the expression of K_v channels. According to their transcriptomes acquired during developmental stages, L1 and L2 neurons are more similar to each other than to L3 neurons (Tan et al. 2015). However, L1 and L2 contrast encoding also differ which might be shaped by the expression of different voltage-gated channels. RNA-seq datasets can be used to compare voltage-gated channel expression profiles (Davis et al. 2020), and identified channel candidates can be manipulated using the fly genetic toolbox. A functional analysis of cell-type specific RNAseq data from adults might therefore reveal differentially expressed candidate genes that developmental studies did not identify. Furthermore, both L1 and L2 neurons in other flies receive lateral inhibition (Laughlin et al. 1989), and thus L1 properties can also be assessed using spatial stimulation. Genetic silencing of

the neurons providing lateral inputs in the lamina or centrifugal inputs from the medulla could reveal the circuit mechanisms shaping L1 and L2 neurons.

L3 neuron properties in other flies display a strong K_d current (Rusanen et al. 2016). Shaw K_d channels are more highly expressed in L3 neurons than L2 neurons, providing a candidate for shaping L3 (Davis et al. 2020). Pharmacological and genetic Shaw manipulations are required to test a possible Shaw contribution in L3 neurons. Furthermore, transcription factors also differentiate the lamina neurons and are required for the layered projection of the lamina neurons (Tan et al. 2015; Peng et al. 2018; Santiago et al. 2021). L3 neurons specifically express the transcriptional repressor Fezf (Santiago et al. 2021), and Fezf mutant L3 neurons exhibit transient responses (Sporar et al., unpublished). Thus, the downstream targets of Fezf can provide valuable candidates for shaping L3 responses. Taken together, a combination of molecular and circuit mechanisms shape the distinct properties of LMCs, and the fly genetic tools combined with RNA-seq and physiological assays is optimal for revealing LMC specialization. The insights from how molecular and circuit mechanisms lead to distinct LMCs might improve our causal understanding of cell-type specializations in neural circuits in different brain regions and species.

ON and OFF pathways both require a luminance gain to achieve their contrast representations in rapidly changing luminances. Lamina neurons L1 and L3 both provide this rapid luminance gain but have different functional roles in ON and OFF pathways. Isolating these roles is crucial for understanding neural computation and behavior in natural scenes where ON and OFF stimuli are present together. The majority of L3 outputs go to the ON pathway neuron Mi9 (Takemura et al. 2013; Strother et al. 2014). One can try to isolate the L3 ON pathway function by silencing L3-Mi9 connections, specifically using STAB-like methods. L1 is known to provide functional inputs to the OFF pathway neuron Tm9 (Fisher et al. 2015). Still, for a complete understanding of the L1 contribution to the OFF pathway, the direct connections of L1 relaying information to the OFF pathway must be first revealed. The inputs from L1 to Tm9 can be carried by the GABAergic C2 and C3 interneurons or the wide-field Dm neurons (Takemura et al. 2013; Nern et al. 2015). Thus genetic silencing of L1 and assessing the function of these neurons can narrow down candidates that can carry L1 signals to Tm9. Once identified, the neuron mediating L1 to Tm9 connections can be silenced and the effects on the Tm9 neurons can be observed via physiology methods to reveal the functional role of L1 in OFF circuits. STAB-like methods can also isolate L1 contribution to the OFF pathway and assess the functional importance in natural settings.

The rapid luminance gain arises in the OFF circuitry in distinct third-order neurons, the medulla neurons Tm1 and Tm9. Thanks to the luminance gain, Tm1 neurons can represent contrasts in changing luminances stably, whereas Tm9 neurons boost low luminance contrast representations. For both neurons, spatial pooling is vital for luminance gain, yet which circuits mediate this spatial pooling is unknown. The plausible candidates are the wide-field horizontal Dm neurons. Optogenetics identified several Dm neurons that functionally connect with Tm9 neurons (Lopez et al. 2020). We have also shown that a glutamate-gated chloride channel is responsible for the luminance gain in Tm9, narrowing these Dm candidates to glutamatergic ones. Genetic silencing of these neurons while investigating Tm9 contrast representations in changing luminances would reveal the Dm neuron candidate that provides the spatial inputs. The spatial extent of the glutamatergic input of around 22° could narrow down further Dm neuron candidates according to how many columns they span. Imaging Dm neurons would reveal their contrast and luminanc encoding properties which would be helpful for identifying candidates for implementing luminance gain in medulla neurons. For Tm1 neurons, all the above experiments apply, but GABAergic neurons should also be taken into account since there was no evidence for a glutamatergic mechanism. Furthermore, spatial pooling extends of Tm1 and Tm9 neurons can be matched to the luminance statistics of natural scenes that flies are exposed to test if the spatial filters are optimal to compute the relevant luminance levels.

Why does the fly need two channels with a rapid luminance gain that lead to different contrast representations and how do Tm1 and Tm9 neurons achieve their distinct characteristics? Similar to the suggestions above for L3 non-linear luminance sensitivity, statistical analysis of luminance distributions in natural scenes can provide clues on the existence of two distinct luminance gain channels. The functional role of these distinct channels can be further investigated by silencing either Tm1 and Tm9 and visualizing the effects on the motion-sensitive neurons or behavior. In these experiments, stimulus design is essential since the effects can only be captured using appro-

priate stimuli. One can map the receptive field (RF) of motion-sensitive neurons and induce rapid luminance changes using natural scenes in the RF and observe how the contrast or direction representations change upon Tm neurons silencing. Another approach is to see if two luminance gain channels are a wide phenomena or arise due to specific lightning conditions that the *Drosophila* lives in. Using species that live in different environments, one could check their medulla neurons for luminance gain channels and compare them with the environmental luminance statistics. This is in principle possible in the era of genome editing, and other Drosophila species have been used for genetic manipulations and calcium imaging (CSeeholzer et al. 2018). Another difference between Tm1 and Tm9 neurons is that they use different molecular mechanisms for luminance gain control. Tm9 properties rely on GluClalphaα but how GluClalphaα implements a luminance gain is not known. A promising hypothesis is that GluClalphaα mediates a shunting inhibition, leading to the normalization of Ach input coming to the Tm9 dendrites. Biophysical models can test the feasibility of this hypothesis. Then cell-type specific RNAseq and LOF approaches can also be applied to identify the Ach receptor involved in this mechanism. Electrophysiology could be used to characterize the role of GluClalphaα on Tm9 membrane properties and assess if it provides a shunting inhibition as done for T4 neurons (Groschner et al. 2022), but electrophysiological recordings from medulla neurons are very challenging to perform given the size of neurons in the fly brain. The molecular mechanism of Tm1 neurons is currently unknown. A promising candidate is the $GABA_A$ receptors since some Dm neurons are GABAergic (Nern et al. 2015). Rdl flpSTOP allele exist and can be used to achieve cell-type specific LOF of $GABA_A$ receptors in Tm1 neurons to test this hypothesis (Fisher et al. 2017). The answer to Tm1 and Tm9 differences could either be due to the difference in molecular mechanisms or difference in inputs, or a combination.

Our worked revealed that behavioral responses to ON stimuli also underlie luminance gain control. The circuit implementation for the luminance gain in the ON pathway is yet to be identified. Similar to what I did in this thesis, calcium imaging of the major ON pathway neurons will reveal the location of luminance gain. L3 neurons, for example, provide inputs to Mi9 and Mi1 (Takemura et al. 2013), which makes them promising candidates for implementing the ON pathway luminance gain. OFF behavior in rapidly changing luminances is different than ON behavior which could be reflected in the contrast representations of ON pathway neurons. After identifying and characterizing the luminance gain in the ON pathway, a modeling approach can combine the findings to create a framework on how contrast is stably represented during natural scene viewing.

Convergence and divergence of cell-types characterizes information processing in neural circuits, including vertebrate and invertebrate visual circuits. Due to this intricate architecture, individual cell-types can be involved in signal processing differently via their distinct synaptic connections. A causal understanding of neural computations thus requires isolating and manipulating distinct synaptic connections of synaptic partners. STAB is a genetically based protease-mediated approach to silence synapses between specific cell-types to achieve this aim. If successful, STAB will be the first example of such synapse-specific manipulations. STAB can easily be implemented across different sensory modalities or central circuits in the fly system, but also provides opportunities to perform synapse-specific manipulations in other organisms amenable to transgenesis, such as rodents and zebrafish.

STAB is already in a promising state but further testing and potential optimizations will be needed to improve STAB activity and applicability. An essential component of STAB is the TEVp which targets the essential synaptic proteins on the other side of the synapse. We recently successfully tested a TEV protease variant with improved folding and stability using mutagenesis. *In vivo* experiments for recapitulating known LOF phenotypes is next required to functionally test the improved TEVp. Further mutations could be aimed to increase the catalytic activity of TEVp (Sanchez et al. 2020). As we have done so far, these mutations can be initially tested *in vitro* in S2 cells and then applied *in vivo*. Establishing a highly efficient TEVp will be very fruitful for improving STAB and other TEVp-dependent approaches in the fly system.

TEVcs can be integrated into any synaptic protein using endogenous protein modification methods such as RMCE or CRISPR-Cas9. However, some possible problems are worth considering while integrating TEVcs. 1) Tag insertions can disrupt a protein, 2) TEVcs might be hidden in the complex structure of the proteins, hindering TEVp mediated cleavage or 3) cleavage might not lead to the disruption of protein. A rapid platform to optimize TEVcs insertions could be useful for extending the STAB applicability. By overexpressing the TEVcs integrated channels in *in vitro* systems such as

S2 cells, HEK cells or oocytes, one can examine if the TEVcs is cleavable and the functional consequences upon TEVcs insertion and cleavage via electrophysiology. A high throughput approach like this can be used to test different TEVcs insertions to isolate the optimal ones for further use *in vivo*.

STAB is a chronic manipulation approach and limitations of chronic manipulation approaches, such as homeostatic compensatory mechanisms, can be circumvented by temporal control of manipulations. In fact, temporal control could be combined with the STAB approach targeting the voltage-gated calcium channel Cacophony, as temperature-sensitive *cac* alleles exist which could be used in trans to *cac[flpTEV]*. Thinking of alternative approaches, temporal control of synaptic manipulations could also be achieved by generating a synapse specific activity block using the dominant-negative temperature-sensitive dynamin allele Shibire^{ts} (Kitamoto 2001). One possible design is to modify an existing trans-synaptic tracing tool called TRACT which is based on an artificial ligand-receptor pair that are expressed in cells making contacts (Huang et al. 2017). Upon activation, the receptor undergoes intracellular proteolysis of a transcription factor, ultimately leading to transcriptional regulation of the downstream cell. Instead of the transcription factor, one can integrate Shibire^{ts} since upon release from the receptor, Shibire^{ts} then might result in the elimination of endocytosis only upon temperature increase.

No matter which of these approaches will be useful in the end, the successful establishment of STAB or a STAB-like tool will allow to analyze circuit architecture at synaptic resolution. As highlighted above, combining such a genetics approach with an *in vivo* analysis of neural circuits will further our understanding how specific, behaviorally relevant computations, can be implemented within neural networks.

9 | Bibliography

Ahrens, Misha B. et al. (May 2013). Whole-brain functional imaging at cellular resolution using light-sheet microscopy. en. Nature Methods *10*.5, 413–420. ISSN: 1548-7105. DOI: 10.1038/nmeth.2434. URL: https://www.nature.com/articles/nmeth.2434 (visited on 05/06/2022).

Albadri, Shahad, Del Bene, Filippo, and Revenu, Céline (May 2017). Genome editing using CRISPR/Cas9-based knock-in approaches in zebrafish. eng. Methods (San Diego, Calif.) *121-122*, 77–85. ISSN: 1095-9130. DOI: 10.1016/j.ymeth.2017.03.005.

Ammer, Georg et al. (Aug. 2015). Functional Specialization of Neural Input Elements to the Drosophila ON Motion Detector. eng. Current biology: CB *25*.17, 2247–2253. ISSN: 1879-0445. DOI: 10.1016/j.cub.2015.07.014.

Arshavsky, Vadim Y., Lamb, Trevor D., and Pugh, Edward N. (Mar. 2002). G Proteins and Phototransduction. en. Annual Review of Physiology *64*.1, 153–187. ISSN: 0066-4278, 1545-1585. DOI: 10.1146/annurev.physiol.64.082701.102229. URL: https://www.annualreviews.org/doi/10.1146/annurev.physiol.64.082701.102229 (visited on 05/10/2022).

Asari, Hiroki and Meister, Markus (Nov. 2012). Divergence of visual channels in the inner retina. eng. Nature Neuroscience *15*.11, 1581–1589. ISSN: 1546-1726. DOI: 10.1038/nn.3241.

Baden, Tom and Hedwig, Berthold (Nov. 2010). Primary afferent depolarization and frequency processing in auditory afferents. eng. The Journal of Neuroscience: The Official Journal of the Society for Neuroscience *30*.44, 14862–14869. ISSN: 1529-2401. DOI: 10.1523/JNEUROSCI.2734-10.2010.

Baden, Tom et al. (Jan. 2016). The functional diversity of retinal ganglion cells in the mouse. en. Nature *529*.7586, 345–350. ISSN: 1476-4687. DOI: 10.1038/nature16468. URL: https://www.nature.com/articles/nature16468 (visited on 05/06/2022).

Bae, J. Alexander et al. (May 2018). Digital Museum of Retinal Ganglion Cells with Dense Anatomy and Physiology. eng. Cell *173*.5, 1293–1306.e19. ISSN: 1097-4172. DOI: 10.1016/j.cell.2018.04.040.

Baines, R. A. et al. (Mar. 2001). Altered electrical properties in Drosophila neurons developing without synaptic transmission. eng. The Journal of Neuroscience: The Official Journal of the Society for Neuroscience *21*.5, 1523–1531. ISSN: 1529-2401.

Bates, Alexander S. et al. (Aug. 2020). Complete Connectomic Reconstruction of Olfactory Projection Neurons in the Fly Brain. en. Current Biology *30*.16, 3183–3199.e6. ISSN: 09609822. DOI: 10.1016/j.cub.2020.06.042. URL: https://linkinghub.elsevier.com/retrieve/pii/S0960982220308587 (visited on 05/22/2022).

Baylor, D. A. and Hodgkin, A. L. (Nov. 1974). Changes in time scale and sensitivity in turtle photoreceptors. eng. The Journal of Physiology *242*.3, 729–758. ISSN: 0022-3751. DOI: 10.1113/jphysiol.1974.sp010732.

Bellen, Hugo J., Tong, Chao, and Tsuda, Hiroshi (July 2010). 100 years of Drosophila research and its impact on vertebrate neuroscience: a history lesson for the future. eng. Nature Reviews. Neuroscience *11*.7, 514–522. ISSN: 1471-0048. DOI: 10.1038/nrn2839.

Berger, Hans (Dec. 1929). Über das Elektrenkephalogramm des Menschen. de. Archiv für Psychiatrie und Nervenkrankheiten *87*.1, 527–570. ISSN: 1433-8491. DOI: 10.1007/BF01797193. URL: https://doi.org/10.1007/BF01797193 (visited on 05/04/2022).

Berndt, André et al. (Feb. 2009). Bi-stable neural state switches. en. Nature Neuroscience *12*.2, 229–234. ISSN: 1546-1726. DOI: 10.1038/nn.2247. URL: https://www.nature.com/articles/nn.2247 (visited on 05/06/2022).

Binda, Paola and Morrone, Maria Concetta (Sept. 2018). Vision During Saccadic Eye Movements. en. Annual Review of Vision Science *4*.1, 193–213. ISSN: 2374-4642, 2374-4650. DOI: 10.1146/annurev-vision-091517-034317. URL: https://www.annualreviews.org/doi/10.1146/annurev-vision-091517-034317 (visited on 05/09/2022).

Boynton, Robert M. and Whitten, David N. (Dec. 1970). Visual Adaptation in Monkey Cones: Recordings of Late Receptor Potentials. en. Science *170*.3965, 1423–1426. ISSN: 0036-8075, 1095-9203. DOI: 10.1126/science.170.3965.1423. URL: https://www.science.org/doi/10.1126/science.170.3965.1423 (visited on 05/10/2022).

Brand, A. H. and Perrimon, N. (June 1993). Targeted gene expression as a means of altering cell fates and generating dominant phenotypes. eng. Development (Cambridge, England) *118*.2, 401–415. ISSN: 0950-1991. DOI: 10.1242/dev.118.2.401.

Brankatschk, M. and Eaton, S. (Aug. 2010). Lipoprotein Particles Cross the Blood-Brain Barrier in Drosophila. en. Journal of Neuroscience *30*.31, 10441–10447. ISSN: 0270-6474, 1529-2401. DOI: 10.1523/JNEUROSCI.5943-09.2010. URL: https://www.jneurosci.org/lookup/doi/10.1523/JNEUROSCI.5943-09.2010 (visited on 05/28/2022).

Briggman, Kevin L., Helmstaedter, Moritz, and Denk, Winfried (Mar. 2011). Wiring specificity in the direction-selectivity circuit of the retina. en. Nature *471*.7337, 183–188. ISSN: 1476-4687. DOI: 10.1038/nature09818. URL: https://www.nature.com/articles/nature09818 (visited on 05/06/2022).

Broadie, Kendal et al. (Sept. 1995). Syntaxin and synaptobrevin function downstream of vesicle docking in drosophila. en. Neuron *15*.3, 663–673. ISSN: 0896-6273. DOI: 10.1016/0896-6273(95)90154-X. URL: https://www.sciencedirect.com/science/article/pii/089662739590154X (visited on 05/19/2022).

Burkhardt, Dwight A. (Mar. 1994). Light adaptation and photopigment bleaching in cone photoreceptors in situ in the retina of the turtle. eng. The Journal of Neuroscience: The Official Journal of the Society for Neuroscience *14*.3 Pt 1, 1091–1105. ISSN: 0270-6474.

Burkhardt, Dwight A. et al. (Mar. 1984). Symmetry and constancy in the perception of negative and positive luminance contrast. EN. JOSA A *1*.3, 309–316. ISSN: 1520-8532. DOI: 10.1364/JOSAA.1.000309. URL: https://opg.optica.org/josaa/abstract.cfm?uri=josaa-1-3-309 (visited on 04/19/2022).

Burns, Marie E and Baylor, Denis A (Mar. 2001). Activation, Deactivation, and Adaptation in Vertebrate Photoreceptor Cells. en. Annual Review of Neuroscience *24*.1, 779–805. ISSN: 0147-006X, 1545-4126. DOI: 10.1146/annurev.neuro.24.1.779. URL: https://www.annualreviews.org/doi/10.1146/annurev.neuro.24.1.779 (visited on 05/10/2022).

Byri, Sunitha et al. (June 2015). The Triple-Repeat Protein Anakonda Controls Epithelial Tricellular Junction Formation in Drosophila. en. Developmental Cell *33*.5, 535–548. ISSN: 15345807. DOI: 10.1016/j.devcel.2015.03.023. URL: https://linkinghub.elsevier.com/retrieve/pii/S1534580715002191 (visited on 05/28/2022).

Cachero, Sebastian et al. (Dec. 2020). BAcTrace, a tool for retrograde tracing of neuronal circuits in Drosophila. en. Nature Methods *17*.12, 1254–1261. ISSN: 1548-7105. DOI: 10.1038/s41592-020-00989-1. URL: https://www.nature.com/articles/s41592-020-00989-1 (visited on 04/21/2022).

Carandini, M. and Heeger, D. J. (May 1994). Summation and division by neurons in primate visual cortex. eng. Science (New York, N.Y.) *264*.5163, 1333–1336. ISSN: 0036-8075. DOI: 10.1126/science.8191289.

Carandini, Matteo (Apr. 2012). From circuits to behavior: a bridge too far? en. Nature Neuroscience *15*.4, 507–509. ISSN: 1546-1726. DOI: 10.1038/nn.3043. URL: https://www.nature.com/articles/nn.3043 (visited on 05/04/2022).

Carandini, Matteo and Heeger, David J. (Nov. 2011). Normalization as a canonical neural computation. Nature reviews. Neuroscience *13*.1, 51–62. ISSN: 1471-003X. DOI: 10.1038/nrn3136. URL: https://www.ncbi.nlm.nih.gov/pmc/articles/PMC3273486/ (visited on 04/19/2022).

Carandini, Matteo, Heeger, David J., and Movshon, J. Anthony (Nov. 1997). Linearity and Normalization in Simple Cells of the Macaque Primary Visual Cortex. en. Journal of Neuroscience *17*.21, 8621–8644. ISSN: 0270-6474, 1529-2401. DOI: 10.1523/JNEUROSCI.17-21-08621.1997. URL: https://www.jneurosci.org/content/17/21/8621 (visited on 05/15/2022).

Cesaratto, Francesca et al. (Oct. 2015). Engineered tobacco etch virus (TEV) protease active in the secretory pathway of mammalian cells. en. Journal of Biotechnology *212*, 159–166. ISSN: 01681656. DOI: 10.1016/j.jbiotec.2015.08.026. URL: https://linkinghub.elsevier.com/retrieve/pii/S016816561530105X (visited on 04/06/2022).

Chen, Beth L., Hall, David H., and Chklovskii, Dmitri B. (Mar. 2006). Wiring optimization can relate neuronal structure and function. en. Proceedings of the National Academy of Sciences *103*.12, 4723–4728. ISSN: 0027-8424, 1091-6490. DOI: 10.1073/pnas.0506806103. URL: https://pnas.org/doi/full/10.1073/pnas.0506806103 (visited on 05/06/2022).

Chen, Tsai-Wen et al. (July 2013). Ultrasensitive fluorescent proteins for imaging neuronal activity. en. Nature *499*.7458, 295–300. ISSN: 1476-4687. DOI: 10.1038/nature12354. URL: https://www.nature.com/articles/nature12354 (visited on 05/06/2022).

Choi, Sue-Yeon et al. (Nov. 2005). Encoding light intensity by the cone photoreceptor synapse. eng. Neuron *48*.4, 555–562. ISSN: 0896-6273. DOI: 10.1016/j.neuron.2005.09.011.

Cicerone, C M and Green, Daniel G. (Apr. 1980). Light adaptation within the receptive field centre of rat retinal ganglion cells. en. The Journal of Physiology *301*.1, 517–534. ISSN: 00223751. DOI: 10.1113/jphysiol.1980.sp013221. URL: https://onlinelibrary.wiley.com/doi/10.1113/jphysiol.1980.sp013221 (visited on 05/14/2022).

Clark, Damon A. and Demb, Jonathan B. (Oct. 2016). Parallel Computations in Insect and Mammalian Visual Motion Processing. English. Current Biology *26*.20, R1062–R1072. ISSN: 0960-9822. DOI: 10.1016/j.cub.2016.08.003. URL: https://www.cell.com/current-biology/abstract/S0960-9822(16)30915-0 (visited on 05/09/2022).

Clark, Damon A. et al. (June 2011). Defining the Computational Structure of the Motion Detector in Drosophila. en. Neuron *70*.6, 1165–1177. ISSN: 08966273. DOI: 10.1016/j.neuron.2011.05.023. URL: https://linkinghub.elsevier.com/retrieve/pii/S0896627311004417 (visited on 05/12/2022).

Cohen, Ethan, Sterling, Peter, and Boycott, Brian Blundell (Dec. 1990). Convergence and divergence of cones onto bipolar cells in the central area of cat retina. Philosophical Transactions of the Royal Society of London. Series B: Biological Sciences *330*.1258, 323–328. DOI: 10.1098/rstb.1990.0202. URL: https://royalsocietypublishing.org/doi/10.1098/rstb.1990.0202 (visited on 05/06/2022).

Cohen, Marlene R. and Newsome, William T. (Apr. 2004). What electrical microstimulation has revealed about the neural basis of cognition. eng. Current Opinion in Neurobiology *14*.2, 169–177. ISSN: 0959-4388. DOI: 10.1016/j.conb.2004.03.016.

Collins, Catherine A and DiAntonio, Aaron (Feb. 2007). Synaptic development: insights from Drosophila. en. Current Opinion in Neurobiology *17*.1, 35–42. ISSN: 09594388. DOI: 10.1016/j.conb.2007.01.001. URL: https://linkinghub.elsevier.com/retrieve/pii/S0959438807000037 (visited on 05/07/2022).

Cook, Boaz et al. (May 2000). Phospholipase C and termination of G-protein-mediated signalling in vivo. en. Nature Cell Biology *2*.5, 296–301. ISSN: 1476-4679. DOI: 10.1038/35010571. URL: https://www.nature.com/articles/ncb0500_296 (visited on 05/10/2022).

Crick, F. and Koch, C. (1990). Some reflections on visual awareness. eng. Cold Spring Harbor Symposia on Quantitative Biology *55*, 953–962. ISSN: 0091-7451. DOI: 10.1101/sqb.1990.055.01.089.

Crocker, Amanda et al. (May 2016). Cell-Type-Specific Transcriptome Analysis in the Drosophila Mushroom Body Reveals Memory-Related Changes in Gene Expression. eng. Cell Reports *15*.7, 1580–1596. ISSN: 2211-1247. DOI: 10.1016/j.celrep.2016.04.046.

Cronin, Michelle A., Lieu, Minh-Ha, and Tsunoda, Susan (July 2006). Two stages of light-dependent TRPL-channel translocation in *Drosophila* photoreceptors. en. Journal of Cell Science *119*.14, 2935–2944. ISSN: 1477-9137, 0021-9533. DOI: 10.1242/jcs.03049. URL: https://journals.biologists.com/jcs/article/119/14/2935/29003/Two-stages-of-light-dependent-TRPL-channel (visited on 05/19/2022).

Crook, Joanna D., Packer, Orin S., and Dacey, Dennis M. (Jan. 2014). A synaptic signature for ON- and OFF-center parasol ganglion cells of the primate retina. eng. Visual Neuroscience *31*.1, 57–84. ISSN: 1469-8714. DOI: 10.1017/S0952523813000461.

Cui, Jinjuan and Pan, Zhuo-Hua (2008). Two Types of Cone Bipolar Cells Express Voltage-Gated Na+ Channels in the Rat Retina. Visual neuroscience *25*.5-6, 635–645. ISSN: 0952-5238. DOI: 10.1017/S0952523808080851. URL: https://www.ncbi.nlm.nih.gov/pmc/articles/PMC2650833/ (visited on 05/11/2022).

Cuttle, M. F. et al. (May 1995). Diurnal modulation of photoreceptor potassium conductance in the locust. en. Journal of Comparative Physiology A *176*.3, 307–316. ISSN: 1432-1351. DOI: 10.1007/BF00219056. URL: https://doi.org/10.1007/BF00219056 (visited on 05/10/2022).

Davidson, Elmer H. and Freeman, Robert B. (Jan. 1965). Brightness constancy under a gradient of illumination. en. Psychonomic Science *2*.1, 349–350. ISSN: 2197-9952. DOI: 10.3758/BF03343492. URL: https://doi.org/10.3758/BF03343492 (visited on 05/15/2022).

Davis, Fred P. et al. (Aug. 2018). A genetic, genomic, and computational resource for exploring neural circuit function. en. bioRxiv. DOI: 10.1101/385476. URL: https://doi.org/10.1101/385476 (visited on 06/25/2019).

– (Jan. 2020). A genetic, genomic, and computational resource for exploring neural circuit function. eLife *9*. Ed. by Hugo J. Bellen and K VijayRaghavan, e50901. ISSN: 2050-084X. DOI: 10.7554/eLife.50901. URL: https://doi.org/10.7554/eLife.50901 (visited on 05/15/2022).

Davis, Graeme W. (July 2006). Homeostatic control of neural activity: from Phenomenology to Molecular Design. en. Annual Review of Neuroscience *29*.1, 307–323. ISSN: 0147-006X, 1545-4126. DOI: 10.1146/annurev.neuro.28.061604.135751. URL: http://www.annualreviews.org/doi/10.1146/annurev.neuro.28.061604.135751 (visited on 07/25/2019).

Davison, Jon M. et al. (Apr. 2007). Transactivation from Gal4-VP16 transgenic insertions for tissue-specific cell labeling and ablation in zebrafish. eng. Developmental Biology *304*.2, 811–824. ISSN: 0012-1606. DOI: 10.1016/j.ydbio.2007.01.033.

Deisseroth, Karl (Sept. 2015). Optogenetics: 10 years of microbial opsins in neuroscience. en. Nature Neuroscience *18*.9, 1213–1225. ISSN: 1546-1726. DOI: 10.1038/nn.4091. URL: https://www.nature.com/articles/nn.4091 (visited on 05/21/2022).

Demb, Jonathan B. and Singer, Joshua H. (Nov. 2015). Functional Circuitry of the Retina. en. Annual Review of Vision Science *1*.1, 263–289. ISSN: 2374-4642, 2374-4650. DOI: 10.1146/annurev-vision-082114-035334. URL: https://www.annualreviews.org/doi/10.1146/annurev-vision-082114-035334 (visited on 05/03/2022).

DeVries, S. H. (Dec. 2000). Bipolar cells use kainate and AMPA receptors to filter visual information into separate channels. eng. Neuron *28*.3, 847–856. ISSN: 0896-6273. DOI: 10.1016/s0896-6273(00)00158-6.

Dolph, Patrick J. et al. (June 1993). Arrestin Function in Inactivation of G Protein-Coupled Receptor Rhodopsin in Vivo. en. Science *260*.5116, 1910–1916. ISSN: 0036-8075, 1095-9203. DOI: 10.1126/science.8316831. URL: https://www.science.org/doi/10.1126/science.8316831 (visited on 05/11/2022).

Drews, Michael S. et al. (Jan. 2020). Dynamic Signal Compression for Robust Motion Vision in Flies. en. Current Biology *30*.2, 209–221.e8. ISSN: 0960-9822. DOI: 10.1016/j.cub.2019.10.035. URL: https://www.sciencedirect.com/science/article/pii/S0960982219313752 (visited on 04/19/2022).

Dubs, Andreas (1982). The spatial integration of signals in the retina and lamina of the fly compound eye under different conditions of luminance. en. Journal of Comparative Physiology ? A *146*.3, 321–343. ISSN: 0340-7594, 1432-1351. DOI: 10.1007/BF00612703. URL: http://link.springer.com/10.1007/BF00612703 (visited on 05/15/2022).

Dunn, Felice A., Lankheet, Martin J., and Rieke, Fred (Oct. 2007). Light adaptation in cone vision involves switching between receptor and post-receptor sites. en. Nature *449*.7162, 603–606. ISSN: 1476-4687. DOI: 10.1038/nature06150. URL: https://www.nature.com/articles/nature06150 (visited on 04/19/2022).

Dyakova, Olga and Nordström, Karin (Dec. 2017). Image statistics and their processing in insect vision. en. Current Opinion in Insect Science *24*, 7–14. ISSN: 22145745. DOI: 10.1016/j.cois.2017.08.002. URL: https://linkinghub.elsevier.com/retrieve/pii/S221457451730010X (visited on 05/24/2022).

Eichner, Hubert et al. (June 2011). Internal Structure of the Fly Elementary Motion Detector. en. Neuron *70*.6, 1155–1164. ISSN: 08966273. DOI: 10.1016/j.neuron.2011.03.028. URL: https://linkinghub.elsevier.com/retrieve/pii/S089662731100376X (visited on 05/26/2022).

Euler, Thomas (Aug. 2001). Dendritic processing. Current Opinion in Neurobiology *11*.4, 415–422. ISSN: 09594388. DOI: 10.1016/S0959-4388(00)00228-2. URL: https://linkinghub.elsevier.com/retrieve/pii/S0959438800002282 (visited on 05/28/2022).

Euler, Thomas, Detwiler, Peter B., and Denk, Winfried (Aug. 2002). Directionally selective calcium signals in dendrites of starburst amacrine cells. en. Nature *418*.6900, 845–852. ISSN: 1476-4687. DOI: 10.1038/nature00931. URL: https://www.nature.com/articles/nature00931 (visited on 05/09/2022).

Euler, Thomas et al. (Aug. 2014). Retinal bipolar cells: elementary building blocks of vision. en. Nature Reviews Neuroscience *15*.8, 507–519. ISSN: 1471-0048. DOI: 10.1038/nrn3783. URL: https://www.nature.com/articles/nrn3783 (visited on 05/11/2022).

Fain, G. L. et al. (Jan. 2001). Adaptation in vertebrate photoreceptors. eng. Physiological Reviews *81*.1, 117–151. ISSN: 0031-9333. DOI: 10.1152/physrev.2001.81.1.117.

Faisal, A. Aldo, Selen, Luc P. J., and Wolpert, Daniel M. (Apr. 2008). Noise in the nervous system. en. Nature Reviews Neuroscience *9*.4, 292–303. ISSN: 1471-0048. DOI: 10.1038/nrn2258. URL: https://www.nature.com/articles/nrn2258 (visited on 05/06/2022).

Fendl, Sandra, Vieira, Renee Marie, and Borst, Alexander (Oct. 2020). Conditional protein tagging methods reveal highly specific subcellular distribution of ion channels in motion-sensing neurons. eLife *9*. Ed. by Claude Desplan et al., e62953. ISSN: 2050-084X. DOI: 10.7554/eLife.62953. URL: https://doi.org/10.7554/eLife.62953 (visited on 05/06/2022).

Fenno, Lief, Yizhar, Ofer, and Deisseroth, Karl (2011). The development and application of optogenetics. eng. Annual Review of Neuroscience *34*, 389–412. ISSN: 1545-4126. DOI: 10.1146/annurev-neuro-061010-113817.

Ffrench-Constant, R H et al. (Aug. 1991). Molecular cloning and transformation of cyclodiene resistance in Drosophila: an invertebrate gamma-aminobutyric acid subtype A receptor locus. en. Proceedings of the National Academy of Sciences *88*.16, 7209–7213. ISSN: 0027-8424, 1091-6490. DOI: 10.1073/pnas.88.16.7209. URL: https://pnas.org/doi/full/10.1073/pnas.88.16.7209 (visited on 05/18/2022).

Fischbach, K. -F. and Dittrich, A. P. M. (Dec. 1989). The optic lobe of Drosophila melanogaster. I. A Golgi analysis of wild-type structure. en. Cell and Tissue Research *258*.3, 441–475. ISSN: 1432-0878. DOI: 10.1007/BF00218858. URL: https://doi.org/10.1007/BF00218858 (visited on 05/06/2022).

Fisher, Yvette E. et al. (Dec. 2015). A Class of Visual Neurons with Wide-Field Properties Is Required for Local Motion Detection. en. Current Biology *25*.24, 3178–3189. ISSN: 09609822. DOI: 10.1016/j.cub.2015.11.018. URL: https://linkinghub.elsevier.com/retrieve/pii/S0960982215014128 (visited on 05/11/2022).

Fisher, Yvette E. et al. (Feb. 2017). FlpStop, a tool for conditional gene control in Drosophila. eLife *6*. Ed. by Kristin Scott, e22279. ISSN: 2050-084X. DOI: 10.7554/eLife.22279. URL: https://doi.org/10.7554/eLife.22279 (visited on 05/07/2022).

Frazor, Robert A. and Geisler, Wilson S. (May 2006). Local luminance and contrast in natural images. en. Vision Research *46*.10, 1585–1598. ISSN: 0042-6989. DOI: 10.1016/j.visres.2005.06.038. URL: https://www.sciencedirect.com/science/article/pii/S0042698905005559 (visited on 04/19/2022).

Freeman, Daniel K., Graña, Gilberto, and Passaglia, Christopher L. (Aug. 2010). Retinal Ganglion Cell Adaptation to Small Luminance Fluctuations. Journal of Neurophysiology *104*.2, 704–712. ISSN: 0022-3077. DOI: 10.1152/jn.00767.2009. URL: https://www.ncbi.nlm.nih.gov/pmc/articles/PMC4971895/ (visited on 05/14/2022).

Freifeld, Limor et al. (June 2013). GABAergic Lateral Interactions Tune the Early Stages of Visual Processing in Drosophila. en. Neuron *78*.6, 1075–1089. ISSN: 0896-6273. DOI: 10.1016/j.neuron.2013.04.024. URL: https://www.sciencedirect.com/science/article/pii/S0896627313003267 (visited on 05/11/2022).

Fries, Pascal et al. (Nov. 1997). Synchronization of oscillatory responses in visual cortex correlates with perception in interocular rivalry. en. Proceedings of the National Academy of Sciences *94*.23, 12699–12704. ISSN: 0027-8424, 1091-6490. DOI: 10.1073/pnas.94.23.12699. URL: https://pnas.org/doi/full/10.1073/pnas.94.23.12699 (visited on 05/04/2022).

Frolov, Roman, Immonen, Esa-Ville, and Weckström, Matti (Apr. 2016). Visual ecology and potassium conductances of insect photoreceptors. eng. Journal of Neurophysiology *115*.4, 2147–2157. ISSN: 1522-1598. DOI: 10.1152/jn.00795.2015.

Gandhi, Sunil P. and Stevens, Charles F. (June 2003). Three modes of synaptic vesicular recycling revealed by single-vesicle imaging. eng. Nature *423*.6940, 607–613. ISSN: 0028-0836. DOI: 10.1038/nature01677.

García-Otín, Angel Luis and Guillou, Florian (Jan. 2006). Mammalian genome targeting using site-specific recombinases. eng. Frontiers in Bioscience: A Journal and Virtual Library *11*, 1108–1136. ISSN: 1093-9946. DOI: 10.2741/1867.

Gaudry, Quentin et al. (Jan. 2013). Asymmetric neurotransmitter release enables rapid odour lateralization in Drosophila. eng. Nature *493*.7432, 424–428. ISSN: 1476-4687. DOI: 10.1038/nature11747.

Gengs, Chaoxian et al. (Nov. 2002). The target of Drosophila photoreceptor synaptic transmission is a histamine-gated chloride channel encoded by ort (hclA). eng. The Journal of Biological Chemistry *277*.44, 42113–42120. ISSN: 0021-9258. DOI: 10.1074/jbc.M207133200.

Geurten, Bart R. H. et al. (Oct. 2014). Saccadic body turns in walking Drosophila. Frontiers in Behavioral Neuroscience *8*. ISSN: 1662-5153. DOI: 10.3389/fnbeh.2014.00365. URL: http://journal.frontiersin.org/article/10.3389/fnbeh.2014.00365/abstract (visited on 05/25/2022).

Gjorgjieva, Julijana, Sompolinsky, Haim, and Meister, Markus (Sept. 2014). Benefits of pathway splitting in sensory coding. eng. The Journal of Neuroscience: The Official Journal of the Society for Neuroscience *34*.36, 12127–12144. ISSN: 1529-2401. DOI: 10.1523/JNEUROSCI.1032-14.2014.

Gohl, Daryl M. et al. (Mar. 2011). A versatile in vivo system for directed dissection of gene expression patterns. en. Nature Methods *8*.3, 231–237. ISSN: 1548-7105. DOI: 10.1038/nmeth.1561. URL: https://www.nature.com/articles/nmeth.1561 (visited on 05/07/2022).

Golgi, Camillo (1873). Sulla struttura della sostanza grigia del cervello. Gazz. Med. Ital. (Lombardia) 33, 244–246.

Gomez, Juan L. et al. (Aug. 2017). Chemogenetics revealed: DREADD occupancy and activation via converted clozapine. en. Science *357*.6350, 503–507. ISSN: 0036-8075, 1095-9203. DOI: 10.1126/science.aan2475. URL: https://www.science.org/doi/10.1126/science.aan2475 (visited on 05/06/2022).

Gratz, Scott J. et al. (July 2015a). CRISPR-Cas9 genome editing in Drosophila. Current protocols in molecular biology / edited by Frederick M. Ausubel ... [et al.] *111*, 31.2.1–31.2.20. ISSN: 1934-3639. DOI: 10.1002/0471142727.mb3102s111. URL: https://www.ncbi.nlm.nih.gov/pmc/articles/PMC4506758/ (visited on 05/31/2022).

Gratz, Scott J. et al. (2015b). Precise Genome Editing of Drosophila with CRISPR RNA-Guided Cas9. eng. Methods in Molecular Biology (Clifton, N.J.) *1311*, 335–348. ISSN: 1940-6029. DOI: 10.1007/978-1-4939-2687-9_22.

Gray, Charles M. et al. (Mar. 1989). Oscillatory responses in cat visual cortex exhibit inter-columnar synchronization which reflects global stimulus properties. en. Nature *338*.6213, 334–337. ISSN: 1476-4687. DOI: 10.1038/338334a0. URL: https://www.nature.com/articles/338334a0 (visited on 05/04/2022).

Green, Daniel G. (Nov. 1971). Light Adaptation in the Rat Retina: Evidence for Two Receptor Mechanisms. en. Science *174*.4009, 598–600. ISSN: 0036-8075, 1095-9203. DOI: 10.1126/science.174.4009.598. URL: https://www.science.org/doi/10.1126/science.174.4009.598 (visited on 05/10/2022).

Green, Daniel G. and Powers, M. K. (1982). Mechanisms of light adaptation in rat retina. eng. Vision Research *22*.2, 209–216. ISSN: 0042-6989. DOI: 10.1016/0042-6989(82)90120-1.

Green, Daniel G. et al. (Apr. 1975). Retinal mechanisms of visual adaptation in the skate. eng. The Journal of General Physiology *65*.4, 483–502. ISSN: 0022-1295. DOI: 10.1085/jgp.65.4.483.

Grimes, William N. et al. (Mar. 2010). Retinal Parallel Processors: More than 100 Independent Microcircuits Operate within a Single Interneuron. Neuron *65*.6, 873–885. ISSN: 0896-6273. DOI: 10.1016/j.neuron.2010.02.028. URL: https://www.ncbi.nlm.nih.gov/pmc/articles/PMC2967021/ (visited on 05/06/2022).

Groschner, Lukas N. et al. (Mar. 2022). A biophysical account of multiplication by a single neuron. en. Nature *603*.7899, 119–123. ISSN: 1476-4687. DOI: 10.1038/s41586-022-04428-3. URL: https://www.nature.com/articles/s41586-022-04428-3 (visited on 05/15/2022).

Gu, Yuchun et al. (July 2005). Mechanisms of Light Adaptation in Drosophila Photoreceptors. en. Current Biology *15*.13, 1228–1234. ISSN: 0960-9822. DOI: 10.1016/j.cub.2005.05.058. URL: https://www.sciencedirect.com/science/article/pii/S0960982205006184 (visited on 05/10/2022).

Guerrero, Giovanna et al. (Sept. 2005). Heterogeneity in synaptic transmission along a Drosophila larval motor axon. eng. Nature Neuroscience *8*.9, 1188–1196. ISSN: 1097-6256. DOI: 10.1038/nn1526.

Gunaydin, Lisa A. et al. (Mar. 2010). Ultrafast optogenetic control. en. Nature Neuroscience *13*.3, 387–392. ISSN: 1546-1726. DOI: 10.1038/nn.2495. URL: https://www.nature.com/articles/nn.2495 (visited on 05/06/2022).

Hall, T.S. (1972). *Treatise of Man: French Text with Translation and Commentary, trans. Thomas Steele Hall*. Harvard University Press.

Hamada, Fumika N. et al. (July 2008). An internal thermal sensor controlling temperature preference in Drosophila. en. Nature *454*.7201, 217–220. ISSN: 1476-4687. DOI: 10.1038/nature07001. URL: https://www.nature.com/articles/nature07001 (visited on 05/21/2022).

Harder, Ben et al. (May 2008). TEV protease-mediated cleavage in *Drosophila* as a tool to analyze protein functions in living organisms. en. BioTechniques *44*.6, 765–772. ISSN: 0736-6205, 1940-9818. DOI: 10.2144/000112884. URL: https://www.future-science.com/doi/10.2144/000112884 (visited on 05/28/2022).

Hardie, R. C. (June 1989). A histamine-activated chloride channel involved in neurotransmission at a photoreceptor synapse. en. Nature *339*.6227, 704–706. ISSN: 1476-4687. DOI: 10.1038/339704a0. URL: https://www.nature.com/articles/339704a0 (visited on 05/11/2022).

Hateren, J H van and Schaaf, A van der (Mar. 1998). Independent component filters of natural images compared with simple cells in primary visual cortex. Proceedings of the Royal Society B: Biological Sciences *265*.1394, 359–366. ISSN: 0962-8452. URL: https://www.ncbi.nlm.nih.gov/pmc/articles/PMC1688904/ (visited on 05/09/2022).

Hateren, J. H. van (Dec. 1997). Processing of natural time series of intensities by the visual system of the blowfly. eng. Vision Research *37*.23, 3407–3416. ISSN: 0042-6989. DOI: 10.1016/s0042-6989(97)00105-3.

Heisenberg, Martin and Buchner, Erich (Jan. 1977). The rôle of retinula cell types in visual behavior ofDrosophila melanogaster. en. Journal of comparative physiology *117*.2, 127–162. ISSN: 1432-1351. DOI: 10.1007/BF00612784. URL: https://doi.org/10.1007/BF00612784 (visited on 05/10/2022).

Henning, Miriam et al. (Jan. 2022). Populations of local direction–selective cells encode global motion patterns generated by self-motion. en. Science Advances *8*.3, eabi7112. ISSN: 2375-2548. DOI: 10.1126/sciadv.abi7112. URL: https://www.science.org/doi/10.1126/sciadv.abi7112 (visited on 05/25/2022).

Henry, Gilbert L. et al. (Oct. 2012). Cell type–specific genomics of Drosophila neurons. en. Nucleic Acids Research *40*.19, 9691–9704. ISSN: 1362-4962, 0305-1048. DOI: 10.1093/nar/gks671. URL: https://academic.oup.com/nar/article/40/19/9691/2414604 (visited on 05/06/2022).

Hodge, James J.L. (Aug. 2009). Ion Channels to Inactivate Neurons in Drosophila. Frontiers in Molecular Neuroscience *2*, 13. ISSN: 1662-5099. DOI: 10.3389/neuro.02.013.2009. URL: https://www.ncbi.nlm.nih.gov/pmc/articles/PMC2741205/ (visited on 05/06/2022).

Honkanen, Anna et al. (Apr. 2017). Insect photoreceptor adaptations to night vision. Philosophical Transactions of the Royal Society B: Biological Sciences *372*.1717, 20160077. ISSN: 0962-8436. DOI: 10.1098/rstb.2016.0077. URL: https://www.ncbi.nlm.nih.gov/pmc/articles/PMC5312026/ (visited on 05/10/2022).

Horne, Jane Anne et al. (Nov. 2018). A resource for the Drosophila antennal lobe provided by the connectome of glomerulus VA1v. en. eLife *7*, e37550. ISSN: 2050-084X. DOI: 10.7554/eLife.37550. URL: https://elifesciences.org/articles/37550 (visited on 05/06/2022).

Hu, Caiping, Bi, Anding, and Pan, Zhuo-Hua (Apr. 2009). Differential expression of three T-type calcium channels in retinal bipolar cells in rats. eng. Visual Neuroscience *26*.2, 177–187. ISSN: 1469-8714. DOI: 10.1017/S0952523809090026.

Huang, Ting-hao et al. (Dec. 2017). Tracing neuronal circuits in transgenic animals by transneuronal control of transcription (TRACT). eLife *6*. Ed. by Mani Ramaswami, e32027. ISSN: 2050-084X. DOI: 10.7554/eLife.32027. URL: https://doi.org/10.7554/eLife.32027 (visited on 05/07/2022).

Hubel, D. H. and Wiesel, T. N. (Oct. 1959). Receptive fields of single neurones in the cat's striate cortex. en. The Journal of Physiology *148*.3, 574–591. ISSN: 00223751. DOI: 10.1113/jphysiol.1959.sp006308. URL: http://doi.wiley.com/10.1113/jphysiol.1959.sp006308 (visited on 04/18/2019).

Hubel, David H. (Mar. 1957). Tungsten Microelectrode for Recording from Single Units. en. Science *125*.3247, 549–550. ISSN: 0036-8075, 1095-9203. DOI: 10.1126/science.125.3247.549. URL: https://www.science.org/doi/10.1126/science.125.3247.549 (visited on 05/04/2022).

Hubel, David H. and Wiesel, T. N. (Jan. 1962). Receptive fields, binocular interaction and functional architecture in the cat's visual cortex. en. The Journal of Physiology *160*.1, 106–154. ISSN: 00223751. DOI: 10.1113/jphysiol.1962.sp006837. URL: https://onlinelibrary.wiley.com/doi/10.1113/jphysiol.1962.sp006837 (visited on 05/04/2022).

Ichinose, T., Fyk-Kolodziej, B., and Cohn, J. (June 2014). Roles of ON Cone Bipolar Cell Subtypes in Temporal Coding in the Mouse Retina. en. Journal of Neuroscience *34*.26, 8761–8771. ISSN: 0270-6474, 1529-2401. DOI: 10.1523/JNEUROSCI.3965-13.2014. URL: https://www.jneurosci.org/lookup/doi/10.1523/JNEUROSCI.3965-13.2014 (visited on 05/26/2022).

Idrees, Saad and Münch, Thomas A. (Nov. 2020). *Different contrast encoding in ON and OFF visual pathways*. en. preprint. Neuroscience. DOI: 10.1101/2020.11.25.398230. URL: http://biorxiv.org/lookup/doi/10.1101/2020.11.25.398230 (visited on 05/14/2022).

Izquierdo, I. and Medina, J. H. (Oct. 1998). On brain lesions, the milkman and Sigmunda. eng. Trends in Neurosciences *21*.10, 423–426. ISSN: 0166-2236. DOI: 10.1016/s0166-2236(98)01279-x.

Jarsky, Tim et al. (July 2011). A Synaptic Mechanism for Retinal Adaptation to Luminance and Contrast. en. Journal of Neuroscience *31*.30, 11003–11015. ISSN: 0270-6474, 1529-2401. DOI: 10.1523/JNEUROSCI.2631-11.2011. URL: https://www.jneurosci.org/content/31/30/11003 (visited on 05/11/2022).

Jeanne, James M. and Wilson, Rachel I. (Dec. 2015). Convergence, Divergence, and Reconvergence in a Feedforward Network Improves Neural Speed and Accuracy. eng. Neuron *88*.5, 1014–1026. ISSN: 1097-4199. DOI: 10.1016/j.neuron.2015.10.018.

Jenett, Arnim et al. (Oct. 2012). A GAL4-driver line resource for Drosophila neurobiology. eng. Cell Reports *2*.4, 991–1001. ISSN: 2211-1247. DOI: 10.1016/j.celrep.2012.09.011.

Joesch, M. et al. (Jan. 2013). Functional Specialization of Parallel Motion Detection Circuits in the Fly. en. Journal of Neuroscience *33*.3, 902–905. ISSN: 0270-6474, 1529-2401. DOI: 10.1523/JNEUROSCI.3374-12.2013. URL: https://www.jneurosci.org/lookup/doi/10.1523/JNEUROSCI.3374-12.2013 (visited on 05/26/2022).

Joesch, Maximilian et al. (Nov. 2010). ON and OFF pathways in Drosophila motion vision. en. Nature *468*.7321, 300–304. ISSN: 0028-0836, 1476-4687. DOI: 10.1038/nature09545. URL: http://www.nature.com/articles/nature09545 (visited on 05/12/2022).

Jonas, Peter, Bischofberger, Josef, and Sandkühler, Jürgen (July 1998). Corelease of Two Fast Neurotransmitters at a Central Synapse. en. Science *281*.5375, 419–424. ISSN: 0036-8075, 1095-9203. DOI: 10.1126/science.281.5375.419. URL: https://www.science.org/doi/10.1126/science.281.5375.419 (visited on 05/16/2022).

Joselevitch, Christina, Klooster, Jan, and Kamermans, Maarten (Oct. 2020). *VOLTAGE-GATED POTASSIUM CHANNELS CONTROL THE GAIN OF ROD-DRIVEN LIGHT RESPONSES IN MIXED-INPUT ON BIPOLAR CELLS*. en. preprint. Neuroscience. DOI: 10.1101/2020.10.10.334417. URL: http://biorxiv.org/lookup/doi/10.1101/2020.10.10.334417 (visited on 05/15/2022).

Jun, James J. et al. (Nov. 2017). Fully integrated silicon probes for high-density recording of neural activity. en. Nature *551*.7679, 232–236. ISSN: 1476-4687. DOI: 10.1038/nature24636. URL: https://www.nature.com/articles/nature24636 (visited on 05/04/2022).

Juusola, M. and Hardie, R. C. (Jan. 2001). Light adaptation in Drosophila photoreceptors: I. Response dynamics and signaling efficiency at 25 degrees C. eng. The Journal of General Physiology *117*.1, 3–25. ISSN: 0022-1295. DOI: 10.1085/jgp.117.1.3.

Juusola, M., Uusitalo, R. O., and Weckström, M. (Jan. 1995). Transfer of graded potentials at the photoreceptor-interneuron synapse. eng. The Journal of General Physiology *105*.1, 117–148. ISSN: 0022-1295. DOI: 10.1085/jgp.105.1.117.

Kane, Nanci S. et al. (Dec. 2000). Drug-resistant *Drosophila* indicate glutamate-gated chloride channels are targets for the antiparasitics nodulisporic acid and ivermectin. en. Proceedings of the National Academy of Sciences *97*.25, 13949–13954. ISSN: 0027-8424, 1091-6490. DOI: 10.1073/pnas.240464697. URL: https://pnas.org/doi/full/10.1073/pnas.240464697 (visited on 05/18/2022).

Katz, Ben and Minke, Baruch (2009). Drosophila photoreceptors and signaling mechanisms. Frontiers in Cellular Neuroscience *3*. ISSN: 1662-5102. URL: https://www.frontiersin.org/article/10.3389/neuro.03.002.2009 (visited on 05/10/2022).

Ketkar, Madhura D. et al. (Feb. 2020). Luminance Information Is Required for the Accurate Estimation of Contrast in Rapidly Changing Visual Contexts. en. Current Biology *30*.4, 657–669.e4. ISSN: 09609822. DOI: 10.1016/j.cub.2019.12.038. URL: https://linkinghub.elsevier.com/retrieve/pii/S0960982219316719 (visited on 05/19/2022).

Ketkar, Madhura D. et al. (Mar. 2022). First-order visual interneurons distribute distinct contrast and luminance information across ON and OFF pathways to achieve stable behavior. en. eLife *11*, e74937. ISSN: 2050-084X. DOI: 10.7554/eLife.74937. URL: https://elifesciences.org/articles/74937 (visited on 04/11/2022).

Kilpeläinen, Markku, Nurminen, Lauri, and Donner, Kristian (Feb. 2011). Effects of Mean Luminance Changes on Human Contrast Perception: Contrast Dependence, Time-Course and Spatial Specificity. en. PLOS ONE *6*.2, e17200. ISSN: 1932-6203. DOI: 10.1371/journal.pone.0017200. URL: https://journals.plos.org/plosone/article?id=10.1371/journal.pone.0017200 (visited on 04/22/2022).

Kitamoto, Toshihiro (May 2001). Conditional modification of behavior inDrosophila by targeted expression of a temperature-sensitiveshibire allele in defined neurons. en. Jour-

nal of Neurobiology *47*.2, 81–92. ISSN: 0022-3034, 1097-4695. DOI: 10.1002/neu.1018. URL: https://onlinelibrary.wiley.com/doi/10.1002/neu.1018 (visited on 04/21/2022).

Klapoetke, Nathan C. et al. (Mar. 2014). Independent optical excitation of distinct neural populations. en. Nature Methods *11*.3, 338–346. ISSN: 1548-7105. DOI: 10.1038/nmeth.2836. URL: https://www.nature.com/articles/nmeth.2836 (visited on 05/06/2022).

Klumpp, D. J. et al. (July 1995). The Shaker-like potassium channels of the mouse rod bipolar cell and their contributions to the membrane current. eng. The Journal of Neuroscience: The Official Journal of the Society for Neuroscience *15*.7 Pt 1, 5004–5013. ISSN: 0270-6474.

Konstantinides, Nikolaos et al. (July 2018). Phenotypic Convergence: Distinct Transcription Factors Regulate Common Terminal Features. en. Cell *174*.3, 622–635.e13. ISSN: 00928674. DOI: 10.1016/j.cell.2018.05.021. URL: https://linkinghub.elsevier.com/retrieve/pii/S0092867418306330 (visited on 05/06/2022).

Krapp, H. G., Hengstenberg, B., and Hengstenberg, R. (Apr. 1998). Dendritic structure and receptive-field organization of optic flow processing interneurons in the fly. eng. Journal of Neurophysiology *79*.4, 1902–1917. ISSN: 0022-3077. DOI: 10.1152/jn.1998.79.4.1902.

Krapp, H. G. and Hengstenberg, R. (Dec. 1996). Estimation of self-motion by optic flow processing in single visual interneurons. eng. Nature *384*.6608, 463–466. ISSN: 0028-0836. DOI: 10.1038/384463a0.

Krashes, Michael J. et al. (Oct. 2009). A Neural Circuit Mechanism Integrating Motivational State with Memory Expression in Drosophila. en. Cell *139*.2, 416–427. ISSN: 00928674. DOI: 10.1016/j.cell.2009.08.035. URL: https://linkinghub.elsevier.com/retrieve/pii/S0092867409011052 (visited on 05/21/2022).

Kroll, Noam (May 2014). *5 Reasons Your Day For Night Footage Doesn't Look Right*. Blog. URL: https://www.premiumbeat.com/blog/5-reasons-day-for-night-footage-doesnt-look-right/ (visited on 05/30/2022).

Lai, Sen-Lin and Lee, Tzumin (May 2006). Genetic mosaic with dual binary transcriptional systems in Drosophila. eng. Nature Neuroscience *9*.5, 703–709. ISSN: 1097-6256. DOI: 10.1038/nn1681.

Laughlin, S. B. (Oct. 1981). A Simple Coding Procedure Enhances a Neuron's Information Capacity. en. Zeitschrift für Naturforschung C *36*.9-10, 910–912. ISSN: 1865-7125, 0939-5075. DOI: 10.1515/znc-1981-9-1040. URL: https://www.degruyter.com/document/doi/10.1515/znc-1981-9-1040/html (visited on 05/19/2022).

– (1989). THE ROLE OF SENSORY ADAPTATION IN THE RETINA. en. Journal of Experimental Biology *146*, 39–62.

Laughlin, S. B. and Hardie, Roger C. (Dec. 1978). Common strategies for light adaptation in the peripheral visual systems of fly and dragonfly. en. Journal of comparative physiology *128*.4, 319–340. ISSN: 1432-1351. DOI: 10.1007/BF00657606. URL: https://doi.org/10.1007/BF00657606 (visited on 04/22/2022).

Laughlin, S. B., Howard, J, and Blakeslee, Barbara (Sept. 1987). Synaptic limitations to contrast coding in the retina of the blowfly Calliphora. EN. Proceedings of the Royal Society of London. Series B. Biological Sciences. DOI: 10.1098/rspb.1987.0054. URL: https://royalsocietypublishing.org/doi/epdf/10.1098/rspb.1987.0054 (visited on 04/25/2022).

Laughlin, S. B. and Osorio, Daniel (1989). Mechanisms for neural signal enhancement in the blowfly compound eye. en. Journal of Experimental Biology *144*.1, 113–146.

Lee, Barry B. et al. (Dec. 1990). Luminance and chromatic modulation sensitivity of macaque ganglion cells and human observers. en. Journal of the Optical Society of

America A *7*.12, 2223. ISSN: 1084-7529, 1520-8532. DOI: 10.1364/JOSAA.7.002223. URL: https://opg.optica.org/abstract.cfm?URI=josaa-7-12-2223 (visited on 05/19/2022).

Lee, Pei-Tseng et al. (Mar. 2018). A gene-specific T2A-GAL4 library for Drosophila. eLife *7*. Ed. by K VijayRaghavan, e35574. ISSN: 2050-084X. DOI: 10.7554/eLife.35574. URL: https://doi.org/10.7554/eLife.35574 (visited on 05/07/2022).

Lee, Wei-Chung Allen et al. (Apr. 2016). Anatomy and function of an excitatory network in the visual cortex. en. Nature *532*.7599, 370–374. ISSN: 1476-4687. DOI: 10.1038/nature17192. URL: https://www.nature.com/articles/nature17192 (visited on 05/06/2022).

Leonhardt, Aljoscha et al. (May 2016). Asymmetry of Drosophila ON and OFF motion detectors enhances real-world velocity estimation. en. Nature Neuroscience *19*.5, 706–715. ISSN: 1546-1726. DOI: 10.1038/nn.4262. URL: https://www.nature.com/articles/nn.4262 (visited on 05/12/2022).

Lessing, Derek and Bonini, Nancy M. (June 2009). Maintaining the brain: insight into human neurodegeneration from Drosophila melanogaster mutants. eng. Nature Reviews. Genetics *10*.6, 359–370. ISSN: 1471-0064. DOI: 10.1038/nrg2563.

Li, Hongjie et al. (Nov. 2017). Classifying Drosophila Olfactory Projection Neuron Subtypes by Single-Cell RNA Sequencing. eng. Cell *171*.5, 1206–1220.e22. ISSN: 1097-4172. DOI: 10.1016/j.cell.2017.10.019.

Lin, Chun-Chieh and Potter, Christopher J (Aug. 2016a). Editing Transgenic DNA Components by Inducible Gene Replacement in *Drosophila melanogaster*. en. Genetics *203*.4, 1613–1628. ISSN: 1943-2631. DOI: 10.1534/genetics.116.191783. URL: https://academic.oup.com/genetics/article/203/4/1613/6065842 (visited on 05/07/2022).

Lin, John Y. et al. (Oct. 2013). ReaChR: a red-shifted variant of channelrhodopsin enables deep transcranial optogenetic excitation. en. Nature Neuroscience *16*.10, 1499–1508. ISSN: 1546-1726. DOI: 10.1038/nn.3502. URL: https://www.nature.com/articles/nn.3502 (visited on 05/06/2022).

Lin, Michael Z. and Schnitzer, Mark J. (Sept. 2016b). Genetically encoded indicators of neuronal activity. en. Nature Neuroscience *19*.9, 1142–1153. ISSN: 1546-1726. DOI: 10.1038/nn.4359. URL: https://www.nature.com/articles/nn.4359 (visited on 05/06/2022).

Littleton, J.Troy and Ganetzky, Barry (Apr. 2000). Ion Channels and Synaptic Organization. en. Neuron *26*.1, 35–43. ISSN: 08966273. DOI: 10.1016/S0896-6273(00)81135-6. URL: https://linkinghub.elsevier.com/retrieve/pii/S0896627300811356 (visited on 05/16/2022).

Liu, Che-Hsiung et al. (Sept. 2008). Ca2+-dependent metarhodopsin inactivation mediated by calmodulin and NINAC myosin III. eng. Neuron *59*.5, 778–789. ISSN: 1097-4199. DOI: 10.1016/j.neuron.2008.07.007.

Llinás, Rodolfo Riascos (2002). *I of the vortex: from neurons to self*. eng. 1. paperback ed. A Bradford book. Cambridge, Mass. London: MIT Press. ISBN: 9780262621632 9780262122337.

Llinás, Rodolfo Riascos and Ribary, U (Mar. 1993). Coherent 40-Hz oscillation characterizes dream state in humans. en. Proceedings of the National Academy of Sciences *90*.5, 2078–2081. ISSN: 0027-8424, 1091-6490. DOI: 10.1073/pnas.90.5.2078. URL: https://pnas.org/doi/full/10.1073/pnas.90.5.2078 (visited on 05/04/2022).

Lopez, Ramos Traslosheros and Giordano, Luis (Dec. 2020). Receptive field organization of motion computation in the fly: a study of cell types and their variability. eng. DOI: 10.53846/goediss-8344. URL: https://ediss.uni-goettingen.de/handle/21.11130/00-1735-0000-0005-1507-C (visited on 05/26/2022).

Luan, Haojiang et al. (Nov. 2006). Refined spatial manipulation of neuronal function by combinatorial restriction of transgene expression. eng. Neuron *52*.3, 425–436. ISSN: 0896-6273. DOI: 10.1016/j.neuron.2006.08.028.

Luo, Liqun (Sept. 2021). Architectures of neuronal circuits. en. Science *373*.6559, eabg7285. ISSN: 0036-8075, 1095-9203. DOI: 10.1126/science.abg7285. URL: https://www.science.org/doi/10.1126/science.abg7285 (visited on 05/06/2022).

MacEvoy, Sean P. and Paradiso, Michael A. (July 2001). Lightness constancy in primary visual cortex. en. Proceedings of the National Academy of Sciences *98*.15, 8827–8831. ISSN: 0027-8424, 1091-6490. DOI: 10.1073/pnas.161280398. URL: https://pnas.org/doi/full/10.1073/pnas.161280398 (visited on 04/22/2022).

Macpherson, Lindsey J. et al. (Dec. 2015). Dynamic labelling of neural connections in multiple colours by trans-synaptic fluorescence complementation. en. Nature Communications *6*.1, 10024. ISSN: 2041-1723. DOI: 10.1038/ncomms10024. URL: http://www.nature.com/articles/ncomms10024 (visited on 05/24/2022).

Madabattula, Surya T. et al. (June 2015). Quantitative Analysis of Climbing Defects in a Drosophila Model of Neurodegenerative Disorders. en. Journal of Visualized Experiments 100, 52741. ISSN: 1940-087X. DOI: 10.3791/52741. URL: http://www.jove.com/video/52741/quantitative-analysis-climbing-defects-drosophila-model (visited on 05/22/2022).

Maisak, Matthew S. et al. (Aug. 2013). A directional tuning map of Drosophila elementary motion detectors. en. Nature *500*.7461, 212–216. ISSN: 0028-0836, 1476-4687. DOI: 10.1038/nature12320. URL: http://www.nature.com/articles/nature12320 (visited on 05/19/2022).

Mante, Valerio et al. (Dec. 2005). Independence of luminance and contrast in natural scenes and in the early visual system. en. Nature Neuroscience *8*.12, 1690–1697. ISSN: 1097-6256, 1546-1726. DOI: 10.1038/nn1556. URL: http://www.nature.com/articles/nn1556 (visited on 04/19/2022).

Marder, Eve and Goaillard, Jean-Marc (July 2006). Variability, compensation and homeostasis in neuron and network function. en. Nature Reviews Neuroscience *7*.7, 563–574. ISSN: 1471-003X, 1471-0048. DOI: 10.1038/nrn1949. URL: http://www.nature.com/articles/nrn1949 (visited on 07/25/2019).

Marr, David (1982). *Vision: A computational investigation into the human representation and processing of visual information.* San Francisco: Freeman & Co.

Marr, Elizabeth and Potter, Christopher J. (Dec. 2021). Base Editing of Somatic Cells Using CRISPR–Cas9 in Drosophila. The CRISPR Journal *4*.6, 836–845. ISSN: 2573-1599. DOI: 10.1089/crispr.2021.0062. URL: https://www.liebertpub.com/doi/abs/10.1089/crispr.2021.0062 (visited on 05/07/2022).

Marvin, Jonathan S. et al. (Nov. 2018). Stability, affinity, and chromatic variants of the glutamate sensor iGluSnFR. en. Nature Methods *15*.11, 936–939. ISSN: 1548-7105. DOI: 10.1038/s41592-018-0171-3. URL: https://www.nature.com/articles/s41592-018-0171-3 (visited on 05/26/2022).

Masland, Richard H. (Jan. 2012). The tasks of amacrine cells. en. Visual Neuroscience *29*.1, 3–9. ISSN: 0952-5238, 1469-8714. DOI: 10.1017/S0952523811000344. URL: https://www.cambridge.org/core/product/identifier/S0952523811000344/type/journal_article (visited on 05/09/2022).

Masse, Nicolas Y., Turner, Glenn C., and Jefferis, Gregory S.X.E. (Aug. 2009). Olfactory Information Processing in Drosophila. en. Current Biology *19*.16, R700–R713. ISSN: 09609822. DOI: 10.1016/j.cub.2009.06.026. URL: https://linkinghub.elsevier.com/retrieve/pii/S0960982209013013 (visited on 05/22/2022).

Matulis, Catherine A. et al. (Jan. 2020). Heterogeneous Temporal Contrast Adaptation in Drosophila Direction-Selective Circuits. en. Current Biology *30*.2, 222–236.e6. ISSN:

09609822. DOI: 10.1016/j.cub.2019.11.077. URL: https://linkinghub.elsevier.com/retrieve/pii/S0960982219315799 (visited on 05/14/2022).

McCulloch, Warren S. and Pitts, Walter (Dec. 1943). A logical calculus of the ideas immanent in nervous activity. en. The bulletin of mathematical biophysics *5*.4, 115–133. ISSN: 1522-9602. DOI: 10.1007/BF02478259. URL: https://doi.org/10.1007/BF02478259 (visited on 05/04/2022).

McKemy, David D., Neuhausser, Werner M., and Julius, David (Mar. 2002). Identification of a cold receptor reveals a general role for TRP channels in thermosensation. en. Nature *416*.6876, 52–58. ISSN: 1476-4687. DOI: 10.1038/nature719. URL: https://www.nature.com/articles/nature719 (visited on 05/21/2022).

McNaughton, Bruce L., O'Keefe, John, and Barnes, Carol A. (Aug. 1983). The stereotrode: A new technique for simultaneous isolation of several single units in the central nervous system from multiple unit records. en. Journal of Neuroscience Methods *8*.4, 391–397. ISSN: 0165-0270. DOI: 10.1016/0165-0270(83)90097-3. URL: https://www.sciencedirect.com/science/article/pii/0165027083900973 (visited on 05/04/2022).

Meier, Matthias and Borst, Alexander (May 2019). Extreme Compartmentalization in a Drosophila Amacrine Cell. en. Current Biology *29*.9, 1545–1550.e2. ISSN: 09609822. DOI: 10.1016/j.cub.2019.03.070. URL: https://linkinghub.elsevier.com/retrieve/pii/S0960982219303987 (visited on 05/06/2022).

Meinertzhagen, I. A. and Sorra, K. E. (2001). Synaptic organization in the fly's optic lamina: few cells, many synapses and divergent microcircuits. eng. Progress in Brain Research *131*, 53–69. ISSN: 0079-6123. DOI: 10.1016/s0079-6123(01)31007-5.

Meister, M., Pine, J., and Baylor, D. A. (Jan. 1994). Multi-neuronal signals from the retina: acquisition and analysis. eng. Journal of Neuroscience Methods *51*.1, 95–106. ISSN: 0165-0270. DOI: 10.1016/0165-0270(94)90030-2.

Mimura, K. (Feb. 1976). Some spatial properties in the first optic ganglion of the fly. en. Journal of Comparative Physiology ? A *105*.1, 65–82. ISSN: 0340-7594, 1432-1351. DOI: 10.1007/BF01380054. URL: http://link.springer.com/10.1007/BF01380054 (visited on 05/15/2022).

Min, Soohong et al. (Feb. 2021). Control of feeding by Piezo-mediated gut mechanosensation in Drosophila. eLife *10*. Ed. by Claude Desplan and Piali Sengupta, e63049. ISSN: 2050-084X. DOI: 10.7554/eLife.63049. URL: https://doi.org/10.7554/eLife.63049 (visited on 05/19/2022).

Mo, Alisa et al. (June 2015). Epigenomic Signatures of Neuronal Diversity in the Mammalian Brain. eng. Neuron *86*.6, 1369–1384. ISSN: 1097-4199. DOI: 10.1016/j.neuron.2015.05.018.

Molina-Obando, Sebastian et al. (Sept. 2019). ON selectivity in the Drosophila visual system is a multisynaptic process involving both glutamatergic and GABAergic inhibition. eLife *8*. Ed. by Claude Desplan et al., e49373. ISSN: 2050-084X. DOI: 10.7554/eLife.49373. URL: https://doi.org/10.7554/eLife.49373 (visited on 05/06/2022).

Nagarkar-Jaiswal, Sonal et al. (Mar. 2015). A library of MiMICs allows tagging of genes and reversible, spatial and temporal knockdown of proteins in Drosophila. en. eLife *4*, e05338. ISSN: 2050-084X. DOI: 10.7554/eLife.05338. URL: https://elifesciences.org/articles/05338 (visited on 07/25/2019).

Nagy, A. (Feb. 2000). Cre recombinase: the universal reagent for genome tailoring. eng. Genesis (New York, N.Y.: 2000) *26*.2, 99–109. ISSN: 1526-954X.

Nässel, Dick R. (Mar. 2018). Substrates for Neuronal Cotransmission With Neuropeptides and Small Molecule Neurotransmitters in Drosophila. Frontiers in Cellular Neuroscience *12*, 83. ISSN: 1662-5102. DOI: 10.3389/fncel.2018.00083. URL: https://www.ncbi.nlm.nih.gov/pmc/articles/PMC5885757/ (visited on 05/19/2022).

Nern, Aljoscha, Pfeiffer, Barret D., and Rubin, Gerald M. (June 2015). Optimized tools for multicolor stochastic labeling reveal diverse stereotyped cell arrangements in the fly visual system. en. Proceedings of the National Academy of Sciences *112*.22. ISSN: 0027-8424, 1091-6490. DOI: 10.1073/pnas.1506763112. URL: https://pnas.org/doi/full/10.1073/pnas.1506763112 (visited on 05/06/2022).

Nicolaï, Laura J. J. et al. (Nov. 2010). Genetically encoded dendritic marker sheds light on neuronal connectivity in *Drosophila*. en. Proceedings of the National Academy of Sciences *107*.47, 20553–20558. ISSN: 0027-8424, 1091-6490. DOI: 10.1073/pnas.1010198107. URL: https://pnas.org/doi/full/10.1073/pnas.1010198107 (visited on 05/16/2022).

Nicoll, Roger A. and Malenka, Robert C. (July 1998). A Tale of Two Transmitters. en. Science *281*.5375, 360–361. ISSN: 0036-8075, 1095-9203. DOI: 10.1126/science.281.5375.360. URL: https://www.science.org/doi/10.1126/science.281.5375.360 (visited on 05/16/2022).

Normann, R. A. and Perlman, I. (Jan. 1979). The effects of background illumination on the photoresponses of red and green cones. eng. The Journal of Physiology *286*, 491–507. ISSN: 0022-3751. DOI: 10.1113/jphysiol.1979.sp012633.

Normann, Richard A. and Werblin, Frank S. (Jan. 1974). Control of Retinal Sensitivity. en. Journal of General Physiology *63*.1, 37–61. ISSN: 1540-7748, 0022-1295. DOI: 10.1085/jgp.63.1.37. URL: https://rupress.org/jgp/article/63/1/37/31217/Control-of-Retinal-Sensitivity-I-Light-and-Dark (visited on 04/19/2022).

O'Kane, Cahir J. (2011). "Drosophila as a Model Organism for the Study of Neuropsychiatric Disorders". en. *Molecular and Functional Models in Neuropsychiatry*. Ed. by Jim J. Hagan. Berlin, Heidelberg: Springer, pp. 37–60. ISBN: 9783642197031. DOI: 10.1007/7854_2010_110. URL: https://doi.org/10.1007/7854_2010_110 (visited on 05/07/2022).

Odermatt, Benjamin, Nikolaev, Anton, and Lagnado, Leon (Feb. 2012). Encoding of Luminance and Contrast by Linear and Nonlinear Synapses in the Retina. en. Neuron *73*.4, 758–773. ISSN: 08966273. DOI: 10.1016/j.neuron.2011.12.023. URL: https://linkinghub.elsevier.com/retrieve/pii/S0896627312000475 (visited on 05/14/2022).

Oesch, Nicholas W. and Diamond, Jeffrey S. (Dec. 2011). Ribbon synapses compute temporal contrast and encode luminance in retinal rod bipolar cells. en. Nature Neuroscience *14*.12, 1555–1561. ISSN: 1546-1726. DOI: 10.1038/nn.2945. URL: https://www.nature.com/articles/nn.2945 (visited on 05/11/2022).

Olsen, Shawn R. and Wilson, Rachel I. (Oct. 2008a). Cracking neural circuits in a tiny brain: new approaches for understanding the neural circuitry of Drosophila. en. Trends in Neurosciences *31*.10, 512–520. ISSN: 0166-2236. DOI: 10.1016/j.tins.2008.07.006. URL: https://www.sciencedirect.com/science/article/pii/S0166223608001823 (visited on 05/07/2022).

– (Apr. 2008b). Lateral presynaptic inhibition mediates gain control in an olfactory circuit. en. Nature *452*.7190, 956–960. ISSN: 1476-4687. DOI: 10.1038/nature06864. URL: https://www.nature.com/articles/nature06864 (visited on 05/15/2022).

Otchy, Timothy M. et al. (Dec. 2015). Acute off-target effects of neural circuit manipulations. en. Nature *528*.7582, 358–363. ISSN: 1476-4687. DOI: 10.1038/nature16442. URL: https://www.nature.com/articles/nature16442 (visited on 05/06/2022).

Owald, David, Lin, Suewei, and Waddell, Scott (Sept. 2015). Light, heat, action: neural control of fruit fly behaviour. Philosophical Transactions of the Royal Society B: Biological Sciences *370*.1677, 20140211. ISSN: 0962-8436. DOI: 10.1098/rstb.2014.0211. URL: https://www.ncbi.nlm.nih.gov/pmc/articles/PMC4528823/ (visited on 05/07/2022).

Pankova, Katarina and Borst, Alexander (Sept. 2016). RNA-Seq Transcriptome Analysis of Direction-Selective T4/T5 Neurons in Drosophila. en. PLOS ONE *11*.9, e0163986. ISSN: 1932-6203. DOI: 10.1371/journal.pone.0163986. URL: https://journals.plos.org/plosone/article?id=10.1371/journal.pone.0163986 (visited on 05/06/2022).

Pauli, Andrea et al. (Feb. 2008). Cell-Type-Specific TEV Protease Cleavage Reveals Cohesin Functions in Drosophila Neurons. en. Developmental Cell *14*.2, 239–251. ISSN: 15345807. DOI: 10.1016/j.devcel.2007.12.009. URL: https://linkinghub.elsevier.com/retrieve/pii/S1534580707004868 (visited on 05/28/2022).

Peabody, Nathan C. et al. (Mar. 2009). Characterization of the Decision Network for Wing Expansion in Drosophila Using Targeted Expression of the TRPM8 Channel. en. Journal of Neuroscience *29*.11, 3343–3353. ISSN: 0270-6474, 1529-2401. DOI: 10.1523/JNEUROSCI.4241-08.2009. URL: https://www.jneurosci.org/content/29/11/3343 (visited on 05/21/2022).

Peng, Jing et al. (Mar. 2018). Drosophila Fezf coordinates laminar-specific connectivity through cell-intrinsic and cell-extrinsic mechanisms. eLife *7*. Ed. by Liqun Luo, e33962. ISSN: 2050-084X. DOI: 10.7554/eLife.33962. URL: https://doi.org/10.7554/eLife.33962 (visited on 05/18/2022).

Peron, Simon, Chen, Tsai-Wen, and Svoboda, Karel (June 2015). Comprehensive imaging of cortical networks. en. Current Opinion in Neurobiology. Large-Scale Recording Technology (32) *32*, 115–123. ISSN: 0959-4388. DOI: 10.1016/j.conb.2015.03.016. URL: https://www.sciencedirect.com/science/article/pii/S0959438815000719 (visited on 05/06/2022).

Pfeiffer, Barret D et al. (Oct. 2010). Refinement of Tools for Targeted Gene Expression in Drosophila. en. Genetics *186*.2, 735–755. ISSN: 1943-2631. DOI: 10.1534/genetics.110.119917. URL: https://academic.oup.com/genetics/article/186/2/735/6063613 (visited on 05/05/2022).

Pfeiffer, Barret D., Truman, James W., and Rubin, Gerald M. (Apr. 2012). Using translational enhancers to increase transgene expression in *Drosophila*. en. Proceedings of the National Academy of Sciences *109*.17, 6626–6631. ISSN: 0027-8424, 1091-6490. DOI: 10.1073/pnas.1204520109. URL: https://pnas.org/doi/full/10.1073/pnas.1204520109 (visited on 05/07/2022).

Poggio, Tomaso et al. (Oct. 2017). Why and when can deep-but not shallow-networks avoid the curse of dimensionality: A review. en. International Journal of Automation and Computing *14*.5, 503–519. ISSN: 1476-8186, 1751-8520. DOI: 10.1007/s11633-017-1054-2. URL: http://link.springer.com/10.1007/s11633-017-1054-2 (visited on 05/29/2022).

Politi, Yoav et al. (May 2014). Paternal Mitochondrial Destruction after Fertilization Is Mediated by a Common Endocytic and Autophagic Pathway in Drosophila. en. Developmental Cell *29*.3, 305–320. ISSN: 15345807. DOI: 10.1016/j.devcel.2014.04.005. URL: https://linkinghub.elsevier.com/retrieve/pii/S1534580714002044 (visited on 05/28/2022).

Potter, Christopher J. et al. (Apr. 2010). The Q system: a repressible binary system for transgene expression, lineage tracing, and mosaic analysis. eng. Cell *141*.3, 536–548. ISSN: 1097-4172. DOI: 10.1016/j.cell.2010.02.025.

Pugh, E. N., Nikonov, S, and Lamb, T. D. (Aug. 1999). Molecular mechanisms of vertebrate photoreceptor light adaptation. en. Current Opinion in Neurobiology *9*.4, 410–418. ISSN: 0959-4388. DOI: 10.1016/S0959-4388(99)80062-2. URL: https://www.sciencedirect.com/science/article/pii/S0959438899800622 (visited on 05/11/2022).

Purpura, Keith et al. (Jan. 1990). Light adaptation in the primate retina: Analysis of changes in gain and dynamics of monkey retinal ganglion cells. en. Visual Neuroscience

4.1, 75–93. ISSN: 0952-5238, 1469-8714. DOI: 10.1017/S0952523800002789. URL: https://www.cambridge.org/core/product/identifier/S0952523800002789/type/journal_article (visited on 05/19/2022).

Ramón y Cajal, Santiago (1888). Estructura de los centros nerviosos de las aves. Rev. Trim. Histol. Norm. Patol. 1, 1–10.

Ramos-Traslosheros, Giordano, Henning, Miriam, and Silies, Marion (May 2018). Motion detection: cells, circuits and algorithms. Neuroforum *24*.2, A61–A72. ISSN: 2363-7013. DOI: 10.1515/nf-2017-A028. URL: https://www.degruyter.com/document/doi/10.1515/nf-2017-A028/html (visited on 05/10/2022).

Ramos-Traslosheros, Giordano and Silies, Marion (Aug. 2021). The physiological basis for contrast opponency in motion computation in Drosophila. en. Nature Communications *12*.1, 4987. ISSN: 2041-1723. DOI: 10.1038/s41467-021-24986-w. URL: https://www.nature.com/articles/s41467-021-24986-w (visited on 05/14/2022).

Ratliff, Charles P. et al. (Oct. 2010). Retina is structured to process an excess of darkness in natural scenes. en. Proceedings of the National Academy of Sciences *107*.40, 17368–17373. ISSN: 0027-8424, 1091-6490. DOI: 10.1073/pnas.1005846107. URL: https://pnas.org/doi/full/10.1073/pnas.1005846107 (visited on 05/24/2022).

Ravi, Sneha et al. (Nov. 2018). Pathway-Specific Asymmetries between ON and OFF Visual Signals. en. Journal of Neuroscience *38*.45, 9728–9740. ISSN: 0270-6474, 1529-2401. DOI: 10.1523/JNEUROSCI.2008-18.2018. URL: https://www.jneurosci.org/content/38/45/9728 (visited on 05/12/2022).

Reichardt, Werner, Poggio, Tomaso, and Hausen, Klaus (Jan. 1983). Figure-ground discrimination by relative movement in the visual system of the fly. en. Biological Cybernetics *46*.1, 1–30. ISSN: 1432-0770. DOI: 10.1007/BF00595226. URL: https://doi.org/10.1007/BF00595226 (visited on 05/15/2022).

Reiff, Dierk F et al. (Aug. 2010). Visualizing retinotopic half-wave rectified input to the motion detection circuitry of Drosophila. en. Nature Neuroscience *13*.8, 973–978. ISSN: 1097-6256, 1546-1726. DOI: 10.1038/nn.2595. URL: http://www.nature.com/articles/nn.2595 (visited on 05/11/2022).

Rieger, Dirk et al. (Oct. 2007). The Fruit Fly *Drosophila melanogaster* Favors Dim Light and Times Its Activity Peaks to Early Dawn and Late Dusk. en. Journal of Biological Rhythms *22*.5, 387–399. ISSN: 0748-7304, 1552-4531. DOI: 10.1177/0748730407306198. URL: http://journals.sagepub.com/doi/10.1177/0748730407306198 (visited on 05/10/2022).

Rieke, Fred and Rudd, Michael E. (Dec. 2009). The Challenges Natural Images Pose for Visual Adaptation. en. Neuron *64*.5, 605–616. ISSN: 0896-6273. DOI: 10.1016/j.neuron.2009.11.028. URL: https://www.sciencedirect.com/science/article/pii/S0896627309009441 (visited on 04/20/2022).

Rivera-Alba, Marta et al. (Dec. 2011). Wiring economy and volume exclusion determine neuronal placement in the Drosophila brain. Current biology : CB *21*.23, 2000–2005. ISSN: 0960-9822. DOI: 10.1016/j.cub.2011.10.022. URL: https://www.ncbi.nlm.nih.gov/pmc/articles/PMC3244492/ (visited on 05/10/2022).

Rohwedder, Astrid et al. (Mar. 2016). Four Individually Identified Paired Dopamine Neurons Signal Reward in Larval Drosophila. en. Current Biology *26*.5, 661–669. ISSN: 0960-9822. DOI: 10.1016/j.cub.2016.01.012. URL: https://www.sciencedirect.com/science/article/pii/S0960982216000622 (visited on 05/19/2022).

Rowitch, D. H. et al. (Oct. 1999). Sonic hedgehog regulates proliferation and inhibits differentiation of CNS precursor cells. eng. The Journal of Neuroscience: The Official Journal of the Society for Neuroscience *19*.20, 8954–8965. ISSN: 1529-2401.

Ruderman, Daniel L. and Bialek, William (Aug. 1994). Statistics of natural images: Scaling in the woods. en. Physical Review Letters *73*.6, 814–817. ISSN: 0031-9007. DOI: 10.

1103/PhysRevLett.73.814. URL: https://link.aps.org/doi/10.1103/PhysRevLett.73.814 (visited on 05/12/2022).

Rusanen, Juha and Weckström, Matti (Apr. 2016). Frequency-selective transmission of graded signals in large monopolar neurons of blowfly Calliphora vicina compound eye. eng. Journal of Neurophysiology *115*.4, 2052–2064. ISSN: 1522-1598. DOI: 10.1152/jn.00747.2015.

Sanchez, Mateo I and Ting, Alice Y (Feb. 2020). Directed evolution improves the catalytic efficiency of TEV protease. Nature methods *17*.2, 167–174. ISSN: 1548-7091. DOI: 10.1038/s41592-019-0665-7. URL: https://www.ncbi.nlm.nih.gov/pmc/articles/PMC7004888/ (visited on 05/19/2022).

Sanes, Joshua R. and Zipursky, S. Lawrence (Apr. 2010). Design principles of insect and vertebrate visual systems. eng. Neuron *66*.1, 15–36. ISSN: 1097-4199. DOI: 10.1016/j.neuron.2010.01.018.

– (June 2020). Synaptic Specificity, Recognition Molecules, and Assembly of Neural Circuits. en. Cell *181*.6, 1434–1435. ISSN: 0092-8674. DOI: 10.1016/j.cell.2020.05.046. URL: https://www.sciencedirect.com/science/article/pii/S0092867420306796 (visited on 05/07/2022).

Santiago, Ivan J. et al. (Mar. 2021). *Drosophila* Fezf functions as a transcriptional repressor to direct layer-specific synaptic connectivity in the fly visual system. en. Proceedings of the National Academy of Sciences *118*.13, e2025530118. ISSN: 0027-8424, 1091-6490. DOI: 10.1073/pnas.2025530118. URL: https://pnas.org/doi/full/10.1073/pnas.2025530118 (visited on 05/19/2022).

Scheffer, Louis K et al. (Sept. 2020). A connectome and analysis of the adult Drosophila central brain. eLife *9*. Ed. by Eve Marder et al., e57443. ISSN: 2050-084X. DOI: 10.7554/eLife.57443. URL: https://doi.org/10.7554/eLife.57443 (visited on 05/06/2022).

Schiller, P. H., Sandell, J. H., and Maunsell, J. H. (Sept. 1986). Functions of the ON and OFF channels of the visual system. eng. Nature *322*.6082, 824–825. ISSN: 0028-0836. DOI: 10.1038/322824a0.

Schlegel, Philipp, Costa, Marta, and Jefferis, Gregory SXE (Dec. 2017). Learning from connectomics on the fly. en. Current Opinion in Insect Science. Neuroscience * Pheromones *24*, 96–105. ISSN: 2214-5745. DOI: 10.1016/j.cois.2017.09.011. URL: https://www.sciencedirect.com/science/article/pii/S2214574517301578 (visited on 05/06/2022).

Schnapf, J L et al. (Aug. 1990). Visual transduction in cones of the monkey Macaca fascicularis. The Journal of Physiology *427*, 681–713. ISSN: 0022-3751. URL: https://www.ncbi.nlm.nih.gov/pmc/articles/PMC1189952/ (visited on 05/09/2022).

Scott, Ethan K. et al. (Apr. 2007). Targeting neural circuitry in zebrafish using GAL4 enhancer trapping. en. Nature Methods *4*.4, 323–326. ISSN: 1548-7105. DOI: 10.1038/nmeth1033. URL: https://www.nature.com/articles/nmeth1033 (visited on 05/05/2022).

Seeholzer, Laura F. et al. (July 2018). Evolution of a central neural circuit underlies Drosophila mate preferences. en. Nature *559*.7715, 564–569. ISSN: 1476-4687. DOI: 10.1038/s41586-018-0322-9. URL: https://www.nature.com/articles/s41586-018-0322-9 (visited on 05/30/2022).

Serbe, Etienne et al. (Feb. 2016). Comprehensive Characterization of the Major Presynaptic Elements to the Drosophila OFF Motion Detector. en. Neuron *89*.4, 829–841. ISSN: 08966273. DOI: 10.1016/j.neuron.2016.01.006. URL: https://linkinghub.elsevier.com/retrieve/pii/S0896627316000076 (visited on 07/25/2019).

Shapley, Robert and Enroth-Cugell, Christina (Jan. 1984). Chapter 9 Visual adaptation and retinal gain controls. en. Progress in Retinal Research *3*, 263–346. ISSN: 0278-4327. DOI: 10.1016/0278-4327(84)90011-7. URL: https://www.sciencedirect.com/science/article/pii/0278432784900117 (visited on 04/19/2022).

Shekhar, Karthik et al. (Aug. 2016). Comprehensive Classification of Retinal Bipolar Neurons by Single-Cell Transcriptomics. eng. Cell *166*.5, 1308–1323.e30. ISSN: 1097-4172. DOI: 10.1016/j.cell.2016.07.054.

Shinomiya, Kazunori et al. (Jan. 2019a). Comparisons between the ON- and OFF-edge motion pathways in the Drosophila brain. eLife *8*. Ed. by Alexander Borst and K VijayRaghavan, e40025. ISSN: 2050-084X. DOI: 10.7554/eLife.40025. URL: https://doi.org/10.7554/eLife.40025 (visited on 05/06/2022).

Shinomiya, Kazunori et al. (2019b). The Organization of the Second Optic Chiasm of the Drosophila Optic Lobe. Frontiers in Neural Circuits *13*. ISSN: 1662-5110. URL: https://www.frontiersin.org/article/10.3389/fncir.2019.00065 (visited on 05/27/2022).

Silies, Marion et al. (July 2013). Modular Use of Peripheral Input Channels Tunes Motion-Detecting Circuitry. en. Neuron *79*.1, 111–127. ISSN: 08966273. DOI: 10.1016/j.neuron.2013.04.029. URL: https://linkinghub.elsevier.com/retrieve/pii/S0896627313003607 (visited on 05/11/2022).

Spitschan, Manuel et al. (June 2016). Variation of outdoor illumination as a function of solar elevation and light pollution. en. Scientific Reports *6*.1, 26756. ISSN: 2045-2322. DOI: 10.1038/srep26756. URL: https://www.nature.com/articles/srep26756 (visited on 04/25/2022).

Srinivasan, M. V., Laughlin, S. B., and Dubs, A. (Nov. 1982). Predictive coding: a fresh view of inhibition in the retina. eng. Proceedings of the Royal Society of London. Series B, Biological Sciences *216*.1205, 427–459. ISSN: 0950-1193. DOI: 10.1098/rspb.1982.0085.

St. Pierre, Susan E. et al. (Jan. 2014). FlyBase 102—advanced approaches to interrogating FlyBase. en. Nucleic Acids Research *42*.D1, D780–D788. ISSN: 0305-1048, 1362-4962. DOI: 10.1093/nar/gkt1092. URL: https://academic.oup.com/nar/article-lookup/doi/10.1093/nar/gkt1092 (visited on 05/16/2022).

Sternson, Scott M. and Roth, Bryan L. (2014). Chemogenetic tools to interrogate brain functions. eng. Annual Review of Neuroscience *37*, 387–407. ISSN: 1545-4126. DOI: 10.1146/annurev-neuro-071013-014048.

Stöckl, Anna L., Ribi, Willi A., and Warrant, Eric J. (Jan. 2016). Adaptations for nocturnal and diurnal vision in the hawkmoth lamina: Visual Adaptations in the Hawkmoth Lamina. en. Journal of Comparative Neurology *524*.1, 160–175. ISSN: 00219967. DOI: 10.1002/cne.23832. URL: http://doi.wiley.com/10.1002/cne.23832 (visited on 07/25/2019).

Strother, James A., Nern, Aljoscha, and Reiser, Michael B. (May 2014). Direct Observation of ON and OFF Pathways in the Drosophila Visual System. en. Current Biology *24*.9, 976–983. ISSN: 09609822. DOI: 10.1016/j.cub.2014.03.017. URL: https://linkinghub.elsevier.com/retrieve/pii/S0960982214002760 (visited on 07/25/2019).

Svensson, Erik et al. (2019). General Principles of Neuronal Co-transmission: Insights From Multiple Model Systems. Frontiers in Neural Circuits *12*. ISSN: 1662-5110. URL: https://www.frontiersin.org/article/10.3389/fncir.2018.00117 (visited on 05/16/2022).

Takagi, Suguru et al. (Dec. 2017). Divergent Connectivity of Homologous Command-like Neurons Mediates Segment-Specific Touch Responses in Drosophila. en. Neuron *96*.6, 1373–1387.e6. ISSN: 0896-6273. DOI: 10.1016/j.neuron.2017.10.030. URL: https://www.sciencedirect.com/science/article/pii/S089662731731022X (visited on 05/06/2022).

Takemura, Shin-ya et al. (Aug. 2013). A visual motion detection circuit suggested by Drosophila connectomics. en. Nature *500*.7461, 175–181. ISSN: 1476-4687. DOI: 10.1038/nature12450. URL: https://www.nature.com/articles/nature12450 (visited on 05/06/2022).

Takemura, Shin-ya et al. (Apr. 2017). The comprehensive connectome of a neural substrate for 'ON' motion detection in Drosophila. en. eLife *6*, e24394. ISSN: 2050-084X. DOI: 10.7554/eLife.24394. URL: https://elifesciences.org/articles/24394 (visited on 07/25/2019).

Talay, Mustafa et al. (Nov. 2017). Transsynaptic Mapping of Second-Order Taste Neurons in Flies by trans-Tango. en. Neuron *96*.4, 783–795.e4. ISSN: 08966273. DOI: 10.1016/j.neuron.2017.10.011. URL: https://linkinghub.elsevier.com/retrieve/pii/S0896627317309790 (visited on 04/08/2022).

Tammero, Lance F. and Dickinson, Michael H. (Feb. 2002). The influence of visual landscape on the free flight behavior of the fruit fly *Drosophila melanogaster*. en. Journal of Experimental Biology *205*.3, 327–343. ISSN: 1477-9145, 0022-0949. DOI: 10.1242/jeb.205.3.327. URL: https://journals.biologists.com/jeb/article/205/3/327/33097/The-influence-of-visual-landscape-on-the-free (visited on 05/25/2022).

Tan, Liming et al. (Dec. 2015). Ig Superfamily Ligand and Receptor Pairs Expressed in Synaptic Partners in Drosophila. Cell *163*.7, 1756–1769. ISSN: 0092-8674. DOI: 10.1016/j.cell.2015.11.021. URL: https://www.ncbi.nlm.nih.gov/pmc/articles/PMC4804707/ (visited on 05/18/2022).

Tasic, Bosiljka et al. (Feb. 2016). Adult mouse cortical cell taxonomy revealed by single cell transcriptomics. en. Nature Neuroscience *19*.2, 335–346. ISSN: 1546-1726. DOI: 10.1038/nn.4216. URL: https://www.nature.com/articles/nn.4216 (visited on 05/05/2022).

Taylor, WR and Smith, RG (Oct. 2011). Trigger features and excitation in the retina. Current opinion in neurobiology *21*.5, 672–678. ISSN: 0959-4388. DOI: 10.1016/j.conb.2011.07.001. URL: https://www.ncbi.nlm.nih.gov/pmc/articles/PMC3463620/ (visited on 05/16/2022).

Thoreson, Wallace B. and Mangel, Stuart C. (Sept. 2012). Lateral interactions in the outer retina. eng. Progress in Retinal and Eye Research *31*.5, 407–441. ISSN: 1873-1635. DOI: 10.1016/j.preteyeres.2012.04.003.

Tkačik, Gašper et al. (June 2011). Natural Images from the Birthplace of the Human Eye. en. PLOS ONE *6*.6, e20409. ISSN: 1932-6203. DOI: 10.1371/journal.pone.0020409. URL: https://journals.plos.org/plosone/article?id=10.1371/journal.pone.0020409 (visited on 05/31/2022).

Tran, Nicholas M. et al. (Dec. 2019). Single-Cell Profiles of Retinal Ganglion Cells Differing in Resilience to Injury Reveal Neuroprotective Genes. eng. Neuron *104*.6, 1039–1055.e12. ISSN: 1097-4199. DOI: 10.1016/j.neuron.2019.11.006.

Tsetsenis, T. et al. (Nov. 2014). Direct Visualization of Trans-Synaptic Neurexin-Neuroligin Interactions during Synapse Formation. en. Journal of Neuroscience *34*.45, 15083–15096. ISSN: 0270-6474, 1529-2401. DOI: 10.1523/JNEUROSCI.0348-14.2014. URL: https://www.jneurosci.org/lookup/doi/10.1523/JNEUROSCI.0348-14.2014 (visited on 05/18/2022).

Tuthill, John C. et al. (July 2013). Contributions of the 12 Neuron Classes in the Fly Lamina to Motion Vision. en. Neuron *79*.1, 128–140. ISSN: 08966273. DOI: 10.1016/j.neuron.2013.05.024. URL: https://linkinghub.elsevier.com/retrieve/pii/S0896627313004443 (visited on 05/15/2022).

Urban, Evelin et al. (Aug. 2014). The Cohesin Subunit Rad21 Is Required for Synaptonemal Complex Maintenance, but Not Sister Chromatid Cohesion, during Drosophila Female Meiosis. en. PLoS Genetics *10*.8. Ed. by R. Scott Hawley, e1004540. ISSN: 1553-7404. DOI: 10.1371/journal.pgen.1004540. URL: https://dx.plos.org/10.1371/journal.pgen.1004540 (visited on 05/28/2022).

Uusitalo, R. O., Juusola, M., and Weckström, M. (May 1995). Graded responses and spiking properties of identified first-order visual interneurons of the fly compound eye. eng.

Journal of Neurophysiology *73*.5, 1782–1792. ISSN: 0022-3077. DOI: 10.1152/jn.1995.73.5.1782.

Vaidya, Avinash R. et al. (Aug. 2019). Lesion Studies in Contemporary Neuroscience. en. Trends in Cognitive Sciences *23*.8, 653–671. ISSN: 1364-6613. DOI: 10.1016/j.tics.2019.05.009. URL: https://www.sciencedirect.com/science/article/pii/S1364661319301329 (visited on 05/06/2022).

Vaney, David I., Sivyer, Benjamin, and Taylor, W. Rowland (Mar. 2012). Direction selectivity in the retina: symmetry and asymmetry in structure and function. en. Nature Reviews Neuroscience *13*.3, 194–208. ISSN: 1471-0048. DOI: 10.1038/nrn3165. URL: https://www.nature.com/articles/nrn3165 (visited on 05/11/2022).

Venken, Koen J. T. and Bellen, Hugo J. (Mar. 2005). Emerging technologies for gene manipulation in Drosophila melanogaster. eng. Nature Reviews. Genetics *6*.3, 167–178. ISSN: 1471-0056. DOI: 10.1038/nrg1553.

Venken, Koen J. T., Simpson, Julie H., and Bellen, Hugo J. (Oct. 2011a). Genetic Manipulation of Genes and Cells in the Nervous System of the Fruit Fly. English. Neuron *72*.2, 202–230. ISSN: 0896-6273. DOI: 10.1016/j.neuron.2011.09.021. URL: https://www.cell.com/neuron/abstract/S0896-6273(11)00872-5 (visited on 05/07/2022).

Venken, Koen J. T. et al. (Sept. 2011b). MiMIC: a highly versatile transposon insertion resource for engineering Drosophila melanogaster genes. en. Nature Methods *8*.9, 737–743. ISSN: 1548-7105. DOI: 10.1038/nmeth.1662. URL: https://www.nature.com/articles/nmeth.1662 (visited on 05/05/2022).

Vlasits, Anna L. et al. (Sept. 2014). Visual Stimulation Switches the Polarity of Excitatory Input to Starburst Amacrine Cells. en. Neuron *83*.5, 1172–1184. ISSN: 0896-6273. DOI: 10.1016/j.neuron.2014.07.037. URL: https://www.sciencedirect.com/science/article/pii/S0896627314006485 (visited on 05/11/2022).

Weckström, M., Hardie, R. C., and Laughlin, S. B. (1991). Voltage-activated potassium channels in blowfly photoreceptors and their role in light adaptation. eng. The Journal of Physiology *440*, 635–657. ISSN: 0022-3751. DOI: 10.1113/jphysiol.1991.sp018729.

Weckström, M. and Laughlin, S. B. (Jan. 1995). Visual ecology and voltage-gated ion channels in insect photoreceptors. eng. Trends in Neurosciences *18*.1, 17–21. ISSN: 0166-2236. DOI: 10.1016/0166-2236(95)93945-t.

Wehrhahn, Christian, Poggio, Tomaso, and Bülthoff, Heinrich (Sept. 1982). Tracking and chasing in houseflies (Musca): An analysis of 3-D flight trajectories. en. Biological Cybernetics *45*.2, 123–130. ISSN: 0340-1200, 1432-0770. DOI: 10.1007/BF00335239. URL: http://link.springer.com/10.1007/BF00335239 (visited on 05/25/2022).

Wernet, Mathias F., Huberman, Andrew D., and Desplan, Claude (Dec. 2014). So many pieces, one puzzle: cell type specification and visual circuitry in flies and mice. en. Genes & Development *28*.23, 2565–2584. ISSN: 0890-9369, 1549-5477. DOI: 10.1101/gad.248245.114. URL: http://genesdev.cshlp.org/lookup/doi/10.1101/gad.248245.114 (visited on 07/25/2019).

Wernet, Mathias F. et al. (Mar. 2006). Stochastic spineless expression creates the retinal mosaic for colour vision. en. Nature *440*.7081, 174–180. ISSN: 1476-4687. DOI: 10.1038/nature04615. URL: https://www.nature.com/articles/nature04615 (visited on 05/10/2022).

Wienisch, Martin and Klingauf, Jurgen (Aug. 2006). Vesicular proteins exocytosed and subsequently retrieved by compensatory endocytosis are nonidentical. eng. Nature Neuroscience *9*.8, 1019–1027. ISSN: 1097-6256. DOI: 10.1038/nn1739.

Wietek, Jonas et al. (Apr. 2014). Conversion of channelrhodopsin into a light-gated chloride channel. eng. Science (New York, N.Y.) *344*.6182, 409–412. ISSN: 1095-9203. DOI: 10.1126/science.1249375.

Wu, Jinglin et al. (Mar. 2021). Parallel Synaptic Acetylcholine Signals Facilitate Large Monopolar Cell Repolarization and Modulate Visual Behavior in Drosophila. eng. The Journal of Neuroscience: The Official Journal of the Society for Neuroscience *41*.10, 2164–2176. ISSN: 1529-2401. DOI: 10.1523/JNEUROSCI.2388-20.2021.

Wu, Mark N and Bellen, Hugo J. (Oct. 1997). Genetic dissection of synaptic transmission in Drosophila. en. Current Opinion in Neurobiology *7*.5, 624–630. ISSN: 0959-4388. DOI: 10.1016/S0959-4388(97)80081-5. URL: https://www.sciencedirect.com/science/article/pii/S0959438897800815 (visited on 05/19/2022).

Wu, S. M. (Aug. 1992). Feedback connections and operation of the outer plexiform layer of the retina. eng. Current Opinion in Neurobiology *2*.4, 462–468. ISSN: 0959-4388. DOI: 10.1016/0959-4388(92)90181-j.

Yamamoto, Mutsuya et al. (July 2003). Reversible Suppression of Glutamatergic Neurotransmission of Cerebellar Granule Cells *In Vivo* by Genetically Manipulated Expression of Tetanus Neurotoxin Light Chain. en. The Journal of Neuroscience *23*.17, 6759–6767. ISSN: 0270-6474, 1529-2401. DOI: 10.1523/JNEUROSCI.23-17-06759.2003. URL: https://www.jneurosci.org/lookup/doi/10.1523/JNEUROSCI.23-17-06759.2003 (visited on 05/06/2022).

Yang, Helen H. and Clandinin, Thomas R. (Sept. 2018). Elementary Motion Detection in *Drosophila* : Algorithms and Mechanisms. en. Annual Review of Vision Science *4*.1, 143–163. ISSN: 2374-4642, 2374-4650. DOI: 10.1146/annurev-vision-091517-034153. URL: https://www.annualreviews.org/doi/10.1146/annurev-vision-091517-034153 (visited on 05/12/2022).

Yang, Helen H. et al. (June 2016). Subcellular Imaging of Voltage and Calcium Signals Reveals Neural Processing In Vivo. en. Cell *166*.1, 245–257. ISSN: 00928674. DOI: 10.1016/j.cell.2016.05.031. URL: https://linkinghub.elsevier.com/retrieve/pii/S0092867416305827 (visited on 05/22/2022).

Yang, Hui et al. (Sept. 2013). One-step generation of mice carrying reporter and conditional alleles by CRISPR/Cas-mediated genome engineering. eng. Cell *154*.6, 1370–1379. ISSN: 1097-4172. DOI: 10.1016/j.cell.2013.08.022.

Yuste, Rafael (Aug. 2015). From the neuron doctrine to neural networks. eng. Nature Reviews. Neuroscience *16*.8, 487–497. ISSN: 1471-0048. DOI: 10.1038/nrn3962.

Zeng, Hongkui and Sanes, Joshua R. (Sept. 2017). Neuronal cell-type classification: challenges, opportunities and the path forward. eng. Nature Reviews. Neuroscience *18*.9, 530–546. ISSN: 1471-0048. DOI: 10.1038/nrn.2017.85.

Zhang, Chi and McCall, Maureen A. (Jan. 2012). Receptor targets of amacrine cells. eng. Visual Neuroscience *29*.1, 11–29. ISSN: 1469-8714. DOI: 10.1017/S0952523812000028.

Zhang, Feng et al. (Apr. 2007). Multimodal fast optical interrogation of neural circuitry. en. Nature *446*.7136, 633–639. ISSN: 1476-4687. DOI: 10.1038/nature05744. URL: https://www.nature.com/articles/nature05744 (visited on 05/06/2022).

Zheng, Lei et al. (May 2006). Feedback network controls photoreceptor output at the layer of first visual synapses in Drosophila. eng. The Journal of General Physiology *127*.5, 495–510. ISSN: 0022-1295. DOI: 10.1085/jgp.200509470.

10 | Acknowledgements

"You have to suffer for your Ph.D." is the motto of many people who talk about doing a Ph.D. There are many places where doing a Ph.D. takes an enormous toll on someone's mental and physical health. I am very privileged and lucky to say that my journey was very different; it was wonderful. With its ups and downs, natural to every process in life, it was full of learning, growth, discoveries, and a ton of fun! Mondays were not gloomy days for me but rather the start of something exciting. More importantly, I realized more and more about what I cherish most in life and how I want to shape my future during this journey. I need to acknowledge that it is not me who made this journey as awesome as it was, but rather the people surrounding me or with whom my life intersected. Thus, I would like to reflect on people who supported me, inspired me with their unique perspectives and ideas, and shaped a part of this fantastic journey. I would like to express my deepest gratitude to:

First and foremost, **Marion Silies** for being a fantastic advisor in so many aspects and showing me a very positive side of academia. Your passion for science is definitely contagious and luckily, no mask can block that! Your constructive criticism and deep knowledge improved me so much, including critical thinking, coming up with new ideas, analyzing and interpreting results, writing and presenting. I am grateful for your outstanding support and encouragement, which kept me going during the difficult parts of my Ph.D. I deeply appreciate the trust, freedom and support you gave me for shaping my interests, even if they were not sometimes aligned with the immediate interests of the lab. Thanks to this, I now know much more about where my deepest interests lie and how I want to shape my life. I feel so privileged to have worked in Silies lab under your guidance and will try to follow your example in outstanding leadership in the future.

Silvio Rizzoli for his constructive criticism and ideas to further develop my project and giving me encouragement during the TAC meetings. Thank you very much for your time to meet me even before my Ph.D. to discuss the project ideas. I also appreciate your guidance and support for the projects I started later in my Ph.D.. Thank you, **Jan Clemens**, for the feedback, new ideas, and support during the TAC meetings and for being available for emailing or meeting up to discuss my projects. Thank you Silvio Rizzoli and Jan Clemens very much for your time and expertise in evaluating my work.

Jochen Staiger, **Tobias Moser** and **Alexander Ecker** for being my extended thesis examination board members. Thank you very much for sharing your time and expertise in evaluating my work.

Current and previous members of the **IMPRS Neurosciences team**, the late **Michael Hörner, Sandra, Mirja, Jonas** and **Franziska**. The more I live in Germany and deal with German bureaucracy the more I appreciate your never-ending support in any type of organizational work. Your friendly and warm attitude always makes it a pleasure to talk with you and makes it very easy to ask for help. Thanks for organizing the great retreats where it felt like returning to a family house, reminding us of the warm atmosphere we all experienced daily during our Master's days. Thank you very much, Jonas, for your support in extending my thesis and for trying your best to find me a mentor during the mentoring program. A big thanks to the **GGNB office** for organizing great courses that improved me in so many ways, from teaching to programming to communicating my science.

Neuromatch organizers for organizing a fantastic summer course with a great philosophy of making high-quality education accessible and science fairer. I have learned a lot as a TA and an organizer and met with like-minded people who are passionate about science and making a positive

impact in the world. Similarly, I am also grateful to **TReND in Africa** team for allowing me to organize a programming course with fantastic volunteers and meet with students all around Africa. Throughout these experiences, I have seen that merging my passion for science and teaching with my desire to do good for the world is possible.

All my friends at the **Silies lab**. Silies lab is amazing not just with research but also with its warm and diverse environment and amazing people. Thank you everyone for bringing your passion for science, sharp minds, and warm and fun attitude. I had the chance to get to know many of you personally and formed great friendships. I know I can not thank everyone enough but I would still like to mention some of the people who made this journey incredible. Thank you:

Sebastian, for your very special place in this journey. In our first interaction at our Master's program, you made me believe that you really saw the winning lottery numbers in your dream and failed to buy the ticket in real life by some unfortunate sequence of events. Real or not, I would probably never believe a story like this if it was coming from someone else's mouth. You are a truly genuine, interested, open-minded person and a caring friend. Plus, thanks for being so passionate about science and being so good at having constructive discussions, which helped me a lot during my academic journey. When it comes to novelty, you are full of it!

Juan, for your academic and personal contribution to my life. You are a great friend with some contrasting qualities compared to me, which I find a great source of growth. Your eye for detail and questioning mindset is remarkable. Thanks to this, I could improve my code, experimental paradigms, and my science.

Miriam, for being a very supportive and cheerful friend. The great discussions we had over any topic contributed greatly to my growth and my science. Collaborating with you on your project was also a highlight of my Ph.D. An extra thanks for always opening up your place for social gatherings with Jonas.

Madhura, for your extensive conceptual knowledge and innovative ideas, which formed the basis of one of my projects. It was great to collaborate with you and Sebastian and learn from everyone's strengths. It is always fruitful to discuss with you since you delve deep into concepts to put our findings into a broad framework that inspires further experiments.

Luis, for your critical questions and comments on the science and for showing me your skill to zoom out and look at things from a very broad perspective to ask the right questions.

Jonas Peper, for your humorous and relaxed attitude and your molecular biology expertise and sharp intellect, which leads to great ideas to improve the tool project.

Christine, Simone and Jonas Chojetzki for your excellent technical support. Thanks Jonas Chojetzki, for becoming a good friend with whom I can have great fun and talk about any personal topic.

Katja, for being my supervisor during my first experience at the Silies lab and showing me how to do great dissections.

Freya, for being a motivated, critical thinking, resilient and patient student. It was great fun to work with you and I am happy to see that you're continuously improving in the lab! Thanks **Nare**, for showing your passion for science and extreme desire to learn in such a short amount of time in your lab rotation.

The newcomers of the Silies lab, **Maria, Neel, Jacqueline and Annika**. You keep the awesome atmosphere ongoing and add on with your unique personalities. Special thanks to Jacqueline for your time and your fast-learning of experimental methods that contributed to my project.

Chris, for sharing your passion for science in our short discussions. I admire your skills for building a two-photon imaging setup from scratch. I am looking forward to learning more from you.

Carlotta, for your passion for science and great questions and advice during lab meetings which made me reflect on some aspects that I was missing. An extra thanks for taking me with you and giving me the first amazing outdoor climbing experience of my life!

Carlotta's lab, **Giovanni, Sofia and Leticia** for extending our warm atmosphere by being so friendly and passionate about science.

Everyone in our department for making this journey great!

My **non-lab friends** from Istanbul, Göttingen, Mainz, from summer-schools and conferences. Thank you my friends for life (Aras, Tolgi, Ufuk ...) from Istanbul for being so interested in what I do and always asking why I work with fruit flies and asking when I will get the Nobel prize. Special thanks to IMPRS Master's friends for making me feel at home during my stay in Göttingen after a couple of days of arrival and for sticking with me until now.

Marli, for many many things, including your endless unconditional love and support that enabled me to write the whole day for 2 months while still keeping my mood high. Being with you and your approach to life enriches me and makes me grow in all areas, including scientific thinking. I am lucky to be able to share all my interests with you, talk freely about anything and just be who I am.

Last but not least, I would like to share my deepest gratitude to **my family**. I can enjoy such a great life in Germany doing what I love (including at work and outside work) only because of the freedom, trust, love and support you gave me. You encouraged and supported me to explore my diverse interests and gave me the security in case I failed. Consciously and unconsciously, I learned and still learning a lot from you, which I benefit from in my daily life and my big life choices. I would like to point out a few things that I find extremely valuable for my journey. Thanks mum, for being very caring and always considering my well-being and providing a warm family environment with my sister. Thanks dad, for shaping my interest in deep topics of life by talking to me about your book collection ranging from Darwin to Richard Dawkins and being an example with your logical and organized approach. Thanks a lot also for showing me how important it is to pursue your interests outside work and be a multi-faceted person. Thanks aunt for your never-ending encouragement and support and your valuable insights from academia. Thanks Aysegul for the warm environment, being interested in my life and offering your support and encouragement. An additional thanks for introducing me to mindfulness and meditation, which changed my perspectives on life that nothing has ever done before.

11 | Appendix

11.1 List of Abbreviations

BPC	Bipolar Cell
Dm	Distal medulla
EM	Electron Microscopy
GABA	Gamma-Aminobutyric acid
GFP	Green Fluorescent Protein
GOF	Gain of Function
IPL	Inner Plexiform Layer
K_a	Voltage gated potassium channels with fast-inactivating A-type currents
K_d	Voltage gated potassium channels with a delayed rectifier current
K_v	Voltage gated potassium channels
LMC	Lamina Monopolar Cell
LOF	Loss of Function
LPTC	Lobula Plate Tangential Cell
Mi	Medulla-intrinsic
MiMIC	Minos-mediated integration cassette
Nlg	Neuroligin
nSyb	neural Synaptobrevin
OPL	Outer Plexiform Layer
RF	Receptive field
RGC	Retinal Ganglion Cell
RMCE	Recombinase Mediated Casette Exchange
STAB	Synapse Targeted Activity Block
Tm	Transmedullary

11.2 List of Figures

11.3 List of Tables

12 | Declaration

Herewith I declare, that I prepared the Doctoral Thesis ‘Molecular and circuit analysis of stable contrast processing in the visual system’ on my own and with no other sources and aids than quoted.

Mainz, 31.05.2022

Burak Gür